

Parasitology Research Monographs 18

Heinz Mehlhorn
Jian Li
Kai Wu *Editors*

Malaria Control and Elimination in China

A successful Guide from Bench
to Bedside

 Springer

Parasitology Research Monographs

Volume 18

Series Editor

Heinz Mehlhorn, Department of Parasitology, Heinrich Heine University,
Düsseldorf, Germany

This book series “Parasitology Research Monographs” presents carefully refereed volumes on selected parasitological topics. Parasites have an increasing impact on animal and human health in the present times of globalization and global warming. Parasites may be agents of diseases and- often at the same time- vectors of other agents of disease such as viruses, bacteria, fungi, protozoa and/or worms. The growth in knowledge of parasitic physiology, cell structure, biotechnological and genetic approaches, ecology, therapeutic capabilities, vaccination, immunology, diagnosis, transmission pathways and many other aspects of parasitology is increasing dramatically, even in the face of the breakthroughs that have already been made. Reflecting these most recent achievements and the importance of parasites as a threat to human and animal health, the series’ broad scope concentrates on particularly hot topics emerging from the scientific community. Chapters offer compact but intense insights into the ongoing research and into the methods and technologies used to control parasites. The volumes in the series build on these topics, and the volume editors are well-known experts in their respective fields. Each volume offers 10 to 20 comprehensive reviews covering all relevant aspects of the topic in focus.

Heinz Mehlhorn • Jian Li • Kai Wu
Editors

Malaria Control and Elimination in China

A successful Guide from Bench to
Bedside

 Springer

Editors

Heinz Mehlhorn
Department of Parasitology
Heinrich Heine University
Düsseldorf, Germany

Jian Li
School of Basic Medical Sciences
Hubei University of Medicine
Shiyan City, China

Kai Wu
Wuhan Center for Disease Control and
Prevention
Wuhan City, China

ISSN 2192-3671

ISSN 2192-368X (electronic)

Parasitology Research Monographs

ISBN 978-3-031-32901-2

ISBN 978-3-031-32902-9 (eBook)

<https://doi.org/10.1007/978-3-031-32902-9>

© The Editor(s) (if applicable) and The Author(s), under exclusive license to Springer Nature Switzerland AG 2023

This work is subject to copyright. All rights are solely and exclusively licensed by the Publisher, whether the whole or part of the material is concerned, specifically the rights of translation, reprinting, reuse of illustrations, recitation, broadcasting, reproduction on microfilms or in any other physical way, and transmission or information storage and retrieval, electronic adaptation, computer software, or by similar or dissimilar methodology now known or hereafter developed.

The use of general descriptive names, registered names, trademarks, service marks, etc. in this publication does not imply, even in the absence of a specific statement, that such names are exempt from the relevant protective laws and regulations and therefore free for general use.

The publisher, the authors, and the editors are safe to assume that the advice and information in this book are believed to be true and accurate at the date of publication. Neither the publisher nor the authors or the editors give a warranty, expressed or implied, with respect to the material contained herein or for any errors or omissions that may have been made. The publisher remains neutral with regard to jurisdictional claims in published maps and institutional affiliations.

This Springer imprint is published by the registered company Springer Nature Switzerland AG
The registered company address is: Gewerbestrasse 11, 6330 Cham, Switzerland

Contents

1	Malaria Epidemiology in China: A Historical Review	1
	Jianhai Yin	
2	A Fact Sheet on Malaria: Global Status and Significant Species . . .	19
	Heinz Mehlhorn	
3	Malaria-Free in China: A Story of More than 70 Years	33
	Jun Feng	
4	Malaria Parasites: Species, Life Cycle, and Morphology	49
	Kai Wu	
5	Pathogenesis and Clinical Features of Malaria	71
	Huilong Chen	
6	Morphology of Malaria Parasites at the Erythrocytic Stage	87
	Kai Wu	
7	Immunodiagnosis of Malaria	199
	Jianhai Yin, He Yan, and Jian Li	
8	Molecular Basis of Malaria Pathogenesis	211
	Su-Jin Li, Zhenghui Huang, and Lubin Jiang	
9	Artificial Intelligence and Deep Learning in Malaria Diagnosis	225
	Min Fu and Zuodong Li	
10	Current Treatments for Malaria	253
	Xiaonan Song and Jian Li	
11	Artemisinin Resistance in <i>Plasmodium falciparum</i> Malaria	267
	Xiaoxing Wang, Bo Xiao, and Lubin Jiang	
12	Traditional Chinese Medicines for Malaria Therapy	279
	Changhua Lu, Lilei Wang, and Wei Wang	
	Index	291



Malaria Epidemiology in China: A Historical Review

1

Jianhai Yin

Abstract

Malaria is an ancient disease that used to be widespread in most parts of China, dominated by *Plasmodium vivax* and *P. falciparum*, seriously threatening people's health. In this chapter, the malaria epidemic in China from ancient times to the present was briefly reviewed. The Chinese nation has made important contributions to the fight against malaria, especially after the founding of the People's Republic of China. No indigenous malaria cases have been reported since 2017 after nearly 70 years of unremitting efforts, and China officially achieved the elimination of malaria on June 30, 2021. However, China will likely see a resurgence in malaria cases due to the thousands of imported cases and the distribution of the malaria vector *Anopheles* mosquitoes in the defined areas. Therefore, it is essential to maintain and strengthen the sensitivity of surveillance and response through capacity building and the research and development of new technologies based on the established and improved multisectoral cooperative mechanism under the unified leadership of the government, thereby effectively consolidating the achievements of malaria elimination in China.

Keywords

Malaria · Epidemiology · Historical records · Control · Elimination · Re-establishment · China

J. Yin (✉)

National Institute of Parasitic Diseases, Chinese Center for Disease Control and Prevention (Chinese Center for Tropical Diseases Research), Shanghai, China

1.1 Introduction

Malaria is an ancient disease that is caused by *Plasmodium* parasites transmitted by female *Anopheles* mosquitoes, and the history of malaria outbreaks is thought to date back to the beginnings of civilization. It is a devastating and life-threatening disease with global distribution, resulting in many people losing lives, and is even considered the cause of major military defeats and the disappearance of some nations. Fortunately, with the advancement of the global malaria control process (Litsios 2020), an increasing number of countries have entered the malaria preelimination stage or the elimination stage, and a total of 25 countries have been considered to be on track to reduce indigenous malaria cases to zero by 2025 in the E-2025 initiative after the E-2020 initiative, which was launched by the World Health Organization (WHO) (WHO 2021b, 2021d), although progress has stalled according to the malaria cases and deaths estimated in the world malaria reports in recent years and the negative impact of the coronavirus disease 2019 (COVID-19) pandemic on the implementation of malaria prevention and control measures and the availability of antimalarial treatment (WHO 2021c). For instance, the estimated number of cases in 85 endemic countries in the world reached 241 million, and the estimated number of deaths reached 627,000 in 2020 according to the latest World Malaria Report 2021 (WHO 2021c).

Looking back at the history of malaria, the earliest record of malaria was found in the inscriptions on oracle bones and bronze wares during the Shang-Yin period, which had the pictograph of “malaria” in Chinese, indicating that malaria was prevalent in China 3000 years ago (Tang et al. 2012). Moreover, Hippocrates, a Greek physician in the fourth century BC, linked malaria to the summer/fall, marshes, and splenomegaly and first described the different types of malaria depending upon the periodicity of the fever, thereby completely rejecting its demonic origin (Cunha and Cunha 2008). This explanation remained until 1880 when Laverin discovered that the malaria parasite in the blood of people with malaria was the cause of the disease (Cox 2010; Hempelmann and Krafts 2013). Laverin also won a Nobel Prize for this work in 1907. Another four Nobel Prizes associated with malaria were awarded: Youyou Tu in 2015 for the discovery of artemisinin, a drug that is now the dominant treatment for malaria (Tu 2011, 2016); Paul Müller in 1947 for the synthetic pesticide formula dichlorodiphenyltrichloroethane; Julius Wagner-Jauregg in 1927 for the induction of malaria as a pyrotherapy procedure in the treatment of paralytic dementia; and Ronald Ross in 1902 for the discovery and significance of mosquitoes in the biology of the causative agents in malaria (Talapko et al. 2019).

In the long-term struggle against malaria, the Chinese nation has made outstanding contributions to human understanding of malaria and the prevention and treatment of malaria. In more than 2000 years since the Qin and Han Dynasties, there have been many records about malaria from the earliest medical classic “Huangdi Neijing, Inner Canon of the Yellow Emperor” to the Ming and Qing dynasties, which described the malaria causes, symptoms, diagnosis, and treatment methods (Tu 2016). In particular, the records of Qinghao in *A Handbook of Prescriptions for*

Emergencies by Ge Hong in the Eastern Jin Dynasty (approximately 317–420 AD) provide important inspiration for the method of extracting active ingredients in the early stage of artemisinin development in China (Ge 300–400 A.D.), and the artemisinin-based antimalarial drug has been developed, which has made a proud contribution to the world (Chen 2014).

China was certified malaria-free by the WHO on June 30, 2021 (Feng et al. 2021; Zhou 2021). In this chapter, we briefly review the malaria epidemic in China from ancient times to the present.

1.2 Malaria Epidemiology Before the Founding of the People's Republic of China

Malaria is also commonly known as “miasma” and some other dialects in China, and it is an ancient parasitic disease that was distributed extensively throughout history, although there was a lack of systematic epidemic statistical reports before the founding of the People's Republic of China. Fortunately, the historical records and documents of serious epidemics in different regions have been collected and reviewed by Prof. Zujie Zhou and Prof. Linghua Tang, et al. in Chinese (Tang et al. 2012; Zhou 1991). It was recorded that the prevalence of malaria increased from north to south and from west to east, and *Plasmodium vivax*, *P. falciparum*, and *P. ovale* were identified in surveys conducted in some representative malaria transmission areas, including Yunnan, Guangxi, Guizhou, Guangdong, Fujian, Jiangxi, Sichuan, Zhejiang, Anhui, Jiangsu, Hebei, and Liaoning, from 1924 to 1947. Furthermore, the epidemic could be exacerbated by population movements due to wars, natural disasters, large-scale construction projects, etc., resulting in economic decline and people's livelihood withering. In this section, we reorganize and briefly describe the epidemiological history of malaria in different geographical and administrative divisions in the Chinese mainland before the founding of the People's Republic of China mainly based on two books (Tang et al. 2012; Zhou 1991).

1.2.1 Malaria in Southwest China (Yunnan, Guizhou, Tibet, Sichuan, and Chongqing)

In Yunnan, there were records of malaria infections and epidemics among soldiers as early as the Three Kingdoms period. In the poem “Xin Feng Zhe Bi Weng,” written by the Tang Dynasty poet Juyi Bai, he heard that there was a river named Lu in Yunnan, and it would be filled with miasmas when the pepper flowers wither in summer, which was a sight ravaged by malaria. Taihe (now Dali) experienced heavy malaria epidemics in the thirteenth year of Tianbao (AD 754) in the Tang Dynasty recorded in the “Zi Zhi Tong Jian (Comprehensive Mirror for Aid in Government)” (Guang 2012). Since then, there have been many records about the rampant prevalence of malaria in the local areas in the history books and local chronicles of various dynasties. During the 7 years of the construction of the Yunnan

section of the Yunnan-Vietnam Railway, which began in 1904, a total of 200,000–300,000 migrant workers from Yunnan, Sichuan, Guangdong, Guangxi, and other places were recruited and severely affected by malaria without enough medical protection, resulting in 60,000–70,000 people dying of malaria (<https://baijiahao.baidu.com/s?id=1715864376600876896&wfr=spider&for=pc>). In Simao, the trade center in the southern part of Yunnan, the malaria outbreak in 1919 lasted for 30 years, and the malaria parasite rate of the surveyed residents was 76.5% in 1936, while the incidence rate of malaria from January to September of the previous year was 72.9%, resulting in many deaths and serious population reduction (only 944 people left in 1949 from more than 30,000 original population of the urban area). Likewise, more than 30,000 people died due to a malaria epidemic in Yunxian County in a few years since 1933, the incidence of malaria in this county was 94.9%, and the rate of malaria parasites reached 49.1% in 1941 (Tang et al. 2012; Zhou 1991).

The annals of Guizhou Province also recorded malaria as early as the Warring States Period (Tang et al. 2012; Zhou 1991). In the Ming Dynasty, Shouren Wang, a Chinese philosopher, was demoted to Longchang, and he wrote in the “Xiuwen County Chronicle” that so many miasmas were distributed in Guizhou and that people living there were very afraid of malaria. Furthermore, there was a folk song in the southern part of Guizhou Province that says, “When you walk to Shimenkan, the ghost will shout behind you; when you walk to Meizikou, the ghost will wait behind you; when you walk to Sanmengou, the King of Hell will take his life.” At the end of the Qing Dynasty, more than 3000 people among more than 5000 cavalymen stationed in Pojiao Village under Anlong County in southwestern Guizhou died of malaria in a few years. In 1936, Prof. Yongzheng Yao and others found that the splenomegaly rate of school children was 35.9%, and the malaria parasite rate was 50.4%, of which *P. falciparum* accounted for 72.9%, in Pojiao, Sandaokou and other places in Guizhou. In the following 2 years, Prof. Huaijie Gan surveyed more than 5,800 school children in more than 10 counties in southwestern, northern, and central Guizhou. The malaria parasite rate varied from 1.8% to 51.3%, and *P. falciparum* was the most common, especially in the southwest and south. From 1939 to 1940, Prof. Jingsheng Guo surveyed 24 counties and cities and found that malaria infection was the most serious in southwestern and southern Guizhou. Among the three counties of Luodian, Ceheng, and Wangmo, the malaria parasite rate of children under 12 years old was more than 25%, and falciparum malaria accounted for 75%. In Songtao County, which is close to Hunan in the northeast, the malaria parasite rate in children could also be as high as 29.3%, and more than half were *P. falciparum*.

In Tibet, malaria cases were distributed in Moutuo, Chayu, and other counties in the Yarlung Zangbo River and Chayu River valleys in southeastern Tibet, as well as in areas below the altitude of 1500 m in the southern Himalayas, with Moutuo being the majority.

Malaria was endemic throughout the basin and periphery of Sichuan Province. In the 23rd year of Guangxu’s reign (1897), malaria was prevalent in Chongqing, and nearly half of the population fell ill. Between 1934 and 1937, malaria cases

accounted for approximately 1.4–2.1% of the inpatients, with vivax malaria accounting for approximately 53%, falciparum malaria accounting for 41%, and malariae malaria accounting for 6% in more than 10 hospitals in Chongqing, Yibin, Kangding, Fuling, Mianzhu, Guanghan, Leshan, Ya'an, and Chengdu. Meanwhile, the malaria species were distributed significantly differently in different areas; the proportion of falciparum malaria ranged from 1.9% to 69.1%, with the highest in Ya'an, Mianzhu, Guanghan, Fuling, and Leshan counties and the lowest in Zhong County. Furthermore, malaria was prevalent, and the splenomegaly rate of adolescents reached 18% in Chongqing in the autumn of 1939 due to the internal relocation of government agencies and the westward migration of refugees. Malaria cases accounted for 20% of the total number of patients, and the highest rate reached 42% in the eight relocation areas. After that, the number of falciparum malaria cases in the suburbs of Gele Mountain increased greatly between 1940 and 1945, and the mortality rate reached 7.7%. In other parts of the province, malaria was also widespread. In 1948, it was reported that falciparum malaria accounted for 93.3% of the malaria cases in Luzhou, and vivax malaria accounted for 97.4% in Chengdu, and some malariae malaria cases were also present.

1.2.2 Malaria in South Central China (Henan, Hubei, Hunan, Guangxi, Guangdong, and Hainan)

In Henan Province, “malaria is in Zheng” was recorded in the “Zuo Spring and Autumn Period”(Zuo), which indicated that malaria was prevalent in Xinzheng more than 2000 years ago. In 1815, during the reign of Emperor Jiaqing of the Qing Dynasty, the malaria epidemic in southern and eastern Shandong also spread to Shangqiu and Luyi in eastern Henan. The malaria epidemic caused by the flood in 1931 had a great impact on the eastern and central parts of Henan Province, and the frequent mobilization of the army led to a major malaria epidemic in the province. For instance, a malaria outbreak occurred in Kaifeng, Henan Province, due to the heavy rain in July and August and the mobilization of soldiers. Moreover, among the positive blood samples for *Plasmodium*, *P. vivax*, *P. falciparum*, and *P. malariae* accounted for 77.8%, 17.39%, and 4.44%, respectively. In addition, there were also a certain number of falciparum malaria cases in Xinyang, Queshan, Zhumadian, and Dengxian. Since then, many malaria epidemics have occurred in Xinyang, Zhengzhou, Kaifeng, and Xichuan County in the mountainous area of southwestern Henan.

In the Yuan Dynasty, famous Medical Scientists of Danxi Zhu once listed Hubei Province as one of the places with a serious malaria epidemic. Taking Yichang as an example, malaria epidemics occurred successively in the ninth to sixteenth years of Guangxu (1883–1890), 1911, 1916, and 1938. In 1931, when the Yangtze River flooded, falciparum malaria was widespread among the malaria cases in Hankou, accounting for 69.4%. Usually, malaria cases in Hankou accounted for approximately 1.9–2.3% of the hospitalized patients, and falciparum malaria and vivax

malaria accounted for approximately 40% each, with some infections of *P. malariae* and mixed infections.

Malaria was endemic throughout Hunan Province. During the Guangxu period of the Qing Dynasty, severe malaria epidemics occurred in Guiyang County in 1875, Jiahe in 1893, and Changde in 1901, and many cases died. After that, there were serious outbreaks of malaria in Hengnan in 1918, Guidong in 1924, Ningyuan in 1926, Huitong on the border of Hunan and Guizhou in 1931, Pingjiang in 1935, Liuyang in 1937, Leiyang in 1944, Rucheng and Lingling in 1945, Guidong in 1947, and Chenxian in 1949. Among them, the incidence of malaria among residents in Lingling and Guidong counties exceeded 50%, with many deaths in the year of the outbreak. Furthermore, the splenomegaly rate of urban primary school students in Chenxian was as high as 69%, the malaria parasite rate was 63%, and those of rural primary school students were as high as 74% and 81%, respectively, being both dominated by vivax malaria, as well as malariae malaria and falciparum malaria.

Guangxi has been also commonly suffered from malaria epidemics for many years. In 1924, more than a thousand of soldiers died of malaria in the troops in Baise, Guangxi, on their march from Guizhou to Guangdong. In 1935, Prof. Lanzhou Feng conducted surveys in 8 counties, including Enyang and Baise in Guangxi, and found that the splenomegaly rate was 3%–58%, and the malaria parasite rate was 7.1%–84.9%. In particular, falciparum malaria accounted for 59% and 37% in Enyang and Longsheng counties, respectively. In 1942, among the 33 households with 115 people in Zhelang Township, Longlin County, north-west Guangxi, 92 people from 20 households suffered from malaria, and 25 people died, of which 5 households died. It was estimated that there were no less than 5 million malaria cases in Guangxi at that time.

The area of Qiong (Hainan Island) and Lei (Leizhou Peninsula) has been called the hometown of miasma since ancient times (Office 2013; Zhang et al. 1901; Zhang 1841). The local chronicles in the Sui Dynasty recorded that “most areas in more than twenty counties in the Lingnan were under the wet and were almost suffered from miasma” (Wei 629). In the autumn of 1923, the Dongjiang River in Guangdong was flooded, and the northern soldiers stationed in Heyuan County on the right bank of the river were suffered an outbreak of malaria (Zhou 1991). Approximately 300–400 patients poured into the hospital every day, and many died. Moreover, more than 700 local residents (only more than 1000 residents in the county) also died of malaria. In addition, malaria epidemics continuously occurred in Qiongzong County and Chengmai County on Hainan Island in 1925, Shantou City and Chaoan County in 1939, Foshan County, Taishan County, and Baisha County on Hainan Island in 1943, and Zhuhai County and Baoting County on Hainan Island in 1944 (Tang et al. 2012; Zhou 1991).

1.2.3 Malaria in Eastern China (Fujian, Shanghai, Jiangsu, Zhejiang, Anhui, Jiangxi, and Shandong)

It was recorded that “Yubo was appointed to Central Fujian and often supported soldiers to catch mountain bandits, but the soldiers all felt malaria when they passed through Zhangpu” in “Su Shen Liang Fang” written by Kuo Shen and Shi Su in the Song Dynasty (Shen and Su). Danxi Zhu described malaria transmission in the south of the Yangtze River in China in the 12th century, with many malaria cases in Fujian, which was in line with the reality that people were more likely to suffer from malaria during the long summer. In the 34th year of Jiaping in the Ming Dynasty, General Jiguang Qi’s troops garrisoned in Pantuoling, southern Fujian, and malaria was rampant in the army, resulting in a large number of deaths of soldiers, which seriously affected the war. In 1932, Prof. Lanzhou Feng conducted malaria investigations in Xiamen and found that the rate of splenomegaly among residents was 75%, and the rates of *Plasmodium* infection among migrant workers and farmers in mountainous areas were 83.3% and 58.1%, respectively, of which *P. falciparum* accounted for 63.5%. Moreover, the sporozoite infection rate of *Anopheles minimus* was 8.6%, and the rate of gastric oocyst infection was 29.8%. Years later, the Fujian Provincial Health Laboratory reported in 1938 that malaria had been prevalent and spread in eastern and southern Fujian and throughout the province in those years, rather than mostly being confined to the mountainous areas of northwestern Fujian in the past. It was estimated that there were at least 4 million malaria cases throughout the year, and the fatality rate was as high as 3% according to the outpatient statistics of the county health centers at that time. In 1948, more than 30,000 people suffered from malaria in Jianning County, which accounted for almost half of the county’s population.

In Jiangsu, there was a serious epidemic of malaria in Suzhou at the beginning of the twentieth century. In the early 1920s, the prevalence of malaria among students at Soochow University was 37.8%, and *P. falciparum* accounted for half of the cases. According to the annual report of Suzhou Hospital in 1930, among the 249 *Plasmodium*-positive cases in blood tests, 39.8% were *P. falciparum*, 49.4% were *P. vivax*, and 10.8% were *P. malariae*. In 1930, malaria was prevalent among people from Anhui, and six other provinces went to Nanjing to build the Sun Yat-Sen Cemetery. The incidence rate reached 71.3% in 1933, of which 84.2% was the first onset after arriving in Nanjing, the rate of splenomegaly was 53.8%, and falciparum malaria accounted for 58.3%. After the Yangtze River flooded in 1931, the rate of splenomegaly was 2.5%, and the malaria parasite rate was 22.6% in 6039 Nanjing residents surveyed by the Department of Health. Moreover, falciparum malaria accounted for half of them, vivax malaria accounted for nearly half, and some sporadic malariae malaria. In the second year, 6976 residents in Nanjing and its suburbs were surveyed; 47% of them had a history of malaria, the splenomegaly rate was 18%, the malaria parasite rate was 13%, and vivax malaria accounted for 65%. However, from August to September in the same year, falciparum malaria accounted for 52%, twice as many as that in other months. Additionally, malaria cases accounted for 2.6% of hospitalized cases in Wuxi and 1.6% in Nanjing according

to incomplete statistics. *P. vivax* malaria, falciparum malaria, and malariae malaria were found, with vivax malaria being the majority.

Zhejiang was once a province with a serious epidemic of falciparum malaria. In Wenzhou, Zhejiang, in the eighth year of Emperor Guangxu's reign (1882), nearly half of the population was infected with malaria. After the Yangtze River flooded in 1931, the splenomegaly rate of the Hangzhou population was 7.2%, and the malaria parasite rate was 39.5%, with *P. falciparum* mainly accounting for 82.4%, as well as *P. vivax* and *P. malariae* according to the surveys conducted by the Department of Health in November of that year. Meanwhile, the splenomegaly rate was 23% in the population in Wukang (today's Deqing), the malaria parasite rate was 21%, and falciparum malaria and vivax malaria were equally divided. However, vivax malaria accounted for the majority of 60%, usually followed by falciparum malaria. For instance, the proportion of falciparum malaria in local malaria cases in 1937 was 27.2% in Hangzhou, 38.9% in Ningbo, 24.0% in Wuxing, 26.5% in Shaoxing, and 20.7% in Wukang, respectively.

Malaria was endemic in Shanghai. An epidemic of vivax malaria was recorded in the tenth year of Guangxu (1884) in the Qing Dynasty. In 1931, the Yangtze River and Huaihe River flooded concurrently, and the number of malaria cases in the disaster-stricken areas along the rivers increased sharply, with the incidence rate reaching up to 60% in some areas. During the autumn and winter of this year, a survey of the victims who fled from Hankou to Shanghai found that the malaria parasite rate was 27.4%, of which *P. falciparum* accounted for 69.4%, *P. vivax* accounted for 13.7%, and *P. malariae* accounted for 16.9%. In 1933, in a survey of school children in Gaoqiao, a suburb of Shanghai, 34.8% of them had a history of malaria within a year, 18.4% had splenomegaly, and the malaria parasite rate was 5.2%, of which *P. vivax* accounted for 59.9%, and *P. falciparum* accounted for 6.4%. In 1936, a survey in the southwestern suburbs of the city showed that 32.7% of the residents and 42.8% of school children had a history of malaria, the rate of splenomegaly in school children was 28.9%, and the malaria parasite rate was 20%. According to the statistics of patients admitted to the hospitals in the early 1930s, the case proportion of malaria was 0.4%, with *P. vivax* as the main type, falciparum malaria was approximately half of the number of vivax malaria cases, and there were also malariae malaria cases and mixed infections.

In the southern Anhui and Dabie Mountains in Anhui Province, malaria has been endemic for a long time. In 1931, the Yangtze River and Huaihe River flooded, the number of malaria cases in the disaster-stricken areas along the rivers increased sharply, and the incidence rate in some areas was as high as 60%. In the winter of that year, falciparum malaria cases in Anqing City accounted for 68.6% of the malaria cases, and mixed infections with vivax malaria were also found. According to the statistics of Wuhu Hospital, malaria cases accounted for 2.8% of the total number of hospitalized patients, and the majority suffered from *P. vivax*, accounting for 84.5%. Meanwhile, there were a few cases infected with *P. falciparum* and *P. malariae*.

From the nineteenth year of Guangxu (1893) in the Qing Dynasty to the early years of the Republic of China, malaria continued to be prevalent in Jiangxi

Province, especially in mountainous and hilly areas. In some counties in the mountainous areas of southern Jiangxi, the annual incidence of malaria reached 75–80%. In the winter of 1931, it was found that the splenomegaly rate of people in Jiujiang, Hukou, Shahe, Nanchang, and other places along the rivers was between 2.2 and 19.5%. All of the affected children in Jiujiang had cases of falciparum malaria, while those of vivax malaria were more common in Nanchang. According to data from the early 1930s, malaria cases accounted for approximately 3.4% among inpatients in Nanchang. Three types of malaria (vivax malaria, falciparum malaria, malariae malaria) were recorded; the former two types were more common, accounting for approximately 40% each, and mixed infections were also seen from time to time.

In Shandong, malaria epidemics were recorded in the Spring and Autumn Periods and the Warring States Period (Tang et al. 2012; Zhou 1991). In the 20th year of Jiaqing (1815) in the Qing Dynasty, malaria was prevalent in Juye, Caoxian, and Dongping in southwestern Shandong. The Jiaodong Peninsula in the nineteenth year of Guangxu's reign (1893), Yantai in 1897, Dongping in 1914, and Juye in 1916 all experienced malaria epidemics. The floods in 1931 also resulted in an outbreak of malaria in Shandong. It was recorded in the local chronicles of Dongming County that "malaria was prevalent in the autumn of the 20th year of the Republic of China, with seven or eight cases out of ten persons in a village, and many of them died, and the disease persisted in the following spring." Subsequently, the malaria epidemic occurred successively in Dong'e in 1932, Dongping in 1937, the whole southwestern Shandong region in 1942, Jinan and other places in 1947.

1.2.4 Malaria in North China (Beijing, Tianjin, Hebei, and Shanxi)

In the tenth year of Tongzhi (1871) in the Qing Dynasty, an outbreak of vivax malaria occurred due to a flood in North China. By 1873, the prevalence of malaria in Beijing and Tianjin reached its peak, with approximately 25–30% of residents getting sick. Reports in 1927 and 1936 showed that there were many cases of vivax malaria, mostly among hospitalized patients in Beijing and its suburbs and Tianjin. In the autumn of 1919, an epidemic of falciparum malaria occurred in nearby local residents of the troops from Hunan and northern Hubei and stationed at the Beijing Racecourse.

In southern Hebei, malaria was severely endemic. For instance, a serious epidemic and many people died of malaria in the ninth year of Jiajing (1530) in the Ming Dynasty were recorded in the chronicle of Xingtai area. In the annals of Lingshou County in the Shijiazhuang area, malaria was prevalent from spring to autumn in the twelfth year of Tongzhi (1873). Furthermore, malaria had spread to every village in this county, and at least one person in one household was sickened, and as many as several family members were affected by malaria from 1940 to 1944. According to a survey conducted by the Southern Hebei Office in 1946, there were more than 540,000 malaria cases in 41 counties, of which there were more than 180,000 cases in 14 counties in the Xingtai area. In 1949, it was estimated that there

were 600,000 malaria cases in the province, with an incidence rate of 15 per thousand.

In Shanxi Province, it was recorded that malaria mostly occurred in Linfen, Yuncheng, and other areas in the southwest. During the Anti-Japanese War of Resistance in 1938, a local malaria epidemic was recorded in Pinglu and Ruicheng counties in the Yuncheng area. Between 1940 and 1943, the border regions and counties of Jincheng and Changzhi adjacent to Hebei and Shandong provinces experienced malaria epidemics.

1.2.5 Malaria in Northwest China (Shaanxi, Xinjiang, Gansu, Qinghai, and Ningxia)

Malaria in Shaanxi Province was prevalent in the Guanzhong Plain and south of the Qinling Mountains. According to incomplete statistics from 1940 to 1948, there were more than 47,000 malaria cases in the province, with an average annual incidence rate of 52/10,000, which were commonly distributed in Shangluo, Weinan, and other special areas, and mainly vivax malaria. However, malaria was rare or nonexistent in the northern part of the province due to drought.

In Xinjiang, malaria cases were reported in Shufu County in southern Xinjiang in 1931. Since then, malaria epidemics or malaria cases have been found in other counties in Kashgar, oases in some counties in Hotan, and counties along the Ili River Basin. Among them, the counties in the Yili region had the largest number of malaria cases, accounting for approximately 64% of the total malaria cases in the autonomous region. Moreover, malaria was scattered along the Kashgar River, Yarkand River, and Hotan River Basin.

In Gansu, Qinghai, and Ningxia, there were no or very few historical data about the prevalence of malaria, mostly due to drought or cold weather.

1.2.6 Malaria in Northeast China (Liaoning, Heilongjiang, Jilin, and Inner Mongolia)

In 1924, there was an epidemic of malaria in Tieling, Liaoning Province, and hundreds of people were affected. After the victory of the Anti-Japanese War of Resistance, malaria was brought into Liaoning with frequent population movements inside and outside the customs, coupled with the swarming transfer of the troops, which led to a severe epidemic of malaria in the local area.

According to records in Heilongjiang Province, there were local epidemics of malaria on the Songnen Plain and Sanjiang Plain. Falciparum malaria has also been found in the Heilongjiang Basin, but it was not endemic.

In Jilin and Inner Mongolia, there are no or very few historical records about malaria, mostly due to drought or cold weather.

1.3 Trend of Malaria Epidemiology in the People's Republic of China (1949–2020)

Before 1949, it was estimated that more than 30 million cases of malaria occurred nationwide each year, and mortality was approximately 1% (Tang et al. 2012). However, through sustained efforts in different control phases, malaria has declined dramatically, to less than 15,000 cases in 2009, and the endemic areas have shrunk greatly (Zhou et al. 2011b). Immediately after, the Chinese government initiated the National Malaria Elimination Programme (NMEP) in 2010, and no indigenous malaria cases have been reported since 2017. China officially achieved the elimination of malaria on June 30, 2021, contributing to the Millennium Development Goals and global eradication of malaria. However, the control and elimination of malaria in China is a tortuous road, and challenges still exist in the post-elimination phase; thus, a systematic review of its roadmap can provide a reference for countries experiencing malaria elimination.

The main objective of this section is to briefly review malaria epidemiology in the different malaria control and elimination phases in P.R. China. In general, there are five phases in the country, namely, (1) the key-point investigation and control phase (1949–1959), (2) the phase in the control of severe epidemics (1960–1979), (3) phase of reducing the incidence rate (1980–1999), (4) phase of consolidating control achievements (2000–2009), and (5) malaria elimination phase (2010–2020).

1.3.1 The Key-Point Investigation and Control Phase (1949–1959)

At the beginning of the founding of the People's Republic of China, there was still a lack of detailed malaria epidemiological data and related information and a serious lack of specialized malaria prevention and control institutions and technical teams. Fortunately, malaria was designated a notifiable disease in 1956, a malaria-reporting mechanism was implemented nationwide, and malaria was listed as one of the diseases to be controlled and eliminated within a set time in the first 5-year National Malaria Control Programme (MOH 1956). Moreover, several baseline data on malaria epidemiology were collected through many surveys in some endemic areas for pilot studies conducted by continuously established professional bodies. In 1958, the malaria incidence rate in China dropped to 215.83/100,000, which declined by 57.2% compared with that in 1956 (505.23/100,000). In addition, four different malaria transmission zones were divided in the country, with different malaria parasite compositions and transmission seasons (MOH 1956; Tang et al. 2012; Yin et al. 2014; Zhou 1981, 1991).

1.3.2 Phase in the Control of Severe Epidemics (1960–1979)

Although the large-scale malaria outbreaks were controlled with a great reduction in malaria morbidity and mortality through the control strategy focusing on mass drug

administration and infectious source control, malaria transmission in this phase was unstable, especially the pandemic transmission of vivax malaria that occurred in the Huang-Huai Plain and central China, including Jiangsu, Shandong, Henan, Anhui, and Hubei Provinces, and there were more than 18,000,000 malaria cases accumulatively reported from each of these five provinces in this phase (Shang et al. 2007; Tang et al. 2012; Zhou 1991). Furthermore, more than 1,000,000 cases were reported from Jiangxi, Zhejiang, Sichuan, Hunan, Fujian, Guangdong, Hebei, Guangxi, Shanghai, and Yunnan, and approximately 1,000,000 cases were reported in other endemic areas (Tang et al. 2012). Additionally, the malaria incidence (257.54/100,000) in 1979 declined by 91.3% compared with that in 1970.

1.3.3 Phase of Reducing Incidence Rate (1980–1999)

In this phase, the integrated control strategies dominated by infectious source management and/or vector control were adopted in mainly accordance with both malaria epidemic characteristics and the distribution of different vectors (mainly *An. sinensis*, *An. minimus*, *An. dirus*, and *An. anthropophagus*) (MOH 1983, 1984, 1986, 1990, 1996). As a result, malaria transmission declined gradually, with case reduction rates of 30–43% during 1982–1988 (Expert Advisory Committee on Parasitic Diseases 1988, 1989; Malaria Commission 1984, 1985, 1986, 1987; MOH 1983, 1986) and approximately 15–25% during 1990–1996, except for 1994 (Expert Advisory Committee on Malaria 1993, 1994; Expert Advisory Committee on Malaria 1995; Expert Advisory Committee on Parasitic Diseases 1991, 1992, 1996, 1997). Moreover, more than 40% of cases were reported from the above five provinces in central China in the first 10 years, while more than 40% of cases were from southern China in the latter 10 years. In endemic areas, *P. vivax* was the predominant malaria parasite species and was widely distributed, and the transmission of *P. falciparum* was successfully blocked in central China in 1995 and has been confined to Yunnan and Hainan Provinces since 1995 (Expert Advisory Committee on Parasitic Diseases 1996, 1997). By 1999, a total of 1321 counties and cities with an incidence rate less than 1 per 10 000 individually, had been confirmed to meet the standard of “effective malaria elimination” (Expert Advisory Committee on Malaria 2000). In addition, malaria deaths dramatically decreased, with less than 70 deaths reported annually.

1.3.4 Phase of Consolidating Control Achievements (2000–2009)

Malaria transmission was unstable, with an incidence between 0.11 per 10,000 and 0.49 per 10,000 in this phase (Expert Advisory Committee on Malaria, 2001; Sheng et al. 2003; Zhou et al. 2005; Zhou et al. 2006a; Zhou et al. 2008, 2009; Zhou et al. 2006b, 2007; Zhou et al. 2011b). Particularly, a resurgence of vivax malaria occurred in Anhui, Henan, Hubei, and Jiangsu Provinces along the Huang-Huai River but was effectively controlled in 2008 through the control strategy of timely

diagnosis and standardized treatment with the strengthened mass antimalarial drug administration for risk groups, vector control, and health education. Furthermore, the direct reporting of any malaria case within 24 h after the finding was realized through the Chinese Information System for Disease Control and Prevention, which was established in 2004. However, there were a large number of suspected malaria cases nationwide. The transmission of *P. falciparum* was still confined to Yunnan and Hainan Provinces and has been interrupted in Hainan since 2010 (Zhou et al. 2011a; Zhou et al. 2011b). Even greater success was that a total of 1687 counties, cities, and districts had not reported 1 indigenous malaria case for at least 3 consecutive years by 2009 (Zhou et al. 2008, 2009, 2011b), and only four counties throughout the country were at an incidence rate of more than 10/10,000. Additionally, less than 100 deaths due to malaria were reported annually.

1.3.5 Malaria Elimination Phase (2010–2020)

The Chinese government initiated the National Malaria Elimination Programme (NMEP) in 2010 with the issue of the “Action Plan for Malaria Elimination in China (2010–2020)” (MOH 2010), and counties in China were stratified into four types (Type I–IV) based on the malaria epidemic reports of 2006–2008, and specific strategies were implemented in each type stratum for better resource allocation (Yin et al. 2013). In 2011, malaria surveillance information management was greatly improved by the establishment of the “National Information Management System for Parasitic Disease Control and Prevention” (Feng et al. 2014). Moreover, a strategy focusing on the “1-3-7” approach in surveillance and response based on the nature of malaria transmission and the biological characteristics of malaria parasites was put forward and implemented successfully between 2013 and 2020 (Cao et al. 2014). In addition, the national malaria diagnosis reference laboratory network has been under establishment since 2011 and has historically covered malaria-endemic provinces by 2016, mainly responsible for the quality control and assurance, training, and maintenance of laboratory competency in malaria parasitological testing (Yin et al. 2022a; Yin et al. 2015). As a result, indigenous cases significantly declined from 1308 in 2011 to 36 in 2015, and the last case was reported from Yunnan Province in April 2016 (Huang et al. 2022), although thousands of imported cases still occur annually and are extensively distributed in every province and each month (Zhang et al. 2019b). Such achievements were inseparable from the high-quality implementation of the “1-3-7” approach, with a full percentage of malaria cases reported within 24 h, 94.5% of them investigated within three days after case reporting, and 93.4% of foci disposed within a week after case reporting (Huang et al. 2022). In addition, each historically malaria-endemic province successfully passed the subnational verification of malaria elimination.

1.4 Conclusions and Perspectives

Malaria has a long history in China and was widely distributed in most parts of the country. Four types of local malaria parasites have been recorded, among which *P. vivax* and *P. falciparum* were the main parasites that seriously threaten people's health. From ancient times to the present, the Chinese nation has made important contributions to the fight against malaria, especially traditional Chinese medicine represented by artemisinin. In addition, after the founding of the People's Republic of China, with nearly 70 years of tremendous investments and intensive interventions, no indigenous malaria cases have been reported since 2017, and China officially achieved the elimination of malaria on June 30, 2021 (Feng et al. 2021; Zhou 2021), contributing to the global eradication of malaria. However, thousands of imported cases were reported annually and were extensively distributed in China, particularly in historically malaria-endemic areas; thus, China will likely see a resurgence in malaria cases if there is persistent importation of malaria cases under the condition that the distribution of the malaria vector *Anopheles* mosquitoes in the defined areas. Therefore, there are still some technical and managerial challenges in the post elimination of malaria in China.

1.4.1 High Burden of Imported Cases, Including Border Malaria

Before the COVID-19 pandemic, approximately 3000 cases annually were reported mainly from Africa and Southeast Asia (Huang et al. 2022), with *P. falciparum* being the most prevalent, followed by *P. vivax*, and the proportion of *P. ovale* has been on the rise for several years and was widely distributed across China throughout the year, particularly in historically malaria-endemic provinces (Zhang et al. 2019b). Moreover, China is severely suffered from border malaria, especially in counties on the China–Myanmar border (Huang et al. 2021a; Huang et al. 2021b; Xu et al. 2021). In addition, malaria infection caused by the bite of positive *Anopheles* mosquitoes after crossing the border has been found at a Chinese construction site on the China–Myanmar border (Yin et al. 2022b).

1.4.2 Undetermined Sources of Malaria Infection

Asymptomatic malaria infections are easily missed by traditional diagnostics in all intensities of malaria transmission, but they contribute far more to the malaria reservoir than previously thought, resulting in the continuous spread of malaria, and symptomatic cases are just the tip of the iceberg of malaria transmission (Cheaveau et al. 2019). Meanwhile, all *Plasmodium* species have asymptomatic infections (Roucher et al. 2014; Tadesse et al. 2017), and asymptomatic infections of *P. falciparum* and *P. vivax* have been reported in some Chinese border counties on the China–Myanmar border (Huang et al. 2017), but no data have been reported in other areas. In addition, the gene deletion of *P. falciparum* histidine-rich protein

(HRP) 2/3 making the RDT detection reagent based on HRP2 unable to detect *P. falciparum* very well has been reported in an increasing number of countries around the world, especially African countries (WHO 2021a), but Africa is the main source of imported cases in China.

1.4.3 Maintenance of Human Resources for Prevention of Malaria Re-Establishment

As a disease is eliminated, there may be less attention to it and fewer resources. However, there is a high risk of malaria re-establishment in China if imported malaria cases cannot be found under the condition that the distribution of the malaria vector *Anopheles* mosquitoes in the defined areas, and the introduced cases have been reported in China and abroad (Sun et al. 2017; Wang et al. 2015; Zhang et al. 2019a). In response to the prevention of malaria re-establishment, human resources for timely detection and appropriate treatment of imported cases, investigation and assessment of transmission risk caused by imported cases, and timely handling of foci or susceptible populations with a re-established transmission risk should be maintained and strengthened (Nasir et al. 2020; Yin et al. 2022b).

In summary, it is essential to maintain and strengthen the sensitivity of surveillance and response to imported malaria through capacity building of malaria diagnosis and treatment, case investigation, laboratory confirmation, epidemiological investigation, and foci disposal, as well as the research and development of new technologies, based on the established and improved multisectoral cooperative mechanism under the unified leadership of the government, thereby effectively consolidating the achievements of malaria elimination in China.

References

- Cao J, Sturrock HJ, Cotter C, Zhou S, Zhou H, Liu Y, Tang L, Gosling RD, Feachem RG, Gao Q (2014) Communicating and monitoring surveillance and response activities for malaria elimination: China's "1-3-7" strategy. *PLoS Med* 11:e1001642
- Cheaveau J, Mogollon DC, Mohon MAN, Golassa L, Yewhalaw D, Pillai DR (2019) Asymptomatic malaria in the clinical and public health context. *Expert Rev Anti-Infect Ther* 17:997–1010
- Chen C (2014) Development of antimalarial drugs and their application in China: a historical review. *Infect Dis Poverty* 3:9
- Cox FE (2010) History of the discovery of the malaria parasites and their vectors. *Parasit Vectors* 3:5
- Cunha CB, Cunha BA (2008) Brief history of the clinical diagnosis of malaria: from Hippocrates to Osler. *J Vector Borne Dis* 45:194–199
- Expert Advisory Committee on Malaria, MoH (1993) [Malaria situation in the People's Republic of China in 1992]. *Zhongguo Ji Sheng Chong Xue Yu Ji Sheng Chong Bing Za Zhi* 11:161–164
- Expert Advisory Committee on Malaria, MoH (1994) [Malaria situation in the People's Republic of China in 1993]. *Zhongguo Ji Sheng Chong Xue Yu Ji Sheng Chong Bing Za Zhi* 12:161–164
- Expert Advisory Committee on Malaria, MoH (1995) [Malaria situation in the People's Republic of China in 1994]. *Zhongguo Ji Sheng Chong Xue Yu Ji Sheng Chong Bing Za Zhi* 13:161–164

- Expert Advisory Committee on Malaria, MoH (2000) [Malaria situation in the People's Republic of China in 1999]. *Zhongguo Ji Sheng Chong Xue Yu Ji Sheng Chong Bing Za Zhi* 18:129–131
- Expert Advisory Committee on Malaria, MoH (2001) Malaria situation in the People's Republic of China in 2000. *Zhongguo Ji Sheng Chong Xue Yu Ji Sheng Chong Bing Za Zhi* 19:257–259
- Expert Advisory Committee on Parasitic Diseases, MoH (1988) [Malaria situation in China, 1987]. *Zhongguo Ji Sheng Chong Xue Yu Ji Sheng Chong Bing Za Zhi* 6:241–244
- Expert Advisory Committee on Parasitic Diseases, MoH (1989) [Malaria situation in China, 1988]. *Zhongguo Ji Sheng Chong Xue Yu Ji Sheng Chong Bing Za Zhi* 7:241–244
- Expert Advisory Committee on Parasitic Diseases, MoH (1991) [Malaria situation in the People's Republic of China in 1990]. *Zhongguo Ji Sheng Chong Xue Yu Ji Sheng Chong Bing Za Zhi* 9:250–253
- Expert Advisory Committee on Parasitic Diseases, MoH (1992) [Malaria situation in the People's Republic of China in 1991]. *Zhongguo Ji Sheng Chong Xue Yu Ji Sheng Chong Bing Za Zhi* 10:161–165
- Expert Advisory Committee on Parasitic Diseases, MoH (1996) [Malaria situation in the People's Republic of China in 1995]. *Zhongguo Ji Sheng Chong Xue Yu Ji Sheng Chong Bing Za Zhi* 14:169–172
- Expert Advisory Committee on Parasitic Diseases, MoH (1997) [Malaria situation in the People's Republic of China in 1996]. *Zhongguo Ji Sheng Chong Xue Yu Ji Sheng Chong Bing Za Zhi* 15:129–132
- Feng J, Zhang L, Xia ZG, Zhou SS, Xiao N (2021) Malaria-free certification in China: achievements and lessons learned from the National Malaria Elimination Programme. *Zoonoses* 1. <https://doi.org/10.15212/ZOONOSES-2021-1002>
- Feng XY, Xia ZG, Vong S, Yang WZ, Zhou SS (2014) Surveillance and response to drive the national malaria elimination program. *Adv Parasitol* 86:81–108
- Ge H (300–400 A.D.) [A handbook of prescriptions for emergencies]
- Guang SM (2012) Comprehensive mirror for aid in government. China Pictorial Publishing House, Beijing
- Hempelmann E, Krafts K (2013) Bad air, amulets and mosquitoes: 2,000 years of changing perspectives on malaria. *Malar J* 12:232
- Huang F, Feng XY, Zhou SS, Tang LH, Xia ZG (2022) Establishing and applying an adaptive strategy and approach to eliminating malaria: practice and lessons learnt from China from 2011 to 2020. *Emerg Microbes Infect* 11:314–325
- Huang F, Li SG, Tian P, Guo XR, Xia ZG, Zhou SS, Zhou HN, Zhou XN (2021a) A retrospective analysis of malaria epidemiological characteristics in Yingjiang County on the China-Myanmar border. *Sci Rep* 11:14129
- Huang F, Takala-Harrison S, Liu H, Xu JW, Yang HL, Adams M, Shrestha B, Mbambo G, Rybock D, Zhou SS et al (2017) Prevalence of clinical and subclinical *Plasmodium falciparum* and *Plasmodium vivax* malaria in two remote rural communities on the Myanmar-China border. *Am J Trop Med Hyg* 97:1524–1531
- Huang F, Zhang L, Tu H, Cui YW, Zhou SS, Xia ZG, Zhou HN (2021b) Epidemiologic analysis of efforts to achieve and sustain malaria elimination along the China-Myanmar border. *Emerg Infect Dis* 27:2869–2873
- Litsios S (2020) The World Health Organization's changing goals and expectations concerning malaria, 1948–2019. *Hist Cienc Saude Manguinhos* 27:145–164
- Malaria Commission, C.o.M.S. (1984) [Malaria control and morbidity in China in 1982]. *Ji Sheng Chong Xue Yu Ji Sheng Chong Bing Za Zhi* 2:1–2
- Malaria Commission, C.o.M.S. (1985) [The malaria situation in 1984 in the People's Republic of China]. *Ji Sheng Chong Xue Yu Ji Sheng Chong Bing Za Zhi* 3:241–243
- Malaria Commission, C.o.M.S. (1986) [The malaria situation in China, 1985]. *Ji Sheng Chong Xue Yu Ji Sheng Chong Bing Za Zhi* 4:241–243
- Malaria Commission, C.o.M.S. (1987) [Malaria situation in China, 1986]. *Zhongguo Ji Sheng Chong Xue Yu Ji Sheng Chong Bing Za Zhi* 5:241–243

- MOH (1956) [Malaria control programme]
- MOH (1983) [Malaria control programme in China, 1983–1985]
- MOH (1984) [Malaria control management regulation]
- MOH (1986) [Malaria control programme in China, 1986–1990]
- MOH (1990) [Malaria control programme in China, 1991–1995]
- MOH (1996) [Malaria control programme in China, 1996–2000]
- MOH (2010) [Action Plan of China Malaria Elimination (2010–2020)]
- Nasir SMI, Amarasekara S, Wickremasinghe R, Fernando D, Udagama P (2020) Prevention of re-establishment of malaria: historical perspective and future prospects. *Malar J* 19:452
- Office, HPLC (2013) *Annals of Hainan Province: Annals of Science and Technology*. Chapter 6: Medical and health technology. Section 3: Disease prevention and control
- Roucher C, Rogier C, Sokhna C, Tall A, Trape JF (2014) A 20-year longitudinal study of *Plasmodium ovale* and *Plasmodium malariae* prevalence and morbidity in a West African population. *PLoS One* 9:e87169
- Shang LY, Chen JS, Li DF, Li P, Su YP, Liu H (2007) Studies on distribution, ecological feature and malaria transmission effect of *Anopheles anthropophagus* in Henan province, China. *J Pathog Biol* 2:304–306
- Shen K, Su S (960-1127 AD) [Su Shen Liang Fang]
- Sheng HF, Zhou SS, Gu ZC, Zheng X (2003) [Malaria situation in the People's Republic of China in 2002]. *Zhongguo Ji Sheng Chong Xue Yu Ji Sheng Chong Bing Za Zhi* 21:193–196
- Sun YW, Yu DM, Chen J, Li X, Wang B, Wang ZJ, Mao LL, Yao WQ (2017) Two individual incidences of vivax malaria in Dandong municipality of Liaoning province. *Chin J Public Health* 33:314–316
- Tadesse FG, van den Hoogen L, Lanke K, Schildkraut J, Tetteh K, Aseffa A, Mamo H, Sauerwein R, Felger I, Drakeley C et al (2017) The shape of the iceberg: quantification of submicroscopic *Plasmodium falciparum* and *Plasmodium vivax* parasitaemia and gametocytaemia in five low endemic settings in Ethiopia. *Malar J* 16:99
- Talapko J, Skrlec I, Alebic T, Jukic M, Vcev A (2019) Malaria: the past and the present. *Microorganisms* 7:179
- Tang LH, Xu LQ, Chen YD (2012) *Parasitic disease control and research in China*. Beijing Science & Technology Press, Beijing
- Tu Y (2011) The discovery of artemisinin (qinghaosu) and gifts from Chinese medicine. *Nat Med* 17:1217–1220
- Tu Y (2016) Artemisinin-A gift from traditional Chinese medicine to the world (nobel lecture). *Angew Chem* 55:10210–10226
- Wang D, Li S, Cheng Z, Xiao N, Cotter C, Hwang J, Li X, Yin S, Wang J, Bai L et al (2015) Transmission risk from imported *Plasmodium vivax* malaria in the China-Myanmar border region. *Emerg Infect Dis* 21:1861–1864
- Wei Z (629) [Sui Chronicle]
- WHO (2021a) Statement by the Malaria Policy Advisory Group on the urgent need to address the high prevalence of pfrp2/3 gene deletions in the Horn of Africa and beyond
- WHO (2021b) World Malaria Day: WHO launches effort to stamp out malaria in 25 more countries by 2025
- WHO (2021c) World Malaria Report 2021. World Health Organization, Geneva
- WHO (2021d) Zeroing in on malaria elimination: final report of the E-2020 initiative. World Health Organization, Geneva
- Xu JW, Lin ZR, Zhou YW, Lee R, Shen HM, Sun XD, Chen QY, Duan KX, Tian P, Ding CL et al (2021) Intensive surveillance, rapid response and border collaboration for malaria elimination: China Yunnan's "3 + 1" strategy. *Malar J* 20:396
- Yin J, Li M, Yan H, Zhou S, Xia Z (2022a) Laboratory diagnosis for malaria in the elimination phase in China: efforts and challenges, vol 16. *Front Med*, p 10
- Yin J, Yan H, Li M (2022b) Prompt and precise identification of various sources of infection in response to the prevention of malaria re-establishment in China. *Infect Dis Poverty* 11:45

- Yin JH, Yan H, Huang F, Li M, Xiao HH, Zhou SS, Xia ZG (2015) Establishing a China malaria diagnosis reference laboratory network for malaria elimination. *Malar J* 14:40
- Yin JH, Yang MN, Zhou SS, Wang Y, Feng J, Xia ZG (2013) Changing malaria transmission and implications in China towards National Malaria Elimination Programme between 2010 and 2012. *PLoS One* 8:e74228
- Yin JH, Zhou SS, Xia ZG, Wang RB, Qian YJ, Yang WZ, Zhou XN (2014) Historical patterns of malaria transmission in China. *Adv Parasitol* 86:1–19
- Zhang L, Feng J, Zhang SS, Xia ZG, Zhou SS (2019a) Epidemiological characteristics of malaria and the progress towards its elimination in China in 2018. *Chin J Parasit Parasitic Dis* 37:241–247
- Zhang SS, Feng J, Zhang L, Ren X, Geoffroy E, Manguin S, Frutos R, Zhou SS (2019b) Imported malaria cases in former endemic and non-malaria endemic areas in China: are there differences in case profile and time to response? *Infect Dis Poverty* 8:61
- Zhang Y, Xing DL, Zhao YQ (1901) [Yazhou Chronicle]
- Zhang YS (1841) [Daoguang Qiongzhou Prefecture Chronicle]
- Zhou SS, Tang LH, Sheng HF (2005) [Malaria situation in the People's Republic of China in 2003]. *Zhongguo Ji Sheng Chong Xue Yu Ji Sheng Chong Bing Za Zhi* 23:385–387
- Zhou SS, Tang LH, Sheng HF, Wang Y (2006a) [Malaria situation in the People's Republic of China in 2004]. *Zhongguo Ji Sheng Chong Xue Yu Ji Sheng Chong Bing Za Zhi* 24:1–3
- Zhou SS, Wang Y, Fang W, Tang LH (2008) [Malaria situation in the People's Republic of China in 2007]. *Zhongguo Ji Sheng Chong Xue Yu Ji Sheng Chong Bing Za Zhi* 26:401–403
- Zhou SS, Wang Y, Fang W, Tang LH (2009) [Malaria situation in the People's Republic of China in 2008]. *Zhongguo Ji Sheng Chong Xue Yu Ji Sheng Chong Bing Za Zhi* 27:457, 455–456
- Zhou SS, Wang Y, Li Y (2011a) [Malaria situation in the People's Republic of China in 2010]. *Zhongguo Ji Sheng Chong Xue Yu Ji Sheng Chong Bing Za Zhi* 29:401–403
- Zhou SS, Wang Y, Tang LH (2006b) [Malaria situation in the People's Republic of China in 2005]. *Zhongguo Ji Sheng Chong Xue Yu Ji Sheng Chong Bing Za Zhi* 24:401–403
- Zhou SS, Wang Y, Tang LH (2007) [Malaria situation in the People's Republic of China in 2006]. *Zhongguo Ji Sheng Chong Xue Yu Ji Sheng Chong Bing Za Zhi* 25:439–441
- Zhou SS, Wang Y, Xia ZG (2011b) [Malaria situation in the People's Republic of China in 2009]. *Zhongguo Ji Sheng Chong Xue Yu Ji Sheng Chong Bing Za Zhi* 29:1–3
- Zhou XN (2021) China declared malaria-free: a milestone in the world malaria eradication and Chinese public health. *Infect Dis Poverty* 10:98
- Zhou ZJ (1981) The malaria situation in the People's Republic of China. *Bull World Health Organ* 59:931–936
- Zhou ZJ (1991) Malaria control and research in China. People's Medical Publishing House, Beijing
- Zuo QM [Zuo Spring and Autumn Period]. <https://so.gushiwen.cn/mingjus/default.aspx?tstr=%e5%b7%a6%e4%bc%a0>



A Fact Sheet on Malaria: Global Status and Significant Species

2

Heinz Mehlhorn

Abstract

This paper considers the recent status of the spreading of malaria, the symptoms of disease and the chances and needs of control. Worldwide many countries have started projects, which target the elimination of malaria in order to protect their inhabitants and tourists. However, final elimination of malaria is far from being totally successful. This is due to the fact that infected persons may travel without symptoms in many countries and spread their infectious load. Furthermore poor countries cannot induce and steer elimination programs. Thus tourists and foreign workers are highly advised to protect themselves by use of repellents when entering endemic countries.

Keywords

Malaria · Endangered regions · Mosquitoes · Vectors · Protection diagnosis · Drugs · Treatment · Control measurements

2.1 Introduction

Earth and thus all organisms on earth are actually hit by a phase of increasing warming up, which endangers already life of plants, animals and humans. Thus, the world community of humans must start activities as soon as possible which target onto:

- Decrease or at least stop global warming at the recent level.
- Eradication of malaria or (at least) keeping it at low levels.

H. Mehlhorn (✉)

Department of Parasitology, Heinrich Heine University Düsseldorf, Düsseldorf, Germany

e-mail: mehlhorn@uni-duesseldorf.de

- Development of new efficacious drugs blocking the spread of the agents of diseases, since efficacy of existing ones is decreasing.

This chapter considers the recent worldwide status of malaria, presents its most important species infecting humans and points to some needed activities.

2.2 Life Cycle and Facts of Worldwide Malaria

1. *Name*: Malaria (Latin: bad air; French: paludisme; German: Wechselfieber = alternating fever).
2. *Geographic distribution*: The disease malaria infects actually humans living between 40° North and 30° South and is worldwide spreading due to global warming and due to tourism, business activities and local wars. Only a few regions in the tropics and subtropics are free from malaria (e.g. the Caribbean countries except for Haiti and Dominican Republic, North Africa, Singapore, and Polynesia). Thus, at least 40% of the world's population live in malaria-endangered regions. About 90% of all human malaria cases noted by WHO are located in regions of tropical Africa. There have been counted up to 280 million malaria cases per year leading to 450 000 death cases. Especially infected children (mostly below the age of 5 years) are highly endangered and die in high numbers. However, in Europe, North America and Australia there are only a few “imported” cases of malaria per year (e.g. Germany ~ 1000 cases per year).
3. *Vectors*: Infected females of species of the mosquito genus *Anopheles* (Figs. 2.1, 2.2) are the main vectors for humans. However, the parasites also may become transmitted by blood transfusions between humans.
4. *Malaria species infecting humans*: Today there are six species documented infecting humans clearly diagnosed, whilst probably several others occur in animals and thus might also infect humans (Figs. 2.2, 2.3, 2.4, and 2.5).
 - 4.1. *Plasmodium falciparum* (*Malaria tropica*): This species is mainly endemic in Africa, Southeast Asia, South and Central America. However, it occurs also in Haiti and in the Dominican Republic as well as infects people living on several islands of the Pacific regions.
 - 4.2. *Plasmodium knowlesi* (*Malaria quartana type*): This species occurs in countries in the East, e.g. Thailand, Borneo, Malaysian peninsula, Myanmar, Philippines, and is spreading from there.
 - 4.3. *Plasmodium malariae* (*Malaria quartana type*): This species is found practically worldwide in all countries into which it has been long endemic and is constantly “imported” by human travellers, business people, soldiers etc.
 - 4.4. *Plasmodium ovale* (*Malaria tertiana type*): This species is found throughout Africa and might be imported from there by tourists and business people to any country of the world.
 - 4.5. *Plasmodium vivax* (*Malaria tertiana type*): This species is spread amongst humans in Southeast Asia, India, Near East, South and Central America, Pacific Islands and East Africa and harms people in many rural regions.

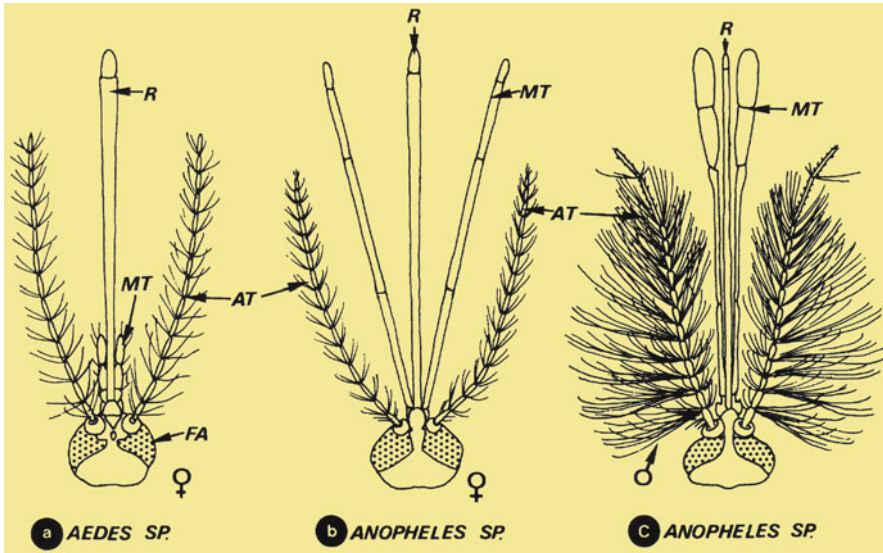


Fig. 2.1 Diagrammatic representation of the antennae of *Aedes* and *Anopheles* species. AT = antennae; FA = compound eyes; MT = maxillar palps; R = labium (sucking channel), Mehlhorn (2016a)



Fig. 2.2 (a) Macrophoto of a female mosquito of the species *Anopheles stephensi* sucking a sugar solution and (b) scanning electron micrograph of a female of the same species in flight position. Mehlhorn (2016a)

- 4.6. *Plasmodium simium* (*Monkey malaria*): This species was found in monkeys in Brazil and also occasionally in rather rare cases in humans. However, the spreading amongst humans might be more common if the number of tests becomes increased.
5. *Incubation periods*: All *Plasmodium* species, which are able to infect humans, are able to induce symptoms of disease and are characterized by different and

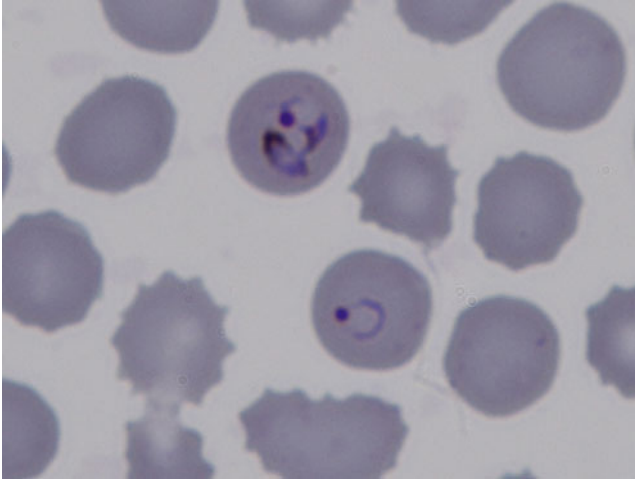


Fig. 2.3 Light micrograph of a smear preparation of erythrocytes containing *Plasmodium knowlesi* stages. The upper erythrocyte contains two dividing stages, the lower one just penetrated a so-called signet ring stage (courtesy of Prof. Dr. PorntipPetmitr, Mahidol University, Bangkok, Thailand)

occasionally varying *incubation periods*. The worldwide published data may vary, which is surely based on several conditions (fitness of the person infected, the amount of injected agents of disease and the age of the person). The published literature mostly reports the following data for common incubation periods:

– <i>Plasmodium falciparum</i>	6–15 days
– <i>Plasmodium knowlesi</i>	10–14 days
– <i>Plasmodium malariae</i>	18–40 days
– <i>Plasmodium ovale</i>	10–18 days (up to months)
– <i>Plasmodium vivax</i>	9–18 days (up to months)
– <i>Plasmodium simium</i>	Their data are probably in the same range, however, there are rather few proven data, since the studied cases are rather low

6. Symptoms of Disease

In principle, the symptoms of disease due to the different human malaria infections are rather similar, but some of them occur more or less common (Tables 2.1, 2.2, and 2.3).

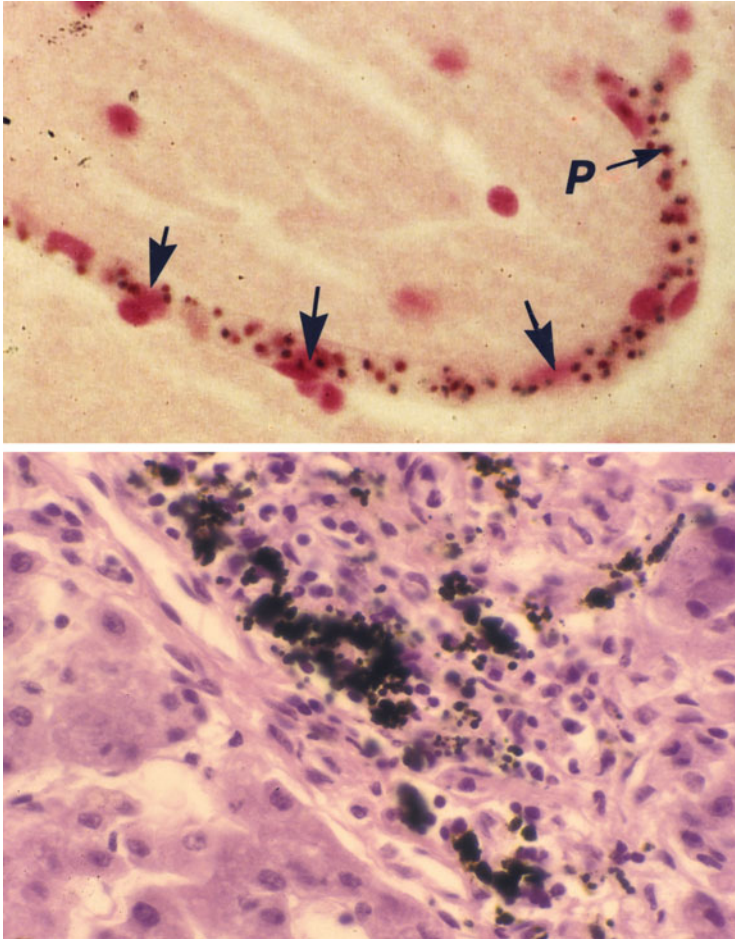


Fig. 2.4 Light micrograph of effects during human infections with *Plasmodium* species; *above*: infested erythrocytes blocking blood vessels (capillary: arrows, P = single parasite); *below*: pigment (derived from destroyed red blood cells) blocking tiny blood vessels. Mehlhorn (2016a)

7. *Diagnosis*: In case patients suffering from *considerable alternating fever* are consulting a physician, it is strongly recommended that he/she asks where the patient had been during the last 3 weeks. In case the patient was in an endemic malaria region the following tests should be performed:

A. Rapid diagnostic test (RDT) testing for *Plasmodium falciparum*

If positive, therapy has to be initiated immediately. If the test results are negative, interpretations are possible as follows:

1. Malaria tropica due to *P. falciparum* is not present, but infections due to other *Plasmodium* species are possible.

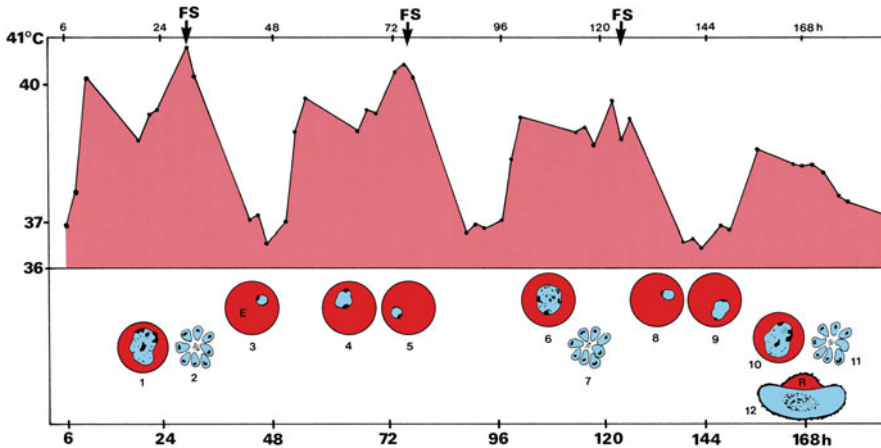


Fig. 2.5 Diagrammatic representation of the fever curve and development of the blood stages of: *Plasmodium falciparum* in an infected human person during four consecutive phases. C Celsius grades of fever; FS high fever phase; h hours. Mehlhorn (2016a)

2. Thus, *direct blood test* should be done using either the *thick droplet method* or the *thin blood smear technique*. Both will show the presence of agents of disease.
3. In any case these tests should be made by experienced persons, since in case of an infection treatment has to be initiated immediately.
8. **Therapy:** Therapy should be done only after a confirmed positive diagnosis by a physician. In order to perform a correct therapy, it is recommended to carry antimalarial drugs along when travelling in endemic malaria regions. If possible, treatment should be carried out exclusively by a physician:

For *uncomplicated malaria* recommended drugs are:

- 20 mg artemether and 120 mg lumefantrine (prescription by a physician).
- Atovaquone/proguanil, dosages depending on the body weight.

For *complicated malaria and in case of pregnancy*: In these cases, a physician has to decide the type of drug and doses to avoid harmful side effects due to the drugs. Relevant further literature for treatment schemes are published in Meyer (2021) and Mehlhorn (2016a, 2016b). In any case, it is recommended to get into contact with a physician, who will prescribe the best version of products needed in malaria regions (Tables 2.4, 2.5, 2.6, 2.7, 2.8, 2.9, and 2.10).

Table 2.1 Symptoms of malaria caused by the different *Plasmodium* species

Species	Fever periods	Anaemia	Brain damages	Incubation period	Spreading of disease
<i>Plasmodium falciparum</i>	20–48 h, depending on the fitness of the infected person	Often high-graded	High-graded, often lethal	8–24 days	Africa, South Asia, Central America, Pacific Islands
<i>Plasmodium knowlesi</i>	Highly variable	Medium grade, depending on age and personal fitness	Medium to low	12–14 days	Southeast Asia, Philippines
<i>Plasmodium malariae</i>	Mostly repeated every 72 h	Medium grade, depending on age and personal fitness	Medium to low	~6 weeks	Africa
<i>Plasmodium ovale</i>	Often varying, up to 48 h	Rare, low-graded	Medium to low	10–17 days	Africa, South Asia
<i>Plasmodium vivax</i>	Strongly varying, up to 48 h	Medium grade, depending on age and personal fitness	Medium to low	9–18 days	South Asia, India, Near East, Central America, East Africa, Pacific Islands
<i>Plasmodium simium</i>	Not determined yet due to lack of sufficient data, it is claimed that this species is a variant of <i>P. vivax</i>	Rare cases observed, no reliable results available	Unknown due to too few data	Variable, few data	Brazil

Table 2.2 Further symptoms of malaria by the different *Plasmodium* species

Species	Prodromal symptoms	Initial paroxysm	Duration of untreated disease	Duration of persistence of parasites in an untreated disease
<i>Plasmodium falciparum</i>	Influenza type	Severe, for 16–36 h	2–3 weeks	6–8 months
<i>Plasmodium knowlesi</i>	Influenza type	Light reaction	?	?
<i>Plasmodium malariae</i>	Influenza type	Light to severe for 10–12 h	3–24 weeks	Up to 30 years
<i>Plasmodium ovale</i>	Influenza type	Light for 10 h	3–8 weeks	Up to 2 years
<i>Plasmodium vivax</i>	Influenza type	Light to severe for 10 h	5–7 years	5–7 years
<i>Plasmodium simium</i>	Influenza type	Not reported	?	?

Table 2.3 Special naming of common malaria types due to repeated fever shivers

Species	Malaria type
<i>Plasmodium vivax</i>	Malaria tertiana
<i>Plasmodium ovale</i>	Malaria tertiana
<i>Plasmodium malariae</i>	Malaria quartana
<i>Plasmodium falciparum</i>	Malaria tropica
<i>Plasmodium knowlesi</i>	Malaria tertiana

Table 2.4 *Plasmodium* species parasitizing humans

Species	Region of distribution	Incubation period (days)	Repeated fever phases	Prepatent period
<i>Plasmodium brasilianum</i>	Brazil and spots in other South American regions	~10	Varying	?
<i>Plasmodium cynomolgi</i>	Asia	~10	Varying	?
<i>Plasmodium falciparum</i>	Africa	7–11	Varying, every 36–48 h	5 days
<i>Plasmodium knowlesi</i>	Asia: Thailand, Malaysia, Philippines, Myanmar and neighbouring regions	10–14	Varying	?
<i>Plasmodium malariae</i>	Worldwide in all malaria regions	10–14	Every 72 h	13–17 days
<i>Plasmodium ovale</i>	Africa, Southwest Asia	10–18	Varying	8 days
<i>Plasmodium simium</i>	Brazil	~10	Varying	?
<i>Plasmodium vivax</i>	Africa, India, Near East, South and Central America, Pacific Islands	10–18	Varying, up to 48 h	8 days

Table 2.5 Comparison of the developmental cycles of the most important *Plasmodium* species parasitizing humans

Species	Prepatent period = interval between infection and the first ability to detect the parasite	Mean of beginning of erythrocytic schizogony	Duration of erythrocytic schizogony	First appearance of gamonts in blood
<i>P. vivax</i>	8 d	13–17 d	48 j	11–13 d
<i>P. ovale</i>	8 d	13–17 d	48 h	20–22 d
<i>P. falciparum</i>	5 d	8–12 d	36–48 h	17–22 d
<i>P. malariae</i>	13–17 d	28–37 d	72 h	24–31 d

d days, *h* hours

Table 2.6 Characteristics of the asexual blood stages of common *Plasmodium* species of humans

Species	Parasite stages in peripheral blood	Size of trophozoites	Number of schizont nuclei	Pigment	Changes in host cells
<i>P. vivax</i>	All	2/3 RBC	12–24	Yellow brownish	Strongly enlarged with Schüffner's dots
<i>P. ovale</i>	All	2/3 RBC	6–12	Light brown	Slightly enlarged, scraggy, surface, Schüffner's dots
<i>P. falciparum</i>	Mostly signet ring stages (trophozoites), gamonts	1/5 RBC	8–24	Scattered: light brown; as lumps dark brown	Mostly none, occasionally Maurer's dots
<i>P. malariae</i>	All	2/5 RBC	6–12 (8 often arranged like a rosette)	Dark brown	None most of the time

RBC red blood cell

Table 2.7 *Plasmodium* species and their induced diseases

Species	Anaemia	Brain problems	Nephritic problems	Recidives	Blackwater fever
<i>Plasmodium brasilianum</i>	+	?	?	?	?
<i>Plasmodium cynomolgi</i>	+/?	?	?	?	?
<i>Plasmodium falciparum</i>	++++	++++	+	-	++++
<i>Plasmodium knowlesi</i>	++	?	+	-	?
<i>Plasmodium malariae</i>	++	++	+++	-	+
<i>Plasmodium ovale</i>	+/?	-/+	-	+	+
<i>Plasmodium simium</i>	+/?	?	?	?	?
<i>Plasmodium vivax</i>	++	-/+	-/+	+	+

Table 2.8 Characteristics of sexual blood stages of *Plasmodium* species of humans (Giemsa-stained)

Species	Shape	Microgamont	Macrogamont
<i>P. vivax</i>	Spherical/ ovoid	10 μ m, nucleus red, cytoplasm pale blue/pink; pigment fine-grained	11 μ m; nucleus small, dark red; cytoplasm blue, plenty of pigment
<i>P. ovale</i>	Spherical/ ovoid	9 μ m, similar to <i>P. vivax</i>	9 μ m, similar to <i>P. vivax</i>
<i>P. falciparum</i>	Sicle- or banana-shaped	9–11 μ m, nucleus big and diffuse; cytoplasm pink; pigment diffusely dispersed	12–14 μ m; central nucleus, red; cytoplasm blue to purple; pigment concentrated around the nucleus
<i>P. malariae</i>	Spherical/ ovoid	7 μ m, like <i>P. vivax</i>	7 μ m, like <i>P. vivax</i>

Table 2.9 Comparison of the clinical symptoms of the different human malaria types

Criteria	<i>P. falciparum</i>	<i>P. vivax</i>	<i>P. ovale</i>	<i>P. malariae</i>
Average incubation period	8–24 days	9–18 days	10–17 days	18–40 days
Prodromal symptoms	Influenza-like	Influenza-like	Influenza-like	Influenza-like
Fever	Daily, recurrent or continuing	Sporadic to daily	Sporadic to daily	Periodically every 72 h
Periodicity of established fever attack	No fever; permanent fever or every 36–48 h	48 h	48 h	72 h
Initial paroxysm	Severe, for 16–36 h	Slight to severe, for 10 h	Slight for 10 h	Slight to severe, for 11 h
Duration of untreated disease	2–3 weeks	3–8 weeks or even longer	2–3 weeks	3–24 weeks
Duration of persistence of parasites in an untreated disease	6–8 months	5–7 years	Up to 2 years	30 years or more
Anaemia	++++	++	+	++
CNS syndrome	++++	+/-	+/-	+/-
Kidney syndrome	+++	+/-	-	+++
Blackwater fever	++++	+	+	+

+ = present, frequency; - = absent

Table 2.10 Malaria prophylaxis (according to the German Society of Tropical Medicine and International Health)

Product	Prophylaxis start	Prophylaxis end	Others
Atovaquone/ Proguanil (Malarone®)	1–2 days before entry into malaria region	7 days after leaving malaria region	Some restrictions
Chloroquine (Resochin®, Weimerquin®, Quensyl®)	With entry of malaria regions without chloroquine resistance	6 weeks after leaving malaria region	Prophylactic dose: 300 mg base per week
Chloroquine plus Proguanil (Paludrine®)	See Proguanil	See Proguanil	
Doxycyclin			In Germany not approved for prophylaxis
Mefloquine (Lariam®)	2 weeks before start of travel to regions without mefloquine resistance	2–3 weeks after return	Caution: mental side effects are possible

Suggested Readings

- Ahmed MA, Cox-Singh J (2015) *Plasmodium knowlesi*—an emerging pathogen. ISBT Sci Ser 10: 134–140
- de Alvarenga DAM, Culleton R, de Pina-Costa A, Rodrigues DF, Bianco C Jr, Silva S, Nunes AJD, de Souza JC Jr, Hirano ZMB, Moreira SB, Pissinatti A, de Abreu FVS, Lisboa Areas AL, Lourenço-de-Oliveira R, Zalis MG, Ferreira-da-Cruz MF, Brasil P, Daniel-Ribeiro CT, de Brito CFA (2018) An assay for the identification of *Plasmodium simium* infection for diagnosis of zoonotic malaria in the Brazilian Atlantic Forest. Sci Rep 8(1):86
- Brasil P, Zalis MG, de Pina-Costa A, Siqueira AM, Júnior CB, Silva S, Areas ALL, Pelajo-Machado M, de Alvarenga DAM, da Silva Santelli ACF, Albuquerque HG, Cravo P, Santos de Abreu FV, Peterka CL, Zanini GM, Suárez Mutis MC, Pissinatti A, Lourenço-de-Oliveira R, de Brito CFA, de Fátima Ferreira-da-Cruz M, Culleton R, Daniel-Ribeiro CT (2017) Outbreak of human malaria caused by *Plasmodium simium* in the Atlantic Forest in Rio de Janeiro: a molecular epidemiological investigation. Lancet Glob Health 5(10):e1038–e1046
- Buery JC, Rodrigues PT, Natal L, Salla LC, Loss AC, Vicente CR, Rezende HR, Duarte AMRC, Fux B, Malafrente RDS, Falqueto A, Cerutti C Jr (2017) Mitochondrial genome of *Plasmodium vivax/simum* detected in an endemic region for malaria in the Atlantic Forest of Espírito Santo state, Brazil: do mosquitoes, simians and humans harbour the same parasite? Malar J 16(1):437
- Carrasquilla G, Barón C, Monsell EM, Cousin M, Walter V, Lefèvre G, Sander O, Fisher LM (2012) Randomized, prospective, three-arm study to confirm the auditory safety and efficacy of artemether-lumefantrine in Colombian patients with uncomplicated *Plasmodium falciparum* malaria. Am J Trop Med Hyg 86(1):75–83
- Cordel H, Cailhol J, Matheron S, Bloch M, Godineau N, Consigny PH, Gros H, Campa P, Bourée P, Fain O, Ralaimazava P, Bouchaud O (2013) Atovaquone-proguanil in the treatment of imported uncomplicated *Plasmodium falciparum* malaria: a prospective observational study of 553 cases. Malar J 12:399
- Costa DC, da Cunha VP, de Assis GM, de Souza Junior JC, Hirano ZM, de Arruda ME, Kano FS, Carvalho LH, de Brito CF (2014) *Plasmodium simium/Plasmodium vivax* infections in southern brown howler monkeys from the Atlantic Forest. Mem Inst Oswaldo Cruz 109(5):641–653
- Cox-Singh J, Davis TM, Lee KS, Shamsul SS, Matusop A, Ratnam S, Rahman HA, Conway DJ, Singh B (2008) *Plasmodium knowlesi* malaria in humans is widely distributed and potentially life threatening. Clin Infect Dis 46(2):165–171
- Führer HP, Noedo H (2014) Recent advances in detection of *Plasmodium ovale*. JCM 52:387–391
- German SocTropmed, travel medicine and global health (DTG): Guideline: diagnostics and therapy of malaria. AWMF online Register 042-001
- Guimares LO et al (2015) Merozoite surface protein-1 genetic diversity in *Plasmodium malariae* and *P. brasilianum*. BMC Infect Dis 15:529
- Hoffmann SL et al (2015) The march towards malaria vaccine. Am J Prev Med 49:S319–S333
- Kugasia IR et al (2014) Recrudescence of *Plasmodium malariae* after quinine. Case Rep Med 2014: 590265
- Lalremruata A, Magris M, Vivas-Martínez S, Koehler M, Esen M, Kempaiah P, Jeyaraj S, Perkins DJ, Mordmüller B, Metzger WG (2015) Natural infection of *Plasmodium brasilianum* in humans: man and monkey share quartan malaria parasites in the Venezuelan Amazon. EBioMedicine 2(9):1186–1192
- Longley RL et al (2015) Malaria vaccines: identifying *Plasmodium falciparum* liver stage targets. Front Microbiol. <https://doi.org/10.3389/fmicb.2015.00960>
- Luo Z et al (2015) The biology of *Plasmodium vivax* explored through genomics. Ann N Y Acad Sci 1342:53–62
- McNair CM (2015) Ectoparasites of medical and veterinary importance: drug resistance and the need for alternative control methods. J Pharm Pharmacol 67(3):351–363
- Mehlhorn H (2016a) Human parasites: diagnosis, treatment, prevention, 1st edn. Springer International Publishing, Cham

- Mehlhorn H (2016b) Encyclopedia of parasitology, 4th edn. Springer, Berlin, London, New York
- Meyer CG (2021) Tropenmedizin: Infektionskrankheiten, 4th edn. Ecomed Medizin, Landsberg
- Mourier T, de Alvarenga DAM, Kaushik A, de Pina-Costa A, Douvropoulou O, Guan Q, Guzmán-Vega FJ, Forrester S, de Abreu FVS, Júnior CB, de Souza Junior JC, Moreira SB, Hirano ZMB, Pissinatti A, Ferreira-da-Cruz MF, de Oliveira RL, Arold ST, Jeffares DC, Brasil P, de Brito CFA, Culleton R, Daniel-Ribeiro CT, Pain A (2021) The genome of the zoonotic malaria parasite *Plasmodium simium* reveals adaptations to host switching. *BMC Biol* 19(1):219
- Popovici Y, Ménard D (2015) Challenges in antimalarial drug treatment for vivax malaria control. *Trends Mol Med* 21(12):776–788
- Richter J et al (2010) What is the evidence for the existence of *Plasmodium ovale* hypnozoites. *Parasitol Res* 107:1285–1290
- Savargaoukar D et al (2014) *Plasmodium malariae* infection—a case of missed infection. *J Vector Borne Dis* 51:149–151
- Singh B, Daneshvar C (2013) Human infections and detection of *Plasmodium knowlesi*. *CMR* 26:165–184
- Spielmann T, Gilberger TW (2015) Critical steps in protein export of *Plasmodium falciparum* blood stages. *Trend Parasitol* 31:514–520
- WHO (2020) Global trends in the burden of malaria. WHO, Geneva
- Willadsen P (2006) Vaccination against ectoparasites. *Parasitology* 133(Suppl):S9–S25



Malaria-Free in China: A Story of More than 70 Years

3

Jun Feng

Abstract

Malaria has been one of the most important public health issues in China's history for approximately 4000 years. After more than 70 years of comprehensive control strategies and interventions, great achievements have been made in malaria control in China, the occurrence of indigenous malaria cases has been steeply reduced, and epidemic regions have been drastically shrunken. This great success in controlling malaria ensures people's health, reduces poverty due to illness, and promotes social and economic development. In 2017, China achieved the target of zero indigenous malaria cases for the first time and has been maintained for 5 consecutive years; thereafter, the World Health Organization certified malaria elimination in China on June 30, 2021. This paper systematically reviews the achievements, experience, and lessons gained from malaria elimination programs and the challenges in the post-elimination phase in China.

Keywords

Malaria · Control · Elimination · China · Challenge

3.1 Introduction

Today, the world still faces great challenges in fighting against malaria. In 2021, 84 countries reported a total of 241 million malaria cases worldwide, with an increase of 2 million cases over the previous year, while the number of malaria

J. Feng (✉)

Shanghai Municipal Center for Disease Control and Prevention, Shanghai, People's Republic of China

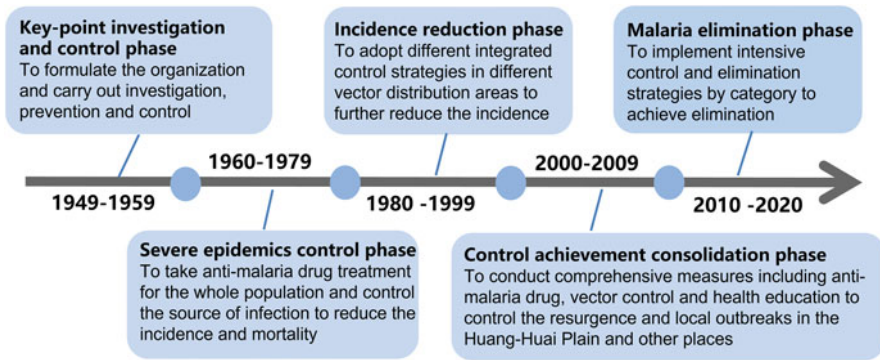
e-mail: fengjun@scdc.sh.cn

Table 3.1 Malaria cases and incidence in different phases of control and elimination in China

Phase	Year coverage	No. of cases	Incidence ^a (1/100,000)
Key-point investigation and control	1949–1959	31,782,036	555.85
Control of severe epidemics	1960–1969	68,842,698	977.86
	1970–1979	114,010,009	1323.68
Reducing incidence rate	1980–1989	12,092,153	120.62
	1990–1999	595,460	5.12
Consolidating the control achievements	2000–2009	352,229	2.87
Elimination phase	2010–2020	38,133	– ^b

^aThe incidence here refers to the average of each cover period

^bSince imported cases were predominant during the elimination phase, we cannot calculate the real incidence

**Fig. 3.1** The strategies and interventions adopted in the 5 phases of the national control and elimination program

deaths reached 619,000 (WHO 2022). Malaria is one of the most important public health issues and has greatly affected human health and economic and social developments in China's history for approximately 4000 years (Tang 1999). Prior to 1949, malaria was widely distributed, with at least 30 million cases reported each year and a mortality rate of approximately 1% (Qian and Tang 2000). After the foundation of the People's Republic of China, the government strived for malaria control and elimination. During the long combat with malaria history, the national malaria control and elimination program is primarily classified into five phases, including the key-point investigation and control phase (1949–1959), the severe epidemic control phase (1960–1979), the incidence reduction phase (1980–1999), the control achievement consolidation phase (2000–2009), and the elimination phase (2010–2020) (Feng et al. 2021c, 2021a) (Table 3.1). The strategies and interventions adopted in each phase are shown in Fig. 3.1. After the implementation of an integrated strategy for malaria control, as well as socioeconomic and environmental development, such as urbanization and alterations in the natural surroundings that

affected the transmission pattern, including changes in malaria vector distribution, the occurrence of indigenous malaria cases has been steeply reduced, and epidemic regions have been drastically shrunken (Feng et al. 2018b). Thus, in May 2010, the former Ministry of Health, together with 12 other ministries, issued the *National Malaria Elimination Action Plan (2010–2020)* (NMEAP), with the objective of eliminating indigenous malaria in nonborder regions before the end of 2015 and eliminating the disease nationwide before the end of 2020 (MOH 2010). The action plan has made great progress, and all 24 endemic provinces, including 258 endemic prefectures and 2158 endemic counties, have completed the malaria verification as scheduled. On June 30th, 2021, the World Health Organization (WHO) formally declared that China had been awarded a malaria-free certification (WHO 2021).

Therefore, in this review, we summarize the achievements and lessons learned from the Chinese national malaria elimination program and propose further efforts to mitigate the challenges that still exist during the elimination phase based on the analysis of malaria incidence patterns since 1950 and changes in case-based malaria reporting data since 2010. The outcomes are likely to demonstrate that malaria elimination is a country-led and country-owned endeavor that can probably help improve malaria surveillance systems in China but also in other elimination countries.

3.2 Achievements

During the 70 years of combatting malaria, various integrated strategies and interventions have been employed for malaria elimination under the principle of “government leadership, multisectoral cooperation and whole-society mobilization.”

3.2.1 The Burden of Malaria Morbidity and Mortality Has Fallen Sharply

Prior to 1949, nearly 30 million malaria cases were reported in China every year. As many as 1829 counties were identified as endemic for malaria in China in the early 1950s, accounting for more than 70% of the total number of counties in the country (Tang 1999). Two large-scale outbreaks occurred in China in the early 1960s and early 1970s, with the number of cases nationwide exceeding 24 million occurring in 1970. Among them, there were approximately 21.98 million malaria cases in the Huanghuai Plain. Since then, the number of cases has been declining, and by 2010, the number of reported malaria cases was reduced to 7855, which accounted for only 0.23% of the total number of reported infectious diseases (Zhou et al. 2011). The number of indigenous malaria cases dropped from 1308 in 2011 to 1 in 2016 (Xia et al. 2012; Zhang et al. 2017). In 2017, the country first reported no indigenous cases and remained at zero from 2018 to 2020, reaching the national malaria elimination standard set by the WHO (Feng et al. 2018a; Xiao et al. 2021; Zhang et al. 2018, 2019, 2020, 2021a) (Fig. 3.2). At the same time, the endemic provinces

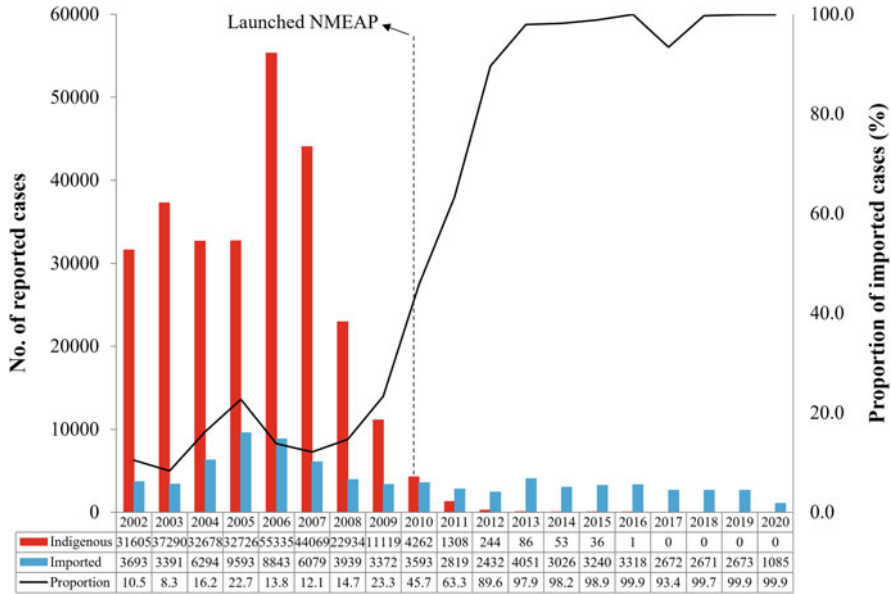


Fig. 3.2 Indigenous and imported cases and their proportions in China, 2002–2020

(municipals, autonomous regions) and counties continued to shrink. In 2011, a total of 155 counties in 13 provinces reported local cases, while in 2016, only 1 local *P. vivax* malaria was reported in Yingjiang County of Yunnan Province. The number of annual deaths suffering from malaria also fell from an average of 2653 per year in the 1950s to 41 per year in the 2000s and then dropped to 17 per year by the 2010s. After 2010, all deaths due to malaria in the country were imported cases (Zhang et al. 2021b).

3.2.2 The Goal of Malaria Elimination Nationwide Was Achieved as Scheduled

To ensure the quality of China’s malaria elimination activities, the former Ministry of Health issued the “Assessment Measures for Malaria Elimination (the 2013 and 2014 versions)” in 2013 and 2014, respectively. The former National Health and Family Planning Commission formulated the “Subnational Verification Implementation Plan for Malaria Elimination” in 2017. In 2019, the National Health Commission (NHC) issued the “Simplifying the Subnational Verification Procedures for Malaria Elimination.” China has implemented malaria elimination verification at the county level since 2013 and has conducted municipal-level malaria elimination verification that has completed all county-level assessments. By the end of 2019, all 2165 endemic counties and all 258 endemic cities had completed the malaria elimination verification in 24 endemic provinces across the whole country. By the

end of June 2020, the NHC organized and completed subnational malaria elimination verification in all 24 endemic provinces. In May 2021, the WHO external assessment panel group conducted an on-site assessment of malaria elimination, including an online assessment of two provinces of Liaoning and Sichuan and field evaluation provinces of Yunnan, Hainan, Anhui, and Hubei. On June 30, the WHO formally declared that China had been awarded a malaria-free certification (WHO 2021).

3.2.3 The “1-3-7” Approach Was Efficient Implemented

In 2011, to couple with the strategy transition from the control stage to the elimination stage, the Parasitic Diseases Information Reporting Management System (PDIRMS) was established to ensure that every case could timely diagnose and appropriately treat to prevent re-establishment. The “1-3-7” approach, referring to case reporting within 1 day, case investigation and reconfirmation within 3 days, foci investigation and disposal within 7 days, was adopted to guide the scientific elimination of malaria in all regions (Cao et al. 2014) (Fig. 3.3). From 2013 to 2020, all cases were reported within 1 day; the epidemiological case investigation rate within

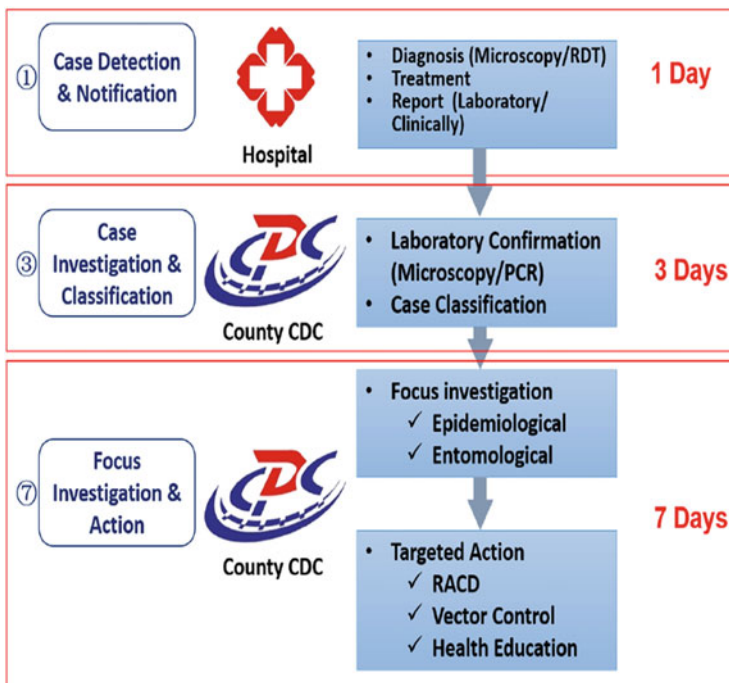


Fig. 3.3 The 1-3-7 approach implemented in China

3 days was 94.5%; and the foci investigation and disposal rate within 7 days was 93.3% (Zhang et al. 2014, 2015, 2016a, 2016b, 2017, 2018, 2019, 2020, 2021a).

3.2.4 Malaria Elimination Capacity Building Was Continuously Strengthened

Every year, technical training is carried out across the country, including malaria diagnosis and treatment in medical institutions, epidemiological and foci investigation, and disposal in CDCs. The training is organized through on-site technical guidance and skills competitions to promote or renew the skills of professional and technical personnel. China has successively established provincial reference laboratories for malaria diagnosis in 24 endemic provinces (Yin et al. 2015). To ensure the quality of malaria elimination activities, the NHC organized a malaria elimination technical expert group to review and analyze each reported case quarterly (2017) or semiannually (since 2018) to ensure that each case is indigenous or imported and that the evidence support is sufficient. The national expert group for severe malaria treatment will review each death case, explore the cause of death, and carry out targeted guidance and training to improve the diagnosis and treatment capabilities (Tu et al. 2019). In addition, the NHC holds an annual national parasitic disease control and prevention technology competition, in which the microscopic examination of malaria parasites is an important part of this competition. Through step-by-step selection, training, and competition, it has played a good role in promoting malaria diagnosis.

3.3 Experiences and Lessons

China has accumulated a wealth of valuable information and experience in the process from malaria control to elimination, especially in the context of building a community with a shared future for humanity and the “Belt and Road” initiative. These experiences are the resources for the historical treasure trove, which not only contributes to the global program in fighting against malaria but also transfers Chinese wisdom to the world.

3.3.1 Strong Government Leadership and Multisectoral Collaboration Are Prerequisites for Malaria Elimination

China's malaria control and prevention is under the unified leadership of governments at all levels, cooperation among health, customs, education, development and reform, and finance departments, and a four-level malaria control and prevention network at the national, provincial, municipal, and county levels undertaken by disease control and prevention institutions and medical institutions. The central government has promulgated and formulated policies, plans, and

technical standards for malaria elimination, with source control as the core and surveillance as the leading role to guide all regions to carry out malaria elimination scientifically. Governments at all levels have incorporated malaria elimination into their regional economic and social development plans and target management assessments, clarified the responsibilities and tasks of each department, strengthened organizational leadership, coordinated management, supervision and assessment, and ensured that work measures are in place. The State Council has established an interministerial joint meeting system for major diseases, including malaria, established leading groups for malaria elimination in 24 malaria-endemic provinces, and established corresponding coordination mechanisms in other regions. Beginning in 1973, a regional joint control and prevention mechanism was established—the five central provinces (Jiangsu, Anhui, Shandong, Hubei, and Henan) jointly prevent and control malaria (Xr 1995), and in 1992, the joint control and prevention mechanism among three southern provinces (Guangdong, Guangxi, and Hainan) was established. In 2017, the original 24 endemic provinces were divided into four joint control and prevention areas (NHC 2018). The regional joint control and prevention mechanism has further improved the timely tracking, data sharing, and experience sharing of mobile personnel information and promoted the process of interprovincial malaria elimination. In the process of malaria control and prevention, the government mobilized control and prevention professionals, scientific researchers from universities and institutes, rural doctors, and the general public to participate in mass prevention and treatment activities, such as large-scale populations taking medicine and insecticide-soaked mosquito nets. In addition, adequate financial support also reflects the strong political will of the central government to eliminate malaria. Since 2010, the central and provincial finance and the Global Fund have invested a total of 1.38 billion yuan as special funds to support malaria elimination. The effective use of various types of funds at all levels has further stabilized the malaria control and prevention team, improved the case surveillance system, standardized the detection, reporting, investigation, and verification of malaria cases and the disposal of epidemic sites, and promoted the knowledge and health education of malaria control and prevention. Continuous deepening has ensured the procurement and supply of antimalarial drugs and related antimalarial materials, laying a solid foundation for China to achieve the goal of eliminating malaria as scheduled.

3.3.2 Rapid and Sensitive Surveillance-Response Systems Are Key to Malaria Elimination

The malaria surveillance system in China has undergone several evolutions. From 1950 to 1985, case reports were mailed; from 1985 to 2003, cases were reported by telephone, computer, or other electronic means; in 2003, an online reporting system was established, and malaria, as one of the legal infectious diseases, began to report through the national infectious disease information. The system reports in real time, and 100% of China's disease control and prevention centers at all levels, 99% of

county-level and above medical and health institutions, and 99% of township health centers have achieved direct online reporting within 24 h. After the NMEAP was launched, the focus of surveillance was shifted to the timely detection of every source of infection and possible transmission spots to provide clues for timely removal of the source of infection and interruption of possible transmission. Therefore, the state launched the special reporting system in 2011 and guided the national malaria elimination work in accordance with the “1-3-7” approach. The “1-3-7” approach technically regulates the discovery, reporting, diagnosis, and treatment of cases, as well as the requirements for source control and epidemic spot disposal (Feng et al. 2016). At present, the “1-3-7” approach is working well and effectively in China, has been included in the WHO technical guidelines for malaria elimination and is being promoted and applied globally (Aung et al. 2020; Kheang et al. 2020; Lertpiriyasuwat et al. 2021; Wang et al. 2017; Wang et al. 2019b; Zhou et al. 2015). For the quality control of the surveillance-response system, the country has exchanged information on malaria epidemics, progress reports on malaria elimination, and featured work experience in a timely manner through weekly report analysis, monthly risk assessments, and quarterly video conferences to discuss and solve existing problems and promote elimination.

3.3.3 Effective Capacity Building Guarantees Malaria Elimination

For the malaria diagnosis and treatment capabilities of medical institutions and the case investigation, laboratory review and epidemiological investigation, and disposal capabilities of disease control institutions, training is organized on a level-by-level basis every year. By 2016, all endemic provinces had established a reference laboratory network. The malaria diagnostic reference laboratory network conducted microscopic examination and PCR for each reported case, providing a reliable basis for clinical treatment and implementation of control and prevention measures. With the establishment and operation of provincial reference laboratories, the proportion of laboratory-confirmed malaria cases has increased substantially (Fig. 3.4). The proportion of clinically diagnosed cases decreased from 22.43% (998/4450) in 2011 to 0.19% (5/2678) in 2019, and no clinically diagnosed cases were reported in 2020 (Xia et al. 2012; Zhang et al. 2020, 2021a). In addition, imported cases of *P. knowlesi* from Malaysia and Indonesia were also identified by PCR in 2014 and 2017 (Pan et al. 2016; Zhou et al. 2018). At the same time, the reference laboratory network regularly organizes external assessment classes for malaria microscopy capabilities organized by the WHO. Currently, each province has at least 1 microscopy expert certified by the WHO.

3.3.4 Technological Innovation Is Crucial to Malaria Elimination

In the process of controlling and eliminating malaria in our country, scientific and technological innovation is crucial. For more than 70 years, scientific research has

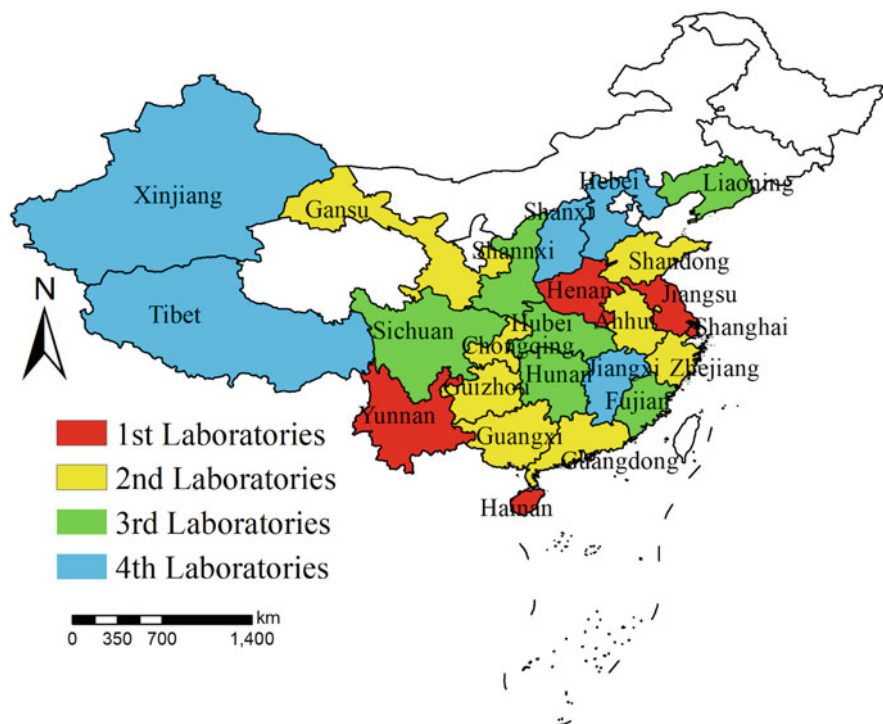


Fig. 3.4 Distribution and classification of the provincial malaria diagnosis reference laboratories

served prevention and treatment, and disease control and prevention institutions at all levels across the country have closely cooperated with universities and scientific research institutes to guide grassroots practice and provide a scientific basis and technical support. Scientific and field research focuses on control strategies and key technical areas, including pathogen biology, vector biology, diagnostics, antimalarial drugs, and control strategies. For example, to explore practical control and prevention strategies and effective and applicable measures, research has been carried out in a number of malaria control and prevention pilots across the country for many years. Problems have been found in the pilots, research programs, and application of new results to guide national malaria prevention work. From 1965 to 1966, research on the control and prevention of malaria in the Huanghuai Plain was carried out; from 1992 to 1994, research on the epidemiological characteristics of the areas where malaria was basically eliminated was conducted (Tang et al. 2012), which provided guidance and technical support for on-site control and prevention; a batch of new antimalarial drugs, such as artemisinin and its derivatives, pyronaphthylidine phosphate, and naphthoquine phosphate, developed by the “523 Research Project” saved tens of millions of malaria infections worldwide (Wang et al. 2019c). In addition, China has actively organized and carried out research on insecticide-impregnated mosquito nets and insecticide resistance and developed

long-term mosquito nets and other vector control products and technologies, which has improved the technical quality of malaria control and prevention (Pan et al. 2001). In the stage of malaria control and elimination in China, scientific research institutions at all levels have created many world-renowned scientific research results, and the timely transformation and application of these scientific research results can ensure the process of malaria control and elimination.

3.3.5 Active International Cooperation Drives Malaria Elimination

Since 2007, with the support of the former Ministry of Health, China has successively launched malaria control and prevention projects with Cambodia, Laos, Myanmar, and Vietnam, established and border malaria joint control and prevention mechanisms, and shared the information and experience of migrant population management. In addition, China has launched a malaria control cooperation project between African and Southeast Asian countries under the framework of the Belt and Road Initiative. For example, the China-UK-Tanzania malaria control and prevention pilot project has explored the “1,7-mRCTR” strategy to effectively reduce the disease burden based on the “1-3-7” approach (Wang et al. 2019a). This is one of the typical cases of applying the experience gained in the process of malaria control and elimination in China to the pilot area. From 2016 to 2019, a China-Australia-Papua New Guinea malaria control pilot project was carried out in Papua New Guinea. International cooperation on malaria has become an important part of China-Africa cooperation, the construction of the “Belt and Road Initiative,” and a priority area of public health cooperation. The survey on the training needs of foreign students on malaria control and prevention shows that the current country-aided malaria control and prevention training programs in Africa can basically meet the needs of foreign students. The design of an international training course on malaria control and prevention provided the basis (Huang et al. 2020; Wang et al. 2016). Through active and effective international cooperation, the goal of eliminating malaria will surely be achieved in other endemic countries and regions around the world.

3.4 Challenges

3.4.1 Maintenance of Non-transmission Status

Achieving malaria elimination in China is not only a great work contributing to contemporary times and bringing benefits for future centuries but also the inevitable requirements and important contents in the succeeding target of Healthy China 2030, promoting the health poverty alleviation program in China. After malaria has been eliminated in some countries and regions around the world, the maintenance of the capacity of the surveillance and response system has been neglected, resulting in a resurgence or even an outbreak (Bauch et al. 2013; Espinoza 2019). In recent years, due to the increasing number of migrant populations overseas, they are likely to

become high-risk groups after arriving in malaria-endemic areas (Feng et al. 2014, 2017, 2020; Feng et al. 2014, 2015a). In addition, imported malaria has brought out high risks to malaria-free localities where *Anopheles* mosquitoes still exist. If the sensitivity and effectiveness of the surveillance and response system cannot be maintained and the source of infection cannot be detected and eliminated in time, the risk of resurgence or even outbreak will still be faced. For example, in 2013, in Shanglin County of Guangxi, nearly 1000 cases were reported in just two months, which brought a great risk of transmission to the local area during the epidemic season (Lin et al. 2015). In 2015, Sanya City of Hainan Province and Dandong City of Liaoning Province, where no local infection cases had been reported for many years, reported indigenous cases (Lin et al. 2016; Sun et al. 2017). In 2018, the introduced *P. vivax* caused by imported cases occurred in Longhui County of Hunan Province (Zhang et al. 2019). Therefore, in the post-elimination phase, it is still necessary to attach great importance to strengthening government leadership and multidepartmental cooperation. Community mobilization and maintenance of the surveillance and response capacity to consolidate the achievements of malaria elimination. The people at high risk who return from malaria-endemic areas such as Africa and Southeast Asia should be the focus.

3.4.2 Strengthen Case Management of Imported Cases

Currently, there are still weak links in the control and prevention of imported malaria. Because the management of imported malaria requires many departments and institutions, the effective management mechanism has not been perfected, so that various management measures cannot be well implemented, or because the migrant population lacks awareness and knowledge on personal protection and hardly seeks malaria diagnosis and treatment. In addition, imported malaria also occurs in nonendemic areas, whereas medical staff often lack the vigilance, diagnosis, and treatment experience of malaria, which often leads to misdiagnosis. Furthermore, due to the lack of necessary diagnostic equipment and effective treatment drugs, *P. falciparum* infections are often not dealt with in a timely and effective manner. This will result in aggravation of the disease burden and even death of patients (Zhang et al. 2016a, 2016b). Therefore, it is necessary to continue to maintain the sensitivity of the surveillance system and guarantee the funds to conduct timely diagnosis and standardized disposal of every imported case. Additionally, the clinical diagnosis and treatment of *P. falciparum* malaria should be further strengthened to avoid severe and fatal cases (Zhang et al. 2021b). Case management, such as timely diagnosis and appropriate treatment, epidemiological case investigation, follow-up of colleagues, and investigation and disposal of foci, should be strengthened.

3.4.3 Innovative Surveillance and Response Technologies

The sensitivity of the surveillance and response system has yet to be improved. Due to the current large flow of primary-level microscopy personnel, the quality of blood tests and reports in many places should be improved. In the post-elimination phase, the ability training and maintenance of personnel should continue to be strengthened. In addition, although rapid diagnostic test strips (RDTs) are currently widely used in malaria, the specificity and sensitivity of RDTs still need to be developed, especially for screening asymptomatic malaria infections. The surveillance and response to imported cases are the main tasks of medical staff at all levels in the country. It is also necessary to strengthen the risk assessment of imported cases to facilitate the early warning and forecasting of cases. In addition, the current surveillance and response system makes it difficult to carry out systematic and effective monitoring of migrant populations, especially in border areas. Therefore, it is still important to conduct active case detection in a timely manner and reduce the risk of malaria transmission in border areas. At present, artemisinin-resistant strains of *P. falciparum* have been found in five countries in the Greater Mekong Subregion (GMS), and genes with single nucleotide polymorphisms (SNPs) related to artemisinin resistance have been reported in *P. falciparum* cases in Africa (Feng et al. 2015b, 2019, 2021b; Yan et al. 2020). It is recommended to rely on the national drug resistance monitoring system network and in accordance with the relevant requirements and implementation plans of the WHO to strengthen the molecular surveillance of artemisinin resistance of imported *P. falciparum* cases.

3.5 Concluding Remarks

In summary, China has achieved great success in malaria elimination programs and has been awarded malaria-free certification by the WHO in 2021. Malaria elimination is a magnificent undertaking with merits and benefits for the future, and it is also a complex global system engineering. On the basis of achieving the milestone goal of eliminating malaria in 2021, China will, as always, actively participate in the global malaria elimination program, cooperate with China-Africa cooperation and construction of the “Belt and Road” initiative, share experience, technology and products of malaria elimination to help control and eliminate malaria in high-endemic areas and countries, and continue to promote the building of a community of human health.

Acknowledgments The work was supported by the key techniques in collaborative control and prevention of major infectious diseases in the Belt and Road (Grant No. 2018ZX10101002-004).

References

- Aung PP, Thein ZW, Hein ZNM, Aung KT, Mon NO, Linn NYY, Thi A, Wai KT, Maung TM (2020) Challenges in early phase of implementing the 1-3-7 surveillance and response approach in malaria elimination setting: a field study from Myanmar. *Infect Dis Poverty* 9:18
- Bauch JA, Gu JJ, Msellem M, Martensson A, Ali AS, Gosling R, Baltzell KA (2013) Perception of malaria risk in a setting of reduced malaria transmission: a qualitative study in Zanzibar. *Malar J* 12:75
- Cao J, Sturrock HJ, Cotter C, Zhou S, Zhou H, Liu Y, Tang L, Gosling RD, Feachem RG, Gao Q (2014) Communicating and monitoring surveillance and response activities for malaria elimination: China's "1-3-7" strategy. *PLoS Med* 11:e1001642
- Espinoza JL (2019) Malaria resurgence in the Americas: an underestimated threat. *Pathogens* 8:11
- Feng J, Hong T, Zhang L, Xia ZG, Zhou SS (2020) Imported malaria cases—China, 2012–2018. *China CDC Wkly* 2:277–284
- Feng J, Kong X, Xu D, Yan H, Zhou H, Tu H, Lin K (2019) Investigation and evaluation of genetic diversity of *Plasmodium falciparum* Kelch 13 polymorphisms imported from Southeast Asia and Africa in Southern China. *Front Public Health* 7:95
- Feng J, Liu J, Feng X, Zhang L, Xiao H, Xia Z (2016) Towards malaria elimination: monitoring and evaluation of the "1-3-7" approach at the China-Myanmar border. *Am J Trop Med Hyg* 95:806–810
- Feng J, Zhang L, Huang F, Yin JH, Tu H, Xia ZG, Zhou SS, Xiao N, Zhou XN (2018a) Ready for malaria elimination: zero indigenous case reported in the People's Republic of China. *Malar J* 17:315
- Feng J, Tu H, Zhang L, Zhang S, Jiang S, Xia Z, Zhou S (2018b) Mapping transmission foci to eliminate malaria in the People's Republic of China, 2010–2015: a retrospective analysis. *BMC Infect Dis* 18:115
- Feng J, Xia Z (2014) Analysis of trends in cases of malaria reported from 2004 to July 2013 in the People's Republic of China (in Chinese). *J Pathog Biol* 9:442–446
- Feng J, Xia ZG, Vong S, Yang WZ, Zhou SS, Xiao N (2014) Preparedness for malaria resurgence in China: case study on imported cases in 2000–2012. *Adv Parasitol* 86:231–265
- Feng J, Xiao H, Xia Z, Zhang L, Xiao N (2015a) Analysis of malaria epidemiological characteristics in the People's Republic of China, 2004–2013. *Am J Trop Med Hyg* 93:293–299
- Feng J, Zhang L, Zhang SS, Xia ZG (2017) Malaria epidemiological characteristics in China, 2005–2015 (in Chinese). *China Trop Med* 17:325
- Feng J, Li J, Yan H, Feng X, Xia Z (2015b) Evaluation of antimalarial resistance marker polymorphism in returned migrant workers in China. *Antimicrob Agents Chemother* 59:326–330
- Feng J, Zhang L, Xia ZG, Zhou SS, Xiao N (2021a) Malaria-free certification in China: achievements and lessons learned from the national malaria elimination programme. *Zoonoses* 1:3–6
- Feng J, Xu D, Kong X, Lin K, Yan H, Feng X, Tu H, Xia Z (2021b) Characterization of *pfmdr1*, *pfcr1*, *pfk13*, *pfubp1*, and *pfap2mu* in travelers returning from Africa with *Plasmodium falciparum* infections reported in China from 2014 to 2018. *Antimicrob Agents Chemother* 65:e0271720
- Feng J, Zhang L, Xia ZG, Xiao N (2021c) Malaria elimination program in China: an eminent milestone in the anti-malaria campaign and challenges in the post-elimination stage (in Chinese). *Chin J Parasitol Parasit Dis* 39:421–428
- Huang LL, Wang D, Shi DD, Li HM, Ma XJ, Duan L, Qian YJ, Wang DQ, Guan YY (2020) [Analysis of demands for trainings related to malaria control in Asia-Pacific countries] (in Chinese). *Chin J Parasitol Parasit Dis* 38:350–353
- Kheang ST, Sovannaroeth S, Barat LM, Dysoley L, Kapella BK, Po L, Nguon S, Gimnig J, Slot R, Samphornarann T, Meng SK, Dissanayake G, AlMossawi HJ, Longacre C, Kak N (2020)

- Malaria elimination using the 1-3-7 approach: lessons from Sampov Loun, Cambodia. *BMC Public Health* 20:544
- Lertpiriyasuwat C, Sudathip P, Kitchakarn S, Areechokchai D, Naowarat S, Shah JA, Sintasath D, Pinyajeerapat N, Young F, Thimasarn K, Gopinath D, Prempreep P (2021) Implementation and success factors from Thailand's 1-3-7 surveillance strategy for malaria elimination. *Malar J* 20: 201
- Lin KM, Li J, Yang YC, Wei SJ, Huang YM, Li JH, Guo CK, Wei HY (2015) Characteristics of imported malaria epidemic in Guangxi, 2013 (in Chinese). *Mod Prev Med* 42:2439–2442
- Lin CY, Chen Z, Wang SQ, Luo PZ, Wu DL, Zheng AJ, Wei JJ (2016) Investigation of a rare local epidemic of *Plasmodium malariae* infection in Sanya City, Hainan Province (in Chinese). *China Trop Med* 16:481–484
- Ministry of Health (2010) National malaria elimination action plan (2010–2020). Ministry of Health, Beijing
- National Health Commission (2018-05-10). Strengthen the standardized management and supervision of malaria elimination. Beijing
- Pan B, Pei F, Ruan CW, Lin RX, Chen YZ, Liu MR, Deng ZH, Ren WF, Liao YB, Li XH (2016) Diagnosis and treatment of the first imported case of *Plasmodium knowlesi* infection in China (in Chinese). *Chin J Parasitol Parasit Dis* 34:513–516
- Pan B, Wu Y, Wu XG, Zhu TH, He Q (2001) Field Evaluation of bednets impregnated with cyfluthrin for the control of malaria transmitted by *Anopheles sinensis* in Guangdong Province, China (in Chinese). *Chin J Parasit Dis Con* 14:165–167
- Qian HL, Tang LH (2000) The achievements and prospects on malaria control and prevention for 50 years in China (in Chinese). *Chin J Epidemiol* 21:225–227
- Sun YW, Yu D, Chen J, Li X, Wang B, Wang ZJ, Mao LL, Yao WQ (2017) Two individual incidences of vivax malaria in Dandong municipality of Liaoning Province (in Chinese). *Chin J Public Health* 33:314–316
- Tang LH (1999) Chinese achievements in malaria control and research (in Chinese). *Chin J Parasitol Parasit Dis* 17:257–259
- Tang LH, Xu L, Chen YD (2012) Parasitic disease control and research in China. Beijing Science and Technology Press, Beijing
- Tu H, Feng J, Zhang L, Zhang SS, Xia ZG, Zhou SS (2019) Audit and quality assessment on malaria case information reported by National information management system for malaria in China in 2017 (in Chinese). *Chin J Parasitol Parasit Dis* 37:41–47
- Wang Q, Wang J, Li TT, Cao J, Xie Z (2016) Analysis of demands of African students for China-Africa malaria prevention training (in Chinese). *Chin J Schisto Control* 28:461–464
- Wang D, Cotter C, Sun X, Bennett A, Gosling RD, Xiao N (2017) Adapting the local response for malaria elimination through evaluation of the 1-3-7 system performance in the China-Myanmar border region. *Malar J* 16:54
- Wang D, Chaki P, Mlacha Y, Gavana T, Michael MG, Khatibu R, Feng J, Zhou ZB, Lin KM, Xia S, Yan H, Ishengoma D, Rumisha S, Mkude S, Mandike R, Chacky F, Dismasi C, Abdulla S, Masanja H, Xiao N, Zhou XN (2019a) Application of community-based and integrated strategy to reduce malaria disease burden in southern Tanzania: the study protocol of China-UK-Tanzania pilot project on malaria control. *Infect Dis Poverty* 8:4
- Wang T, Zhou SS, Feng J, Oo MM, Chen J, Yan CF, Zhang Y, Tie P (2019b) Monitoring and evaluation of intervals from onset of fever to diagnosis before “1-3-7” approach in malaria elimination: a retrospective study in Shanxi Province, China from 2013 to 2018. *Malar J* 18:235
- Wang JG, Xu C, Wong YK, Li YJ, Liao FL, Jiang TL, Tu YY (2019c) Artemisinin, the magic drug discovered from traditional Chinese medicine. *Engineering* 5:32–39
- World Health Organization (2021) From 30 million cases to zero: China is certified malaria-free by WHO. World Health Organization, Geneva
- World Health Organization (2022) World malaria report 2022. World Health Organization, Geneva
- Xia ZG, Yang M, Zhou SS (2012) Malaria situation in the people's Republic of China in 2011 (in Chinese). *Chin J Parasitol Parasit Dis* 30:419–422

- Xiao N, Xu QL, Feng J, Xia ZG, Duan L, Wang DQ, Guan YY, Zhou XN (2021) Approaching malaria elimination in China. *China CDC Wkly* 2:293–297
- Xr W (1995) Analysis on the function and significance of joint malaria prevention in 5 Provinces (in Chinese). *Hubei J Prev Med* 6:1–8
- Yan H, Kong X, Zhang T, Xiao H, Feng X, Tu H, Feng J (2020) Prevalence of *Plasmodium falciparum* Kelch 13 (PfK13) and ubiquitin-specific protease 1 (Pfubp1) gene polymorphisms in returning travelers from Africa reported in Eastern China. *Antimicrob Agents Chemother* 64: e00981–e00920
- Yin JH, Yan H, Huang F, Li M, Xiao HH, Zhou SS, Xia ZG (2015) Establishing a China malaria diagnosis reference laboratory network for malaria elimination. *Malar J* 14:40
- Zhang L, Feng J, Tu H, Yin JH, Xia ZG (2021a) Malaria epidemiology in China in 2020 (in Chinese). *Chin J Parasitol Parasit Dis* 39:195–199
- Zhang L, Feng J, Xia ZG (2014) Malaria situation in the People's Republic of China in 2013 (in Chinese). *Chin J Parasitol Parasit Dis* 32:407–413
- Zhang L, Feng J, Xia ZG, Zhou SS (2020) Epidemiological characteristics of malaria and progress on its elimination in China in 2019 (in Chinese). *Chin J Parasitol Parasit Dis* 38:133–138
- Zhang L, Feng J, Zhang SS, Jiang S, Xia ZG, Zhou SS (2017) Malaria situation in the People's Republic of China in 2016 (in Chinese). *Chin J Parasitol Parasit Dis* 35:515–519
- Zhang L, Feng J, Zhang SS, Xia ZG, Zhou SS (2016a) Malaria situation in the People's Republic of China in 2015 (in Chinese). *Chin J Parasitol Parasit Dis* 34:477–481
- Zhang L, Feng J, Zhang SS, Xia ZG, Zhou SS (2018) The progress of national malaria elimination and epidemiological characteristics of malaria in China in 2017 (in Chinese). *Chin J Parasitol Parasit Dis* 36:201–209
- Zhang L, Feng J, Zhang SS, Xia ZG, Zhou SS (2019) Epidemiological characteristics of malaria and the progress towards its elimination in China in 2018 (in Chinese). *Chin J Parasitol Parasit Dis* 37:241–247
- Zhang L, Tu H, Zhou SS, Xia ZG, Feng J (2021b) Malaria deaths-China, 2011–2020. *China CDC Weekly* 3:360–365
- Zhang L, Zhou SS, Feng J, Fang W, Xia ZG (2015) Malaria situation in the People's Republic of China in 2014 (in Chinese). *Chin J Parasitol Parasit Dis* 33:319–326
- Zhang Q, Geng Q, Sun JL, Zhang ZK, Lai SJ, Zhou S, Li ZJ (2016b) Epidemiological analysis of the deaths of malaria in China, 2005–2014 (in Chinese). *Chin J Prev Med* 50:302–305
- Zhou RM, Song L, Gao LJ, Qian D, Yang CY, Liu Y, Zhao YL, Zhang HW (2018) Diagnosis and analysis of the first imported case of *Plasmodium knowlesi* infection in Henan Province (in Chinese). *Zhengzhou Univ Med Sci* 53:610–613
- Zhou SS, Wang Y, Li Y (2011) Malaria situation in the People's Republic of China in 2010 (in Chinese). *Chin J Parasitol Parasit Dis* 29:401–403
- Zhou SS, Zhang SS, Zhang L, Rietveld AE, Ramsay AR, Zachariah R, Bissell K, Van den Bergh R, Xia ZG, Zhou XN, Cibulskis RE (2015) China's 1-3-7 surveillance and response strategy for malaria elimination: Is case reporting, investigation and foci response happening according to plan? *Infect Dis Poverty* 4:55



Malaria Parasites: Species, Life Cycle, and Morphology

4

Kai Wu

Abstract

Plasmodium parasites are parasitized in vertebrates and female *Anopheles* mosquitoes. Although there are many different species, there are four main species of *Plasmodium* parasites in humans, namely, *Plasmodium falciparum*, *Plasmodium vivax*, *Plasmodium ovale*, and *Plasmodium malariae*. Furthermore, there is a fifth, rarer, human-monkey species, known as *Plasmodium knowlesi*. This chapter describes the biology, life history, and morphological characteristics of human *Plasmodium* to provide a comprehensive understanding of *Plasmodium* in humans.

Keywords

Human *Plasmodium* · Biological characteristics · Life cycle · Morphology

4.1 Etiology and Classification of Malaria

Malaria is an ancient infectious disease that poses a serious threat to human health. There are written records relating to malaria epidemics in China as far back as 3000 years ago. It was not until 1880 in Algeria that Charles-Louis-Alphonse Laveran, a French army doctor, first discovered *Plasmodium* in the blood of patients with fever by microscopic examination. In 1897, Ronald Ross, a British army doctor serving in India, confirmed that the *Anopheles* mosquito was the vector of malaria and elucidated the life cycle of the *Anopheles* mosquito and the mode of transmission of its bite. It was then that the mystery of malaria was unraveled.

K. Wu (✉)

Wuhan, Wuhan City, China

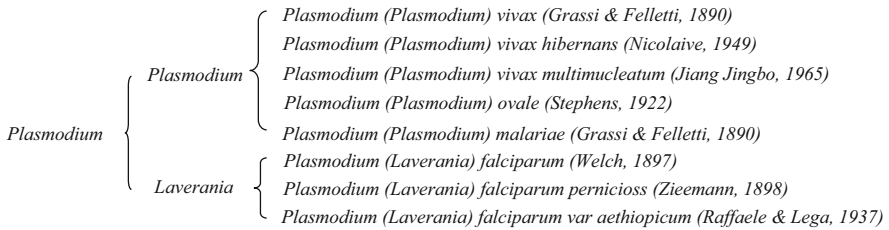


Fig. 4.1 The classification of main human *Plasmodium*

Plasmodium, the causative agent of malaria, is a unicellular eukaryotic protozoan belonging to Sporozoa, the order Eucoccidiales, the family Plasmodiidae, and the genus *Plasmodium*. There are many different species of *Plasmodium*, and the hosts can be amphibians, reptiles, birds, mammals, and other vertebrates, but the hosts of the species are highly specific, and there are significant biological differences between species. There are four main species of human malaria parasites, *Plasmodium falciparum*, *Plasmodium vivax*, *Plasmodium ovale*, and *Plasmodium malariae*, which cause falciparum malaria, Vivax malaria, Ovale malaria, and Quartan malaria, respectively. There are currently eight main named species (or subspecies), with *P. vivax*, *P. ovale*, and *P. malariae* belonging to the subgenus *Plasmodium* and *P. falciparum* belonging to the subgenus *Laverania* (Fig. 4.1). In addition, *P. ovale* contains two subtypes, *P. ovale curtisi* and *P. ovale wallikeri*, but it is controversial whether they are two subspecies. *P. falciparum*, *P. vivax*, and *P. ovale* are only parasitic in humans, whereas *P. malariae* can infect humans and apes in Africa (Xinping and Chuan, 2018; Shaowu et al., 2000; Sutherland et al., 2010).

Plasmodium knowlesi, a monkey *Plasmodium* endemic in the virgin forests of Malaysia, has been shown to cause natural infection from monkey to human, human to human, and human to monkey through mosquito vectors and is recognized as the fifth human *Plasmodium* species. However, *P. knowlesi* infections are less common, have a limited epidemiological range, and do not develop in humans as hyperparasitemia, hence the mild clinical symptoms of *P. knowlesi* infection in humans. Other rare cases of human infection with *Plasmodium simium*, *Plasmodium cynomolgi*, *Plasmodium schwezi*, and *Plasmodium inui* have also been reported in the literature. The route and mode of infection and the degree of risk to humans have yet to be confirmed (Huaimin et al., 2006).

4.2 Life Cycle

The development and reproduction of *Plasmodium* require completion by vertebrates and insect vectors, and the hosts of human *Plasmodium* include humans and *Anopheles*. *Plasmodium* parasitizes human liver parenchyma cells and red blood cells (RBCs). Occasionally, *Plasmodium* may be present outside RBCs in peripheral blood smears, e.g., by released merozoites, or when hemolytic reactions occur

(Chap. 6, Fig. 6.14). In mosquitoes, it parasitizes the mosquito stomach and finally gathers in salivary glands. The four major human *Plasmodium* species share a similar life cycle, which includes the exoerythrocytic (liver stage) and erythrocytic phases in humans and the gametogony and sporogony phases in *Anopheles* mosquitoes. Understanding the life cycle of *Plasmodium* is of great importance to the morphology of *Plasmodium* under the microscope (Xinping and Chuan, 2018; Xiaoqiu, 2007).

4.2.1 Development of *Plasmodium* in Humans

The exoerythrocytic phase is also known as the liver stage. When female *Anopheles* mosquitoes carrying *Plasmodium* sporozoites in salivary glands take a blood meal from humans, the sporozoites with saliva invade human peripheral blood, and they can remain under the skin for several hours. The majority of sporozoites then enter the capillaries, and a very small proportion invade the capillary lymphatics. The sporozoites follow the blood flow into the hepatic sinusoids, cross the Kupffer cell or sinusoidal endothelial cell space, and eventually invade the hepatic parenchymal cells. It takes approximately 30 minutes from the time the sporozoites enter the blood vessels to the time they invade the hepatocytes. Development and asexual schizogony of *Plasmodium* sporozoites are completed in parenchymal cells of the liver, and the development of *Plasmodium* to schizonts is termed schizonts of the exoerythrocytic phase or liver stage. The mature schizonts of the exoerythrocytic phase are 45–60 μm in diameter, which give birth to 10–30,000 merozoites, and escape from the hepatocytes in the form of merozoites, which bud out. After entering the peripheral blood, merozoites release merozoites, some of which are engulfed by macrophages and some of which successfully invade RBCs and begin the development of the erythrocytic phase. The duration of the exoerythrocytic phase varies in *Plasmodium* species, ranging from 6 to 12 days, with 5 to 6 days for *P. falciparum*, 8 days for *P. vivax*, 9 days for *P. ovale*, and 11 to 12 days for *P. malariae*. There are currently two genetically distinct types of sporozoites of *P. vivax* and *P. ovale*, namely, tachysporozoites and bradysporozoites. Tachysporozoites invade hepatocytes and continue to proliferate in the exoerythrocytic phase, releasing liver-stage merozoites that invade RBCs and cause clinical episodes through schizosomal proliferation. Bradysporozoites do not continue developing after invading hepatocytes temporarily but remain dormant (latent period). After a period of dormancy ranging from a few months to a few years (usually longer than 3 months), bradysporozoites develop into mature exoerythrocytic schizonts and release merozoites to invade RBCs to cause clinical symptoms, which is also known as “relapse.” In Wuhan city, an overseas imported case infected with *P. ovale* that had a latent period of more than 14 months was observed, and a case with a latent period of more than 2 years was reported in China. Since no bradysporozoites are observed in either *P. falciparum* or *P. malariae*, there is no relapse of *P. falciparum* or *P. malariae*. However, in Wuhan city, several imported cases infected with *P. malariae* were found to present clinical symptoms after more

than 4 months of returning from overseas countries, which showed a similar latent period with *P. vivax* and *P. ovale*. In fact, the parasitemia density of *P. malariae* is generally lower than that of other species. The extremely low density causes long-term asymptomatic erythrocyte parasitism in *P. malariae*; however, clinical symptoms may occur due to the subsequently increased density.

The erythrocytic phase is also known as the blood stage or RBC stage. Following release to peripheral blood, some merozoites invade RBCs within a few seconds or minutes and develop in RBCs for reproduction by fission, while other merozoites are engulfed by phagocytic cells. The process of merozoite invasion into RBCs includes three consecutive stages. First, merozoites recognize and attach to receptors on the surface of the RBC membrane through specific sites. Second, RBCs are deformed, and the cell membrane is concave around merozoites to form *Plasmodium* vacuoles. Finally, the vacuoles are sealed after merozoite invasion. The merozoites develop into small trophozoites (ring trophozoites or trophozoites of the former forms) in RBCs. After swallowing hemoglobin and other nutrients, the nucleus is enlarged, the cytoplasm is increased, and iron ion-containing pigments are produced by breaking down hemoglobin. The color and shape of the malaria pigments vary somewhat between species of *Plasmodium*. Then, the small trophozoites develop gradually into large trophozoites (late trophozoites or mature trophozoites), also known as an amoeba-like shape, because of their amoeboid movements. The nucleus and cytoplasm of mature trophozoites begin to divide and develop into schizonts. Each nucleus of a mature schizont is surrounded by a piece of cytoplasm, giving it a grainy and clear state. The mature schizonts have 8–32 nuclei (merozoites), and the number of nuclei varies according to the species. When the schizonts are mature, the RBCs are exhausted and then broken. RBC fragments, merozoites, and malarial pigments are released into peripheral blood and cause the onset of clinical symptoms of malaria. Some merozoites are consumed by macrophages, while others reinvade new RBCs and begin a new erythrocytic phase. This cycle is known as the fission proliferation cycle. The duration of the erythrocytic phase varies with *Plasmodium* species, with 36–48 hours for *P. falciparum*, 48 hours for *P. vivax* and *P. ovale*, and 72 hours for *P. malariae*, producing a corresponding fever cycle. After more than ten hours of development in RBCs, the early trophozoites of *P. falciparum* gradually hide in microvessels, blood sinuses, and places with slow blood flow and continue to develop into late trophozoites and schizonts. Therefore, the late trophozoites and schizonts of *P. falciparum* are generally not easily found in peripheral blood, except for severe cases of falciparum malaria. After several fission proliferations of *Plasmodium* in RBCs, merozoites that have invaded RBCs no longer undergo asexual divisions but develop into female (macrogametocytes) and male gametocytes (microgametocytes). At this time, if female *Anopheles* bites and feeds on human blood, the mature female and male gametocytes are sucked into the mosquito's stomach, and sexual reproduction begins. If they remain in humans, they will age and die out spontaneously, being cleared out or simply engulfed by WBCs within 30–60 days. The immature gametocytes of *P. falciparum* are mainly in the microvessels and blood sinuses of the liver, spleen, bone marrow, and other organs. In general, they appear in the peripheral blood after maturity, and the time is

approximately 7–10 days after the emergence of asexual bodies in the peripheral blood. *P. falciparum* can parasitize all types of RBCs, *P. vivax* and *P. ovale* mainly parasitize reticulocytes, and *P. malariae* mostly parasitizes aged RBCs. In addition to new infections in malaria patients, the most common reason leading to the recurrence of clinical symptoms is the massive proliferation of residual *Plasmodium* in blood, which is called “resurgence.” Therefore, no matter what kind of malaria parasite is infected, resurgence is occurring as long as the anti-malaria treatment fails.

4.2.2 Development of *Plasmodium* in Anopheles Mosquito

Gametogenesis: After *Plasmodium* at each stage enters mosquito stomachs by sucking the blood of malaria patients and *Plasmodium* carriers, mature female and male gametocytes continue to develop in the mosquito stomachs, while another asexual *Plasmodium* is digested, including small and large trophozoites, schizonts, and immature gametocytes. Female gametocytes form circular and inactive female gametes following nucleus meiosis. The nucleus of male gametocytes first divides into 4–8 pieces, and the cytoplasm extends 4–8 flagellate filaments, known as the filament phenomenon. Then, each nucleus enters a filament, which detaches from the mother and forms a flagellated male gamete. The male gamete may swim close to female gametes directionally. When in contact with the female gamete, it can burrow into the female gamete within seconds, forming a rounded zygote. The zygote develops into motile and elongated ookinetes. The ookinete passes through the epithelial cells on the mosquito gastric wall and stays between the epithelial cells and the outer elastic fibrous membrane, developing into an oocyst. If the patient's peripheral blood has a long interval between collection and production, then female and male gametes, the filament phenomenon (Figs. 6.25 and 6.57), ookinetes (Fig. 4.2), and other morphologies can also be observed in the peripheral blood smear.

P. vivax ookinetes may be present in human peripheral blood if the time interval from blood collection to the preparation of blood smears is long enough.

Sporozoite reproduction: The oocysts grow and protrude into the wall of the mosquito's stomach in the form of a tumor, and there can be several to dozens, or even more, of oocysts on the wall of the mosquito's stomach. The nuclei and cytoplasm in the oocysts are divided repeatedly and undergo sporozoite reproduction. Mature oocysts are approximately 40–60 μm in diameter and contain approximately 1000–10,000 spindle-shaped sporozoites, which are 10–15 μm long and approximately 1 μm wide, with a nucleus pointed at both ends and a curved body. The sporozoites can be released from the rupture or burrowed out of the oocyst and concentrated in the salivary glands of the mosquito via the hemolymph, developing into mature sporozoites. The duration of *Plasmodium* development in mosquitoes is related to temperature and humidity. The most suitable condition for *Plasmodium* sporozoites reproduction in mosquitoes is at a temperature of 24–26 $^{\circ}\text{C}$ and relative humidity of 75%–80%. A temperature lower than 16 $^{\circ}\text{C}$ or higher than 30 $^{\circ}\text{C}$ will

Fig. 4.2 A *P. vivax* ookinete (Giemsa staining, $\times 1000$)



delay development and may cause degeneration until death. Mature sporozoites escape through the crevice of the oocysts or diffuse into the blood and eventually accumulate in the salivary gland adenocytes. If a female mosquito with sporozoites bites another person, sporozoites inject humans with saliva and initiate development in humans. Under the most suitable conditions, the development time of *Plasmodium* in *Anopheles* mosquitoes is 10–12 days for *P. falciparum*, 9–10 days for *P. vivax*, approximately 16 days for *P. ovale*, and 25–28 days for *P. malariae*.

The biological characteristics and life cycles of the four *Plasmodium* species are shown in Table 4.1 and Fig. 4.3.

4.3 Morphology of Human *Plasmodium* in the Erythrocytic Phase

The basic structure of *Plasmodium* includes the nucleus, cytoplasm and cell membrane. After ingestion of hemoglobin, malaria pigments, a product of digestion and breakdown of hemoglobin, appear in the pRBCs (Fig. 4.4). Blood smears with stainings, such as Giemsa or Wright's staining, show red or purplish red nuclei, blue or dark blue cytoplasm, and brown or black-brown malaria pigments. The four human *Plasmodium* species have the same basic structure, but the morphology of each stage of development varies. In addition to the morphological characteristics of the *Plasmodium* itself, the pRBCs can also change in morphology (Xinping and Chuan, 2018; Xiaoqi, 2007).

Table 4.1 Biological characteristics of four human *Plasmodium* species

<i>Plasmodium</i>	<i>P. falciparum</i>	<i>P. vivax</i>	<i>P. ovale</i>	<i>P. malariae</i>
Duration of the exoerythrocytic phase (Days)	5–6	8	9	11–12
Dormant body	No	Yes	Yes	No
Number of merozoites in the exoerythrocytic phase	30,000	10,000	15,000	15,000
Duration of schizogony in the erythrocytic phase (hours)	36–48	48	48	72
Characteristics of parasitized RBCs (pRBCs)	All types of RBCs	Duffy Positive reticulocyte^a and normoblast	Reticulocyte and normoblast	Aged RBCs
pRBCs morphology	Normal, Maurer's clefts	Enlarged, Schüffner dots	Slightly enlarged, Schüffner dots	Normal or reduced, Ziemann dots
Malarial pigment	Black-brown	Brownish-yellow	Brownish-yellow	Dark-brown
Number of merozoites in the erythrocytic stage	8–26	12–24	6–12	6–12
Morphology of gametocytes	Crescent/Sausage shape	Circular	Circular	Circular
Duration of development in mosquitoes at the most suitable conditions (Days)	10–12	9–10	16	25–28
Malarial pigments in oocyst	Chains and strips	Crown feather	Crossline	Gathered at the edge

^a The merozoites released by *P. vivax* schizonts with Duffy binding protein (DBP) on their surface, which must bind to the Duffy antigen/receptor for chemokine (DARC) of reticulocytes before they can invade the RBCs. In contrast, Fy(a-b-) phenotype RBCs, which lack DARC, are protected from *P. vivax* infection or are at reduced risk of infection

Accumulation of malarial pigments is seen in leukocyte phagocytosis after medical treatment (red arrow), which is often observed in cases with high parasitemias or severe cases.

4.3.1 Morphological Characteristics of the Stages of *Plasmodium* Development in RBCs

The morphological characteristics of *Plasmodium* are grouped into three main developmental stages, namely, the trophozoite, schizont, and gametophyte stages, based on the morphological characteristics of each stage in the pRBCs. The

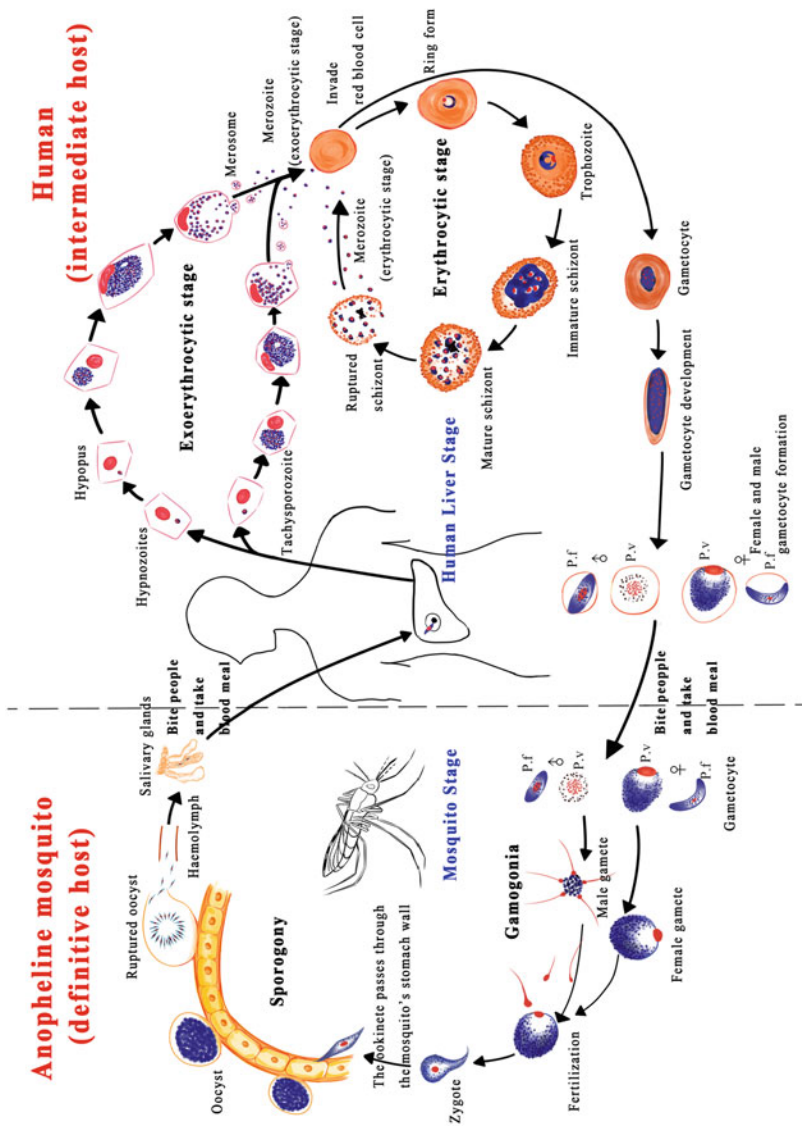


Fig. 4.3 The life cycle of *Plasmodium* species

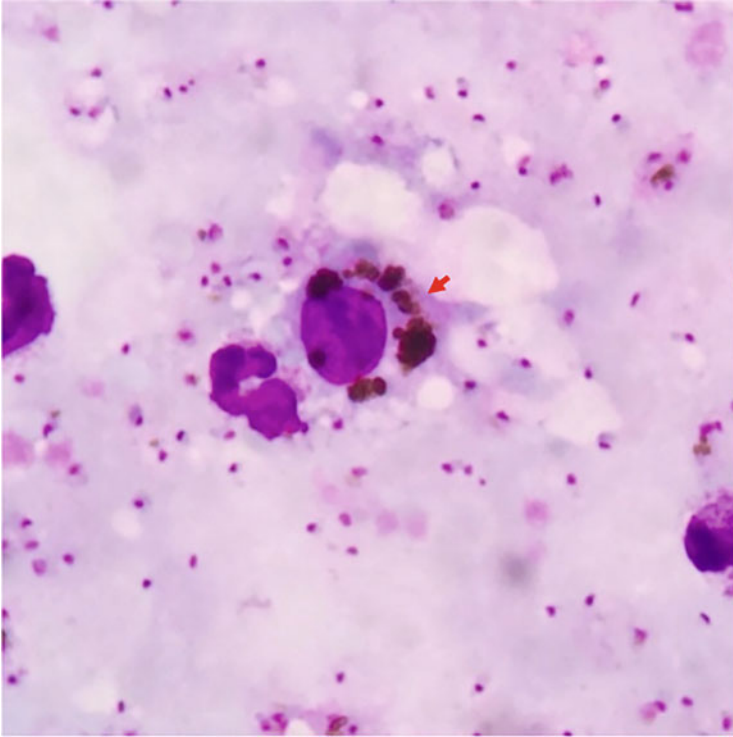


Fig. 4.4 Yellowish- or dark-brown malarial pigments (Giemsa staining, $\times 1000$)

trophozoites and schizonts belong to the asexual stage, and the gametocytes belong to the sexual stage.

I. Trophozoites

Based on morphological characteristics, they can be subdivided into the small trophozoite stage and the large trophozoite stage. Small trophozoites, also known as ring-form and early trophozoites, have a small nucleus, little cytoplasm, a vacuole in the middle and a ring-shaped body. As *Plasmodium* feeds, grows, and develops, the nucleus and cytoplasm increase in size, and pseudopods and malaria pigments appear. Maurer's clefts appear inside pRBCs parasitized by *P. falciparum*, Schüffner's dots appear inside pRBCs parasitized by *P. vivax* and *P. ovale*, and Ziemann's dots appear inside pRBCs parasitized by *P. malariae*. At this point, *Plasmodium* develops into large trophozoites, which can also be called late trophozoites or mature trophozoites. The morphology and size of the large trophozoites vary considerably between *Plasmodium* parasites and are key to morphological differentiation.

II. Schizonts

As the trophozoites mature, the nucleus and cytoplasm begin to divide in a dichotomy called schizonts. The nucleus undergoes repeated divisions, and the

cytoplasm divides as well, with each nucleus surrounded by cytoplasm, called a merozoite. The schizonts can be subdivided into immature (early) schizonts and mature (late) schizonts. The nuclei of immature schizonts are few and tightly packed in undivided cytoplasm, whereas when there are more nuclei, the respective cytoplasm surrounds the nuclei and becomes grainy and clear, and the malaria pigment tends to concentrate; then, the schizonts are mature. The morphology of the schizonts and the number of schizonts vary considerably between *Plasmodium* parasites, which is the key to morphological differentiation.

III. Gametocytes

After *Plasmodium* parasites have undergone several fission proliferations and some merozoites invade RBCs, the nucleus and cytoplasm develop into round, oval or crescent-shaped, sausage-shaped gametocytes. Depending on morphological characteristics, gametocytes can be divided into female and male and can also be subdivided into immature gametocytes and mature gametocytes. The mature gametocyte of *P. falciparum* is crescentic and sausage shaped, which differs markedly from the round, oval-shaped gametocytes of *P. vivax*, *P. ovale*, and *P. malariae*.

4.3.2 Morphological Characteristics of Four Human *Plasmodium* Species in Thin Blood Smears

The morphological characteristics of *Plasmodium* in thin blood smears after Giemsa staining are shown in Table 4.2. The morphology of large (late or mature) trophozoites is sometimes similar to that of nearly mature female gametocytes. The identification is described in Table 4.3.

4.3.3 Morphological Characteristics of Four Human *Plasmodium* Species in Thick Blood Smears

The RBCs of the thick blood smears stacked cascade, *Plasmodium* shrank fold or part of *Plasmodium* was missing, the lysis of RBCs could not be used as a reference, and the hemolysis process also formed more impurities than thin blood smears, resulting in morphological identification being more difficult than thin blood smears. However, thick blood smears have more blood volume and a smaller area, and when RBCs are concentrated, the detection rate of *Plasmodium* is significantly higher than that of thin blood smears and less likely to be missed. The morphological characteristics of *Plasmodium* in thin blood smears after Giemsa staining are shown in Table 4.4.

Figures 4.5, 4.6, 4.7, and 4.8 describe the morphological characteristics of *Plasmodium* in thick and thin blood smears.

Table 4.2 Morphological identification of four *Plasmodium* species on a thin blood smear (Giemsa staining)

<i>Plasmodium</i>		<i>P. falciparum</i>	<i>P. vivax</i>	<i>P. ovale</i>	<i>P. malariae</i>
pRBCs	Size	Normal	Swelling	Normal or slight swelling	Normal or shrinking
	Shape	Normal	Polymorph	Oval or umbrella-arrow, comet-like the edge	Normal
	Color	Normal or slightly purple	Fading	Fading	Normal
Former trophozoites (ring)	Dots	Uneven distribution of a few Maurer's clefts, which appear red and rough	Uniform distribution of lots of Schüffner's dots, which appear red and small	Uniform distribution of red Schüffner's dots, which are larger slightly than that of <i>P. vivax</i>	Light red Ziemann's dots
	Size	Smaller, approximately 1/5–1/6 of the diameter of RBCs	Larger, accounting for approximately 1/3 of the diameter of RBCs	Smaller	Smaller
	Nucleus	1 or 2	1, 2 are rare	1	1
	Cytoplasm	Slender	Thin	Thicker	Thicker
	Malarial pigment	No	No	No	Occasionally tiny, brown particles
Large (late or mature) trophozoites	Size	Smaller	Larger	Medium	Medium
	Nucleus	1 or 2	1, 2 are rare	1	1
	Cytoplasm	Circular, nearly circular or ellipse, inapparent vacuoles	Amoeba-like, it often contains vacuoles	Circular, obvious vacuoles	Ribbon-like, inapparent vacuoles
Immature schizonts	Malarial pigment	Small yellow-brown particles or formation of a black-brown block	Yellowish-brown, small, rhabditiform, scattered in distribution	Brownish and thick	Large dark-brown c distributed along the edges
	Size	Smaller	Larger	Smaller	Smaller
	Nucleus	≥ 2	≥ 2	≥ 2	≥ 2
	Cytoplasm	Circular or nearly circular, disappearance of vacuoles	Circular or irregular, the disappearance of vacuoles	Circular or oval, the disappearance of vacuoles	Circular, the disappearance of vacuoles

(continued)

Table 4.2 (continued)

<i>Plasmodium</i>		<i>P. falciparum</i>	<i>P. vivax</i>	<i>P. ovale</i>	<i>P. malariae</i>
Mature schizonts	Malarial pigment	Black-brown block	Yellowish-brown, uneven distribution or gathering in a heap	Brownish, uneven distribution	Dark-brown, uneven distribution
	Size	Smaller than normal RBCs	Larger than normal RBCs	Less than normal RBCs	Less than normal RBCs
	Merozoites	8–32 but often 8–18, irregular arrangement, smaller	12–24 but often 16–18, irregular arrangement, larger	6–12 but often 8, irregular arrangement	6–12 but often 8, arranged in a flower-like manner
	Malarial pigment	Black-brown block	Yellowish-brown, often gathering in a heap on one side	Brownish, often gathering in a heap centrally or on one side	Dark-brown, often gathering in the center
	Size	Larger	Larger than normal RBCs	Less than normal RBCs	Less than normal RBCs
Female gametocytes	Shape	Crescent, sharp at both ends	Circular	Circular	Circular
	Nucleus	1, smaller, crimson, centered	1, larger, dense, crimson, located on one side	1, smaller, dense, crimson, located on one side	1, smaller, dense, crimson, located on one side
	Cytoplasm	Dark blue	Dark blue	Dark blue	Dark blue
	Malarial pigment	Black-brown, tight distribution around the nucleus	Yellowish-brown, evenly scattered	Brownish, scattered	Dark-brown, evenly scattered
	Size	Larger	Larger than normal RBCs	Less than normal RBCs	Less than normal RBCs
Male gametocytes	Shape	Sausage shape, blunt circle at both ends	Circular	Circular	Circular
	Nucleus	1, larger, light red, located in the center	1, larger, loose, light red, located in the center	1, larger, light red, located in the center	1, larger, light red, located in the center

Cytoplasm	Light blue or light red	Light blue	Light blue	Light blue	Light blue	Light blue
Malarial pigment	Black-brown distributed loosely around the nucleus	Yellowish-brown, evenly scattered	Brownish, scattered	Dark-brown, evenly scattered		

Table 4.3 Morphological identification between large (late or mature) trophozoites and nearly mature female gametocytes

<i>Plasmodium</i>	Female gametocytes	Trophozoites
Size	Almost full of pRBCs	No more than 3/4 size of the pRBCs
Nucleus	One, large and dense, nonstained ribbons around	One, small or ribbon-like, no obvious nonstained ribbons around
Cytoplasm	The edges are clear without vacuoles	The edges are unclear and irregular, with vacuoles
Malarial pigment	More thick particles with even distribution, around nucleus	Less and tiny particles, uneven distribution

Table 4.4 Morphology of human malaria parasites on a thick blood smear

<i>Plasmodium</i>		<i>P. falciparum</i>	<i>P. vivax</i>	<i>P. ovale</i>	<i>P. malariae</i>
Trophozoites of the former (ring)		Small size. Consisted of slender cytoplasm and 1–2 smaller nuclei, always present “i”, “spread the wings,” “v” and “broken ring”	Larger size. Most have one larger nucleus, the cytoplasm is thicker, and always presents larger “i” or “,”	The size is similar to that of the <i>P. vivax</i> with dense cytoplasm and a larger nucleus	Medium size. A larger nucleus and thick cytoplasm form “bird-eye” or “circle”
Large (late or mature) trophozoites	Size	Smaller	Largest among four species	The size is smaller than that of <i>P. vivax</i>	Medium size, it is slightly smaller than that of <i>P. ovale</i>
	Morphology	Often round or nearly circular	Amoeba-like, irregular shape, nucleus located in or outside the cytoplasm, which often shrinks into circles or breaks into pieces	The cytoplasm is dark blue, and the nucleus is larger	Often ribbon-like
Schizonts	Malarial pigment	Tiny or gathered into 1–2 pieces	Tiny and yellowish-brown at an early stage, and then presenting rhabditiform or forming thick particles. The distribution is uneven	Pigment characteristics are similar to <i>P. vivax</i>	Thick particles and obvious
		Smaller and 8–26 merozoites crowded together. Merozoites are also small	Larger and 12–24 dispersed merozoites. Merozoites are small or larger slightly	The size is smaller than that of <i>P. vivax</i> with 6–14 merozoites, larger and distributed closely	Smaller and 6–12 merozoites with scattered distribution. Merozoites are small
Gametocytes		Crescent shape of female gametocytes and sausage shape of male gametocytes, may be folding or partial deletion	Largest among four species, circular and thick malarial pigments. Female gametocytes are larger, nucleus is also larger and leans to one side, cytoplasm is dark blue, male	The gametocyte morphology is similar to <i>P. vivax</i> but the size is smaller than <i>P. vivax</i>	The gametocyte morphology is similar to <i>P. vivax</i> and <i>P. ovale</i> , but the size is more smaller. The malarial pigments are thicker

(continued)

Table 4.4 (continued)

<i>Plasmodium</i>	<i>P. falciparum</i>	<i>P. vivax</i>	<i>P. ovale</i>	<i>P. malariae</i>
Malarial pigment	Tiny yellowish-brown particles at an early stage, then appearing as a black-brown block. The malarial pigment granules of gametophyte are thick and distributed around the nucleus	Tiny yellowish-brown at an early stage rod-like, or forming large, coarse particles. The distribution is uneven	The dark-brown large particles are dispersed	Sometimes small trophozoites with visible dark-brown pigments are thicker, which are distributed along the edges
RBCs	RBCs shadows and Maurer's clefts are seen	RBCs shadows and Schüffner's dots are often seen	Schüffner's dots are visible from the former trophozoites stage	RBCs shadows are seen
Others	Trophozoites of the former (ring) and gametocytes are often seen. Large trophozoites and schizonts are generally not seen	<i>Plasmodium</i> at all erythrocytic stages can often be found	<i>Plasmodium</i> is found at all erythrocytic stages	<i>Plasmodium</i> is found at all erythrocytic stages

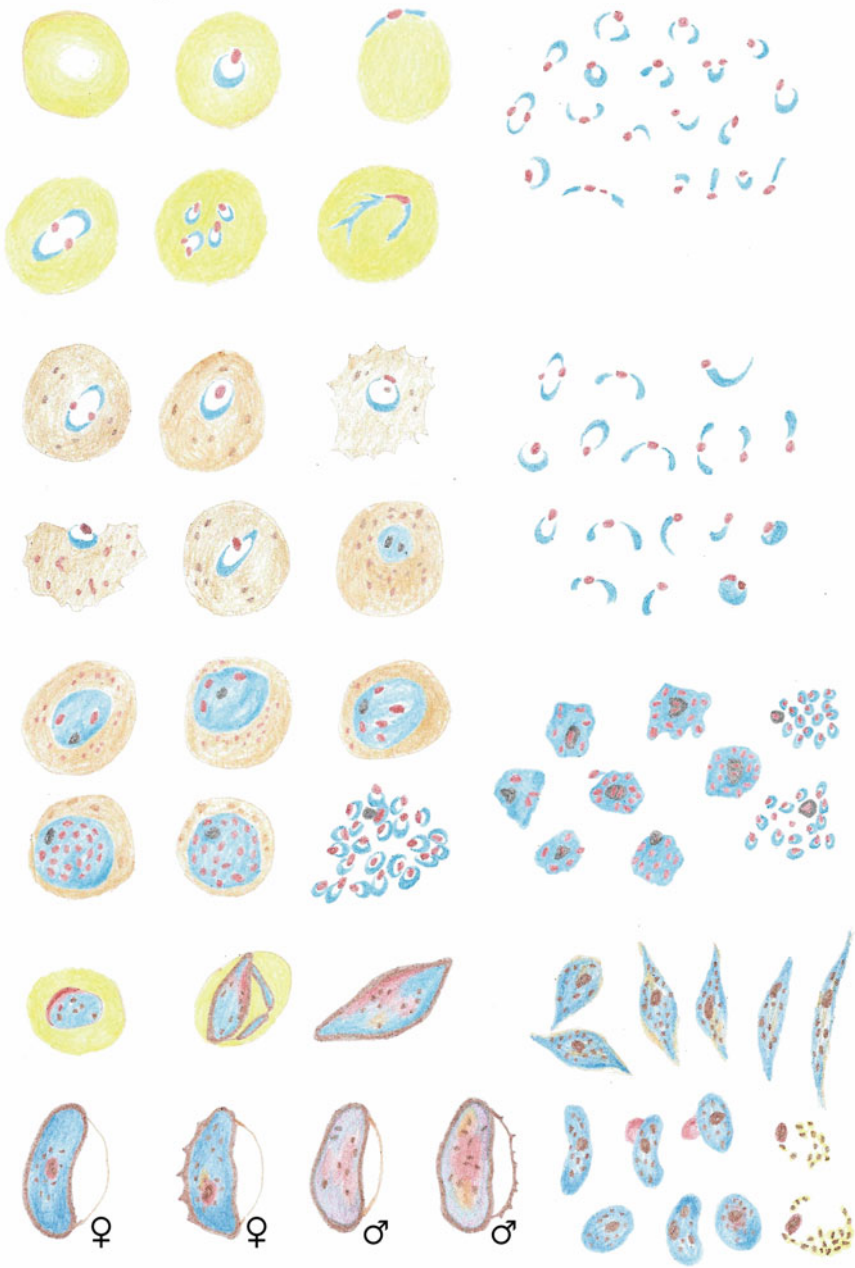


Fig. 4.5 Morphology of *P. falciparum* at the erythrocytic stage

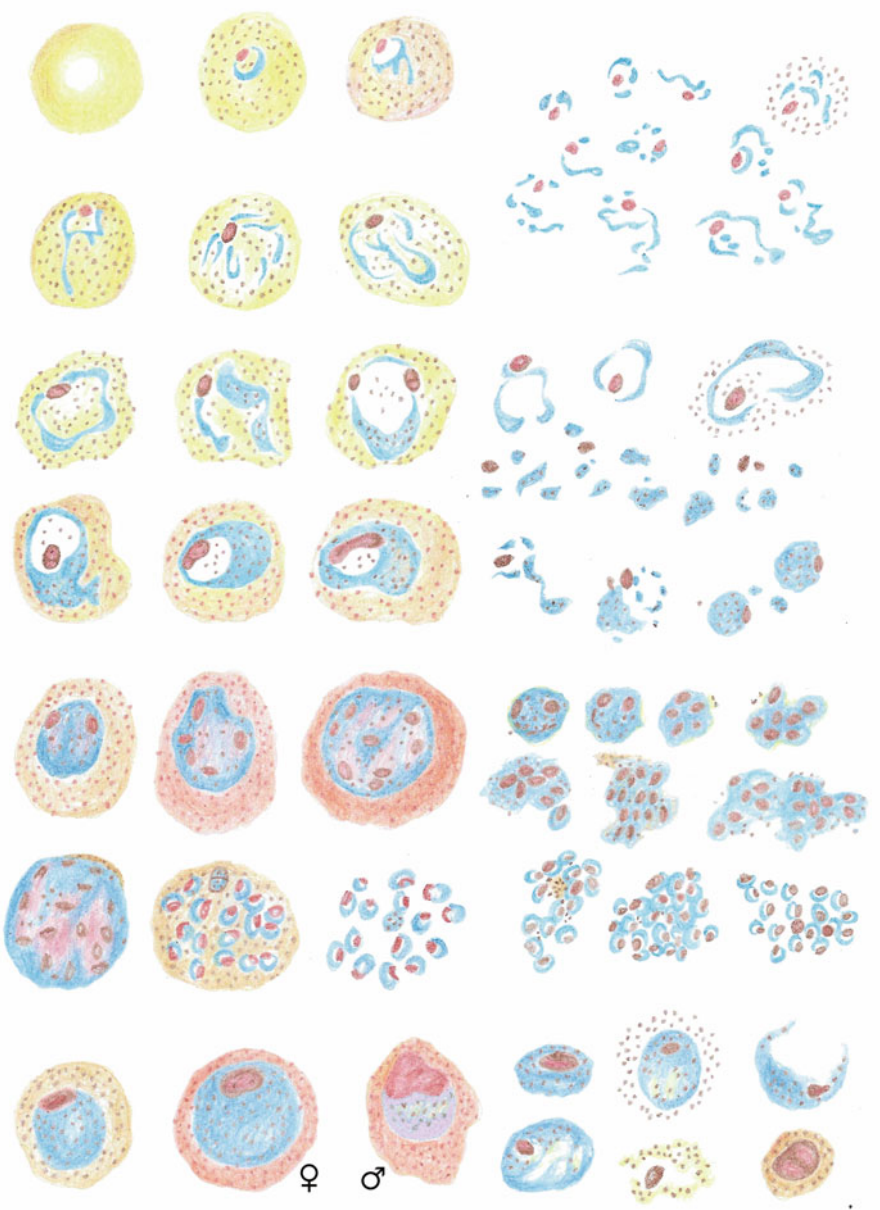


Fig. 4.6 Morphology of *P. vivax* at the erythrocytic stage

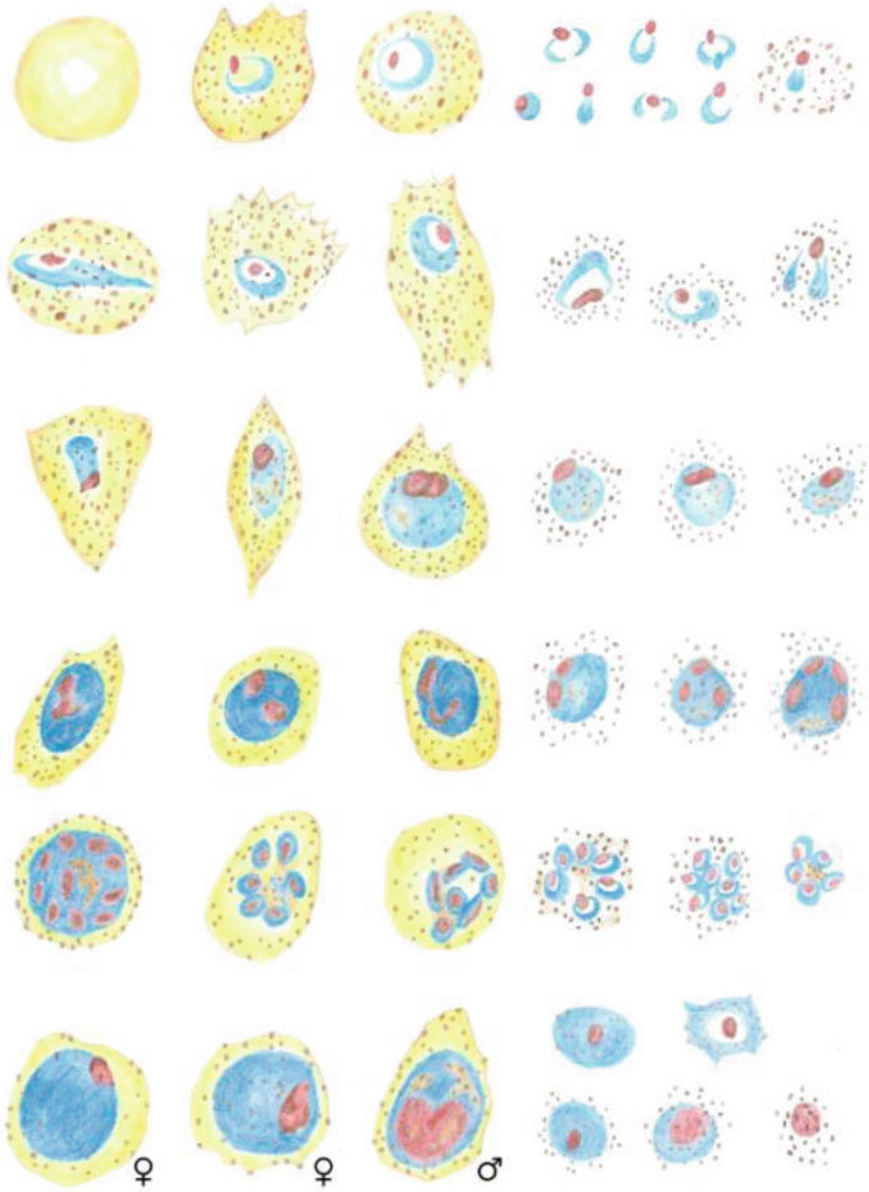


Fig. 4.7 Morphology of *P. ovale* at the erythrocytic stage

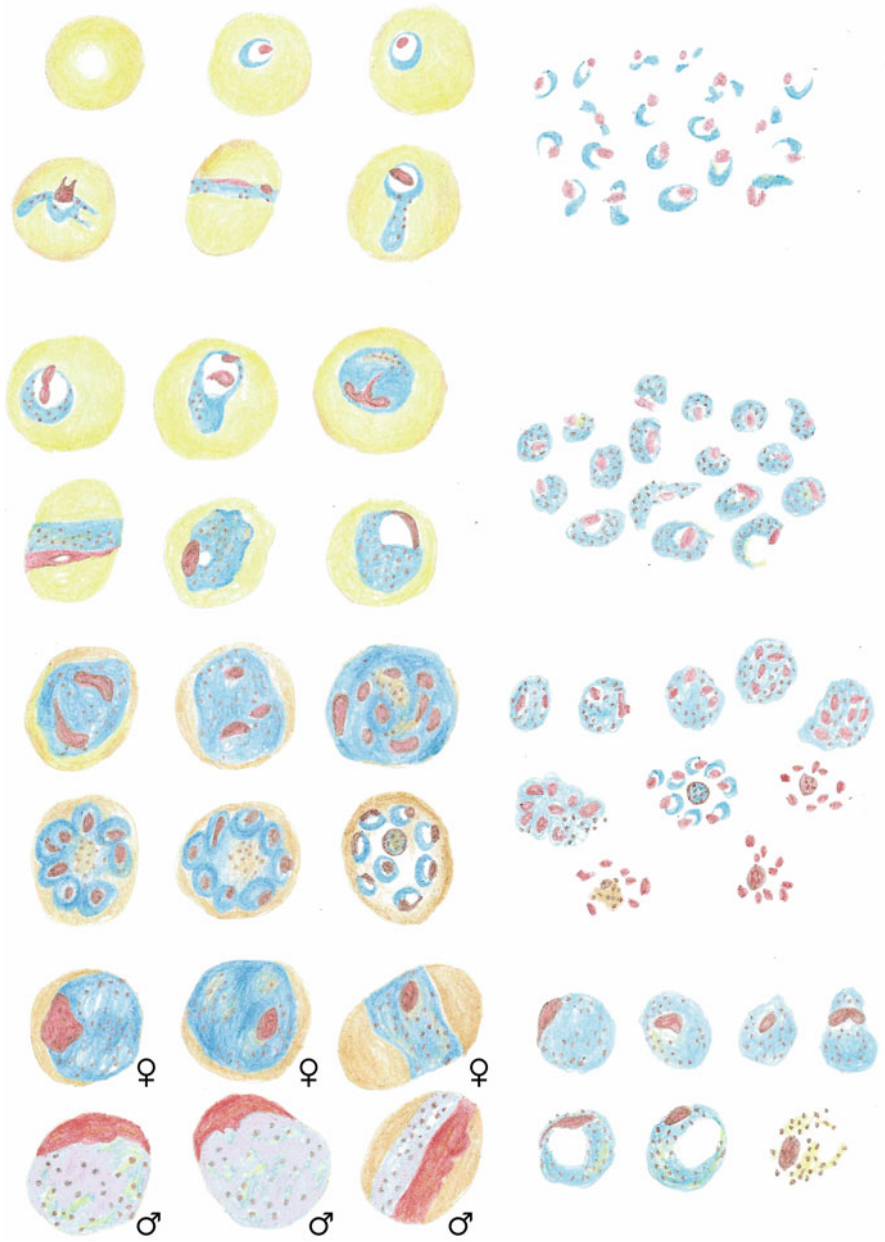


Fig. 4.8 Morphology of *P. malariae* at the erythrocytic stage

References

- Xinping C, Chuan S (2018) Human parasitology (9th edition). People's Medical Publishing House, Beijing, ISBN 978-7-117-26660-4. (in Chinese)
- Huaimin Z, Jun L, Wei Z (2006) Human natural infection of *Plasmodium knowlesi*. Chin J Parasitol Parasitic Dis 24(1):70–71. (in Chinese)
- Shaowu Z, Jiancheng H, Jingbo J (2000) The classification and list of malaria parasites. Chin J Health Lab Technol 10(2):249–256. (in Chinese)
- Sutherland CJ, Tanomsing N, Nolder D et al (2010) Two nonrecombining sympatric forms of the human malaria parasite *Plasmodium ovale* occur globally. J Infect Dis. 201(10):1544–1550. <https://doi.org/10.1086/652240>
- Xiaoqiu Q (2007) Malaria control manual (3rd edition). People's Medical Publishing House, Beijing, ISBN 978-7-117-08857-2. (in Chinese)



Pathogenesis and Clinical Features of Malaria

5

Huilong Chen

Abstract

Understanding the pathogenesis of malaria requires a detailed investigation of the mechanisms of *Plasmodium* invasion, *Plasmodium* biology, and host defense, and by understanding the life history of *Plasmodium*, the impact of *Plasmodium* and host interactions on each other can be elucidated. *Plasmodium falciparum* infection causes the most severe clinical manifestations, and its pathogenesis is the best studied. The clinical presentation of patients with malaria is closely related to the malaria parasites and varies according to local malaria epidemiology, the patient's immune status and age. Populations at high risk of malaria include infants and young children (6–59 months), where severe malaria can occur, and pregnant women, where anemia and low birth weight neonates may occur. In areas where malaria is transmitted year-round, older children and adults develop partial immunity after repeated infections and are therefore at relatively low risk of severe malaria. Treatment of malaria includes antimalarial treatment and symptomatic management, which is difficult given the pathophysiological changes in multiple organ systems involved in severe malaria. This topic will discuss in detail the pathogenesis and clinical features of malaria.

Keywords

Malaria · *Plasmodium* · Pathogenesis · Clinical manifestations · Treatment

H. Chen (✉)

Tongji Hospital, Tongji Medical College, Huazhong University of Science and Technology, Wuhan, China

5.1 Pathogenesis

5.1.1 Pathophysiology

All species of human *Plasmodium* that cause human infection may adhere to the surface of human cells at some point in their life history, but this period is short for all but *Plasmodium falciparum*: more than half of the 48-hour intraerythrocytic phase of *Plasmodium falciparum* is in adhere to the surface of human cells. Adherence to the surface of human cells is an important mechanism in the pathogenesis of *P. falciparum*. As *P. falciparum* matures from ring form to large trophozoites in erythrocytes, they induce the formation of adhesive bumps on the surface of erythrocytes (Newbold et al., 1999; Oh et al., 1997). These bumps consist of a combination of proteins produced by *Plasmodium falciparum* and human-derived proteins. These include *P. falciparum* erythrocyte membrane protein-1 (PFEMP-1; it is the product of *Var* gene expression and is currently considered to be the major cell adhesion factor), KAHRP, PFEMP-2, and PFEMP-3; human-derived proteins include hemosiderin, actin, and band 4.1 proteins (Sharma, 1991; Aikawa, 1988; Sharma, 1997). Each *P. falciparum* has more than 60 different *Var* genes, and the protein product of only one of these genes is present in a single *P. falciparum* (Chookajorn et al., 2008). This bump binds receptors on a variety of cells in the capillaries, including endothelial cells. Common receptors include the intercellular adhesion molecule (ICAM-1) located in the vascular endothelium and the endothelial protein c receptor (ePCR), CD36 on endothelium and platelets, and chondroitin sulfate A (CSA) on placenta (Maubert et al., 2000; Rogerson et al., 1999; Maubert et al., 1997; Chaiyaroj et al., 1996). Binding to the endothelium results in the isolation of *P. falciparum*-infected RBCs (iRBCs) from these small vessels, thus allowing *P. falciparum* to remain absent for a long period of life. The iRBCs are not present in the peripheral circulation for a long period of their life history, thus effectively preventing them from entering the spleen and being phagocytosed. When iRBCs adhere to uninfected red blood cells and form rose node-like masses, a rose node reaction, the masses block the microcirculation and contribute to microvascular disease (Chen et al., 2000). Isolation of iRBCs leads to partial blockage of blood flow, disruption of the endothelial barrier, inflammation, and abnormalities in coagulation. This pathology can occur in vital organs such as the brain, lungs, and kidneys, with the most severe clinical manifestations leading to cerebral malaria (Ponsford et al., 2012). The intravascular lysis of large numbers of *Plasmodium*-infected erythrocytes can lead to hyperhemoglobinemia with back pain, soy sauce-colored urine and, in severe cases, acute renal failure owing to mechanical obstruction of the renal vasculature caused by massive lysis of infected erythrocytes, and, of course, immune-mediated glomerulopathy and alterations in the renal microcirculation are likely to promote the development of renal failure as well (Das, 2008).

Solution of a vascular bed with *Plasmodium* allows for the accumulation of high levels of *Plasmodium* biomass in the host. HRP-2 is a secreted *Plasmodium falciparum* antigen expressed on the erythrocyte membrane, and its expression

indirectly reflects the amount of *Plasmodium* biomass in the circulation and isolated in microvascular structures. Studies suggest that plasma HRP-2 concentrations correlate with the severity of malaria (Dondorp, 2008).

5.1.2 Cytokines

The role of cytokines in the pathogenesis of malaria is extensive and complex. The cytokines TNF- α , IL-6, IL-10, IL-12, IL-18, and macrophage inflammatory protein-1 (MIP-1) are all expressed at elevated levels in malaria infection. However, the role of these cytokines in malaria is not fully understood. The “cytokine storm” hypothesis suggests that in severe malaria, damaging cytokines and small molecules become unregulated, leading to a systemic inflammatory response syndrome (SIRS)-like state with multiorgan and multisystem dysfunction (Fried et al., 2017). However, there is limited evidence of a direct association between severe malaria and SIRS.

Plasmodium infection of hepatocytes activates interferon regulatory factors (IRFs) and induces the secretion of type I interferons (IFNs), which increase the expression and secretion of chemokines by autocrine means, such as CXCL9 and CXCL10. CXCL9 and CXCL10 in turn chemotactically recruit immune cells expressing the chemokine receptor CXCR3, including NK cells, T cells, and NKT cells, to the liver, and these cells in turn inhibit intracellular *Plasmodium* expansion by secreting IFN- γ (Liehl et al., 2014).

Rupture of the exoerythrocytic schizonts releases thousands of merozoites into the bloodstream and invades red blood cells within seconds, with an extremely short exposure to immune cells. Intrinsic immunity is the body's first line of elimination and defense against *Plasmodium* infection, and iRBC rupture stimulates the release of proinflammatory cytokines, including TNF- α . Macrophages that have engulfed iRBCs do not secrete proinflammatory cytokines because of phagosomal acidification (Wu et al., 2015). iRBC rupture releases pathogen-associated molecular patterns (PAMPs) and danger-associated molecular patterns (DAMPs), including microvesicles, hemozoin, and glycosylphosphatidylinositols (GPIs). Dendritic cells (DCs) recognize these PAMPs and DAMPs through pattern recognition receptors (PRRs) and secrete IL-6, TNF- α , and IL-12, and DC-derived IL-12 in turn activates the secretion of IFN- γ by NK cells to activate the clearance of iRBCs (Wu et al., 2015; Stevenson & Riley, 2004). In addition to immune cells, TNF- α can also induce endothelial cell activation, promote chemokine secretion by endothelial cells, recruit inflammatory cells to locally damaged endothelial cells, and cause endothelial barrier damage (Viebig et al., 2005; Rénia et al., 2012).

5.1.3 Hemoglobin and Red Blood Cell Antigen

Hemoglobin and erythrocyte antigens can affect the body's ability to defend itself against malaria to varying degrees. In many parts of the world, the disease burden of malaria has been selected for a range of medically significant traits, including alleles

encoding hemoglobin (Hb), erythrocyte enzymes, and membrane proteins. The following hemoglobinopathies have been identified to defend against malaria infection: hemoglobin S (sickle cell hemoglobin) (Gong et al., 2012; Bunn, 2013); hemoglobin C (Travassos et al., 2015; Kreuels et al., 2010); hemoglobin SC disease (Lin et al., 1989); hemoglobin E (Nagel et al., 1981); hemoglobin F (fetal hemoglobin) (Pasvol et al., 1977); and α and β thalassaemia (Allen et al., 1997; Willcox et al., 1983). The defense mechanism for intraerythrocytic phase *P. falciparum* may involve one or more of the following mechanisms: (1) blocking the entry of merozoites into erythrocytes (Tiffert et al., 2005); (2) inhibition of the intracellular growth of *Plasmodium*; (3) prevention of erythrocyte lysis at the end of *Plasmodium* maturation, thereby preventing the release of merozoites into the circulation; (4) enhanced phagocytosis of iRBCs (Ayi et al., 2004; Bunyaratvej et al., 1986); (5) reduced adhesion of iRBCs to endothelial cells, uninfected erythrocytes, platelets or antigen-presenting cells; and (6) enhanced immune response to malaria infection. A number of potential mechanisms have been identified for hemoglobinopathy resistance to malaria, but it remains unclear which mechanisms play an important role in vivo. Genetic abnormalities in erythrocyte surface antigens and cytoskeletal proteins may also have a defensive role against malaria infection.

5.1.4 Immunity After Infection

Patients living in endemic areas appear to be partially immune to clinical episodes of malaria after repeated infections; the degree of protective immunity appears to be proportional to the intensity of transmission and increases with age (Dondorp et al., 2008). In areas where malaria is highly endemic (e.g., sub-Saharan Africa), near-complete clinical disease resistance is acquired by early adulthood. In low-transmission areas (e.g., Southeast Asia), however, individuals remain at risk of fatal malaria in adulthood and are referred to as “semi-immune.” Individuals infected with malaria in nonendemic areas (e.g., travelers) have a detectable antibody response; however, this response does not protect against initial malaria infection and is only a marker of previous infection (Doolan et al., 2009).

5.1.4.1 Humoral Immune Response

The humoral immune response to malaria appears to be slow, with gradual refinement in the presence of continuous stimulation by different *Plasmodium* species antigens. IgG4, IgE, and IgM are more markedly elevated in patients with severe malaria, while IgG (IgG, IgG1, IgG2, and IgG3) is more markedly elevated in individuals with mild malaria and asymptomatic infections (Leoratti et al., 2008). In addition, individuals who leave endemic areas appear to lose some humoral immune protection; these individuals are “semi-immune,” and their protection is diminished when they return to endemic areas after prolonged periods without *Plasmodium* antigenic stimulation.

5.1.4.2 Cellular Immune Response

The body can defend against hyperplasmidemia through the ability to generate a strong IFN- γ response (mainly via CD56+ γ T cells). (D’Ombrain et al., 2008) Phagocytosis of *Plasmodium* pigments and trophozoites impairs the ability of monocytes and macrophages to mount oxidative bursts, kill ingested pathogens, properly present antigens, and mature into functional dendritic cells. These cells produce TNF- α and other proinflammatory cytokines to mediate and amplify the immune response.

5.2 Clinical Manifestations

5.2.1 Incubation Period

The incubation period is the time between the entry of *Plasmodium* into the human body and the appearance of clinical symptoms and includes the time for the development of the exoerythrocytic phase and the proliferation of several generations of *Plasmodium* in the erythrocytic phase to reach a certain number. The length of the incubation period is related to *Plasmodium* species, the number of sporozoites entering the human body, and the immunity of the body. The incubation period was 7–27 days for *P. falciparum*, 11–25 days for *P. vivax*, 11–16 days for *P. ovale*, and 21–25 days for *P. malariae*. iRBCs release merozoites when they rupture, which can lead to chills, fever, and other clinical manifestations of malaria. Most people infected by *P. falciparum* develop clinical manifestations within 1 month, but longer incubation periods may occur in individuals with partial immunity. *P. vivax* and *P. ovale* are recurring types of *Plasmodium*, which also have an incubation period of approximately 2 weeks but can develop several months after the initial infection owing to activation of residual dormant substrates in the liver (Schwartz et al., 2003). Recurrence usually occurs 3–6 months after recovery. The incubation period for asymptomatic infection of *P. malariae* has been reported to persist for several years on an extremely rare basis. *P. falciparum* and *P. malariae* do not have a dormant period and therefore do not recur. *P. knowlesi* and *P. simium* are among the malaria parasites that infect nonhuman primates, but human infections have been reported in Southeast Asia and Brazil; microscopy and PCR show that *P. knowlesi* is similar to *P. malariae*, and *P. simium* is similar to *P. vivax* (Grigg & Snounou, 2017).

5.2.2 Clinical Manifestations

5.2.2.1 Uncomplicated Malaria

Patients with a positive pathogenic test and mild malaria symptoms are considered to have uncomplicated malaria if they do not show signs of severe malaria (Olliaro et al., 1996). The initial symptoms of malaria are usually nonspecific, including a variety of discomforts, such as fever, chills, malaise, sweating, headache, cough,

anorexia, nausea, vomiting, abdominal pain, diarrhea, arthralgia, and myalgia (Svenson et al., 1995). All *Plasmodium* parasites, including *P. falciparum*, can cause uncomplicated malaria. Early malaria infection usually presents with intermittent fever, typically with sudden onset of chills, high fever, and profuse sweating. In the later stages of infection, the infected red blood cells rupture, with simultaneous rupture of the schizonts and release of merozoites from the red blood cells. The interval is 48 h for *P. vivax* and *P. ovale*, 36–48 h for *P. falciparum* and approximately 72 h for *P. malariae*. *P. malariae* is considered to have more regular intervals than other *Plasmodium* species. With improvements in early diagnosis and treatment, the usual periodic fever is now rare. On examination, signs of anemia and an enlarged spleen that could be palpated under the ribs could be seen. Mild jaundice can occur in patients with falciparum malaria without other complications. Splenomegaly is common in usually healthy patients in high malaria areas and may be the result of repeated malaria infections or other infections. After multiple malaria infections, the spleen often atrophies due to infarction to the point where it is not palpable.

5.2.2.2 Severe Malaria

Clinical manifestations of severe malaria include impaired consciousness with or without seizures, acute respiratory distress syndrome (ARDS), circulatory failure, renal failure, hemoglobinuria, hepatic failure, circulatory failure, and coagulation disorders with or without disseminated intravascular coagulation, acidosis, and hypoglycemia (Trop Med Int Health, 2014; White, 1996).

Although most severe malaria with complications is caused by *P. falciparum*, *P. vivax* infection can also have serious complications. It has been reported that severe vivax malaria may also cause pulmonary complications and ARDS (McGready et al., 2014). High-risk groups of severe malaria include individuals without immunity, patients with impaired immune function (including those without spleen), children aged 6–59 months, and pregnant women (Steketee et al., 2001). The increase in the number of *Plasmodium* is related to the aggravation of the disease. Patients with partial immunity may have obvious parasitemia, but there is almost no obvious clinical manifestation.

Physical examination may include pale skin (severe anemia appearance), ecchymosis, jaundice, and hepatosplenomegaly. Laboratory examination results may include parasitemia (parasitized red blood cells $\geq 4\%$ –10%), anemia, thrombocytopenia, coagulation dysfunction, elevated transaminase, elevated creatinine, acidosis, and hypoglycemia. (McGready et al., 2014; Devarbhavi et al., 2005) Thrombocytopenia and severe anemia often suggest a poor prognosis. (Lampah et al., 2015)

Cerebral malaria is characterized by impaired consciousness, delirium, and seizures. The symptoms of patients may develop slowly or suddenly after convulsions. Its severity depends on a variety of factors, including the species and pathogenicity of *Plasmodium*, host immune response and timely treatment. Risk factors for cerebral malaria include age (children and the elderly), pregnancy, malnutrition, HIV infection, previous history of splenectomy, and host genetic susceptibility. Cerebral malaria is more common in adults without immunization

than in residents in malaria-endemic areas, while cerebral malaria is more common in children in malaria-endemic areas (Hochman et al., 2015; Idro et al., 2007; Ranque et al., 2005; Reyburn et al., 2005). The mortality rate of cerebral malaria is 15%–20%. If treatment is not timely, cerebral malaria can quickly progress to coma or even death. There are more cerebral sequelae in children (approximately 15%) than in adult patients (approximately 3%). Residual defects may include hemiplegia, deafness, epilepsy, language defects, and cognitive impairment. (Mung'Ala-Odera et al., 2004) These sequelae are more common when accompanied by other complications, including severe anemia, hypoglycemia, and acidosis. Postmalarial nervous system syndrome is an autoimmune encephalitis that occurs within 2 months after treatment, and remission of cerebral malaria often manifests as seizures.

ARDS may occur in adults with severe falciparum malaria, and its mechanism is not completely clear. However, it may be related to the isolation of parasitic red blood cells and cytokine-induced alveolar capillary leakage (Taylor et al., 2012). ARDS can even be seen days after antimalarial treatment. In addition to falciparum malaria, ARDS can also be seen in patients with vivax malaria without other complications.

Acute renal injury and even renal failure often occur in severe *P. falciparum* malaria in adults and are less common in children (Conroy et al., 2016). The pathogenesis of renal failure is not completely determined, but it may be closely related to the interference of red blood cell isolation with renal microcirculation blood flow and metabolism. Other possible pathophysiological mechanisms include low blood volume and mechanical obstruction caused by hemolysis. When intravascular hemolysis occurs, a large amount of hemoglobin and malarial pigments may appear in urine, and its mortality is high.

Acidosis is an important cause of death in patients with severe malaria, which can be caused by a variety of factors, including *Plasmodium* isolation interfering with microcirculatory blood flow, causing anaerobic fermentation of host tissue; *Plasmodium* producing lactate; low blood volume; and severe acidosis, often suggesting poor prognosis.

Hypoglycemia is a common complication of severe malaria. The mechanism of hypoglycemia involves the reduction of hepatic gluconeogenesis, the depletion of hepatic glycogen reserve, and the increase of host glucose consumption. Hypoglycemia can lead to poor prognosis, especially for children and pregnant women.

New onset malaria infection is often accompanied by a sudden decrease in hemoglobin concentration, which is related to increased hemolysis and bone marrow suppression. Children with multiple episodes of malaria infection may develop chronic severe anemia in malaria-endemic areas. The mechanisms of anemia in malaria patients include the following: hemolysis of parasitic red blood cells; the isolation and clearance of red blood cells increased in spleen; cytokines inhibit hematopoiesis; red blood cell life shortened; repeated infection and ineffective treatment (Boele van Hensbroek et al., 2010). Anemia caused by falciparum malaria is usually characterized by anemia of positive cells and positive pigments, but reticulocytes are significantly reduced (Roberts et al., 2005). Mild falciparum

malaria often causes mild thrombocytopenia and coagulation disorders. Some patients with severe malaria will have bleeding and even disseminated intravascular coagulation (DIC) (Angchaisuksiri, 2014).

Malaria patients often have mild jaundice due to hemolysis. Severe jaundice can occur in falciparum malaria infection. The causes are hemolysis, hepatocyte injury, and cholestasis. The incidence in adults is higher than that in children. If liver dysfunction is combined with renal injury and other organ dysfunction, it indicates a poor prognosis (Woodford et al., 2018).

5.2.2.3 Malaria Infection During Pregnancy

Compared with nonpregnant women, patients during pregnancy are more prone to severe malaria, such as hypoglycemia and respiratory complications (pulmonary edema and ARDS) (Trans R Soc Trop Med Hyg, 1990). Anemia is a common complication of malaria during pregnancy, and approximately 60% of pregnant women infected with malaria have anemia (Espinoza et al., 2005). Pregnant women are particularly susceptible to *P. falciparum* infection. Infected red blood cells can stay in the placenta, resulting in adverse effects on the fetus, which may be prone to adverse pregnancy outcomes, including spontaneous abortion, premature birth, fetal growth restriction/low birth weight (LBW), stillbirth, congenital infection, and neonatal death. In addition, during treatment, if the antimalarial drugs in the placenta cannot reach the treatment level, the *Plasmodium* retained here may be intermittently released into the peripheral blood, resulting in maternal recurrent infection (Cohee et al., 2016).

5.2.2.4 Recurrent Malaria Infection

The causes of malaria recurrence are treatment failure (resurgence) or reinfection, which are difficult to identify. Both resurgence and relapse showed that the disease recurred after recovery. Resurgence most often occurs in a few days or weeks, and relapse often occurs after months. Resurgence is caused by ineffective treatment, and some *Plasmodium* will remain in the bloodstream. At the time of relapse, the dormant forms are resuscitated in hepatocytes, causing *Plasmodium* parasitemia again. *P. falciparum* infection is a common cause of resurgence, and *P. vivax* and *P. ovale* can reinitiate a few months after the initial infection is cured (usually 3–6 months) because they have dormant forms.

5.3 Treatment

The most important thing in the treatment of malaria is the killing of *Plasmodium* in red blood cells. The choice of antimalarial drugs is based on whether the block is falciparum malaria, the density of *Plasmodium* in the blood, the severity of the disease, whether it comes from a drug-resistant endemic area, the local type of *Plasmodium* resistance, and the availability of local drugs. The World Health Organization (WHO) recommends the use of a combination of an artemisinin derivative and another effective antimalarial drug as the most effective and currently

available method to avoid the development of *Plasmodium* resistance. In addition to antimalarial treatment, symptomatic supportive treatment is critical, especially for severe malaria with severe complications. The basic treatment includes the following aspects: bed rest during the attack and 24 h after the fever subsides, pay attention to vomiting and diarrhea patients by appropriate rehydration, pay attention to warmth when chills are present, physical cooling can be used when fever is present, patients with high fever can be treated with nonsteroidal anti-inflammatory drugs such as ibuprofen and acetaminophen to reduce temperature or glucocorticoids to reduce fever, and patients with serious conditions should be closely monitored for vital signs and water intake and output should be accurately recorded. The patient should be isolated according to insect-borne infectious diseases.

5.3.1 Treatment of Uncomplicated Falciparum Malaria

Uncomplicated falciparum malaria is defined as *P. falciparum* infection with less than 4% parasitemia and no symptoms associated with severe malaria. Hospitalization allows for observation of patient tolerance of antimalarial therapy, monitoring of remission of parasitemia, and further treatment of patients who progress to severe malaria. The following groups may deteriorate rapidly and require consideration of hospitalization, including infants and young children; those with compromised immune function; those without acquired immunity to *Plasmodium*; and those with hyperplasmidemia (4%–10%) without severe manifestations who are vulnerable to the development of severe malaria and may be at risk of treatment failure (World Health Organization, 2015). Therefore, antimalarial treatment should be initiated as soon as possible.

5.3.2 Treatment of Severe Malaria

Severe cases of falciparum malaria are defined by the WHO as the presence of *Plasmodium falciparum* parasitemia in a patient with at least 1 of the following:

- I. Impaired consciousness: Adult Glasgow Coma Score (GCS) <11 or Child–Pugh Coma Score <3.
- II. Poor general condition: General weakness, having to rely on assistance to sit, stand or walk.
- III. Multiple convulsions (>2 episodes in 24 h).
- IV. Acidosis: Alkali surplus >8 mEq/L, plasma bicarbonate level <15 mmol/L or venous plasma lactate \geq 5 mmol/L.
- V. Hypoglycemia: Blood or plasma glucose <2.2 mmol/L (<40 mg/dL).
- VI. Severe anemia: Hemoglobin \leq 5 g/dL or hematocrit \leq 15% in children under 12 years (<7 g/dL or < 20% in adults, respectively) with a *Plasmodium* count >10,000/ μ L.

- VII. Renal impairment: Plasma or serum creatinine $>265 \mu\text{mol/L}$ (3 mg/dL) or blood urea $>20 \text{ mmol/L}$.
- VIII. Jaundice: Plasma or serum bilirubin $>50 \mu\text{mol/L}$ (3 mg/dL) and *Plasmodium* count $>100,000/\mu\text{L}$ (parasitism rate approximately 2%).
- IX. Pulmonary edema: This may be determined by imaging examination, or oxygen saturation $<92\%$ on breathing room air and a respiratory rate >30 breaths/min, often with chest depression and auscultatory twanging.
- X. Significant bleeding: Including repeated or prolonged bleeding from the nose, gums, or venipuncture sites; vomiting blood or black stools.
- XI. Shock: Compensated shock defined as capillary refill time ≥ 3 seconds or presence of a temperature gradient in the leg (mid to proximal) without hypotension. Decompensated shock is defined as a systolic blood pressure $<70 \text{ mmHg}$ in children or $<80 \text{ mmHg}$ in adults with evidence of impaired perfusion (syncope of the extremities or prolonged capillary reperfusion time).
- XII. Hyperplasmodiumemia: Parasitism rate $>10\%$ (or *P. falciparum* density $500,000/\mu\text{L}$).

To reduce the morbidity and mortality of cerebral or severe malaria, a comprehensive treatment approach is needed. Therefore, in addition to the timely initiation of antimalarial treatment for severe malaria, other treatments, including supportive care, symptomatic management, treatment of complications, and enhanced care and prevention of coinfection treatment, are particularly critical for patients with severe malaria.

5.3.2.1 Antimalarial Treatment

The treatment of patients with severe malaria, particularly cerebral malaria, requires the use of rapidly insecticidal antimalarials, administered intramuscularly or intravenously. The choice of antimalarial regimen can be found in Chap. 10.

5.3.2.2 Supporting Treatment

Fluids should be given in appropriate amounts to provide adequate energy, correct metabolic acidosis, and maintain water–electrolyte balance. Give a liquid or semi-liquid diet to those with poor appetite and gradually transition to a high-protein diet during the recovery period and iron supplements to those with anemia.

5.3.2.3 Symptomatic Management and Management of Complications

- I. Fever: Physical cooling (cold towels or ice packs), acetaminophen, or small doses of glucocorticoids may be used to reduce fever in patients with high fever, and ice blankets may be considered to reduce fever if it persists. Attention should be given to rehydration during fever reduction to prevent hypotensive shock due to excessive sweating during fever reduction.
- II. Cerebral edema: Cerebral edema and coma often occur in cerebral malaria and should be treated promptly with dehydration and commonly used clinical dehydrating agents, including mannitol and glycerol fructose.

- III. **Epilepsy:** Seizures can occur in up to 70% of children with severe malaria. Seizures may be generalized or focal, and clinical manifestations may be subtle, such as nystagmus and irregular breathing. In addition to cerebral malaria, other causes of seizures (e.g., hypoglycemia and fever) need to be assessed and managed accordingly. Benzodiazepines are useful first-line drugs for the treatment of seizures, and commonly used drugs include diazepam and lorazepam. If benzodiazepines do not control the seizures, phenobarbital may be given for maintenance.
- IV. **Hypoglycemia:** Hypoglycemia is a common complication of malaria and is a hallmark of severe malaria; it should be suspected in any patient who is comatose or whose condition suddenly deteriorates. Clinical signs of hypoglycemia include seizures and altered consciousness, so blood glucose concentrations should be routinely assessed, preferably with bedside blood glucose monitoring. Intravenous access should be established rapidly in hypoglycemic patients, followed by rapid administration of glucose (10% dextrose). For recurrent hypoglycemia, continuous infusion of 50% high glucose solution by bedside infusion micropump may be considered.
- V. **Hemolytic anemia:** Glucocorticoids are recommended; pay attention to hydration and diuresis, and alkalize the urine with an appropriate amount of sodium bicarbonate infusion; exclude other causes of hemolysis other than the primary disease, such as stopping the use of drugs that may cause hemolysis, such as quinine, primaquine, and other antimalarial drugs; consider transfusion if appropriate for severe anemia, use calcium gluconate or glucocorticoids before transfusion. For patients with severe jaundice, liver protection, and anti-yellowness drugs may be used as appropriate.
- VI. **Shock:** Patients with severe malaria are often hypovolemic. When low peripheral perfusion occurs, including hypotension and cold extremities, a high alert should be given for infectious shock and fluid resuscitation, supplementation of crystalloids and colloids, and the use of vasoactive drugs such as norepinephrine and dopamine should be used as appropriate.
- VII. **Metabolic acidosis:** Consider supplementation with 5% sodium bicarbonate solution for mild metabolic acidosis and continuous renal replacement therapy (CRRT) for severe metabolic acidosis.
- VIII. **Renal injury:** Patients with severe malaria should be closely monitored for urine output, renal function, and urinary routine. Mild kidney injury may be treated with renal protection medication as appropriate. If renal failure is diagnosed, fluid intake should be strictly limited, and if necessary, dialysis should be administered promptly.
- IX. **ARDS:** Patients with severe malaria can also have ARDS. Oxygen therapy can be administered, and noninvasive mechanical ventilation or even invasive mechanical ventilation should be considered if nasal cannula oxygenation fails to correct hypoxemia.
- X. **Coinfection:** Coinfection with bacteria is an important contributor to complications and death in patients with severe malaria. When there is a high clinical suspicion of bacterial infection, empirical antibiotic therapy

should be available, and blood bacterial cultures should be performed promptly.

5.3.3 Treatment of Malaria in Pregnancy

Malaria in pregnancy is an important cause of maternal complications worldwide and can also lead to adverse birth outcomes. Pregnant women are more likely than nonpregnant women to develop complications from malaria infection. Malaria in pregnancy can have serious consequences for both the mother and fetus; therefore, pregnant women with malaria infection should be treated immediately with effective antimalarial drugs to rapidly eliminate the malaria parasite. There are limited data on safety and efficacy to guide treatment and even fewer data on safety in the fetus. Treatment decisions, therefore, need to take into account the clinical severity of the infection, epidemiological resistance patterns, and available information on the safety of a drug or class of drugs used during pregnancy. Amniotic fluid volume, fetal size, and general fetal health should be closely monitored during acute clinical malaria episodes.

References

- Aikawa M (1988) Morphological changes in erythrocytes induced by malarial parasites. *Biol Cell* 64(2):173–181
- Allen SJ, O'Donnell A, Alexander ND et al (1997) alpha+-Thalassemia protects children against disease caused by other infections as well as malaria. *Proc Natl Acad Sci U S A* 94(26): 14736–14741
- Angchaisuksiri P (2014) Coagulopathy in malaria. *Thromb Res* 133(1):5–9
- Ayi K, Turrini F, Piga A, Arese P (2004) Enhanced phagocytosis of ring-parasitized mutant erythrocytes: a common mechanism that may explain protection against falciparum malaria in sickle trait and beta-thalassemia trait. *Blood* 104(10):3364–3371
- Boele van Hensbroek M, Calis JC, Phiri KS et al (2010) Pathophysiological mechanisms of severe anaemia in Malawian children. *PLoS One* 5(9):e12589
- Bunn HF (2013) The triumph of good over evil: protection by the sickle gene against malaria. *Blood* 121(1):20–25
- Bunyaratvej A, Butthep P, Yuthavong Y et al (1986) Increased phagocytosis of Plasmodium falciparum-infected erythrocytes with haemoglobin E by peripheral blood monocytes. *Acta Haematol* 76(2-3):155–158
- Chaiyaroj SC, Angkasekwinai P, Buranakiti A, Looareesuwan S, Rogerson SJ, Brown GV (1996) Cytoadherence characteristics of Plasmodium falciparum isolates from Thailand: evidence for chondroitin sulfate a as a cytoadherence receptor. *Am J Trop Med Hyg* 55(1):76–80
- Chen Q, Schlichtherle M, Wahlgren M (2000) Molecular aspects of severe malaria. *Clin Microbiol Rev* 13(3):439–450
- Chookajorn T, Ponsuwanna P, Cui L (2008) Mutually exclusive var gene expression in the malaria parasite: multiple layers of regulation. *Trends Parasitol* 24(10):455–461
- Cohee LM, Kalilani-Phiri L, Mawindo P et al (2016) Parasite dynamics in the peripheral blood and the placenta during pregnancy-associated malaria infection. *Malar J* 15(1):483
- Conroy AL, Hawkes M, Elphinstone RE et al (2016) Acute kidney injury is common in pediatric severe malaria and is associated with increased mortality. *Open Forum Infect Dis* 3(2):ofw046

- D'Ombra MC, Robinson LJ, Stanicic DI et al (2008) Association of early interferon-gamma production with immunity to clinical malaria: a longitudinal study among Papua New Guinean children. *Clin Infect Dis* 47(11):1380–1387
- Das BS (2008) Renal failure in malaria. *J Vector Borne Dis* 45(2):83–97
- Devarbhavi H, Alvares JF, Kumar KS (2005) Severe falciparum malaria simulating fulminant hepatic failure. *Mayo Clin Proc* 80(3):355–358
- Dondorp AM (2008) Clinical significance of sequestration in adults with severe malaria. *Transfus Clin Biol* 15(1-2):56–57
- Dondorp AM, Lee SJ, Faiz MA et al (2008) The relationship between age and the manifestations of and mortality associated with severe malaria. *Clin Infect Dis* 47(2):151–157
- Doolan DL, Dobaño C, Baird JK (2009) Acquired immunity to malaria. *Clin Microbiol Rev* 22(1): 13–36, Table of Contents.
- Espinoza E, Hidalgo L, Chedraui P (2005) The effect of malarial infection on maternal-fetal outcome in Ecuador. *J Matern Fetal Neonatal Med* 18(2):101–105
- Fried M, Kurtis JD, Swihart B et al (2017) Systemic inflammatory response to malaria during pregnancy is associated with pregnancy loss and preterm delivery. *Clin Infect Dis* 65(10): 1729–1735
- Gong L, Maiteki-Sebuguzi C, Rosenthal PJ et al (2012) Evidence for both innate and acquired mechanisms of protection from *Plasmodium falciparum* in children with sickle cell trait. *Blood* 119(16):3808–3814
- Grigg MJ, Snounou G (2017) *Plasmodium simium*: a Brazilian focus of anthrozoönotic vivax malaria? *Lancet Glob Health* 5(10):e961–e9e2
- Hochman SE, Madaline TF, Wassmer SC et al (2015) Fatal pediatric cerebral malaria is associated with intravascular monocytes and platelets that are increased with HIV coinfection. *mBio* 6(5): e01390–e01315
- Idro R, Ndiritu M, Ogutu B et al (2007) Burden, features, and outcome of neurological involvement in acute falciparum malaria in Kenyan children. *JAMA* 297(20):2232–2240
- Kreuels B, Kreuzberg C, Kobbe R et al (2010) Differing effects of HbS and HbC traits on uncomplicated falciparum malaria, anemia, and child growth. *Blood* 115(22):4551–4558
- Lampah DA, Yeo TW, Malloy M et al (2015) Severe malarial thrombocytopenia: a risk factor for mortality in Papua, Indonesia. *J Infect Dis* 211(4):623–634
- Leoratti FM, Durlacher RR, Lacerda MV et al (2008) Pattern of humoral immune response to *Plasmodium falciparum* blood stages in individuals presenting different clinical expressions of malaria. *Malar J* 7:186
- Liehl P, Zuzarte-Luís V, Chan J et al (2014) Host-cell sensors for *Plasmodium* activate innate immunity against liver-stage infection. *Nat Med* 20(1):47–53
- Lin MJ, Nagel RL, Hirsch RE (1989) Acceleration of hemoglobin C crystallization by hemoglobin S. *Blood* 74(5):1823–1825
- Maubert B, Fievet N, Tami G, Boudin C, Deloron P (2000) Cytoadherence of *Plasmodium falciparum*-infected erythrocytes in the human placenta. *Parasite Immunol* 22(4):191–199
- Maubert B, Guilbert LJ, Deloron P (1997) Cytoadherence of *Plasmodium falciparum* to intercellular adhesion molecule 1 and chondroitin-4-sulfate expressed by the syncytiotrophoblast in the human placenta. *Infect Immun* 65(4):1251–1257
- McGready R, Wongsan K, Chu CS et al (2014) Uncomplicated *Plasmodium vivax* malaria in pregnancy associated with mortality from acute respiratory distress syndrome. *Malar J* 13:191
- Mung'Ala-Odera V, Snow RW, Newton CR (2004) The burden of the neurocognitive impairment associated with *Plasmodium falciparum* malaria in sub-saharan Africa. *Am J Trop Med Hyg* 71(2 Suppl):64–70
- Nagel RL, Raventos-Suarez C, Fabry ME, Tanowitz H, Sicard D, Labie D (1981) Impairment of the growth of *Plasmodium falciparum* in HbEE erythrocytes. *J Clin Invest* 68(1):303–305
- Newbold C, Craig A, Kyes S, Rowe A, Fernandez-Reyes D, Fagan T (1999) Cytoadherence, pathogenesis and the infected red cell surface in *Plasmodium falciparum*. *Int J Parasitol* 29(6): 927–937

- Oh SS, Chishti AH, Palek J, Liu SC (1997) Erythrocyte membrane alterations in *Plasmodium falciparum* malaria sequestration. *Curr Opin Hematol* 4(2):148–154
- Olliaro P, Nevill C, LeBras J et al (1996) Systematic review of amodiaquine treatment in uncomplicated malaria. *Lancet* 348(9036):1196–1201
- Pasvol G, Weatherall DJ, Wilson RJ (1977) Effects of foetal haemoglobin on susceptibility of red cells to *Plasmodium falciparum*. *Nature* 270(5633):171–173
- Ponsford MJ, Medana IM, Prapansilp P et al (2012) Sequestration and microvascular congestion are associated with coma in human cerebral malaria. *J Infect Dis* 205(4):663–671
- Ranque S, Safeukui I, Poudiougou B et al (2005) Familial aggregation of cerebral malaria and severe malarial anemia. *J Infect Dis* 191(5):799–804
- Rénia L, Howland SW, Claser C et al (2012) Cerebral malaria: mysteries at the blood-brain barrier. *Virulence* 3(2):193–201
- Reyburn H, Mbatia R, Drakeley C et al (2005) Association of transmission intensity and age with clinical manifestations and case fatality of severe *Plasmodium falciparum* malaria. *JAMA* 293(12):1461–1470
- Roberts DJ, Casals-Pascual C, Weatherall DJ (2005) The clinical and pathophysiological features of malarial anaemia. *Curr Top Microbiol Immunol* 295:137–167
- Rogerson SJ, Tembenu R, Dobaño C, Plitt S, Taylor TE, Molyneux ME (1999) Cytoadherence characteristics of *Plasmodium falciparum*-infected erythrocytes from Malawian children with severe and uncomplicated malaria. *Am J Trop Med Hyg* 61(3):467–472
- Schwartz E, Parise M, Kozarsky P, Cetron M (2003) Delayed onset of malaria—implications for chemoprophylaxis in travelers. *N Engl J Med* 349(16):1510–1516
- Sharma YD (1991) Knobs, knob proteins and cytoadherence in falciparum malaria. *Int J Biochem* 23(9):775–789
- Sharma YD (1997) Knob proteins in falciparum malaria. *Indian J Med Res* 106:53–62
- Steketee RW, Nahlen BL, Parise ME, Menendez C (2001) The burden of malaria in pregnancy in malaria-endemic areas. *Am J Trop Med Hyg* 64(1–2 Suppl):28–35
- Stevenson MM, Riley EM (2004) Innate immunity to malaria. *Nat Rev Immunol* 4(3):169–180
- Svenson JE, MacLean JD, Gyorkos TW, Keystone J (1995) Imported malaria. Clinical presentation and examination of symptomatic travelers. *Arch Intern Med* 155(8):861–868
- Taylor WRJ, Hanson J, Turner GDH, White NJ, Dondorp AM (2012) Respiratory manifestations of malaria. *Chest* 142(2):492–505
- Tiffert T, Lew VL, Ginsburg H, Krugliak M, Croisille L, Mohandas N (2005) The hydration state of human red blood cells and their susceptibility to invasion by *Plasmodium falciparum*. *Blood* 105(12):4853–4860
- (1990) Severe and complicated malaria. World Health Organization, Division of Control of Tropical Diseases. *Trans R Soc Trop Med Hyg* 84(Suppl 2):1–65
- Travassos MA, Coulibaly D, Laurens MB et al (2015) Hemoglobin C trait provides protection from clinical falciparum malaria in malian children. *J Infect Dis* 212(11):1778–1786
- (2014) Severe malaria. *Trop Med Int Health* 19(Suppl 1):7–131
- Viebig NK, Wulbrand U, Förster R, Andrews KT, Lanzer M, Knolle PA (2005) Direct activation of human endothelial cells by *Plasmodium falciparum*-infected erythrocytes. *Infect Immun* 73(6):3271–3277
- White NJ (1996) The treatment of malaria. *N Engl J Med* 335(11):800–806
- Willcox M, Björkman A, Brohult J (1983) Falciparum malaria and beta-thalassaemia trait in northern Liberia. *Ann Trop Med Parasitol* 77(4):335–347
- Woodford J, Shanks GD, Griffin P, Chalons S, McCarthy JS (2018) The dynamics of liver function test abnormalities after malaria infection: a retrospective observational study. *Am J Trop Med Hyg* 98(4):1113–1119
- World Health Organization (2015) WHO Guidelines Approved by the Guidelines Review Committee. Guidelines for the treatment of malaria. World Health Organization, Geneva. Copyright © World Health Organization 2015.

Wu X, Gowda N, Gowda D (2015) Phagosomal acidification prevents macrophage inflammatory cytokine production to malaria, and dendritic cells are the major source at the early stages of infection: IMPLICATION FOR MALARIA PROTECTIVE IMMUNITY DEVELOPMENT. *J Biol Chem* 290(38):23135–23147



Morphology of Malaria Parasites at the Erythrocytic Stage

6

Kai Wu

Abstract

Microscopy is the gold standard for the laboratory diagnosis of malaria and has the advantages of being rapid, easy to perform, and inexpensive. The aim of microscopic examination is the successful identification of erythrocytic *Plasmodium*, but the ability to correctly and effectively detect *Plasmodium* has always been a difficult task for testers due to the wide variation in *Plasmodium* morphology. This chapter provides a detailed analysis of the basic principles of preparation and staining and the morphological characteristics of the four *Plasmodium* species in the erythrocytic phase in thick and thin blood smears under the microscope to help testers improve the efficiency and quality of microscopy.

Keywords

Microscopic examination · Technical ability · Morphology · Atlas

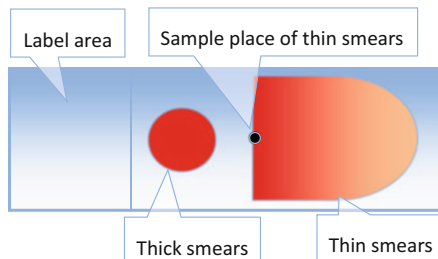
6.1 Microscopic Examination Skills of *Plasmodium*

6.1.1 Preparation and Staining of Blood Smears

Preparation and staining of a blood smear are the foundation of microscopic examination and have a significant impact on the subsequent microscopic examinations of *Plasmodium*, which must be performed carefully. The quality of the smears needs to be optimized by many practices daily. At the same time, anticoagulated blood samples left too long can lead to agglutination, shrinkage, jaggedness, heterogeneity, and hemolysis of RBCs, as well as morphological changes and decay of

K. Wu (✉)
Hubei, Wuhan City, China

Fig. 6.1 Location and morphology of blood smears



Plasmodium, which can affect the determination of microscopic results. Therefore, anticoagulated blood samples should be prepared and stained as soon as possible after collection from the patients. By using Giemsa staining as a standard, the entire process of preparation and staining is explained in this section.

- I. Thick and thin blood smears can be prepared simultaneously on one slide. There is an option to take blood samples directly from the finger or earlobe using a blood collection needle or to use anticoagulation (EDTA or heparin anticoagulation). The volume of blood samples must be strictly limited; 4–5 μL of blood samples are recommended for the preparation of thick blood smears, and 1–2 μL of blood samples are recommended for the preparation of thin blood smears. If too much blood is used, both thick and thin smears may fall off during hemolysis, staining, and rinsing. Excessive blood also prolongs the drying time of thick blood smears and the accumulation of cascading RBCs in thin blood smears. It is not conducive to *Plasmodium* staining, while the darker background also affects microscopic identification. However, malaria patients often show varying degrees of anemia, e.g., when the hematocrit is less than 25% or the hemoglobin is less than 85 g/L or even lower, it is recommended that the anticoagulated blood be left to stand for approximately 15 min, and then deposited RBCs are collected for blood smear preparation. Otherwise, the thick smears are straight forward to fall off during subsequent hemolysis, staining, and rinsing.
- II. Two clean slides are prepared with one for pushing (smooth edges on all four sides of the slide are required) and another for blood smears. The blood smear is divided into three areas, from left to right, in order of label area, thick blood smear, and thin blood smear (Fig. 6.1). In preparation for a thick blood smear, 4–5 μL blood approaching the label area is dripped on the slide, and a corner of the pushing slide is drawn evenly to form a circle around the blood 0.8–1 cm in diameter (Fig. 6.2). In preparation of a thin blood smear, 1–2 μL blood is dripped in the middle of the slide at a distance of approximately 0.5 cm from the thick blood smear at the sample place shown in Fig. 6.1. The short or long side of the pushing slide is chosen according to personal habits, and the blood will spread to both sides within 1–2 seconds when the pushing edge is in contact and connected with the smear slide plane. Push it out at an angle of approximately 30°, either vertical (Fig. 6.3) or parallel (Fig. 6.4), in a way that is 2.5 cm

Fig. 6.2 Preparation of a thick blood smear

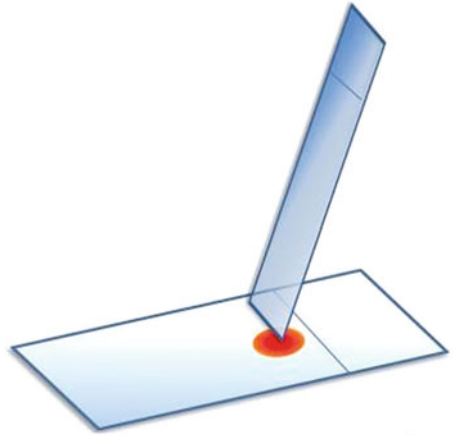


Fig. 6.3 Preparation of a thin blood smear using the vertical pushing method

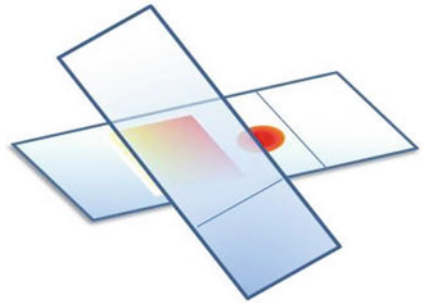
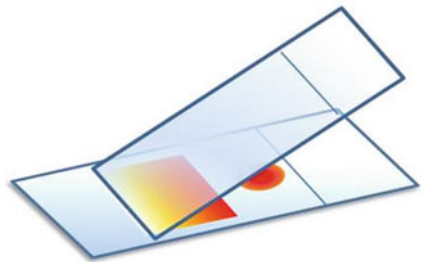


Fig. 6.4 Preparation of a thin blood smear using the parallel pushing method



long of thin blood smear. It is preferable to push out the tongue-like tail, and RBCs should not be stacked under the microscope. If the angle between the blood slide and the pushing slide is small, the thin smear will be long, the RBCs will lay flat, and the RBC gap will be enlarged with a small angle. In contrast, the thin smear will be short, and the RBC gap will be tight or even stacked.

III. The thick blood smear must be naturally dried, while exposure and baking are strictly prohibited. The duration of drying is mainly affected by temperature and humidity. When the temperature is high and dry, the drying time is short, and

conversely, the drying time is longer. If needed, you can also use approximately 25 °C wind or cool wind to promote drying. Finger blood and earlobe blood can be hemolysis and staining immediately after observed drying as there is no anticoagulant, whereas anticoagulant blood takes longer to dry and a time of no less than 30 min is recommended to avoid thick blood smears falling off. Notably, dry storage should be done in such a way as to avoid the adhesion of impurities such as external dust, the parasitic growth of miscellaneous bacteria, and insect intake. Hemolysis must be completed within 48 h in summer and 72 h in winter; otherwise, the thick blood smear may not experience hemolysis because of natural drying and fixation.

- IV. Anhydrous methanol (or anhydrous ethanol) is used for the fixation of thin blood smears (please note that the thick blood smear cannot be fixed at this moment). The thick blood smears are hemolyzed with distilled water, tap water, and water without impurities after the methanol on the thin blood film is completely dry. Water stored for a long period of time is prohibited for use because of the potential presence of microorganisms. Hemolysis is complete when the thick blood smear is milky translucent. Handle the waste fluid after hemolysis carefully to avoid shedding of the thick blood smear, and the blood smears are stained after the second cycle of natural drying. The main component of the working solution for Giemsa staining is water, and in emergency situations, hemolysis of thick blood smears can be skipped, and thin blood smears can be fixed and taken directly to step V using hemolysis while staining. However, this method will result in a deep background of thick blood smears and produce more interfering substances (Fig. 6.7), which may affect the microscopic results.
- V. The Giemsa stock solution should be diluted into a working solution by phosphate buffer solution (PBS) before staining, and a 2–3% concentration is recommended (commercial Giemsa working solution concentrations diluted according to instructions). If the concentration is high, the coloring is deep, and the staining time can be shortened appropriately, Schüffner's dots and Maurer's clefts can be stained. Conversely, the coloring is light, and the staining time is long, but the *Plasmodium* are evenly colored and clear, which facilitates the observation of the internal structure. It can also be diluted with distilled water, pure water, tap water, and other unadulterated water if PBS is not available. The duration of staining was not less than 30 min for *P. falciparum* and 45 min to 1 h for *P. vivax*, *P. ovale*, and *P. malariae* to achieve complete staining of the nucleus, cytoplasm, and malarial pigments. For other rapid staining used in clinical hospitals, such as Wright-Giemsa staining solution, due to its high methanol content, thick blood films should be hemolysis, dried, and then stained according to the steps in the product instructions.

The Giemsa stock solution is configured by placing 10 g of Giemsa powder in a mortar, adding a small amount of glycerol one at a time, grinding as you go, until 500 ml of glycerol is added, and then pouring into a 1-liter narrow-mouth brown bottle. Rinse the residue from the mortar one at a time with an appropriate amount of

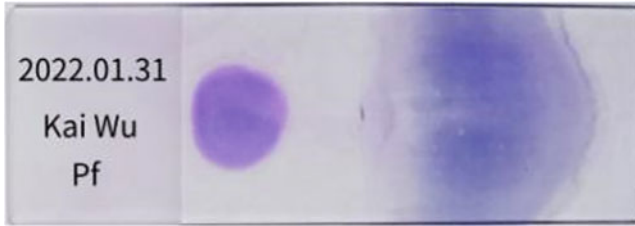


Fig. 6.5 Blood smears of *Plasmodium* on a slide (Giemsa staining)

methanol; pour the rinsed liquid into the same brown bottle until 500 ml of methanol is used. The brown bottle was sealed, shaken well, and placed in a cool place away from light, and then the 1-liter Giemsa stock solution was prepared. It is recommended to use analytical purity for the Giemsa powder, glycerol, and methanol. The prepared stock solution is shaken for a few minutes daily, and after the Giemsa powder has fully dissolved (recommended 30 days), it can be filtered through to remove coarse impurities before use.

VI. At the time of the staining, rinse with distilled, purified, or tap water that is free of impurities. Avoid thick and thin blood smears being rinsed off.

After completion of the staining procedure, the labeling area was marked with the date of the test, the name of the subject, and the results of the test immediately after the microscopic examination (Fig. 6.5). If multiple samples are stained at the same time, they should be marked in the labeling area before smearing. After staining, the smear was dried naturally and stored.

A standard *Plasmodium* blood smear contains a thick and thin blood smear for microscopic examinations. From left to right, the label area, the thick blood smear, and the thin blood smear (Kai et al. 2021).

6.1.2 *Plasmodium* Counting Methods

Hyperparasitemia is an important risk factor for the development of severe malaria. Therefore, *Plasmodium* counting can help guide the type, dose, and course of antimalarial drugs used in clinical treatment. If *Plasmodium* density is high or hyperparasitemia has occurred, treatment with injection should be prioritized to reduce the density as soon as possible, the total dose should be increased, and the course of treatment should be extended to ensure complete clearance of *Plasmodium*. *Plasmodium* should be observed under a 100× oil microscope, examining blood smears sequentially from left to right and top to bottom (Fig. 6.6), avoiding concentration of counts in one area. Thick blood smears are often used for qualification and counting of the sample being examined, while thin blood smears are often used to identify the species and to observe morphology. At least 100 fields

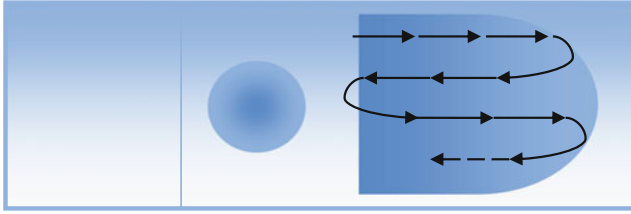


Fig. 6.6 Microscopic examination track

of view of the thick smear were examined before the sample was determined to be negative. In exceptional cases, where very low density may be present, the thick smear should be examined for 200 fields, or the entire thick smear should be examined if necessary.

I. Quantitative count of *Plasmodium* on thick blood smear.

If a count is made on a thick blood smear, the number of white blood cells (WBCs) per microliter of blood needs to be known. When the first *Plasmodium* was captured, all *Plasmodium* and WBCs were counted in each field. If the density of *Plasmodium* is high, a count of 100–200 WBCs is sufficient, but if the density of *Plasmodium* is low, a count of 1000 WBCs is needed. If WBC count is not available, it is calculated as 6, 000 or 8000 WBCs per microliter of blood. *P. falciparum* is prone to hyperparasitemia, and in thick blood smears, the *P. falciparum* rings appear to be full of stars, making counting difficult (Fig. 6.28). In this case, a thin blood smear is used for counting *Plasmodium*. *Plasmodium* density was calculated using the following formula:

$$\begin{aligned} \text{Number of } Plasmodium \text{ in per microliter of blood} &= \frac{\text{Plasmodium}}{\text{WBCs}} \\ &\times \text{Number of WBCs in per microliter of blood} \end{aligned}$$

II. Quantitative count of *Plasmodium* on thin blood smear

If a count is made on the thin blood smear, the number of RBCs per microliter of blood needs to be known, and it is also calculated by males with five million RBCs and females with 4.5 million RBCs per microliter of blood. *Plasmodium* density was calculated using the following formula. When the first *Plasmodium* was captured, all *Plasmodium* and RBCs in each field were counted. If the density of *Plasmodium* was high, up to 1000 RBCs were counted for the parasitic rate; if the density of *Plasmodium* was low, up to 2000 RBCs were counted and examined more if necessary. The parasitic rate of *Plasmodium* varies considerably in different areas of the field on thin smears and should be counted equally in different areas.

Number of *Plasmodium* in per microliter of blood = Parasitism rate of RBCs
× Number of RBCs in per microliter of blood

III. Simple counting method

The distribution of WBCs and *Plasmodium* in thick blood smears can also be uneven, causing some bias in the counts. Sometimes, clinical treatment needs to provide *Plasmodium* density results as soon as possible for reference. Therefore, a quick and easy method of counting can be used. When the first *Plasmodium* was captured, it began to count all *Plasmodium* and WBCs in this field, then space the five fields without counting, and count all *Plasmodium* and WBCs in the sixth field. If there were only *Plasmodium* and no WBCs in the field, the actual number of *Plasmodium* was recorded, while WBCs were recorded as 0. Conversely, record the actual number of WBCs and *Plasmodium* as 0. Record approximately 40–50 fields and use the formula in I above to calculate *Plasmodium* density (Xiaoqiu 2007).

6.1.3 Advantages and Disadvantages of Thick and Thin Blood Smears

- I. Thin blood smear: *Plasmodium* has typical morphology, is easy to recognize and identify, can also be based on the morphology of the pRBCs and is less affected by impurities in the blood smear. However, when the density is low, the distribution of *Plasmodium* is scattered and difficult to detect.
- II. Thick blood smear: With a large volume of blood and a small area, the detection efficiency of *Plasmodium* is approximately 10–30 times higher than that of thin blood smear when RBCs are concentrated. *Plasmodium* is, therefore, easily detected and takes less time. However, thick blood smears have a deep background, lysed RBCs and altered morphology of *Plasmodium*, making it more difficult to distinguish between species.

After treatment with antimalarial drugs, the density of *Plasmodium* decreases rapidly and dramatically, the morphology is altered, and the structure is fragmented, making thin smears difficult to detect.

6.1.4 Identification of Interfering Substances in Blood Smears with *Plasmodium*

During the preparation and staining process, various types of interferences, such as exogenous dust, fungal spores, vegetative cells, stain residues, contaminated other microorganisms, and endogenous blood cell debris, are inevitably present in the blood smears. When the *Plasmodium* morphology is typical and density is higher, it has minimal impact on microscopic identification. However, at lower densities, it

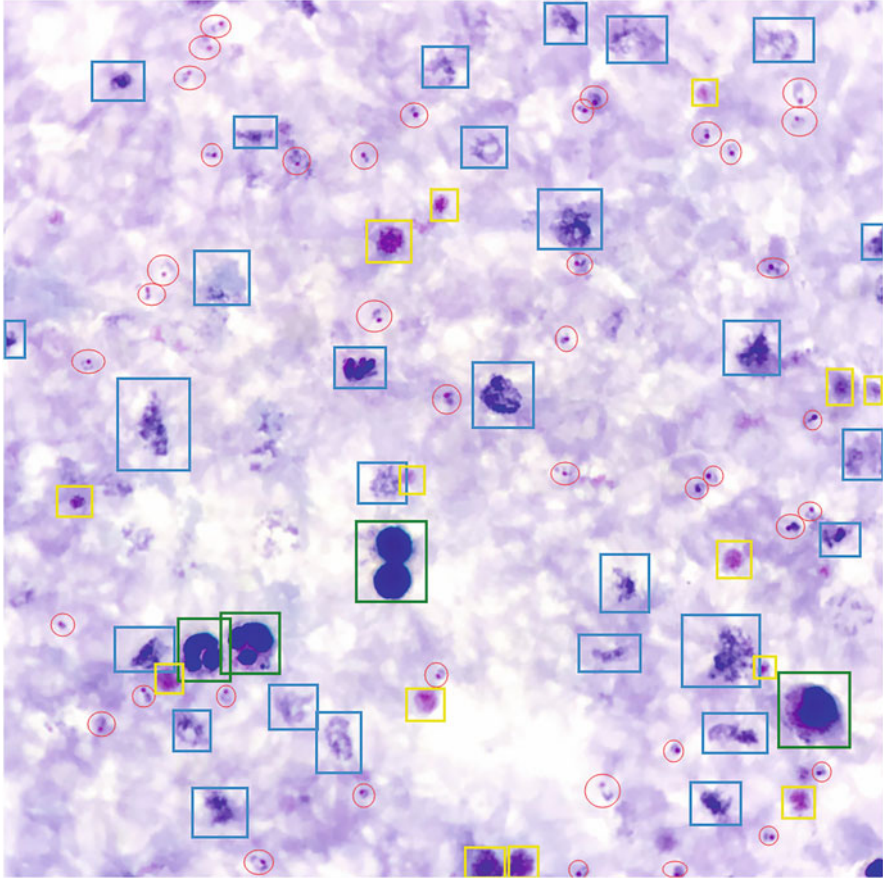


Fig. 6.7 *Plasmodium* and interferences in thick blood smears

can affect microscopic identification and lead to misdiagnosis. In addition, thick blood smears are more affected by interferences than thin blood smears (Fig. 6.7), and it is particularly difficult to distinguish between the nucleus of low-density *P. falciparum* rings and interferences.

During Giemsa staining, if the staining and hemolysis of thick blood smears are synchronous, more interference is produced, and the background is generally darker, which adversely affects the microscopic results when the density is low. The blood cell debris and stain residue produced during hemolysis are shown in the blue box, WBCs are shown in the green box, platelets are shown in the yellow box, and *P. falciparum* rings are shown in the red circle.

- I. Suspected malarial pigments: The residue of staining solution and dust inside the blood smears are often yellowish or dark brown (Fig. 6.8), likely to be mistaken as malarial pigments. The residue and dust particles are generally large and vary in

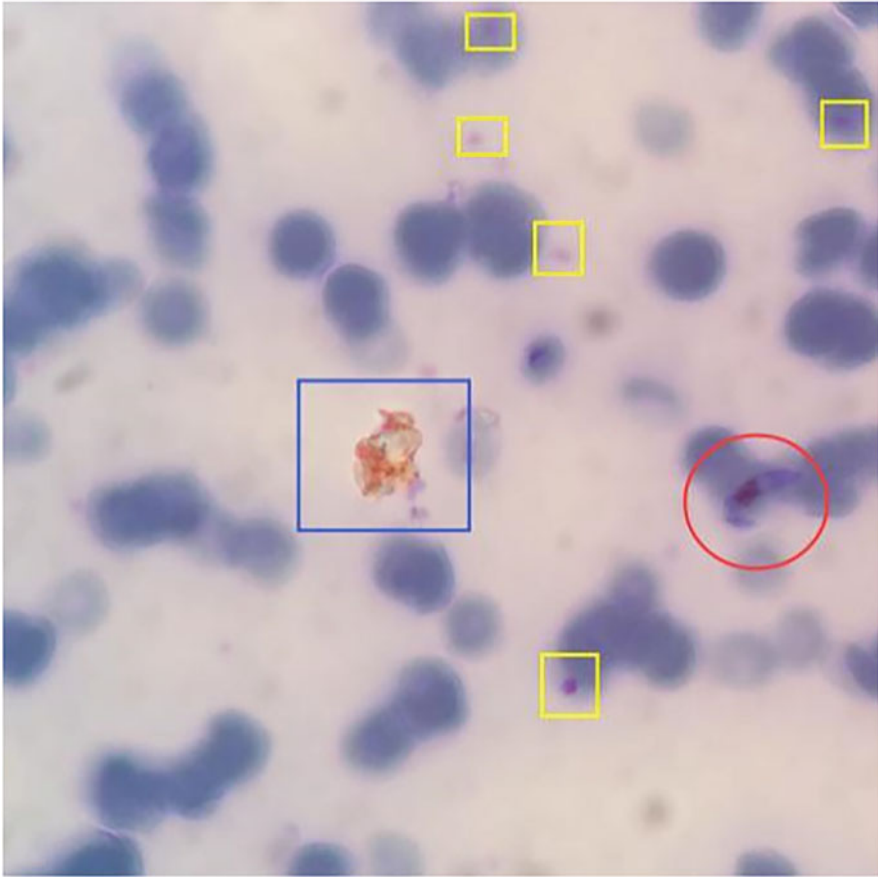


Fig. 6.8 Suspected malaria pigments and *Plasmodium*

size and shape, with abrupt and patchy edges, large distribution and the same type of impurities visible outside the surrounding RBCs. It may be distinguished based on particle size, color, and distribution range. If you turn the slight quasi-focal spiral of the microscope, you may see that the residue of staining solution and dust float above RBCs but not on the same plane as the *Plasmodium*.

The *P. falciparum* female gametocyte is shown in the red circle, and platelets are shown in the yellow box. The brownish-yellow impurity shown in the blue box, which floats above the RBCs, is larger in size, has a disorganized morphology, and has uneven coloring.

II. Suspected *Plasmodium* nucleus: The lysis particles released by bacteria, especially cocci and WBCs, may also appear as red-stained dots, which are likely mistaken as the nucleus of small trophozoites of *Plasmodium*. The Howell-Jolly

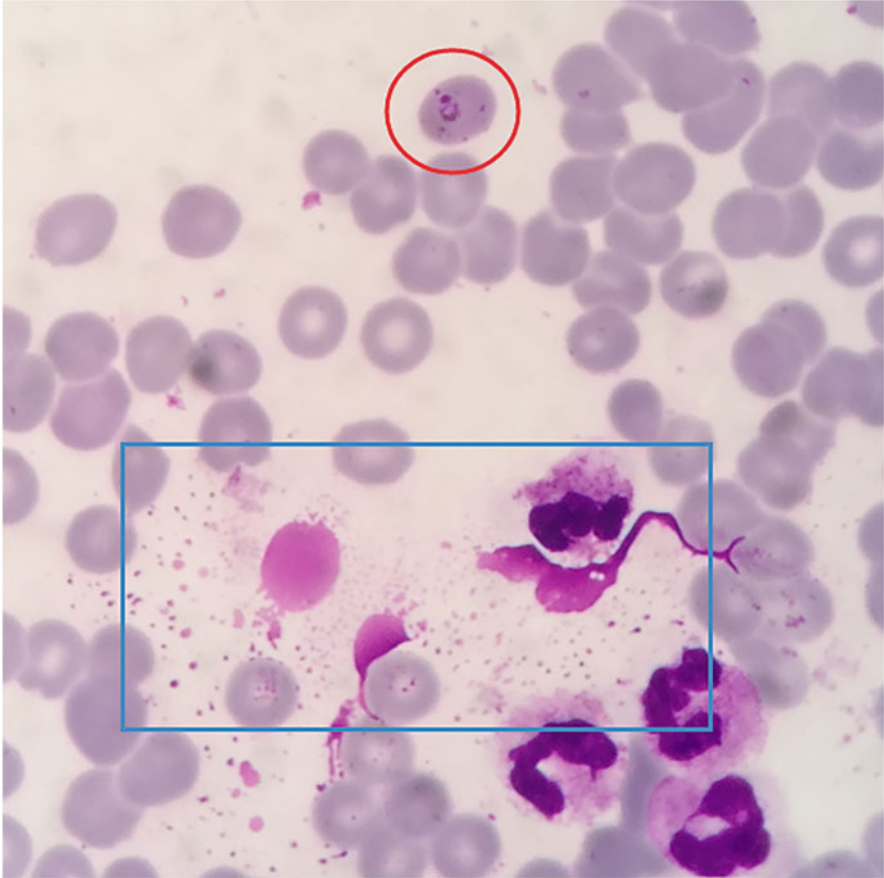


Fig. 6.9 WBC fragments and *Plasmodium*

and Pappenheimer bodies present in anemia are also similar to the nucleus of *P. falciparum*. The nuclei of *P. falciparum* rings are densely colored, reflective, and brightly conspicuous under the microscope. However, the cocci are large in shape and have smooth edges and are often clustered with a wide distribution. The neutrophil and eosinophil particles are lightly colored with neat edges, with WBC debris nearby (Fig. 6.9).

A small trophozoite of *P. falciparum* in pRBCs is shown in the red circle, and the WBC fragments are shown in the blue box. The fragment dots are also red, but they are located outside RBCs, vary in size, are distributed widely and are lightly colored.

III. Suspected *Plasmodium* cytoplasm: The residues of reticulocytes and nuclei of WBCs are usually blue-stained and similar to *Plasmodium* cytoplasm (Fig. 6.7). They are likely to be mistaken as *Plasmodium* due to the presence of red dots.

However, reticulocytes and WBCs often have dark blue nuclei and are large and dense in color. If it resembles large trophozoites, it may be distinguished according to whether the pigments or not and pigment characteristics. If it resembles small trophozoites, it may be determined according to the trophozoite size, whether the refraction is uniform, and whether the nucleus and cytoplasm are on the same plane.

6.2 Morphology of *Plasmodium falciparum*

6.2.1 Small Trophozoites of *P. falciparum* in Thin Blood Smears

The morphology of the small trophozoites of *P. falciparum* is shown in Figs. 6.10, 6.11, and 6.12.

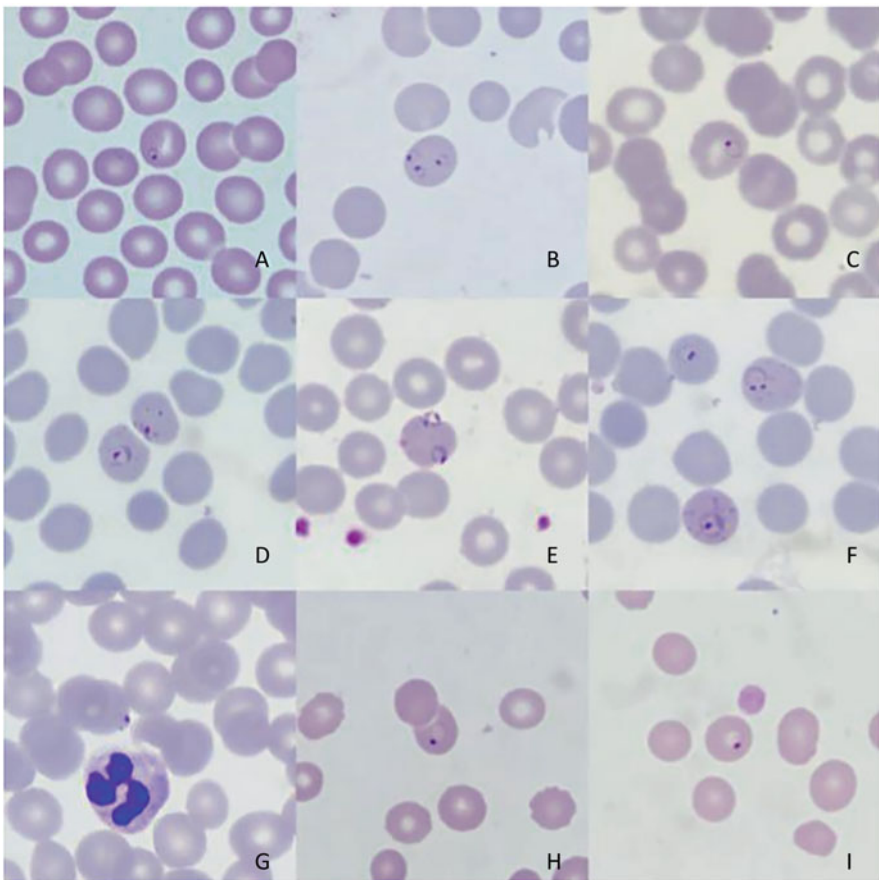


Fig. 6.10 *P. falciparum* small trophozoite (H, I by Wright-Giemsa staining and others by Giemsa staining, $\times 1,000$)

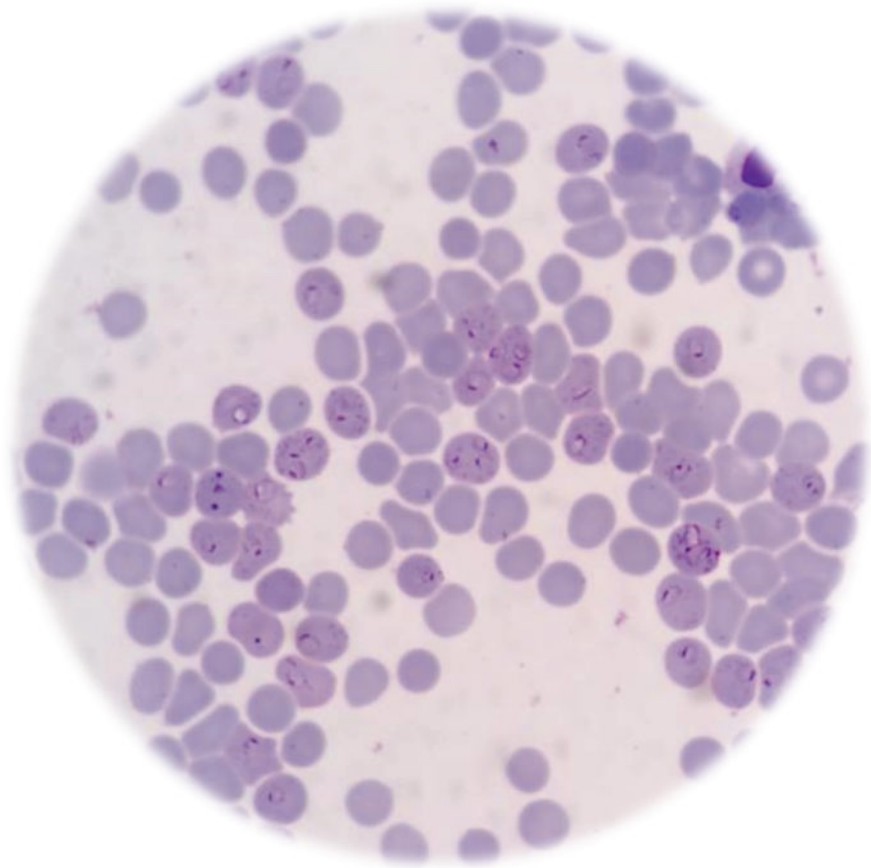


Fig. 6.11 Maurer's clefts of *P. falciparum* (Giemsa staining, $\times 1,000$)

P. falciparum small trophozoite, also known as the former trophozoite, is the most common stage and the key to the identification of *P. falciparum*. After staining, the nucleus is red or dark red, round or oval, small and dense; the cytoplasm is blue, relatively regularly round or oval, forming a ring-like (A–I) or earphone-like (D) shape with the nucleus. For this reason, small trophozoites are also known as ring forms. The size of the ring form varies. When they invade RBCs initially, the ring is small and slender, occupying one-fifth of the pRBCs (AB); as they develop, the ring becomes progressively larger and thicker, occupying up to more than one-third of the pRBCs (DHI), and Maurer's clefts (DF) appear inside the pRBCs, characterized by "thick, few and unevenly distributed." Multiple infections (BEs) are common in *P. falciparum* infection. Rings often protrude from the edge of RBCs (DEG). Sometimes the ring is only partially visible due to slender cytoplasm, the use of antimalarial drugs or staining (G); sometimes the ring is faintly visible or only the nucleus is visible, but there are areas of light or uncolored vacuoles formed by ring

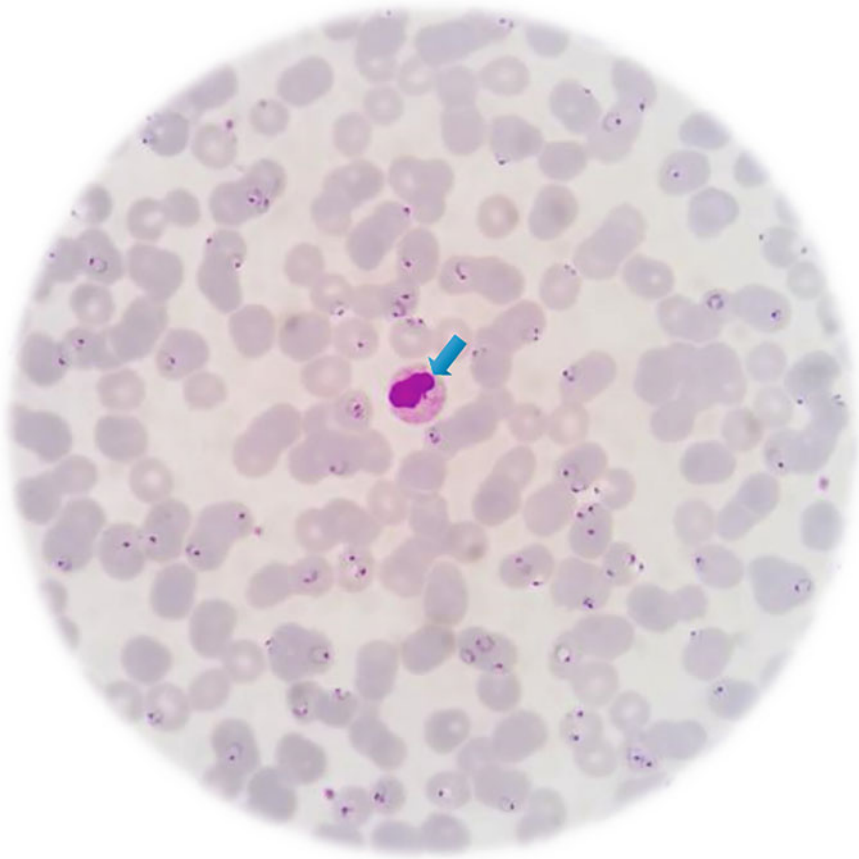


Fig. 6.12 High parasitemia (Giemsa staining, $\times 1,000$)

occupancy within the pRBCs (HI). *P. falciparum* can parasitize all types of RBCs, mainly mature RBCs, and the morphology and size of the pRBCs are generally normal. The red arrows indicate platelets and the blue arrows indicate neutrophils.

Red Maurer's clefts appear in RBCs infected with *P. falciparum*, which are characterized by coarseness, small quantity, and uneven distribution. The appearance of Maurer's clefts is related to the infection intensity, course of the disease, and staining quality. The pRBCs are darker in color than the surrounding RBCs.

High parasitemia frequently occurs in the case of falciparum malaria with a high parasite rate and multiple severe infections. Timely treatment is effective in preventing the development of severe cases. A neutrophilic late juvenile granulocyte is shown by the blue arrow.

6.2.2 Large Trophozoites of *P. falciparum* in Thin Blood Smears

The morphology of the large trophozoites of *P. falciparum* is shown in Figs. 6.13, 6.14, 6.15, 6.16, and 6.17.

Large trophozoites of *P. falciparum* develop from small trophozoites, also known as late trophozoites or mature trophozoites, and are usually accumulated in internal organs such as blood sinuses where blood flow is slow and rare in peripheral blood. When the nucleus and cytoplasm of small trophozoites are enlarged, vacuolated areas tend to fill up, malarial pigments begin to appear and integrate gradually into a brown or black-brown “block” (A-I), which indicates that the small trophozoites develop into large trophozoites. Their cytoplasm is enlarged and thick, and the nucleus and malarial pigments are wrapped in the cytoplasm. The shape is relatively regular (ABDEGHI), or it can also be deformed (CE). Round blocky malarial pigments are remarkable, often 1, occasionally 2. The pRBCs are darker, generally

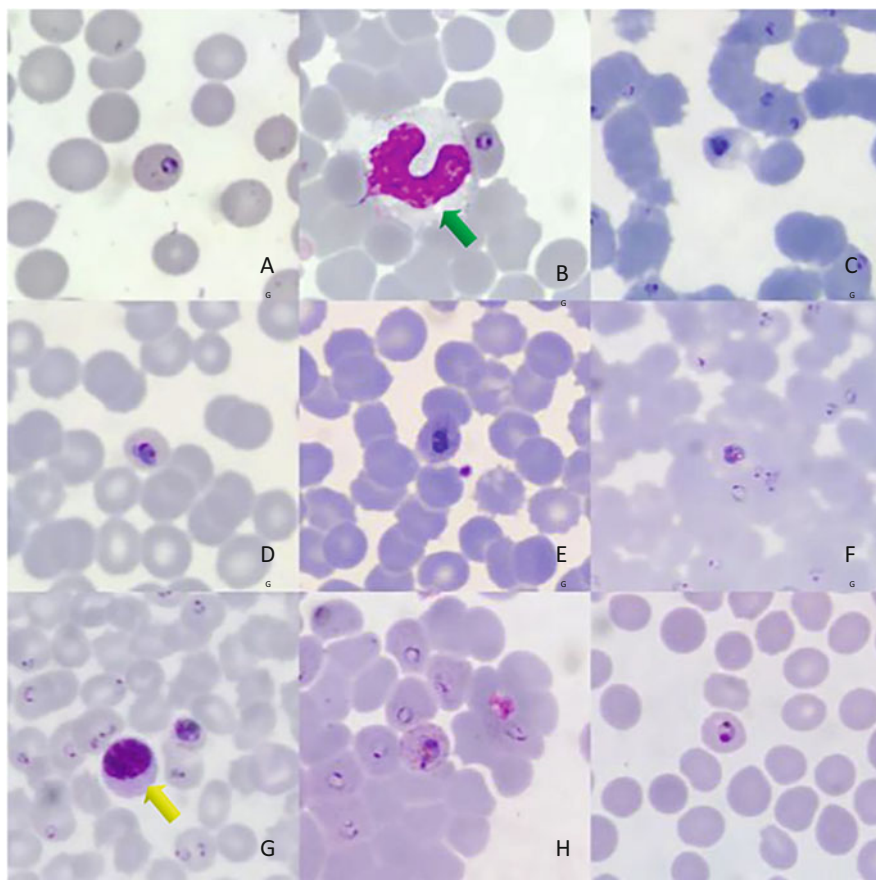


Fig. 6.13 Large trophozoite (Giemsa staining, $\times 1000$)

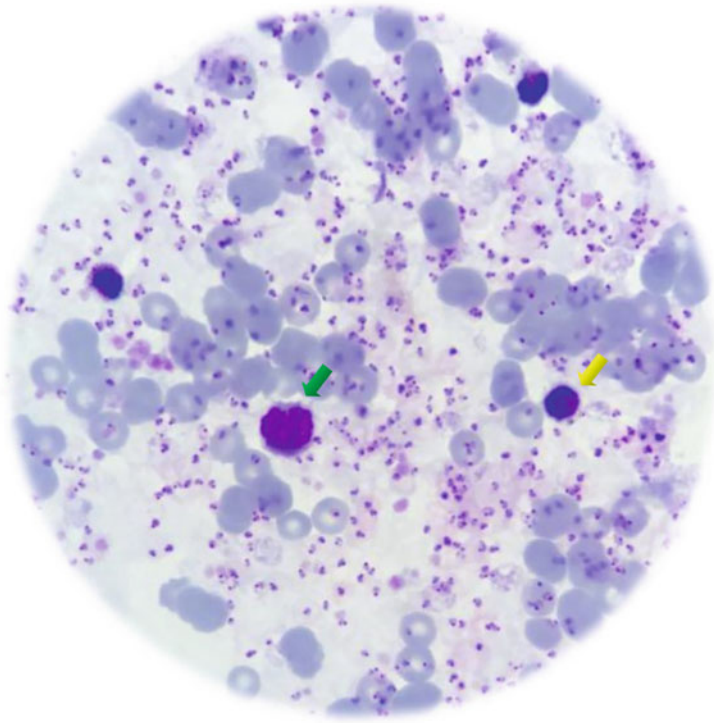


Fig. 6.14 Large trophozoites of *P. falciparum* on a thin blood smear (Giemsa staining, $\times 1000$)

normal in size and morphology, but can be slightly distorted, distended, or distorted by compression of surrounding blood cells (BI). The most remarkable feature of severe or worsening falciparum malaria is the presence of a large number of large trophozoites in peripheral blood. The early morphology of the immature gametophytes of *P. falciparum* is also round or oval, similar in morphology and size to the large trophozoites and more difficult to distinguish. The nucleus of the gametophytes is usually in the center of the cytoplasm, and the malaria pigment is usually yellowish or brownish granular and surrounds the nucleus (Fig. 6.21 a,b,c). The yellow arrows point to lymphocytes and the blue arrows to neutrophils.

Large trophozoites seem to be located outside RBCs because of hemolysis. Meanwhile, RBCs are scarce and aggregate together in a long chain. This is one of the representative characteristics seen in severe cases. Monocytes are indicated by green arrows, and lymphocytes are indicated by yellow arrows.

Plasmodium is deformed, small in size, and has a high parasite rate. The morphology of pRBCs is normal, and no comparable trophozoites or gametocytes are found similar to *P. vivax*.

This figure is captured from a dead case with malaria. Ultrahigh-density RBCs stick together into many long chains and form a grid. This is one of the representative

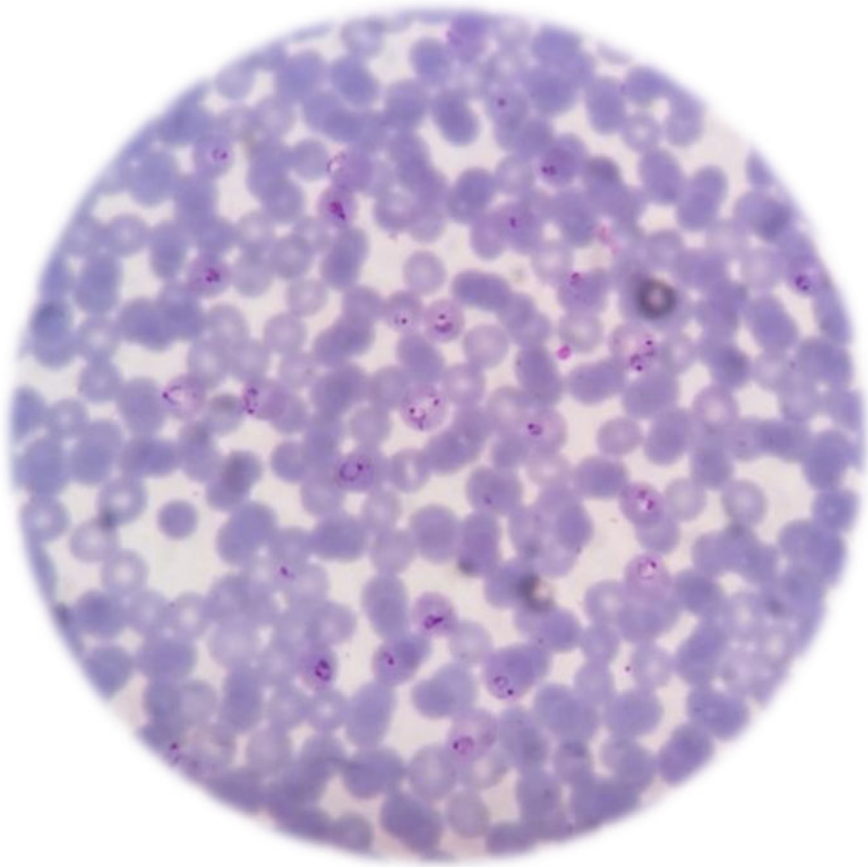


Fig. 6.15 Large trophozoites of *P. falciparum* on a thin blood smear (Giemsa staining, $\times 1000$)

characteristics seen in severe cases. The morphology of large trophozoites shows obvious distortions, but *Plasmodium* are small, the parasitism rate is high, and the pRBCs are normal in morphology and size.

In the view, four *P. falciparum* large trophozoites are parasitized in RBCs, which are small, compact, and relatively regular in morphology, protruding from the edge of the pRBC, and the pRBC are relatively regular in morphology and darker in color than the surrounding RBCs. If the patient is not receiving standardized antimalarial treatment and has multiple relapses in a short period of time or has a long course of disease and is treated repeatedly, the peripheral blood may show a feature of low-density large trophozoites.

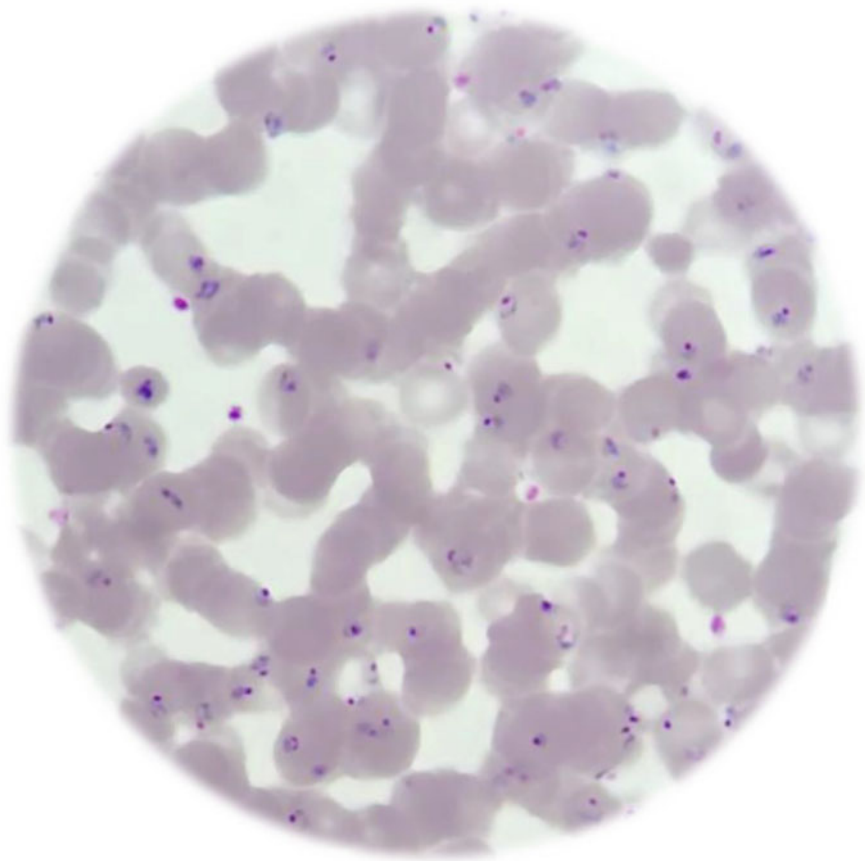


Fig. 6.16 Ring form and large trophozoites of *P. falciparum* on a thin blood smear (Wright-Giemsa staining, $\times 1000$)

6.2.3 Schizonts of *P. falciparum* in Thin Blood Smears

The morphology of the schizonts of *P. falciparum* is shown in Figs. 6.18, 6.19, and 6.20.

P. falciparum schizonts are derived from large trophozoites that undergo dichotomy, usually accumulated in internal organs such as blood sinuses where blood flow is slow and rare in peripheral blood but are also easily observed in the peripheral blood of high parasitemia and severe cases. They can be divided into immature and mature schizonts. The pRBCs are normal or slightly shrinking in this stage. If immature, nuclei are slightly larger, numbering 2 to a dozen, encased in blue cytoplasm, and there are brown or dark-brown masses of distinctive malarial pigments (A–F). Generally, only the nucleus and malarial pigments are seen in mature *P. falciparum* schizonts, while blue cytoplasm is lightly colored or invisible

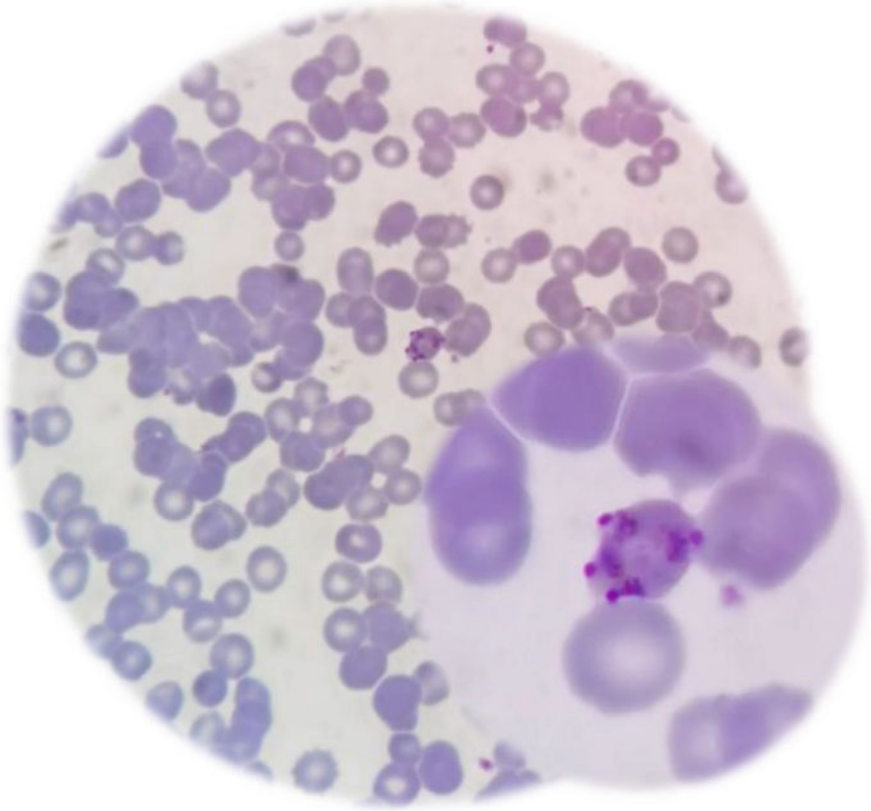


Fig. 6.17 Large trophozoites of *P. falciparum* on a thin blood smear (Giemsa staining, $\times 1000$)

(GHI). The number of nuclei varies from a dozen to two dozen, and merozoites are “small, numerous and intensive distribution,” presenting “grainy and clear,” and tend to approach malarial pigments. Therefore, schizonts are often smaller than the surrounding normal RBCs.

There are two immature schizonts in the view. The schizonts are derived from a large trophozoite dichotomy, both with remarkable brown or dark-brown masses of malaria pigment. The immature schizonts have larger nuclei with distinct blue cytoplasm in clumps, encasing the nucleus and malaria pigments, and a compact body.

A mature schizont of *P. falciparum* has more than ten merozoites and a dark-brown malarial pigment block, which are wrapped in the light-blue cytoplasm. The merozoites are “small, numerous and intensive distribution,” presenting “grainy and clear,” and pRBCs are often smaller than the surrounding normal RBCs.

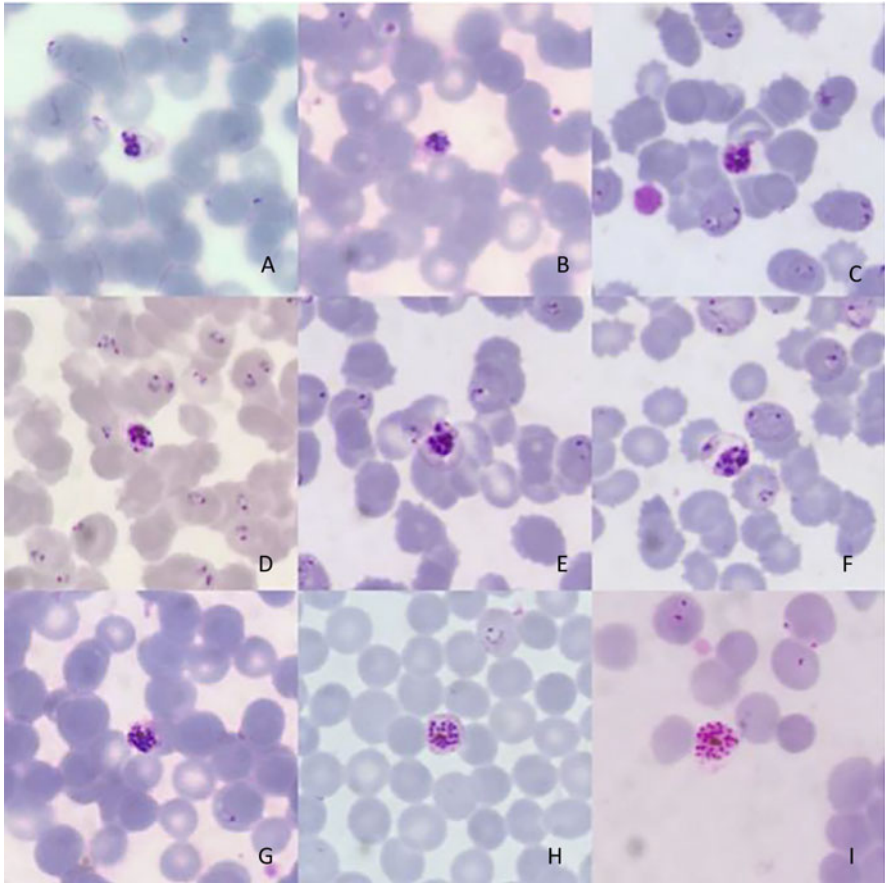


Fig. 6.18 Schizonts of *P. falciparum* (Giemsa staining, $\times 1000$)

6.2.4 Gametocytes of *P. falciparum* in Thin Blood Smears

After *P. falciparum* has undergone several fission proliferations, some of the merozoites invade the RBCs and do not undergo asexual fission but develop into gametophytes. *P. falciparum* gametophytes can be divided into immature and mature gametophytes and by gender into female and male gametophytes. The morphology of the gametophytes of *P. falciparum* is shown in Figs. 6.21, 6.22, 6.23, 6.24, 6.25, and 6.26.

The immature gametophyte at the first stage has a round or oval body with a small, red nucleus, and granular, brown malaria pigments, which surround the nucleus, and the cytoplasm is wrapped around the nucleus and malaria pigments (ABC).

With development, the body extends to the sides and becomes progressively more pointed at both ends, with an obvious oval shape (DEF), shown in development into

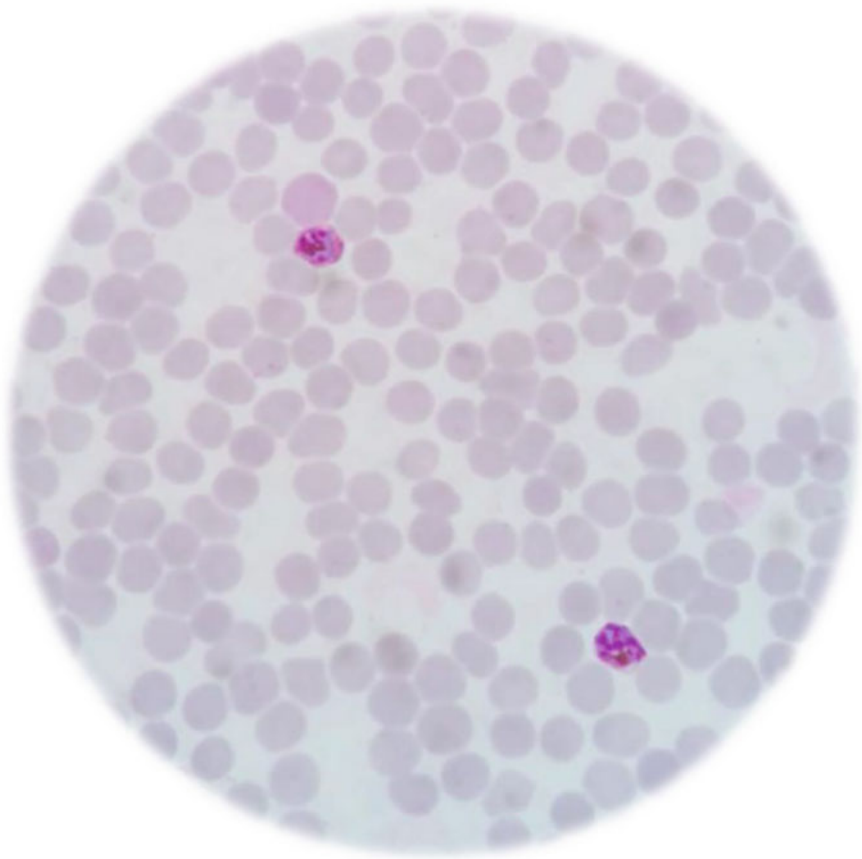


Fig. 6.19 Immature schizonts of *P. falciparum* (Giemsa staining, $\times 1000$)

the second stage of the immature gametophyte when the *Plasmodium* occupies the majority of the pRBCs.

Then, both ends of *Plasmodium* are filled with pRBCs, both ends are pointed, and the pRBCs are seen only contour (GHI), which is the third stage of immature gametophytes.

Thereafter, the fourth stage of immature gametophytes, also known as near-mature gametophytes, is more common in peripheral blood, where the shape is “willow-shaped (JK)” with pointed ends or “cylindry (L)” with flattened ends.

Female gametophytes of *P. falciparum* are more common in peripheral blood than male gametophytes. The red nucleus is usually located in the center of the blue cytoplasm and is surrounded by dark-brown malaria pigment granules. The size is a slightly different, “crescent” shape with rounded ends. Sometimes the outline of a pRBC is also visible, forming a “bow-like” shape (C).

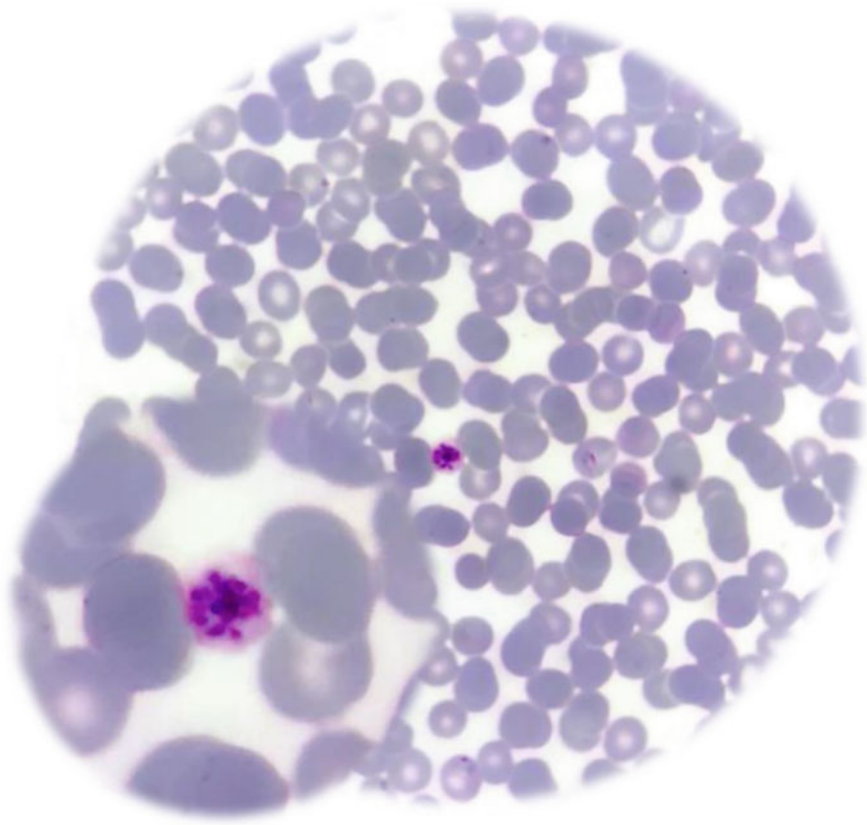


Fig. 6.20 A mature schizont of *P. falciparum* (Giemsa staining, $\times 1000$)

Compared to the female gametophytes, the male gametophytes are relatively more rounded, “sausage-shape,” with a slightly different size and a light-blue cytoplasm, resulting in a reddish coloration due to the red, flabby, and inflated nucleus. Inconspicuous light-blue cytoplasm and faintly visible yellow-brown malarial pigment granules encased in the nucleus. Sometimes the outline of a pRBC is visible, forming a “bow-like” shape (CEGHI).

In falciparum malaria, RBCs often adhere together into a rouleaux or grape-like shape, resulting in gametocytes laminated at RBCs. It is easy to miss detection under conditions of dark background, poor staining (H), small size (EFGI), or folded (EG) and distorted (DFI). However, the nucleus and malaria pigments of the gametophytes are still evident, and the complete body can be seen by twisting the fine quasi-focal spiral of the microscope.

If the duration from blood collection to the preparation of blood smears is long, the mature gametophyte will gradually become rounded and develop into a gamete (A is a female gamete and B is a male gamete), and the morphology is similar to that

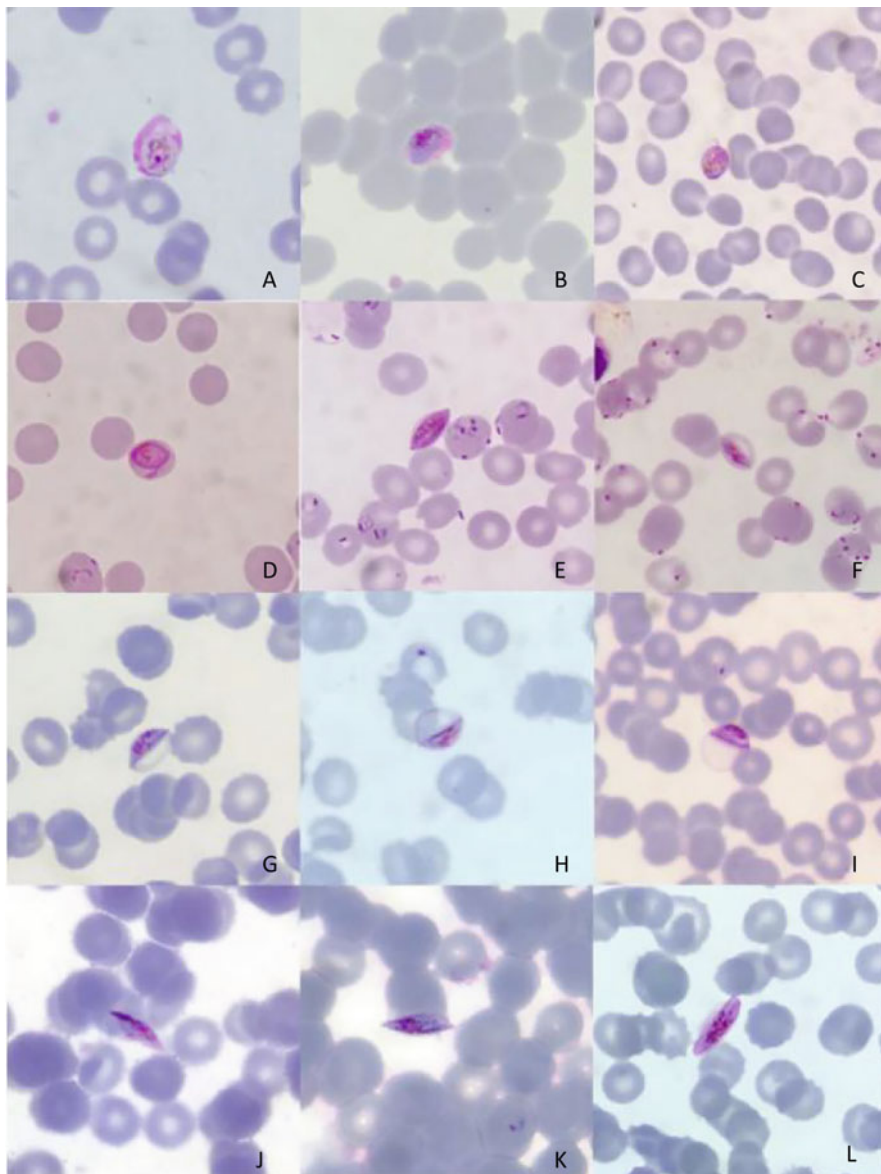


Fig. 6.21 Immature *P. falciparum* gametocytes (Giemsa staining, $\times 1000$)

of *P. vivax* gametocytes. The gametes are only smaller in size, making it difficult to distinguish, and attention should be given to the morphology of other *Plasmodium* forms in the blood smear when identifying them, e.g., the presence of *P. falciparum* rings. The flagellated filament of male gametocytes may be observed in the human

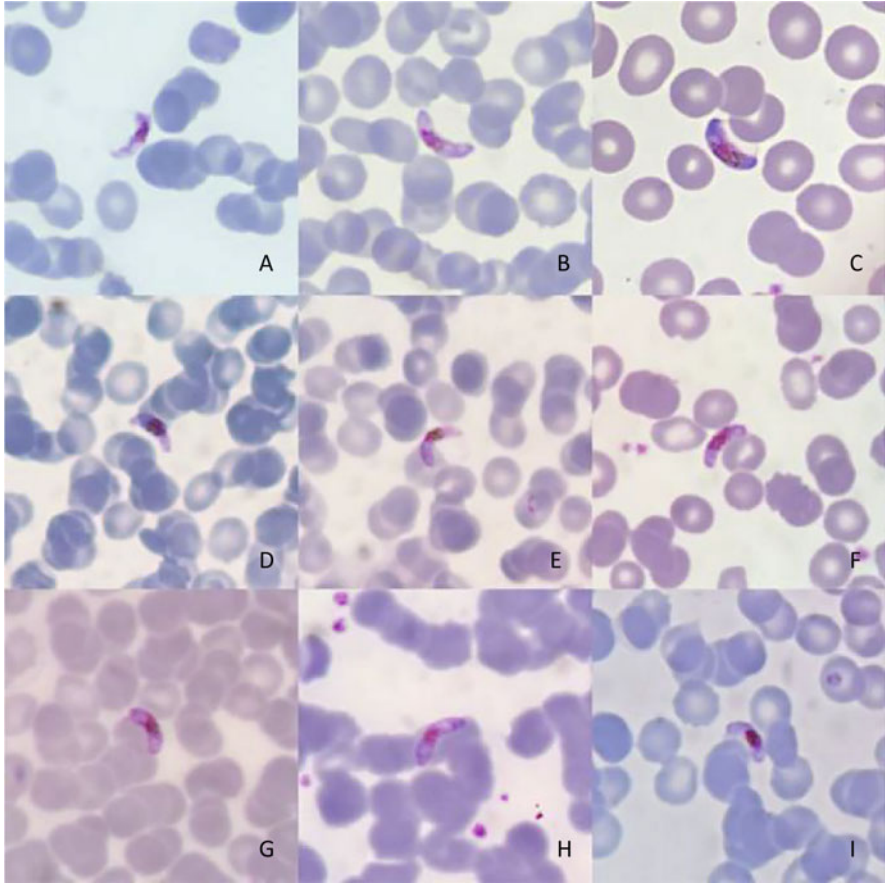


Fig. 6.22 Female gametocytes of *P. falciparum* (Giemsa staining, $\times 1000$)

blood stage; several flagellated filaments extend from the male gamete, and each filament contains a small red nucleus (DEF).

Gametocytes are the destination of development in humans. If only gametocytes are present in the peripheral blood, they are no longer harmful to the patient and can be observed themselves, and the gametocytes will die out within 30–60 days. If there is a high density of gametocytes causing fever or if there is a vector for *P. falciparum* in the surrounding environment, the gametocytes will need to be killed with appropriate medication, such as primaquine phosphate tablets. The yellow arrows point to lymphocytes.

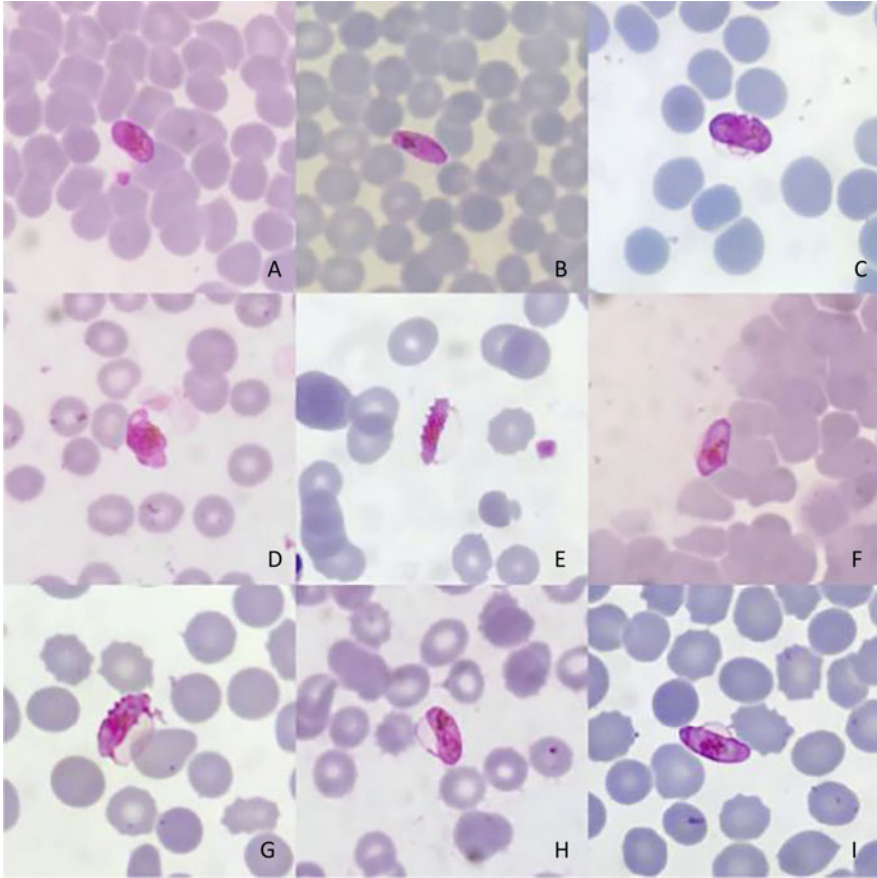


Fig. 6.23 Male gametocytes of *P. falciparum* (Giemsa staining, $\times 1000$)

6.2.5 The Morphology of *P. falciparum* in Thick Blood Smears

The morphology of *P. falciparum* in thick blood smears is shown in Figs. 6.27, 6.28, 6.29, 6.30, 6.31, 6.32, 6.33, 6.34, 6.35, 6.36, 6.37, 6.38, 6.39, and 6.40.

The merozoites of *P. falciparum* schizonts are more tightly packed in thick blood smears, so the schizonts are slightly smaller in thick blood smears, appearing as a dense mass of red clusters. Single merozoite and black–brown malaria pigment can be observed by twisting the fine quasi-focal spiral of the microscope, while pale blue cytoplasm is faintly visible.

The *P. falciparum* immature gametocytes share the same shape on the thin and thick blood smears, but they are reduced in size. Near-mature gametocytes are more easily observed as willow-shaped and cylindrical shapes, which have a red nucleus

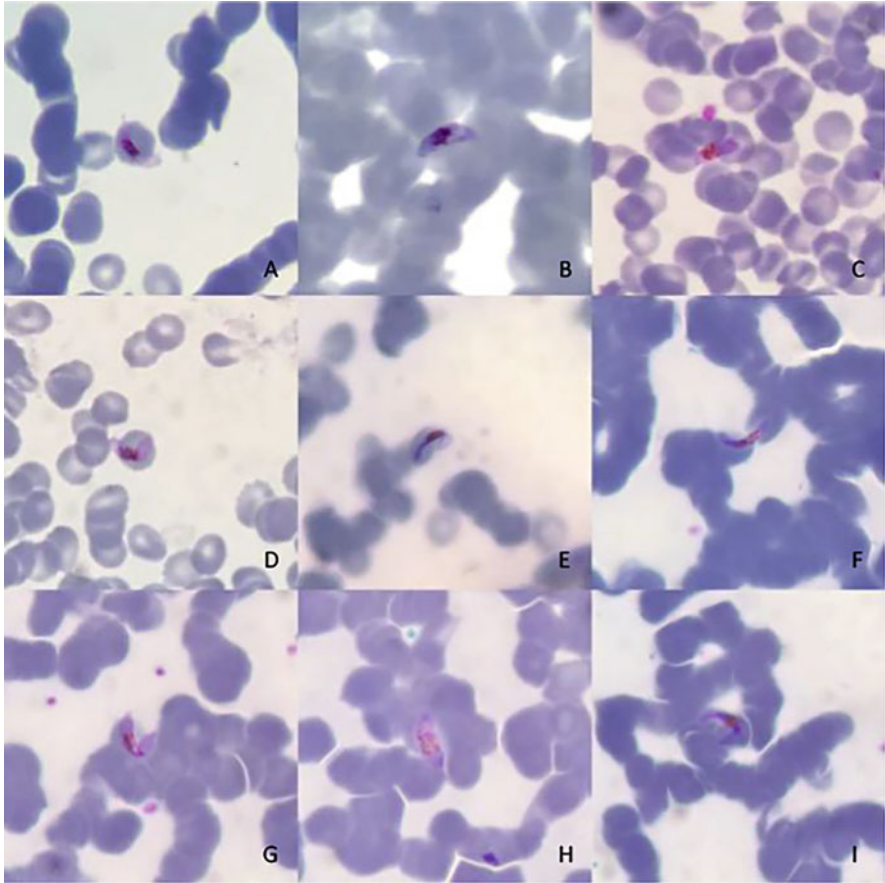


Fig. 6.24 *P. falciparum* gametocytes are laminated among RBCs (Giemsa staining, $\times 1000$)

and brown malaria pigment granules and a compact body with a high contrast to the background.

The *P. falciparum* mature gametocytes share the same shape on the thin and thick blood smears, but they are reduced in size. The red nucleus and brown malaria pigment granules are distinct, but the cytoplasm is similar in color to the background. All gametocytes can be observed by twisting the fine quasi-focal spiral of the microscope.

The *P. falciparum* gametocytes share the same shape on the thin and thick blood smears, but the body appears folded, distorted, and partially missing. When the background is darker, the body is harder to distinguish from the background, but the red nucleus and brown malaria pigment granules are evident. All gametocytes can be observed by twisting the fine collimating spiral.

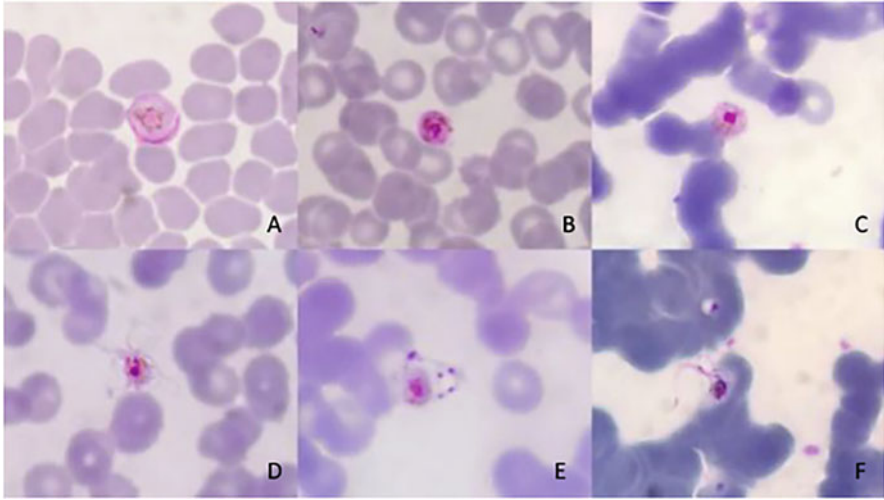


Fig. 6.25 Early appearance of *P. falciparum* gametes at the human blood stage (Giemsa staining, $\times 1000$)

6.2.6 The Morphology of Severe Falciparum Malaria

Falciparum malaria is characterized by acute onset, rapid progression, severe symptoms, and serious complications. Almost all deaths are caused by falciparum malaria. Studies have shown that it is the most important risk factor if the onset-diagnosis time is more than 5 days. Therefore, improving the level of microscopic examination, achieving “early detection, early diagnosis, early treatment” is beneficial to prevent the emergence of severe cases.

In addition to the early diagnosis of falciparum malaria, the early identification of the microscopic morphological characteristics of blood smears of severe cases is also the key to successful treatment and saving lives. The blood smears generally showed high parasitemia, a large number of late-stage parasites, anemia of different degrees, more immature RBCs, abnormal increases in WBC counts, and especially a high percentage of neutrophils. On the other hand, some severe cases are caused by misdiagnosis, which leads to a longer time of onset diagnosis. Although there is symptomatic treatment in the course of the disease, there is no antimalaria treatment. Under the microscope, the density of *Plasmodium* may not be high, but the proportion of late-stage parasites is high, RBCs are rare, and routine blood tests show peripheral blood cell reduction.

The typical morphological characteristics of severe falciparum malaria under a microscope are shown in Figs. 6.41, 6.42, and 6.43. In addition to identifying the *Plasmodium* species, the laboratory technicians of the clinical institutions should also master the knowledge points to provide a timely reference for clinical treatment.

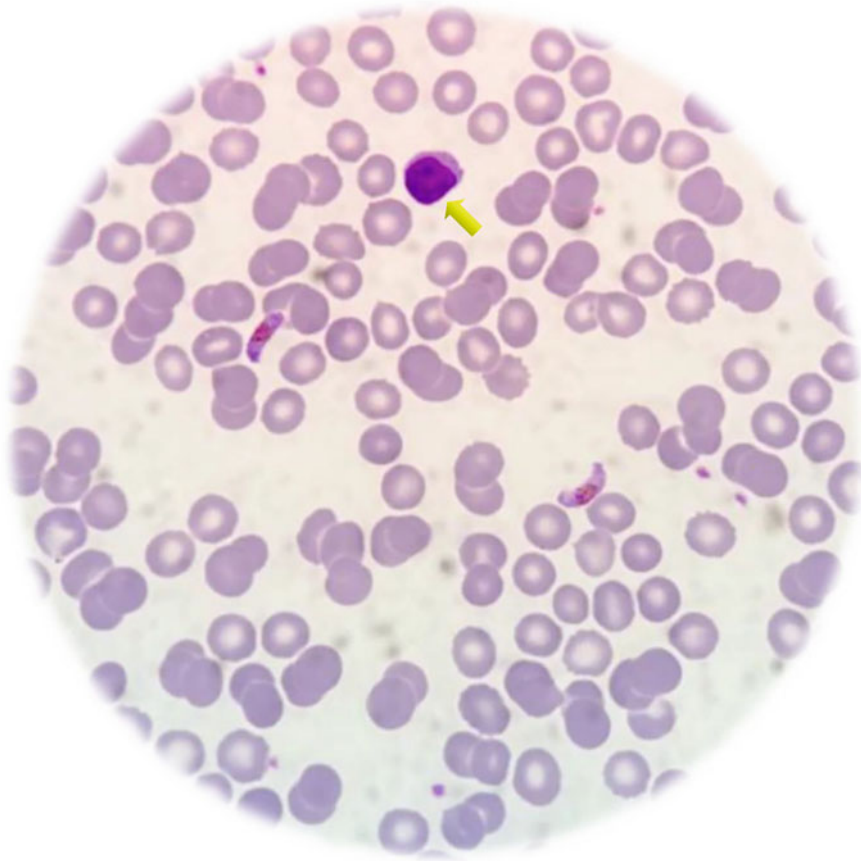


Fig. 6.26 Two female gametocytes of *P. falciparum* (Giemsa staining, $\times 1000$)

In a blood smear from a case of cerebral malaria, the blood smear shows hyperparasitemia, multi-infection, and RBCs adhering together in chains (DFG). The size of small trophozoites is relatively larger with thick cytoplasm, and there are many late-stage *Plasmodium*, such as mature trophozoites (C) and schizonts (D), with elevated WBC counts (A). Due to the very high parasitism rate, leucocyte engulfment of *Plasmodium* is more easily observed, and the nuclei and malaria pigment accumulation are wrapped in WBCs (G). At the same time, Howell-Jolly bodies (EF, indicated by the black arrow) and orthochromatic normoblasts (HI) are common because of the presence of severe anemia. Lymphocytes are indicated by the yellow arrow, and neutrophils are indicated by the blue arrow.

A severe case of falciparum malaria developed respiratory distress syndrome, and blood tests showed severe anemia with low platelet and WBC counts. A blood smear shows hyperparasitemia (A) with few RBCs in a thin blood smear but a high parasitism rate and multiple infections, with orthochromatic normoblasts (D red

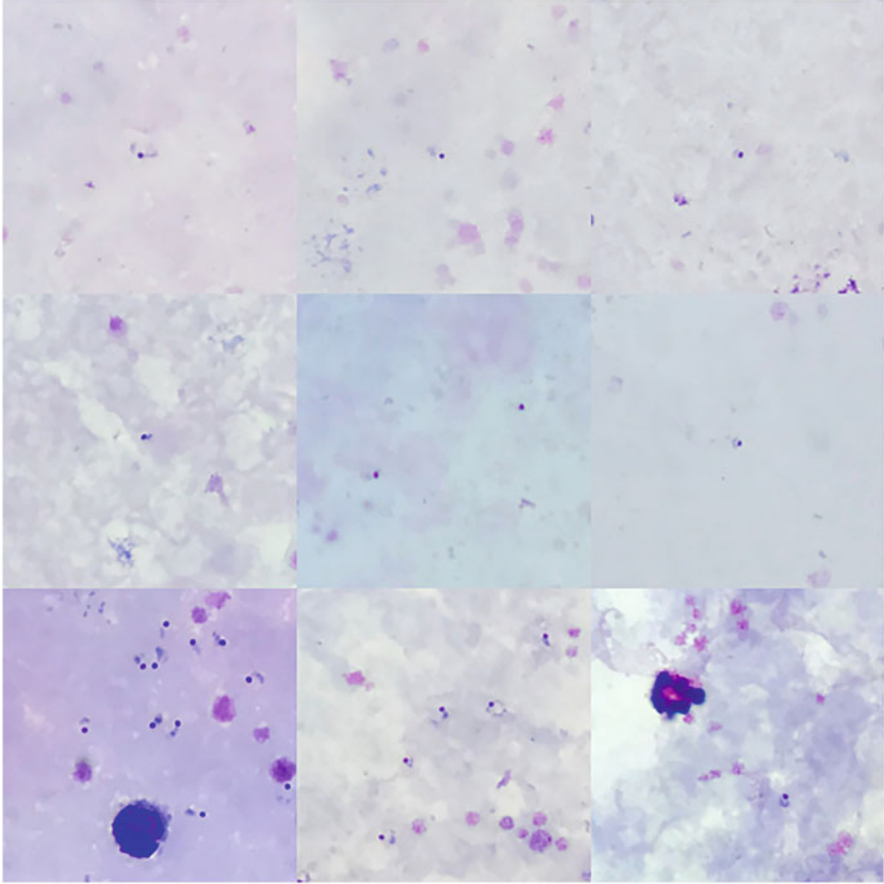


Fig. 6.27 Ring form of *P. falciparum* on a thick blood smear (Giemsa staining, $\times 1000$). Rings of *P. falciparum* are the most important basis for the diagnosis of falciparum malaria. The ring form in thick blood smears is simple and compact, with a reduced size compared to the thin blood smears, and is the smallest form of the various *Plasmodium* species. The nucleus is red, round, dense, and stereoscopic, the cytoplasm is blue, or only the nucleus is visible if the cytoplasm is slender. Due to shrinkage, the cytoplasm can present a “broken ring,” “colon,” “comma,” “semicolon,” and “spread the wings.” Falciparum malaria can develop hyperparasitemia within 3 days of the onset of clinical symptoms. Therefore, rings often appear “full of stars” in view and are easy to identify in thick smears. However, when densities are very low, they can be missed due to small size, excessive interference, or poor staining

circle), polychromatic erythrocytes (E blue circle), macrophages (F blue circle), acanthocytes (BCDFG), and elliptocytes (CHI). The small trophozoites have larger nuclei, with distinct Maurer’s clefts, and more schizonts (GH) and gametocytes (I) appear. Malaria cases, such as the presence of peripheral blood cell reduction, usually have a duration of more than 20 days, are difficult to treat and have a poor

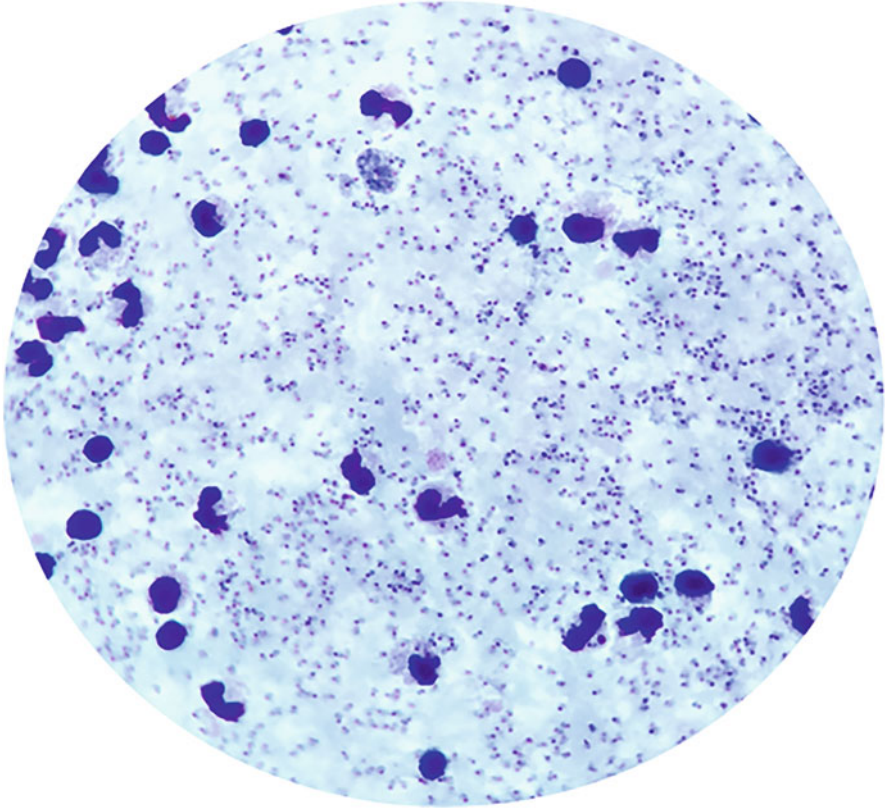


Fig. 6.28 Trophozoites of *P. falciparum* on a thick blood smear (Giemsa staining, $\times 1000$). *P. falciparum* may parasitize various types of RBCs, resulting in a high possibility of developing hyperparasitemia within days. This makes the thick blood smear full of *P. falciparum*, which is uncountable quantities and easily detectable. The above figure shows the morphology of a very high density of *P. falciparum* trophozoites in a thick blood smear, which consisted of a red spherical nucleus and blue, thick cytoplasm, appearing shapes of colon, comma, semicolon, and spread the wings

prognosis. Misdiagnosis or inappropriate methods during the initial treatment, such as inadequate doses or courses of antimalarial treatment and lack of symptomatic adjuvant therapy, will lead to multiple relapses and repeated treatment within a short period of time, with continued deterioration in all test parameters.

In a severe falciparum malaria case in a coma, the initial *P. falciparum* density was more than 300,000 parasites/ μL (A). Intravenous injection of artesunate is used for treatment, with each dose of 120 mg. The injections were given at 0, 12, and 24 h on the first day and then once daily for a total of 7 days and longer. After intravenous injection of artesunate, the density on the first day was greatly reduced (B), and the density on the second day continued to decrease (C). Furthermore, the density

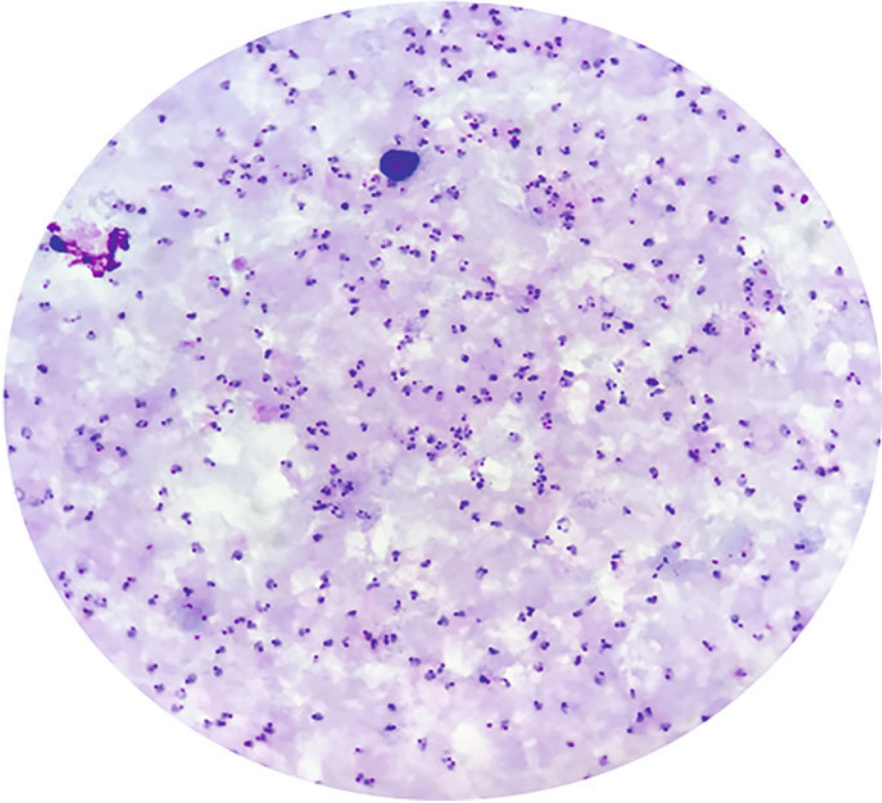


Fig. 6.29 Trophozoites of *P. falciparum* on a thick blood smear (Giemsa staining, $\times 1000$). The above image shows a high density of *P. falciparum* trophozoites in a thick blood smear. The red nucleus appears red, circular, bright, and stereoscopic, and the cytoplasm is blue, thick, and obvious. The nucleus and cytoplasm form colon and exclamation mark shapes. Some rings have already developed into large trophozoites

dropped dramatically from the third day to the fourth day as the WBC count increased (DE). Currently, it is difficult to detect *Plasmodium*. After anti-infective treatment, the WBC count decreased (FGH) from the fifth day to the seventh day. However, large trophozoites can be continuously detected in the peripheral blood until the eighth day (I), and the large trophozoites are significantly smaller than the normal size. There are two possibilities: one is that large trophozoites are not sensitive to artemisinin, and the other is that artemisinin promotes the release of large trophozoites in the viscera into the peripheral blood.

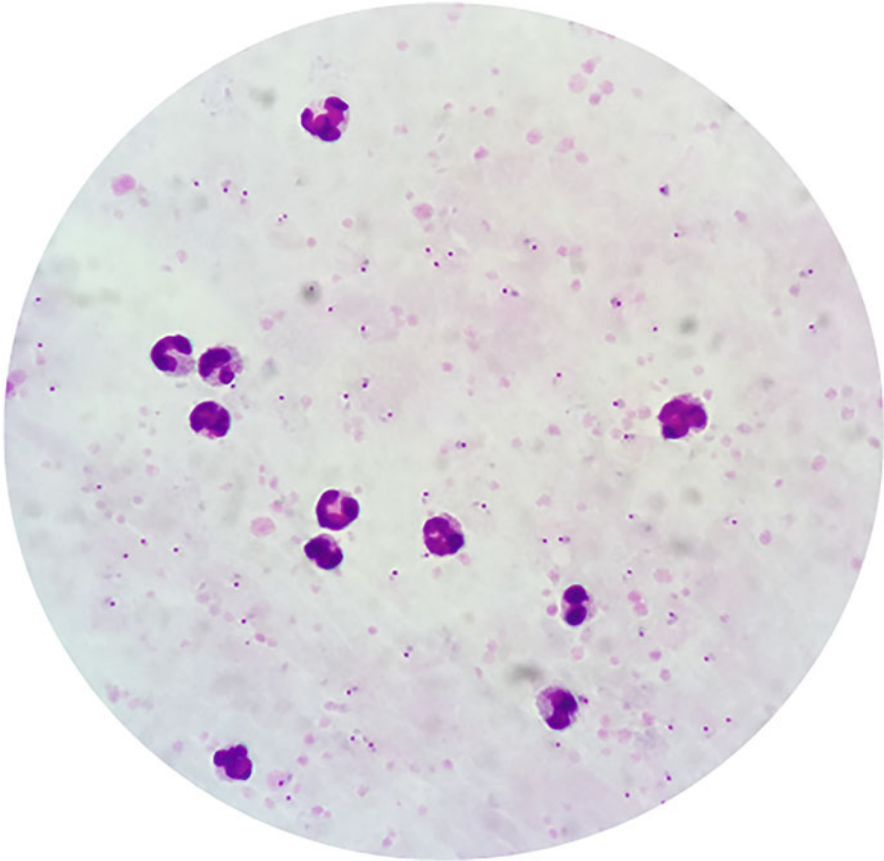


Fig. 6.30 Ring form of *P. falciparum* on a thick blood smear (Giemsa staining, $\times 1000$). The above image exhibits medium-density *P. falciparum* rings in a thick blood smear. The red nucleus appears red, circular, bright, and stereoscopic, and the cytoplasm is blue and slender. The nucleus and cytoplasm form colon and exclamation mark shapes, and some nuclei are visible

6.3 Morphology of *Plasmodium vivax*

6.3.1 Small Trophozoites of *P. vivax* in Thin Blood Smears

The morphology of the small trophozoites of *P. vivax* is shown in Fig. 6.44.

The small trophozoites of *P. vivax* are common at the erythrocytic phase. At the initial stage of *P. vivax* infection, the shape is regular (ABCD), and their size and morphology are difficult to distinguish from small trophozoites of *P. falciparum*. However, they are mostly parasitic on reticulocytes, and pRBCs are therefore slightly larger than the surrounding mature RBCs, and identification also requires

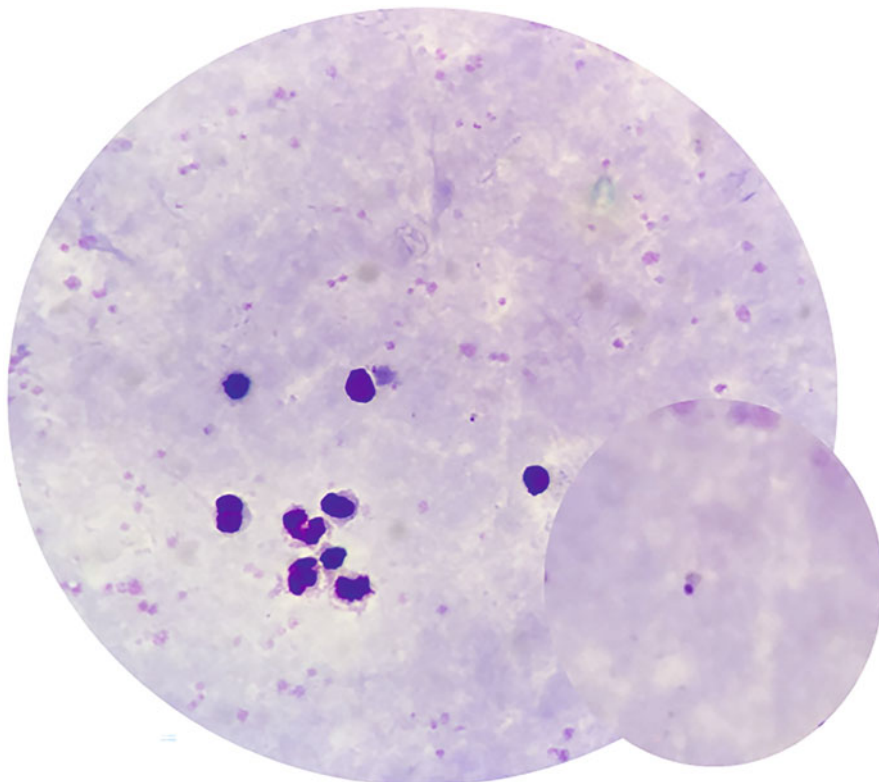


Fig. 6.31 Ring form of *P. falciparum* on a thick blood smear (Giemsa staining, $\times 1000$). Only one ring form of *P. falciparum* is found in the view, and inquiry of epidemiology history and malaria rapid diagnostic tests (RDTs) may help the identification. In peripheral blood, the density of *P. falciparum* is extremely low at the initial stages of onset, after antimalarial treatment and in asymptomatic *Plasmodium* carriers. Therefore, a thin blood smear is very likely to be missed. For monitoring of returnees, initial stages of onset, and re-examinations following medical treatment, great attention should be given to thick blood smears to avoid missed detections.

Following treatment, patients with malaria may remain positive for RDT even if no *Plasmodium* is found in the peripheral blood. Since RDT detects *Plasmodium* lactate dehydrogenase (LDH) or histidine-rich protein II (HRP II), residual LDH or HRP II remains after *Plasmodium* has already been wiped out. The duration of persistence is positively correlated with the density of *Plasmodium*. A higher *Plasmodium* density in the blood may lead to a longer duration of positive RDT results, and positive results may last for one week to several months after negative microscopic examinations based on clinical data. Therefore, RDT positivity does not indicate the presence of *Plasmodium*, and the therapeutic efficacy of antimalarials cannot be evaluated by RDT. The identification of *Plasmodium* infections should be determined by a thick blood smear before discharge from the hospital.

When biochemically testing for LDH, the instrument cannot differentiate human LDH from *Plasmodium* LDH. LDH elevation is partly caused by the destruction of RBCs in malaria patients and partly by the increased production of LDH by *Plasmodium*. LDH is therefore positively correlated with the current density or recent density of *Plasmodium*, and when LDH values reach approximately 1000 U/L, it is indicative of current hyperparasitemia or recent hyperparasitemia according to clinical observations in Wuhan city. If there is a history of epidemic disease, a positive RDT, but no finding *Plasmodium* in a thin blood smear microscopy. Meanwhile, if the LDH is higher than normal, it is strongly recommended that the thick blood smear should be carefully microscopied to avoid missing the test

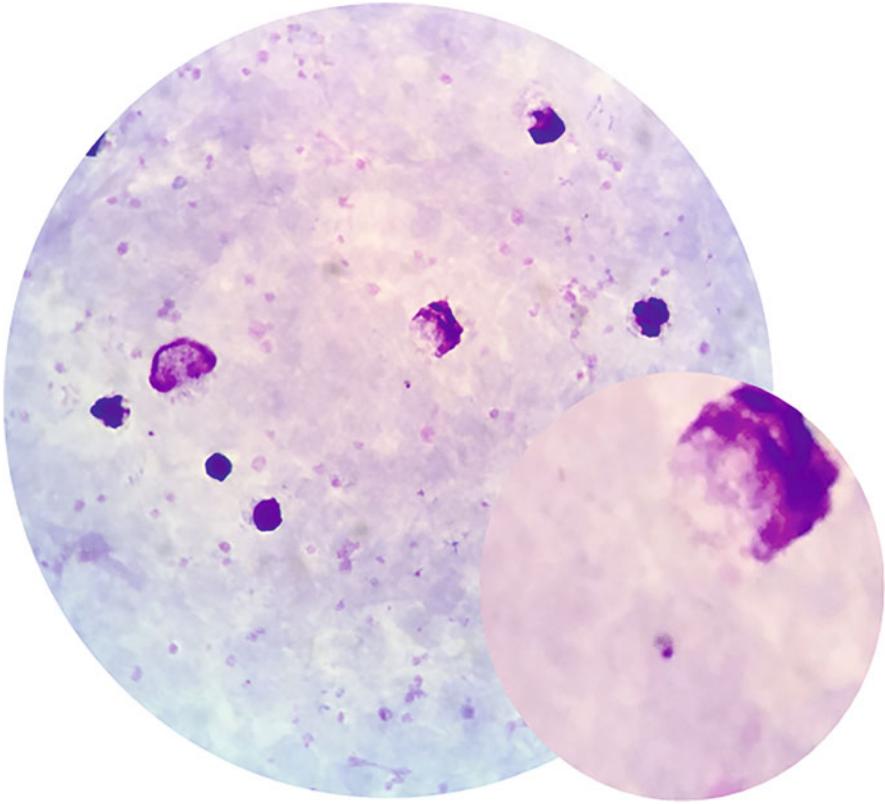


Fig. 6.32 Ring form of *P. falciparum* on a thick blood smear (Giemsa staining, $\times 1000$). Only one *P. falciparum* ring form is found with a small size and compact structure, circular, dark-red dense nucleus, and blue cytoplasm. The overall shape is regular. At this point, the thin blood smear is difficult to detect

judgment by reference to other *Plasmodium* morphologies in the blood smear. As they develop, the cytoplasm of the small trophozoites gradually becomes larger and thicker, the diameter can exceed one-third of the pRBCs, with various irregular deformations (CEFHI) and the appearance of pseudopods (CI), and the appearance of red Schüffner's dots (BCEFGHI) in the pRBCs, characterized by "small, numerous and evenly distributed." The results are a reddish coloration of the pRBCs and various deformations and jaggedness in the shape of the pRBCs in accordance with the small trophozoite shape. When Schüffner's dots are presented, their characteristics and those of Maurer's clefts can be used to distinguish *P. vivax* and *P. ovale* from *P. falciparum*. *P. vivax* can also cause multiple infections (EGH), but this is less common. The green arrow points to monocytes.

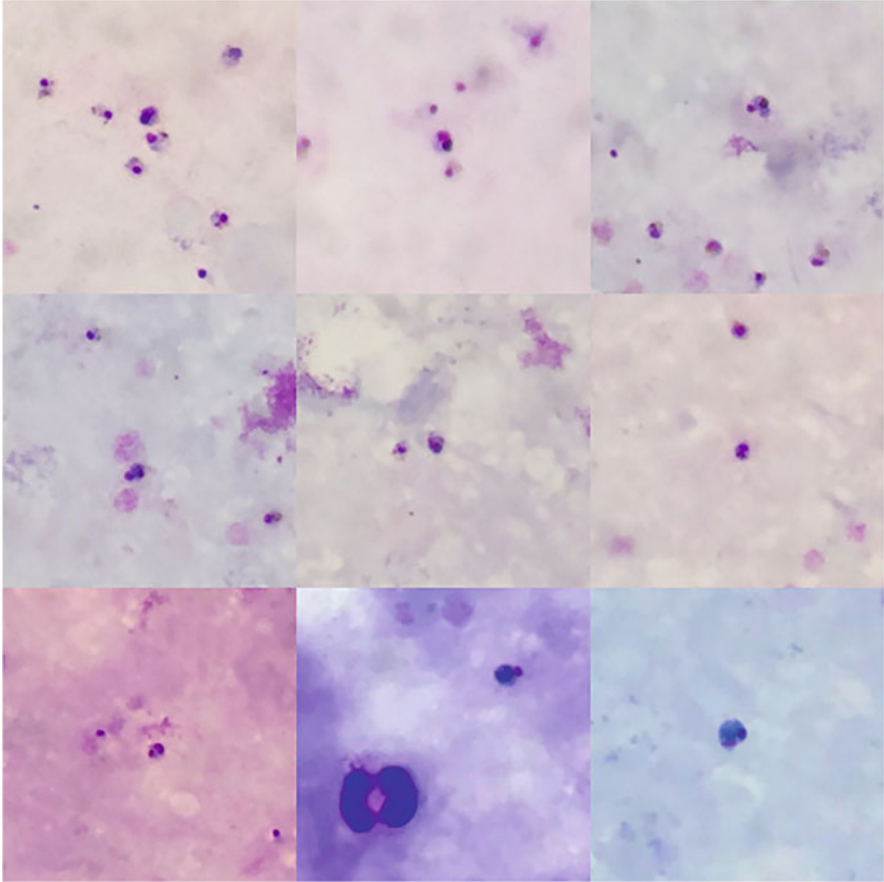


Fig. 6.33 Large trophozoites of *P. falciparum* on a thick blood smear (Giemsa staining, $\times 1000$). Large trophozoites share the shape of thick and thin blood smears; however, large trophozoites in thick smears are slightly smaller in size, and the shape is relatively regular and compact. Nucleus, cytoplasm, and malaria pigment are tightly integrated, and dark-brown blocky malaria pigment can be a key differentiator from other *Plasmodium* species. Sometimes, in thick blood smears, RBCs outline remnants around large trophozoites, and the morphology may be similar to that of *P. vivax* trophozoites and *P. ovale* trophozoites. In this case, the morphology of the other shapes and stages in the same smear and the characteristics of the malaria pigment can be used for identification

6.3.2 Large Trophozoites of *P. vivax* in Thin Blood Smears

The morphology of the large trophozoites of *P. vivax* is shown in Figs. 6.45 and 6.46.

Large trophozoites, also known as late trophozoites, are the most common stage of *P. vivax* in infected human blood, developing from small trophozoites. As the nucleus and cytoplasm of the large trophozoites continue to develop and become

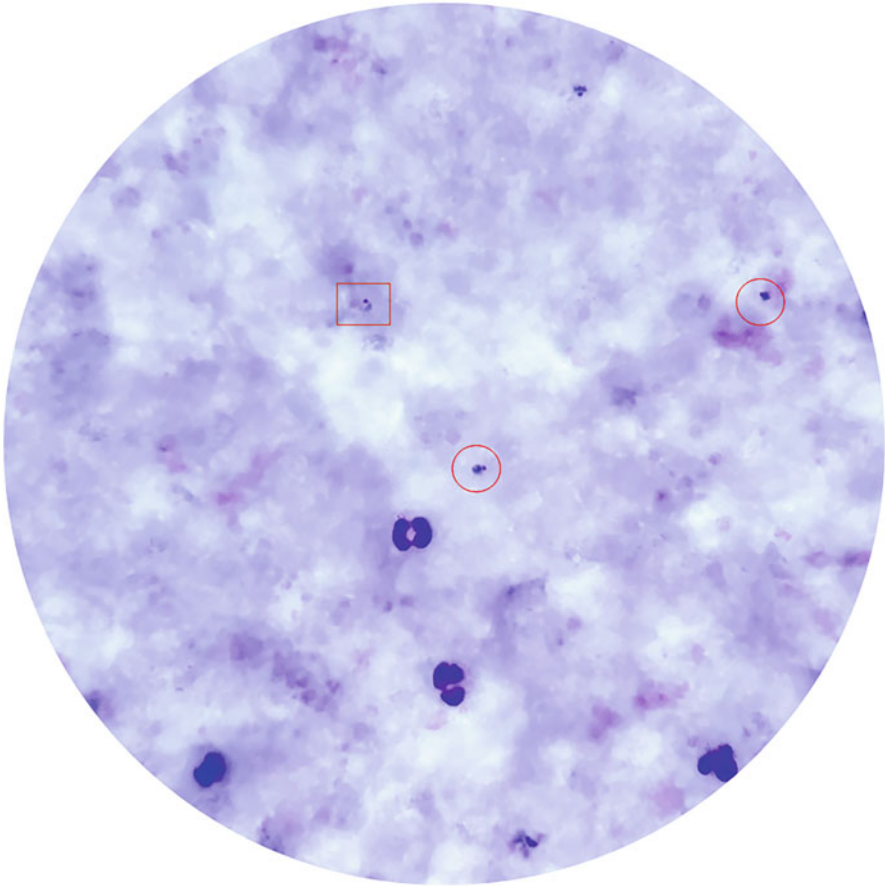


Fig. 6.34 Large trophozoites of *P. falciparum* on a thick blood smear (Giemsa staining, $\times 1000$). Large *P. falciparum* trophozoites are shown in the red circle, and small trophozoites are shown in the red box. The large trophozoites have a large, thick cytoplasm, regular shape, compact structure, and blocky malaria pigment wrapped in cytoplasm, which is sometimes not easily observed but are lower density and are more difficult to detect in thin blood smears. If falciparum malaria has a long course of disease and the dose of antimalarial treatment is inadequate, the peripheral blood will be characterized by predominantly low-density large trophozoites after repeated treatment over a short period of time

enlarged and thicker, they can also be known as mature trophozoites (I), which are morphologically similar to the immature female gametophyte of *P. vivax* and are not easily distinguishable. In contrast to small trophozoites, large trophozoites have a larger cytoplasm, which fills completely or occupies mostly the pRBCs and are polymorphic and amoeboid, with vacuolated areas, but tends to fill out (ABCDFH). The pRBCs are polymorphic and significantly larger than the surrounding RBCs and may even be as large as the WBCs, with obvious Schüffner's dots, characterized by "small, numerous and evenly distributed." The malaria pigments are also obvious, brownish-yellow or brown, mostly granular (ABDG) but also piled up (CH).

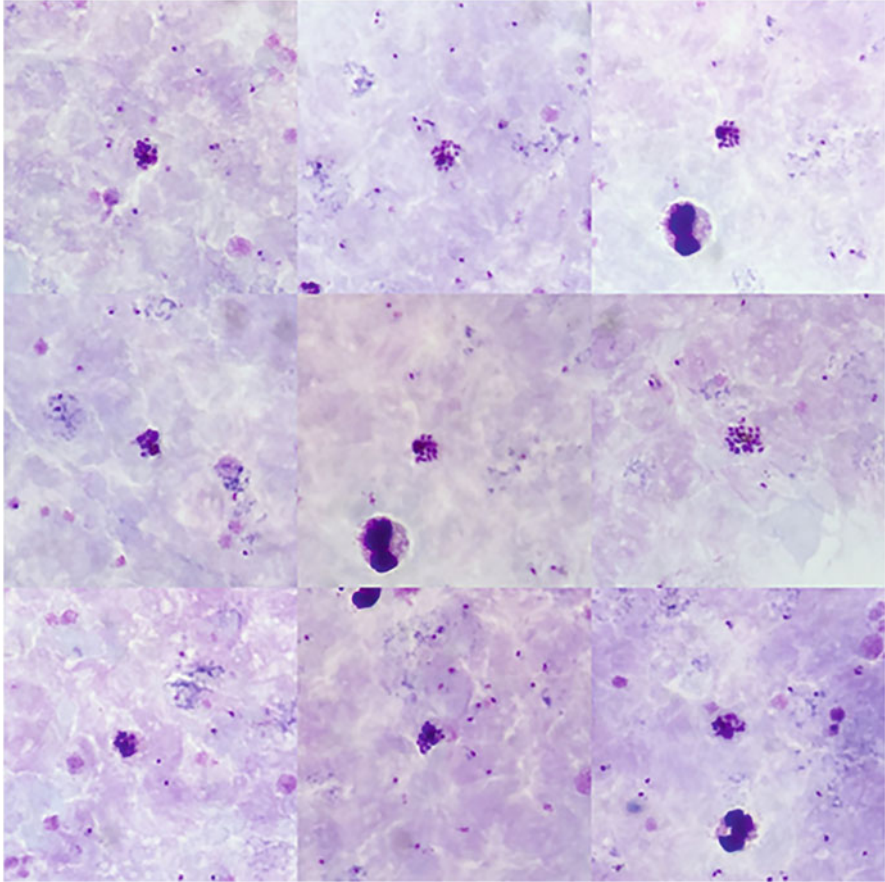


Fig. 6.35 Schizonts of *P. falciparum* on a thick blood smear (Giemsa staining, $\times 1000$). *P. falciparum* schizonts share the same shape on the thin and thick blood smears, merozoites still appear as “small, numerous and intensive distribution”; however, the merozoites are aggregated more closely to form a dense red cluster on a thick blood smear, so the schizonts are slightly smaller in thick blood smears than in thin blood smears, and the blue cytoplasm is harder to observe. By twisting the microscope’s fine quasi-focal spiral, single merozoite, and black-brown blocky malaria pigment are visible. According to the features of malaria pigment and surrounding *Plasmodium* shapes, it can be effectively identified

6.3.3 Schizonts of *P. vivax* in Thin Blood Smears

The morphology of the schizonts of *P. vivax* is shown in Figs. 6.47, 6.48, 6.49, and 6.50.

Immature schizonts of *P. vivax*, which develop from large trophozoite fission, are more common in peripheral blood than mature schizonts at the erythrocytic phase. The schizonts vary in size, and their merozoites are generally larger, with numbers

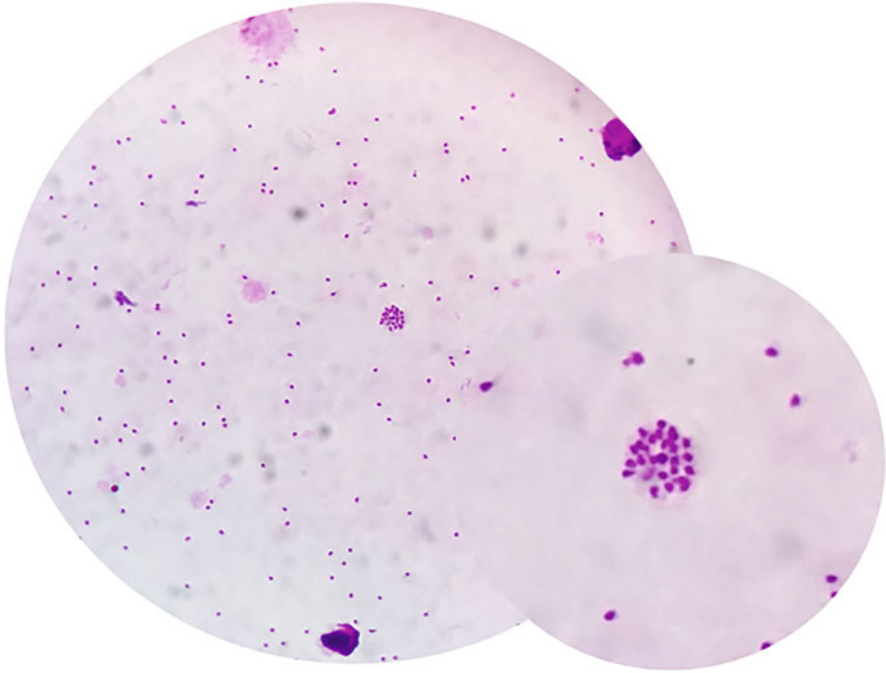


Fig. 6.36 Schizonts of *P. falciparum* on a thick blood smear (Giemsa staining, $\times 1000$). The schizonts share the same shape on the thin and thick blood smears; however, the merozoites are aggregated more closely on a thick blood smear, similar to a dense red cluster. After twisting the fine quasi-focal spiral of the microscope, a single merozoite remains visible. In the view, the schizonts tend to disperse, and surrounding rings are visible, with only the red nucleus being more evident

varying from 2 to a dozen or more (I is close to mature). The malaria pigments are aggregated in “piles,” 1 or 2 piles and are therefore darker and brown in color. The blue cytoplasm is distinct, mass-shaped, and polymorphic, enclosing merozoites and malaria pigments. The pRBCs are also polymorphic, with obvious Schüffner’s dots, even swelling as large as the WBCs.

The platelets are shown as red arrows.

Mature schizonts are less abundant in the peripheral blood at the erythrocytic phase and are more difficult to capture. The number of merozoites ranges from a dozen to two dozen, which is characterized by “small, numerous and scattered.” Each merozoite has its own cytoplasm around the nucleus, presenting “grainy and clear,” indicating that the schizonts have already matured. The malaria pigments are yellowish-brown or dark-brown and aggregated in “piles.” The pRBCs are obviously swollen, and it can be seen that the pRBCs burst and the merozoites disperse (GHI).

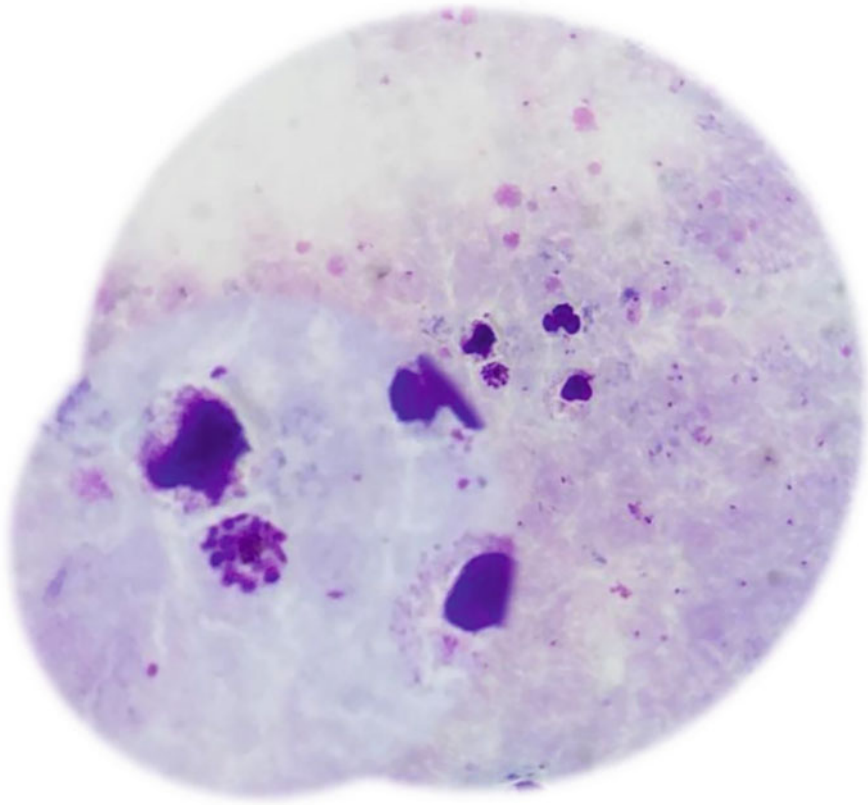


Fig. 6.37 Schizonts of *P. falciparum* on a thick blood smear (Giemsa staining, $\times 1000$)

6.3.4 Gametocytes of *P. vivax* in Thin Blood Smears

The morphology of the gametocytes of *P. vivax* is shown in Figs. 6.51, 6.52, 6.53, 6.54, 6.55, 6.56, 6.57, and 6.58.

Immature female gametocytes are the more common stage in *P. vivax*-infected human blood. Compared with large (mature) trophozoites, the nucleus is larger and more circular, and the cytoplasm is thicker and circular gradually. Immature female gametocytes gradually occupy entire pRBCs. The malarial pigments are yellow-brown, scattered, or aggregated, and pRBCs are obviously swollen with obvious Schüffner's dots. Sometimes, the immature female gametocytes of *P. vivax* are also similar to those of *P. ovale* if they occupy a portion of the pRBCs and if the swelling of the pRBCs is not obvious and has a trailing tail (CDG). At this moment, it must be identified in relation to other *Plasmodium* shapes in the same smear.

Mature female gametocytes are more common in *P. vivax*-infected human blood and are easily detected microscopically because of their large size and dark color. Compared to immature female gametocytes, their red nucleus is large and dense,

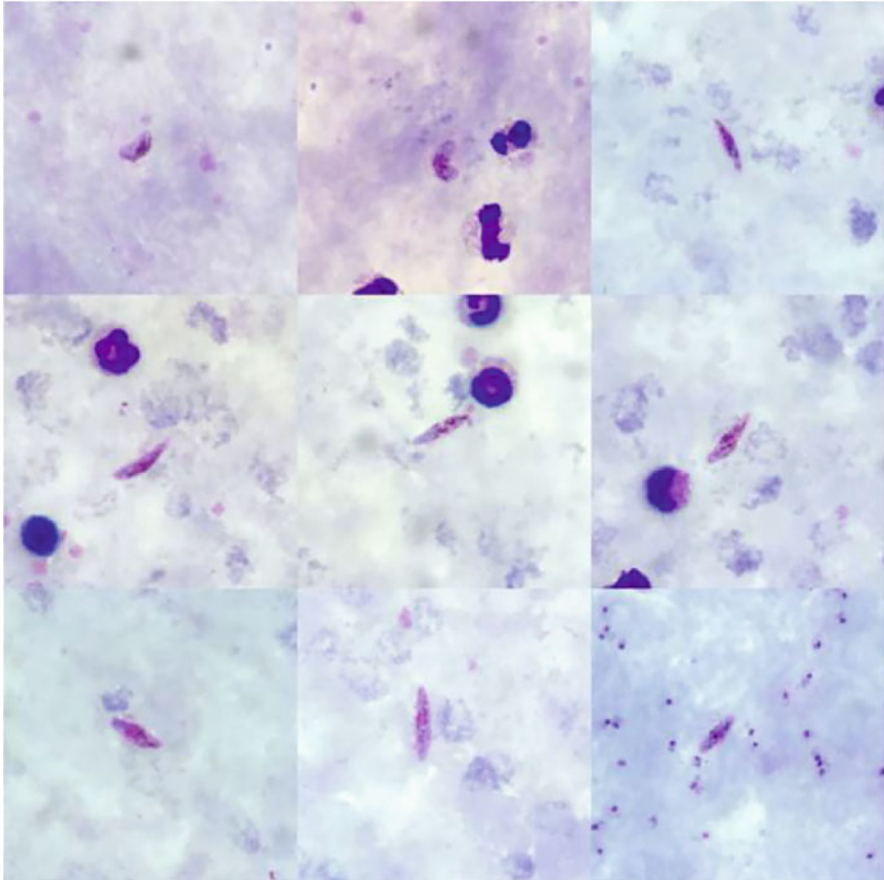


Fig. 6.38 Immature gametocytes of *P. falciparum* on a thick blood smear (Giemsa staining, $\times 1000$)

usually on one side, and the blue cytoplasm is usually regular, round or oval, thick, and darkly colored, with the body occupying the entire pRBC, although other forms may sometimes appear due to compression by surrounding blood cells or for other reasons (GHI). The malaria pigments are yellowish-brown, scattered, or aggregated, the pRBCs are conspicuously distended, sometimes as large as the WBCs, and Schüffner's dots are obvious. The blue arrows point to neutrophils, and the yellow arrows point to lymphocytes. Leukocytes can be used as a reference for the size of malaria parasites.

Lymphocytes are shown in the yellow arrow.

A female gametocyte and a schizont are parasitized in the same RBC (upper), and the flagellate male gamete (red circle) is close to a female gametocyte (down).

Male gametocytes of *P. vivax* are less commonly seen in peripheral blood. They have a round or subcircular body consisting of a loose red nucleus, which is often

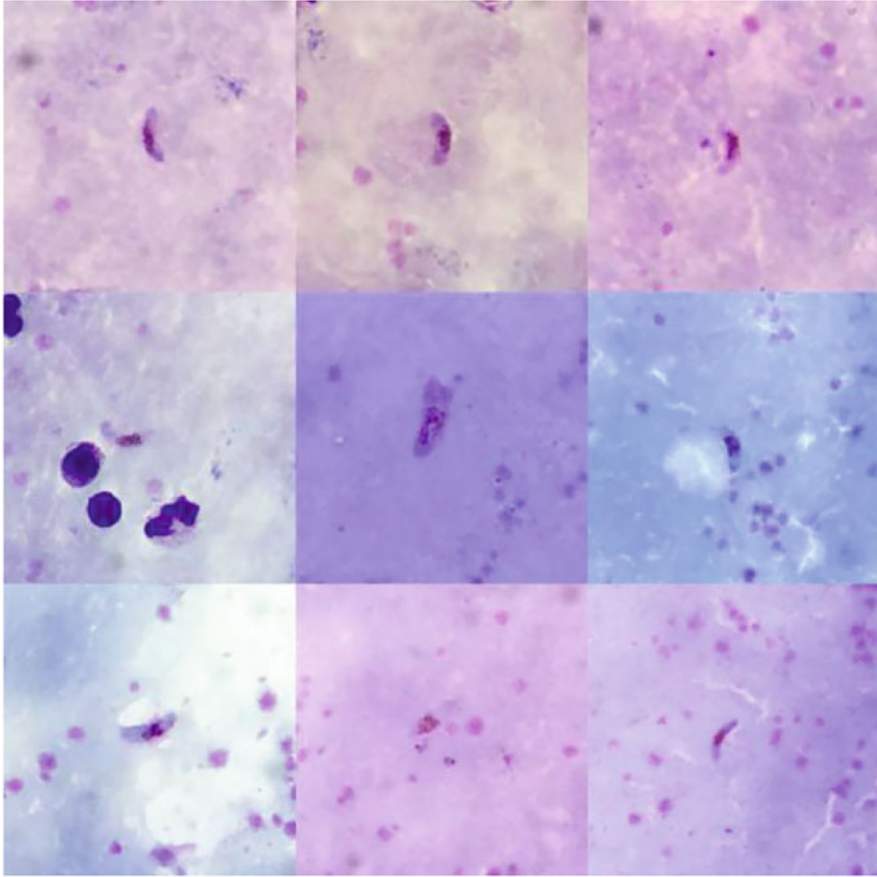


Fig. 6.39 Gametocytes of *P. falciparum* on a thick blood smear (Giemsa staining, $\times 1000$)

located in the center of the body surrounded by brownish-yellow malaria pigments, and a pale blue cytoplasm that is barely visible microscopically, resulting in a reddish coloration of the male gametophytes. Therefore, only the nucleus and malaria pigments are usually observed. If the nucleus is enlarged (CDEG), the cytoplasm and malaria pigments are encapsulated in the nucleus and begin to divide into several pieces (CG), which indicates that the male gametophyte begins to exhibit the filament phenomenon (HI), with several flagellated filaments, each containing nuclei, protruding from the male gametophytes and detaching from the mother to form a flagellated male gamete (H). Giant platelets are also commonly found in the peripheral blood of malaria patients, are red in color and are similar in morphology to *P. vivax* male gametophytes, while the male gametophytes are clear boundary and contain brownish-yellow malaria pigments and Schüffner's dots.

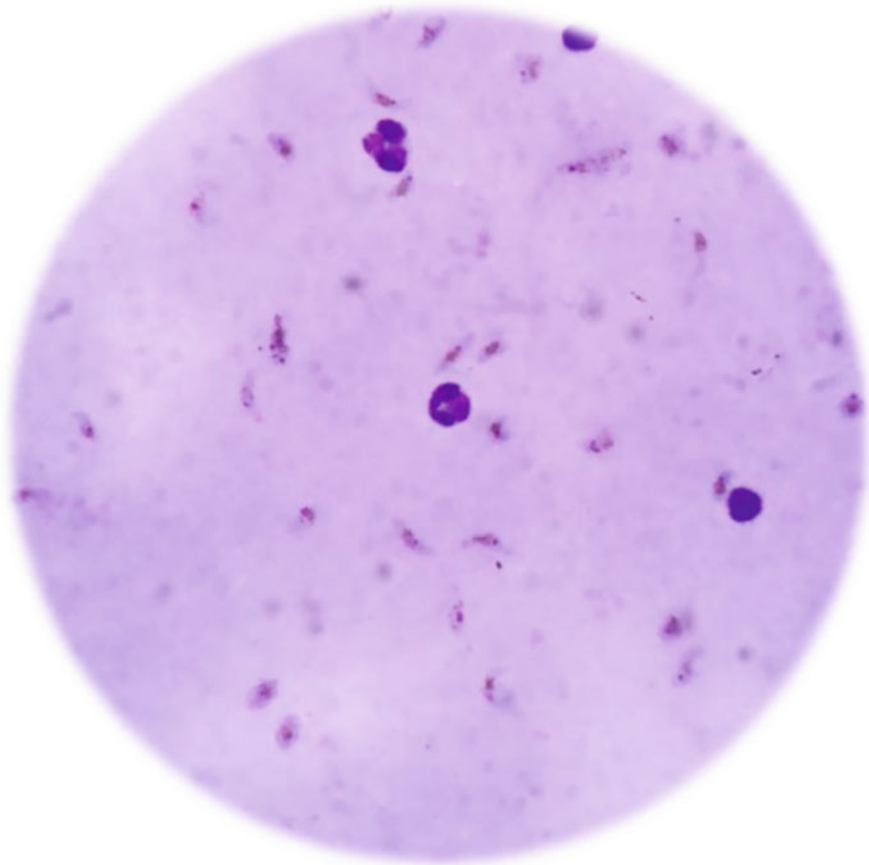


Fig. 6.40 Gametocytes of *P. falciparum* on a thick blood smear (Giemsa staining, $\times 1000$)

6.3.5 The Morphology of *P. vivax* in Thick Blood Smears

Although the parasitism rate of *P. vivax* is low, all stages of the erythrocytic phase can generally be found in the peripheral blood. At the same time, the detection rate is substantially increased by the elevated density of *Plasmodium* due to the aggregated RBCs of thick blood smears. As a result, all stages of *P. vivax* can sometimes be detected in the same field of view. The size is relatively reduced. The morphology of *P. vivax* in thick blood smears is shown in Figs. 6.59, 6.60, 6.61, 6.62, and 6.63.

The morphology of *P. vivax* at initial stages is small and compact, indistinguishable from *P. falciparum* rings in thick blood smears (red circles), and must be identified by the morphological characteristics of the surrounding other stages. In thick blood smears, the trophozoites of *P. vivax* are highly variable in morphology, with concentrated, deformed, disconnected, twisted, folded cytoplasm, but still distinct microscopically, with brownish-yellow malaria pigments wrapped in

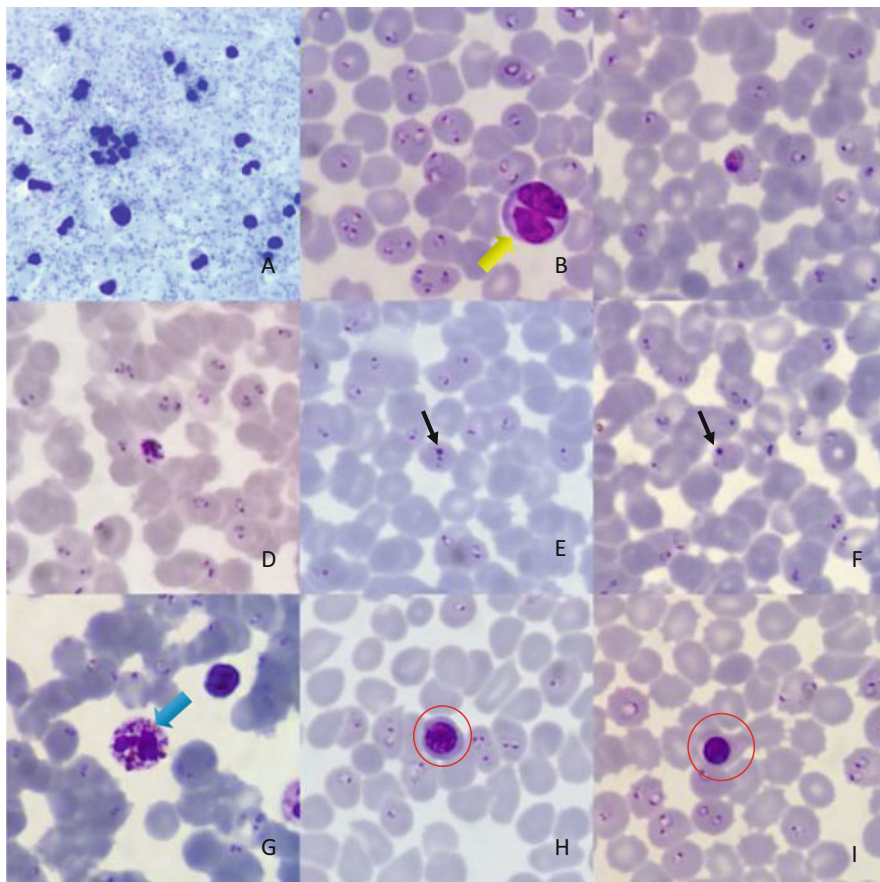


Fig. 6.41 Morphological characteristics of severe cases with falciparum malaria (Giemsa staining, $\times 1000$)

cytoplasm and the remnants or outlines of pRBCs still present on the trophozoites, which are close in size to surrounding WBCs.

The *P. vivax* schizonts share the same shape on thin and thick blood smears, but they are reduced in size, with tightly packed merozoites. The schizonts are close in size to surrounding WBCs. If immature, the merozoites are large and few in number, and the blue cytoplasm is obvious. When mature, the merozoites are small and numerous, the blue cytoplasm is not obvious, and dispersing schizonts can also be observed.

The *P. vivax* gametocytes share the same shape on thin and thick blood smears, but they are slightly reduced in size. The nucleus, cytoplasm, and malaria pigments of the female gametocytes are more pronounced, brownish-yellow malaria pigments encased in blue cytoplasm, and the gametocytes are close in size to surrounding WBCs. The nucleus of the male gametocytes differs from loose and

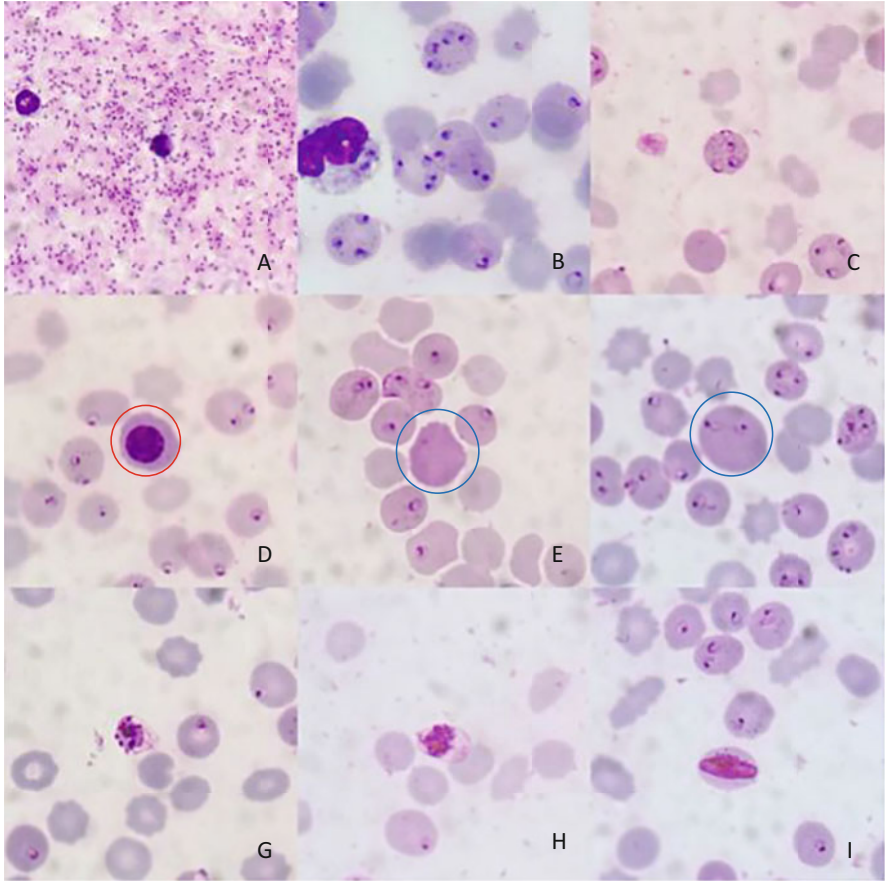


Fig. 6.42 Morphological characteristics of severe cases with falciparum malaria (Giemsa staining, $\times 1000$)

light-colored in the thin smears, becoming dense and bright, surrounded by a ring of granular brownish-yellow malarial pigments (red circle).

The trophozoites are present in various sizes and shapes on a thick blood smear relative to a thin blood smear. The trophozoites appear condensed, twisted, folded, and missing, with a red nucleus and brownish-yellow malaria pigments wrapped in a blue cytoplasm that is far less clear than in the thin blood smears. If the staining is good, the gravelly Schüffner's dots and the outline of pRBC remnants are still faintly visible, and some of the large trophozoites are close in size to those of the surrounding WBCs, which can be used as a reference for the identification of *P. vivax*.

P. vivax is mostly parasitized in reticulocytes. As a result, the density is generally low, leading to easily missed detection on a thin blood smear. Therefore, it must be

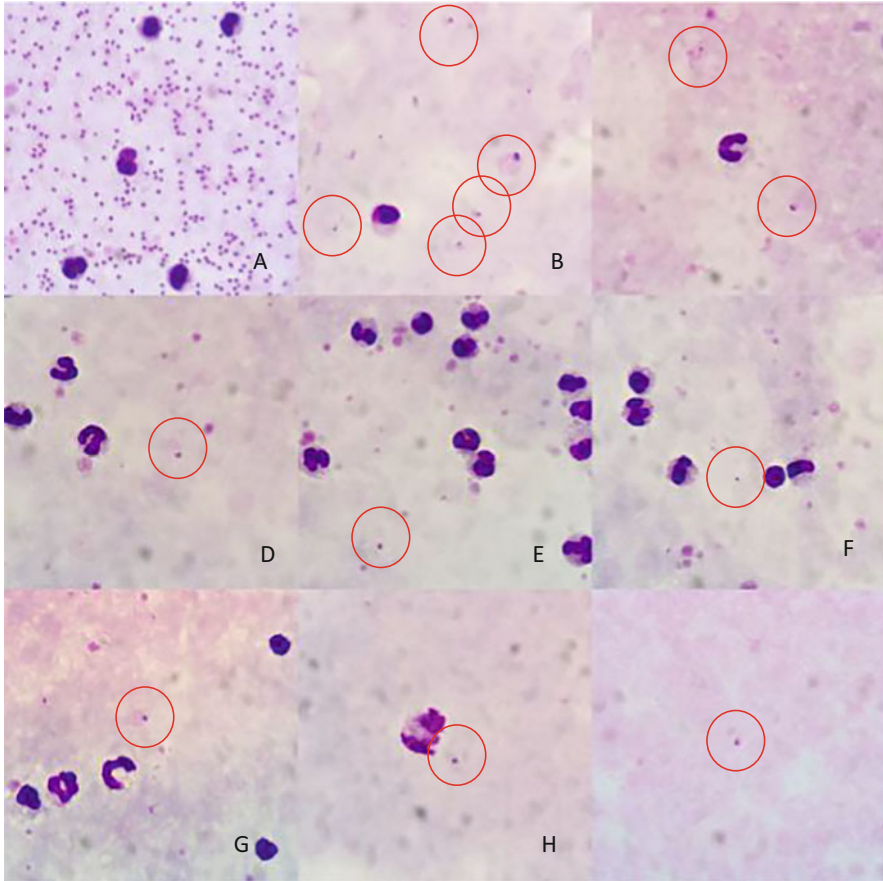


Fig. 6.43 Density and morphology of falciparum malaria high parasitemias after treatment (Giemsa staining, $\times 1000$)

determined by a combination of thick blood smear microscopy, RDT results, and epidemiological history. There is only one immature schizont in the view with approximately 3 or 4 large, closely distributed merozoites. The cytoplasm is blue, and pRBC outlines and Schüffner's dots are visible.

6.4 Morphology of *Plasmodium ovale*

6.4.1 Small Trophozoites of *P. ovale* in Thin Blood Smears

The morphology of the small trophozoites of *P. ovale* is shown in Figs. 6.64 and 6.65.

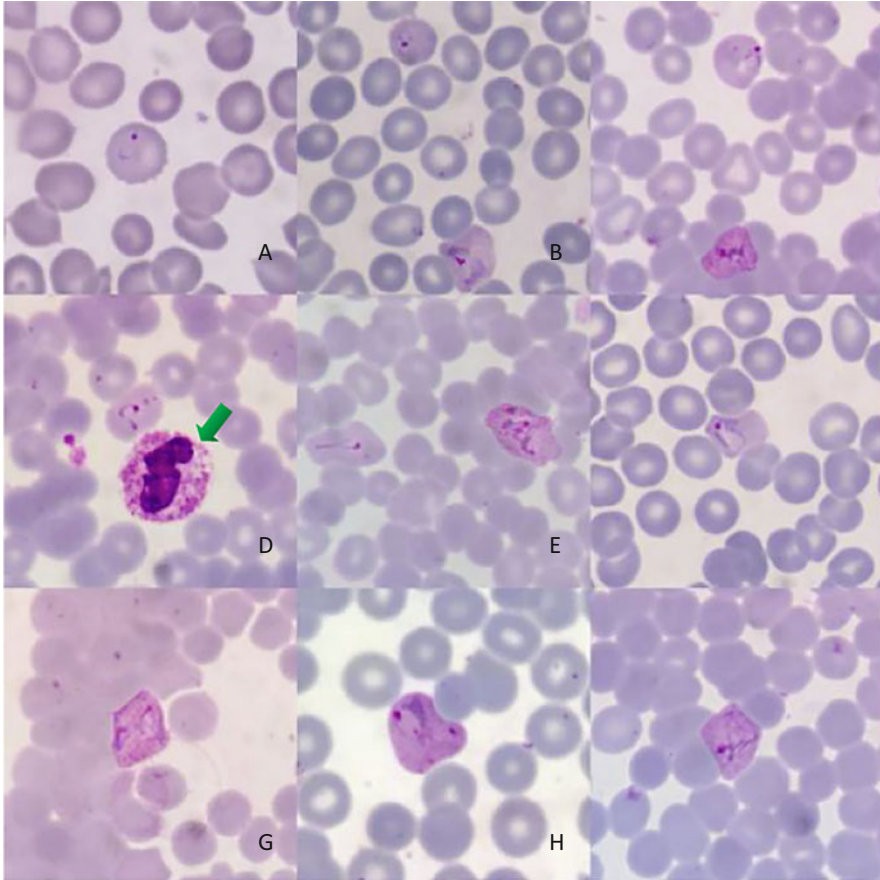


Fig. 6.44 Small trophozoites of *P. vivax* (Giemsa staining, $\times 1000$)

The small trophozoites of *P. ovale* have a red and dense nucleus with a blue, slender, round, or subcircular cytoplasm. The cytoplasm is less abundant when they initially invade RBCs (A) and grows gradually larger as they develop. The size is medium, and the shape is relatively regular. The small trophozoites occupy only a part of the pRBCs. The pRBCs appear as a spiny tail, appearing like an “umbrella, comet-like (FGHI), willow-leaf (AC), or rocket-like (BE),” etc., as if in motion, sometimes with the nucleus surrounded by cytoplasm in a “cat’s eye” shape (GH). Schüffner’s dots appear earlier in pRBCs and are characterized by “small, numerous and evenly distributed.” Multiple infections may be common in *P. ovale*, and the morphology of small trophozoites under a microscope is similar to that of *P. falciparum* rings, which can be determined by the pRBC characteristics and the morphology of other stages of *Plasmodium* in the same blood smear.

The spiny trailing of pRBCs is an important basis for the identification of *P. ovale*, but spiny trailing is often not evident (ABCGH). If the time interval is

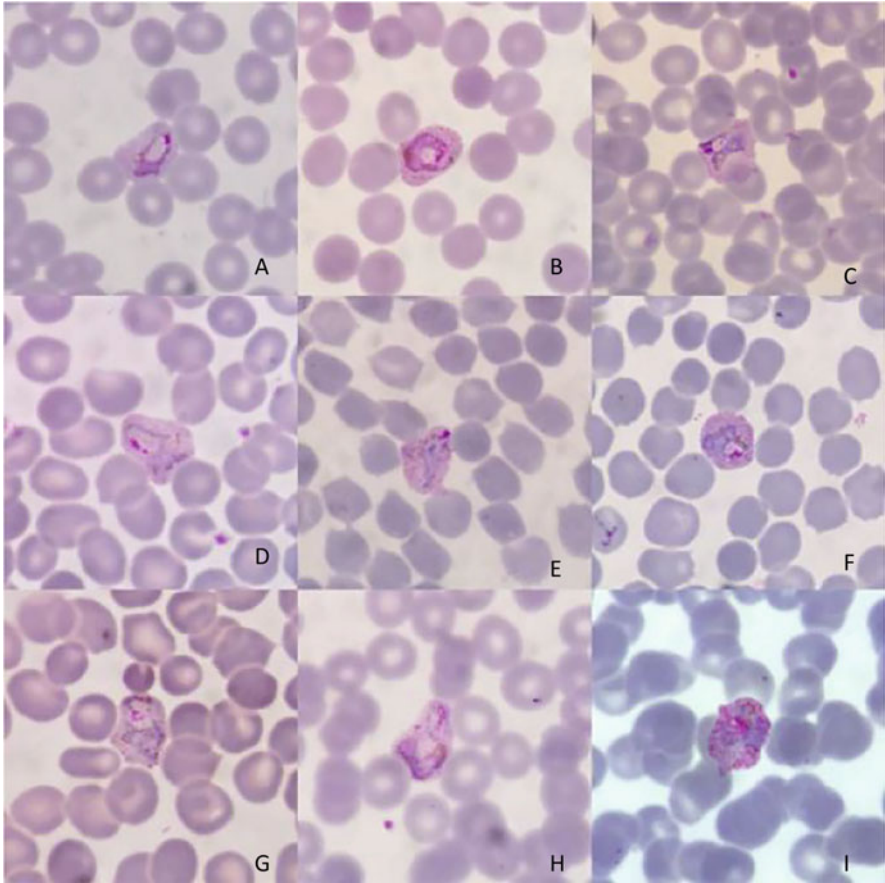


Fig. 6.45 Large trophozoites of *P. vivax* (Giemsa staining, $\times 1000$)

long from peripheral blood collection to smear, the spiny trails often disappear. At the same time, when the parasitism rate is low, small trophozoites often dominate morphology in the blood smear, which is difficult to distinguish from the small trophozoites of other malaria species. These make identification difficult if it cannot be based on the morphology of other stages in the same blood smear. Overall, small trophozoites of *P. ovale* are characterized by a small, compact, regular shape, no obvious cytoplasmic deformation, occupying a small part of the pRBCs, often with a break between the nucleus and cytoplasm (ABCD), or a “cat’s eye” shape (HI), with the pRBCs being normal in size or slightly swollen and deformed (GH), with small Schüffner’s dots.

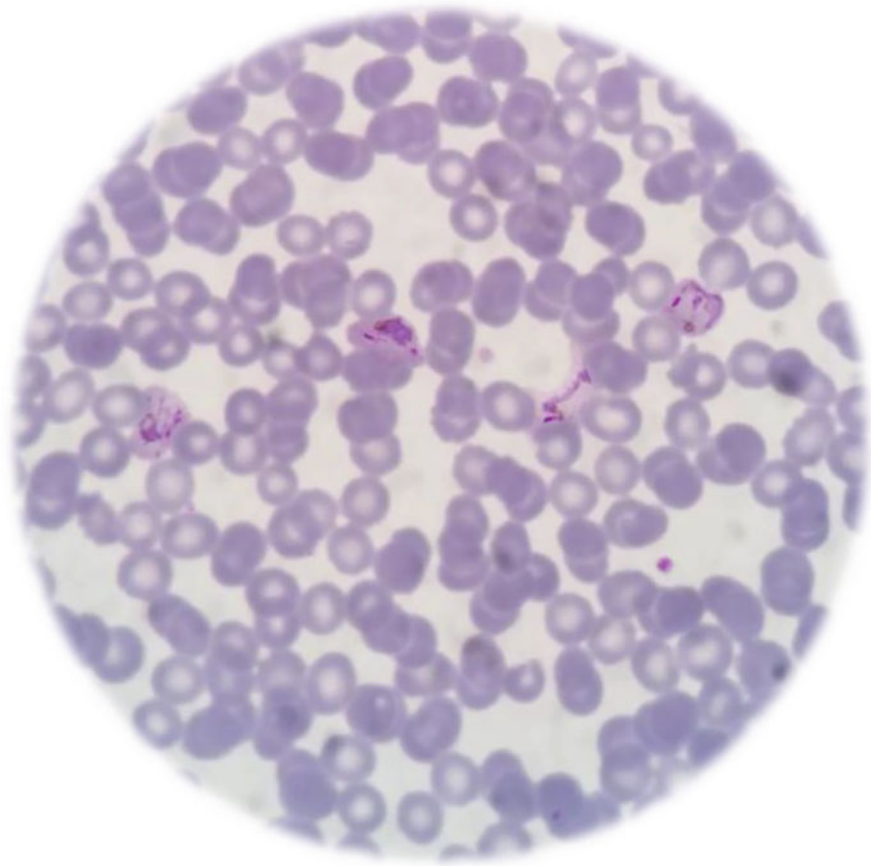


Fig. 6.46 Four large trophozoites of *P. vivax* (Giemsa staining, $\times 1000$)

6.4.2 Large Trophozoites of *P. ovale* in Thin Blood Smears

The morphology of the large trophozoites of *P. ovale* is shown in Fig. 6.66, 6.67, and 6.68.

As the small trophozoites continue to develop, the red nucleus becomes larger, the blue cytoplasm becomes larger and thicker, and brownish-yellow malaria pigments appear, which develop into large trophozoites. Unlike large trophozoites of *P. vivax*, which vary in morphology and size, large trophozoites of *P. ovale* are compact and relatively regular in shape, occupying a portion of the pRBCs with a vacuolated cytoplasm (ABC), but the vacuolated area gradually fills up as they develop (DEFGHI). The pRBCs are normal or slightly swollen in size and may show a distinct spiny trailing tail. Compared to *P. vivax*, their Schüffner's dots are slightly thicker and more pronounced, with a tighter arrangement, resulting in darker staining of the pRBCs. The large trophozoites sometimes appear similar to the

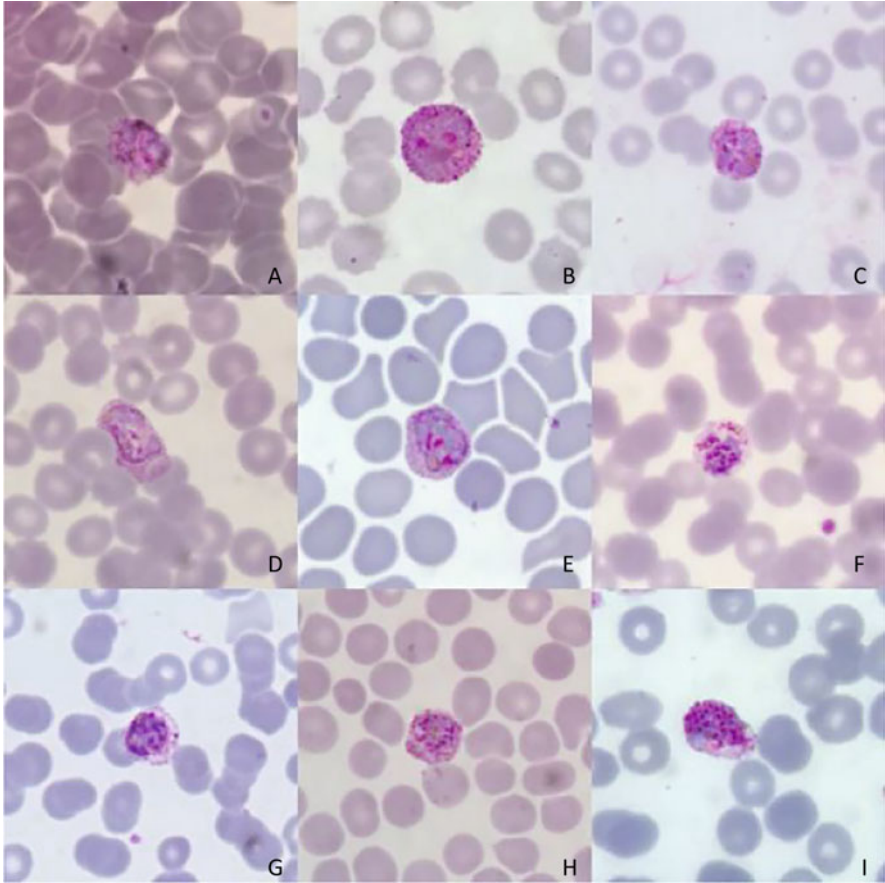


Fig. 6.47 Immature schizonts of *P. vivax* (Giemsa staining, $\times 1000$)

“ribbon-like” (CDEF), which are similar to large trophozoites of *P. malariae*. It can be identified by the characteristics of the pRBCs, such as the presence of spiny trailing and Schüffner’s dots, the characteristics of the malaria pigments and other *Plasmodium* morphology in the same blood smear.

The spiny trailing of pRBCs is an important basis for the identification of *P. ovale*, but spiny trailing is often not evident, and sometimes the pRBCs are obviously swollen and deformed (DG), resulting in a morphology similar to that of *P. vivax*. However, large trophozoites of *P. ovale* are smaller, compact, and regular, occupying a portion of the pRBCs, with *Plasmodium* (egg yolk-like) and pRBCs (egg protein-like) forming a “fried poached-egg” shape. It is also important to consider the overall morphological characteristics of the entire smear and depend on the morphology of typical *Plasmodium*.

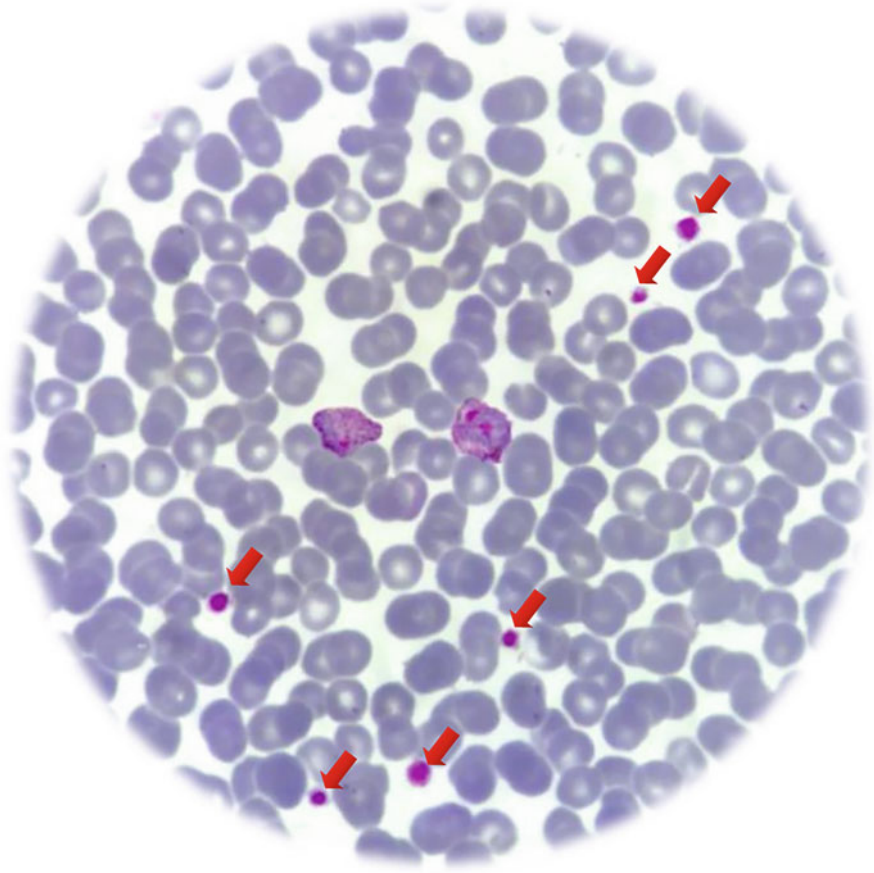


Fig. 6.48 A large trophozoite (left) and an immature schizont (right) of *P. vivax* (Giemsa staining, $\times 1000$)

Compared to the small trophozoites (top), the nucleus and cytoplasm of the large trophozoites (bottom) are large and distinct, and Schüffner's dots are more pronounced in the RBCs parasitized by the large trophozoites.

6.4.3 Schizonts of *P. ovale* in Thin Blood Smears

The morphology of the schizonts of *P. ovale* is shown in Figs. 6.69 and 6.70.

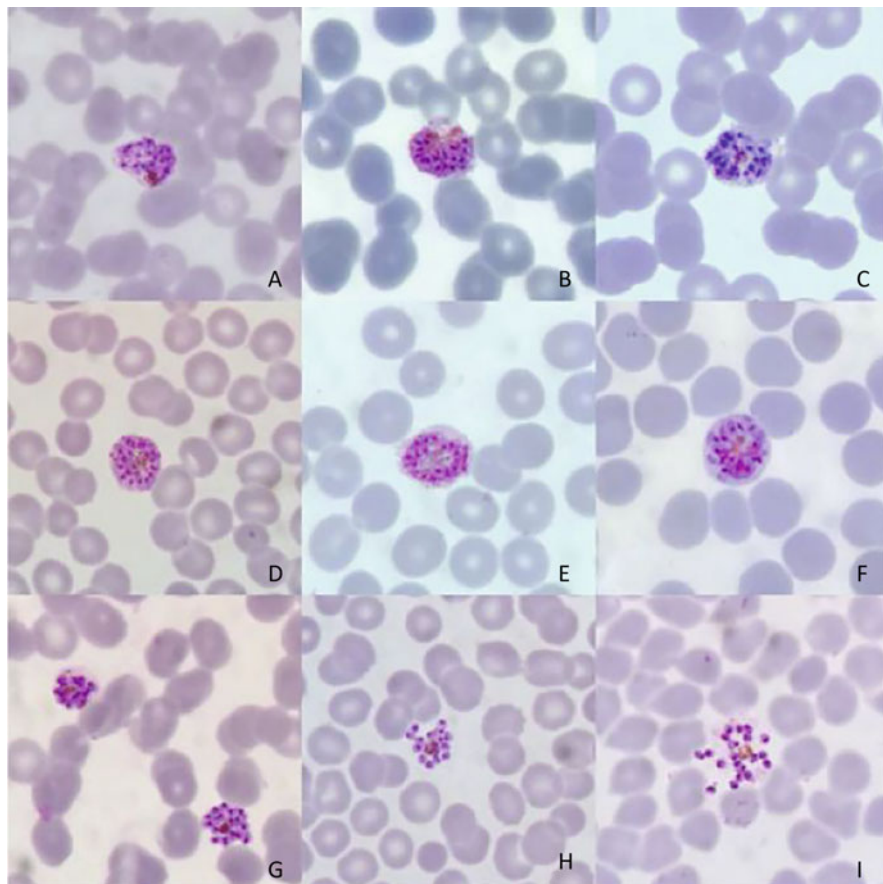


Fig. 6.49 Mature schizonts of *P. vivax* (Giemsa staining, $\times 1000$)

At the erythrocytic phase, immature schizonts of *P. ovale* are more common than mature schizonts. The merozoites are generally 2 (A) to 7 (GHI) and are characterized by “large, few and densely distributed.” Brownish-yellow malaria pigments accumulating on one side, blue cytoplasmic masses, round or oval, closely enclosing merozoites and malaria pigments. The schizonts occupy a portion of the pRBCs and form a “fried poached-egg” shape. If nearly mature, they can also fill most pRBCs (HI). The pRBCs are slightly swollen and deformed, sometimes showing a spiny trailing tail (CEG), which can be beneficial for judgment, and the Schüffner’s dots are even thicker, giving the pRBCs darker staining (I). The blue arrows point to neutrophils.

Compared to immature schizonts, the merozoites of mature schizonts have a number varying from 6 to 12 and are characterized by a “large, small, densely distributed,” each nucleus with a separate cytoplasm surrounding it and showing grainy and clear morphology. Due to the compact structure of schizonts, merozoites,

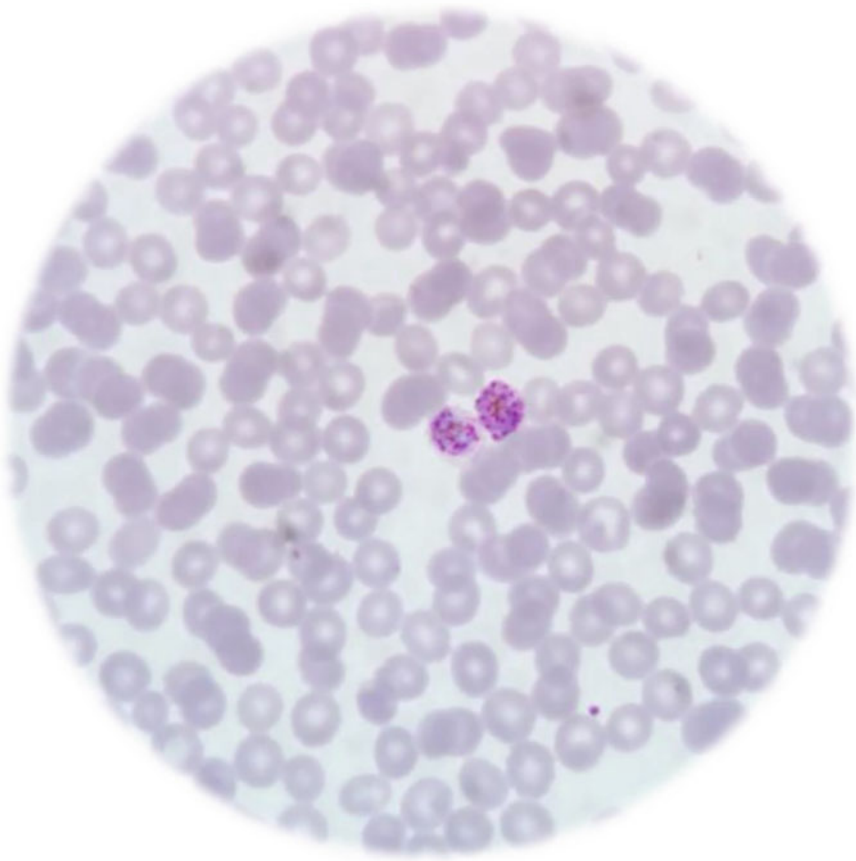


Fig. 6.50 An immature schizont (left) and a mature schizont (right) of *P. vivax* (Giemsa staining, $\times 1000$)

and brownish-yellow malaria pigments are encapsulated in the cytoplasm. The size varies, sometimes being small (ABC), sometimes being large (GH), and occasionally schizonts dispersed (I). The schizonts occupy the majority of the pRBCs, and when the pRBCs have spiny trailing tails (ABCDG), this can be beneficial for a differential diagnosis, as can other *Plasmodium* morphology in the same blood smear (I).

6.4.4 Gametocytes of *P. ovale* in Thin Blood Smears

The morphology of the gametocytes of *P. ovale* is shown in Figs. 6.71 and 6.72.

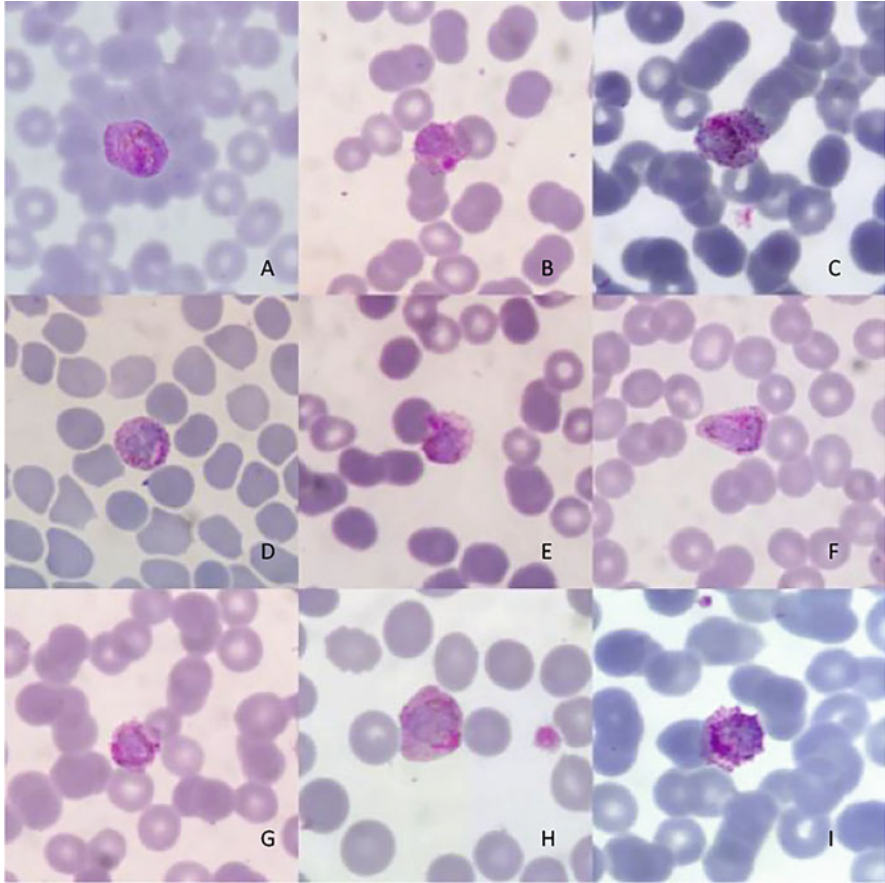


Fig. 6.51 Immature female gametocytes of *P. vivax* (Giemsa staining, $\times 1000$)

The shape of *P. ovale* gametophytes is similar to that of *P. vivax*, with a relatively smaller size. When the nucleus becomes large and dense and the cytoplasm gradually becomes large and round, they develop into gametophytes. The female gametophytes are round or oval, the red nucleus is generally on one side, the malaria pigments are brownish-yellow, aggregated or dispersed granular, and the dark blue cytoplasm is wrapped with the nucleus and malaria pigments. Immature female gametophytes occupy most of the pRBCs (AB). Mature female gametophytes are basically full of the pRBCs. The size and shape of the pRBCs are normal, or swelling and deformation (EF), or spiny tail (C) can still be seen, and the color is deeply stained due to the coarseness of Schüffner's dots. Sometimes, the female gametophyte is also large, and pRBCs are swollen and deformed without a spiny tail (I), which is similar to that of *P. vivax*. Overall, compared to *P. vivax*, Schüffner's dots of *P. ovale* are significantly thicker and more densely distributed, resulting in a

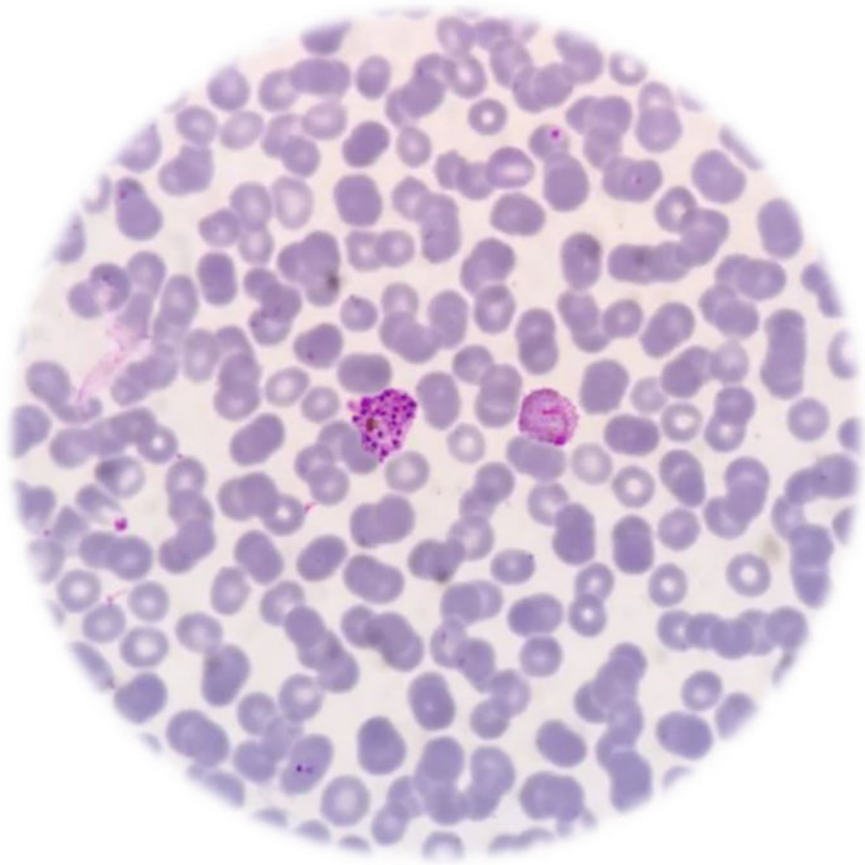


Fig. 6.52 A mature schizont (left) and a nearly mature female gametocyte (right) of *P. vivax* (Giemsa staining, $\times 1000$)

darker-red coloration inside the pRBCs. At the same time, it is also necessary to comprehensively judge the other *Plasmodium* morphology in the same blood smear.

Male gametes of *P. ovale* are less common than female gametophytes in the peripheral blood of the erythrocytic stage. Unlike female gametophytes, the red nucleus of male gametophytes is generally large and loose, with a round or oval cytoplasm that is pale blue, sometimes with inconspicuous cytoplasm and only the nucleus and brownish-yellow malaria pigments (ABC) visible, with Schüffner's dots evident within the pRBCs. As maturation proceeds, the nucleus of the male gametophyte expands, enveloping the cytoplasm, and malaria pigments (I).

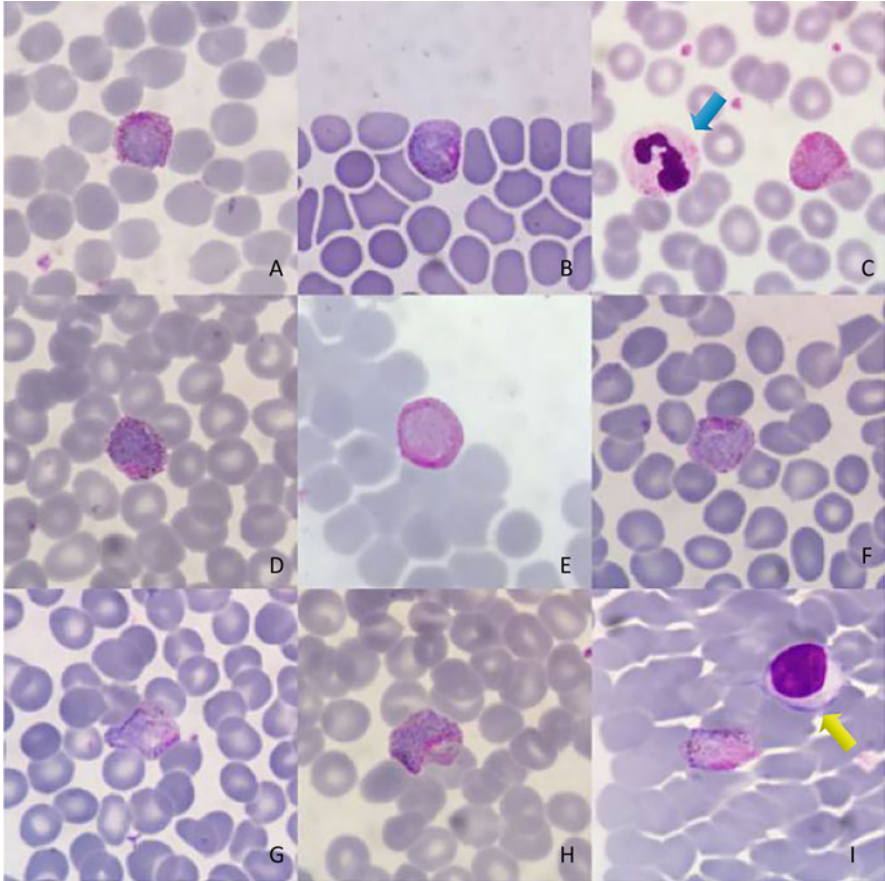


Fig. 6.53 Mature female gametocytes of *P. vivax* (Giemsa staining, $\times 1000$)

6.4.5 The Morphology of *P. ovale* in Thick Blood Smears

Because of its small size and regular and compact shape, *P. ovale* shares the same shape on thin and thick blood smears but is reduced in size. The morphology of *P. ovale* on thick blood smears is shown in Figs. 6.73, 6.74, 6.75, 6.76, 6.77, and 6.78.

The trophozoites of *P. ovale* in thick blood smears were reduced in size and significantly smaller than the surrounding WBCs, which is a remarkable characteristic of *P. ovale* in thick blood smears. Therefore, a preliminary identification can be made by comparing the size of *Plasmodium* with that of WBCs, such as neutrophils. Since Schüffner's dots of *P. ovale* are thicker within pRBCs, Schüffner's dots are still visible in the thick blood smears when the staining is of good quality, as well as the outline of pRBCs.

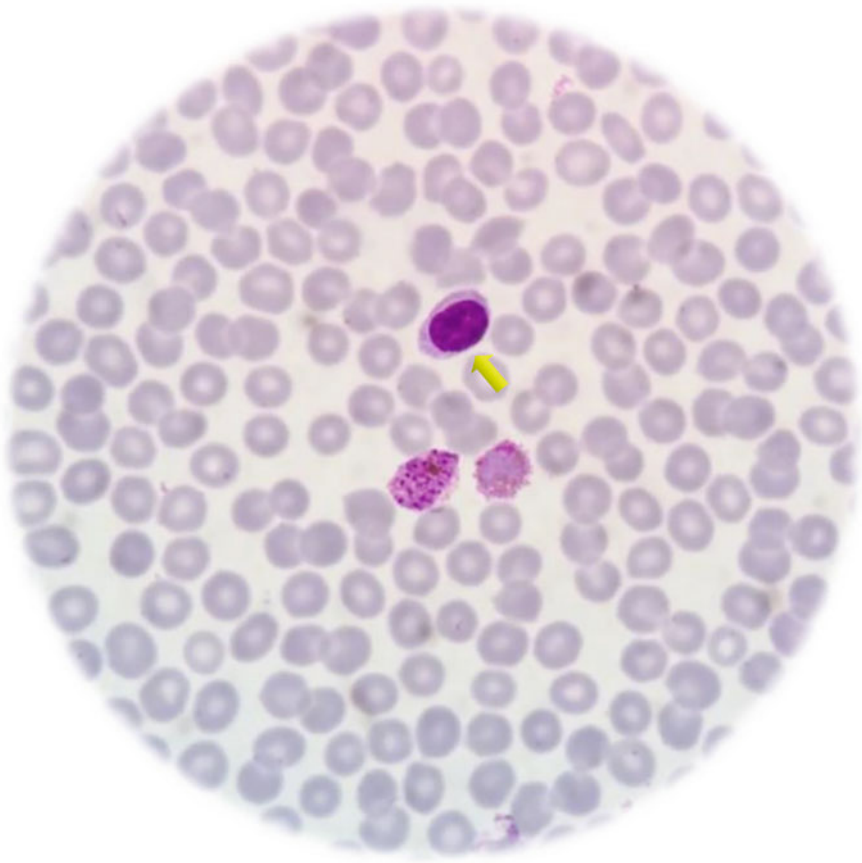


Fig. 6.54 A mature schizont (left) and a mature female gametocyte (right) of *P. vivax* (Giemsa staining, $\times 1000$)

The schizonts of *P. ovale* share the same morphology on thin and thick blood smears. Schuffner's dots are dimly visible, and the *Plasmodium* size is smaller than the surrounding WBCs, which is approximately half of the WBC diameter. *P. ovale* and *P. vivax* may be effectively distinguished according to size. Two trophozoites of *P. ovale* are inside the red circle.

A trophozoite of *P. ovale* is inside the red circle, and male gametocytes are inside the red box; others are female gametocytes. The gametocytes of *P. ovale* share the same morphology on thin and thick blood smears, and the gametocyte shape of *P. ovale* is similar to that of *P. vivax*. However, the size of *P. ovale* at all stages is significantly smaller than that of the surrounding WBCs. Therefore, *P. ovale* and *P. vivax* may be effectively distinguished according to the size of WBCs.

The size of *P. ovale* is relatively small and regular at all life cycle stages, with apparent Schuffner's dots.

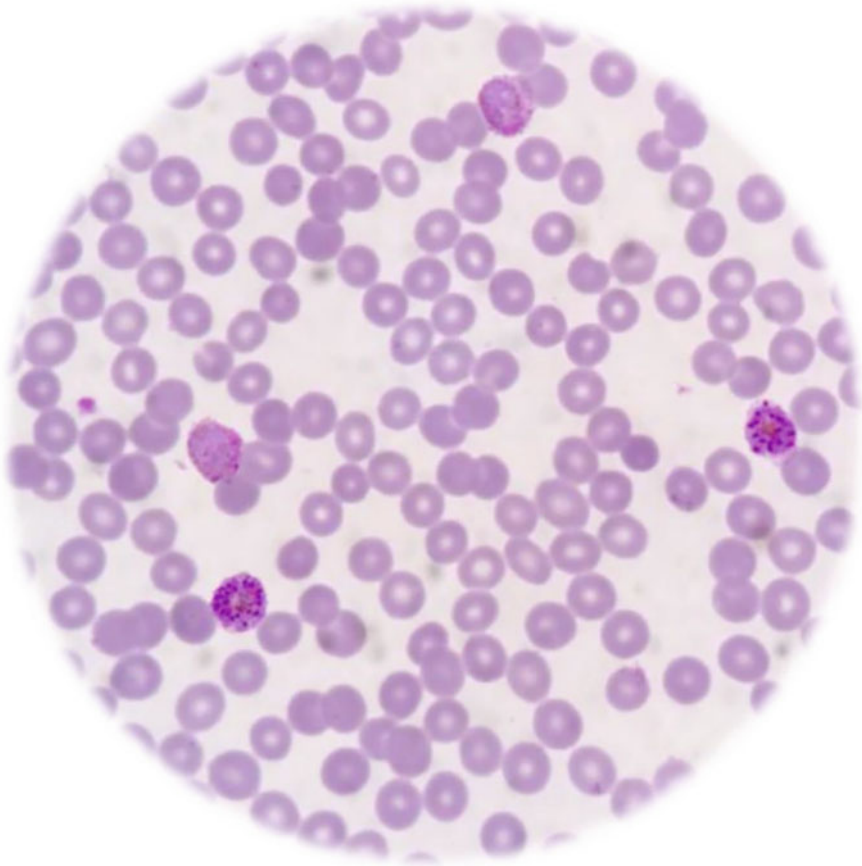


Fig. 6.55 A nearly mature female gametocyte (upper), a mature female gametocyte (left), an immature schizont (right), and a mature schizont (below) of *P. vivax* (Giemsa staining, $\times 1000$)

The parasitism rate of *P. ovale* is generally low, and detection on thin blood smears is more difficult. Therefore, it is necessary to have knowledge of morphology in thick blood smears. There is one female gametocyte of *P. ovale* and two trophozoites in the view. The body is compact, regular in shape, and approximately half the size of the surrounding WBCs.

6.4.6 Identification of *P. ovale* and *P. vivax*

P. ovale is similar to *P. vivax* in terms of morphology. Notably, if *P. ovale* is low in density and atypical in morphology, it is difficult to distinguish it from *P. ovale*. Sometimes, the size of *P. vivax* is small at an early stage and occupies a part of

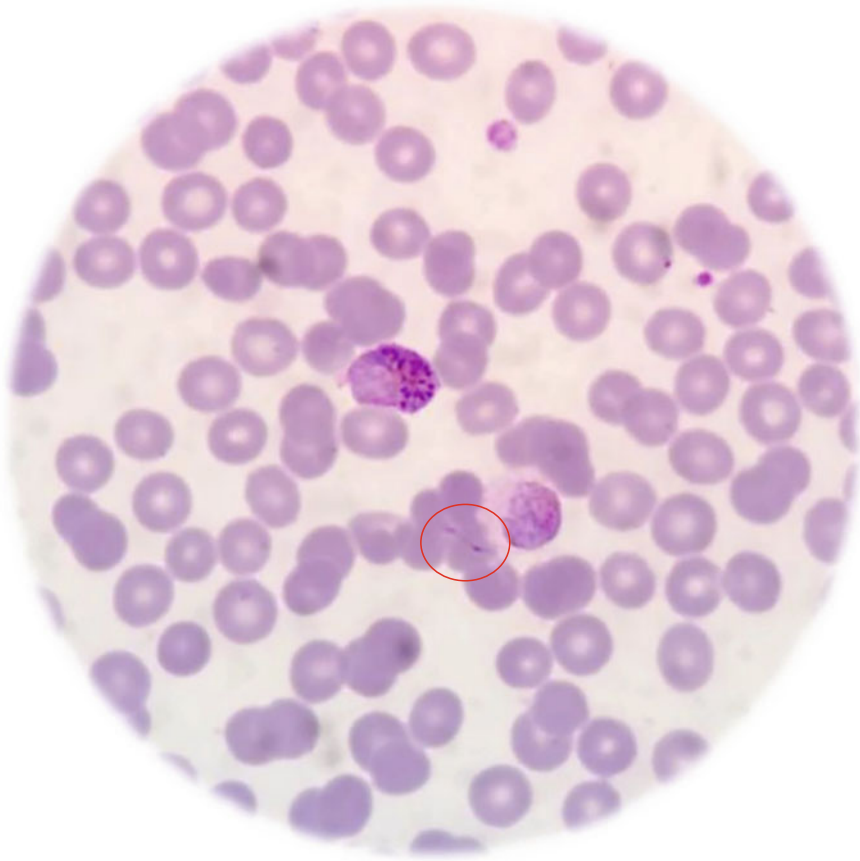


Fig. 6.56 Asynchronization of multiple *P. vivax* infections (Giemsa staining, $\times 1000$)

pRBCs, and the pRBCs have a “serration” or “spiny tail” (Fig. 6.79), which looks like a “fried poached egg.” Therefore, if *P. ovale* is low in density and atypical in morphology, a complete microscopic examination of the whole blood smear is needed. First, the size of *P. ovale* is generally small, and the pRBCs are not swollen. However, the size of *P. vivax* is usually large, resulting in the presence of large and diverse pRBCs. Second, the merozoites of *P. ovale* are large, few, and densely distributed, while the merozoites of *P. vivax* are small, numerous, and scattered. Third, the pRBCs of *P. ovale* have coarse and evenly and tightly distributed Schuffner’s dots, which are dark-red or purplish-red on blood smears and remain visible on thick blood smears. The pRBCs of *P. vivax* have tiny and “gravel-like” Schuffner’s dots, and the pRBCs are relatively shallow in color and may form pRBC shadows on thick blood smears. Finally, the small trophozoites of *P. ovale* are frequently low in density, showing the morphological characteristics of the nucleus

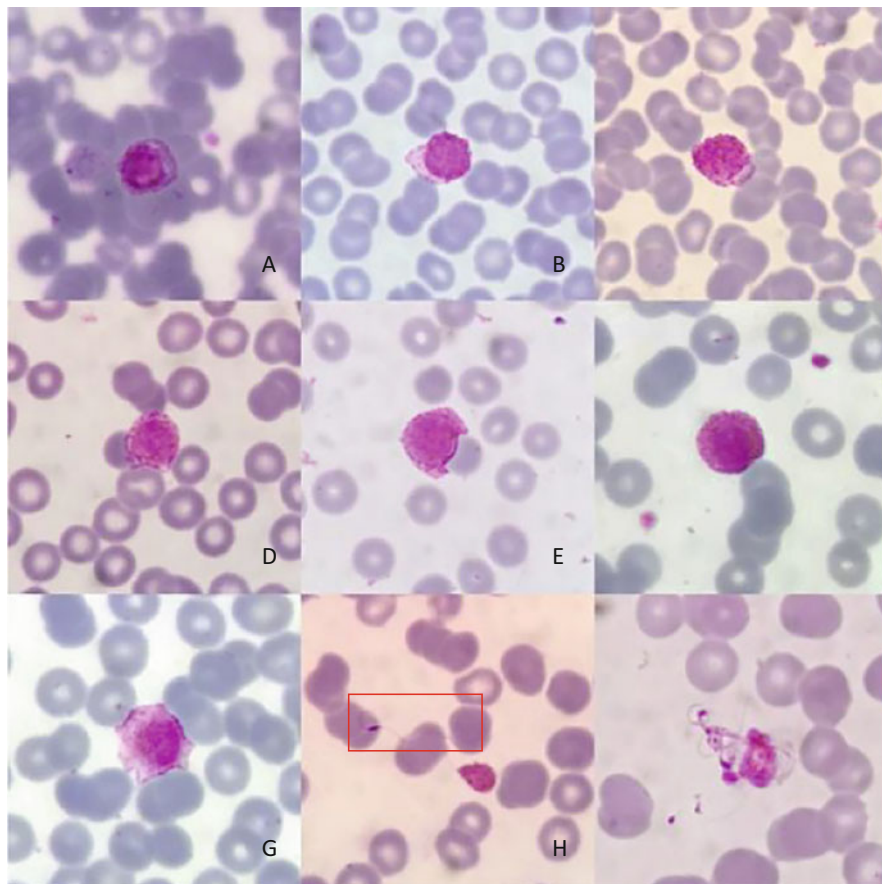


Fig. 6.57 Male gametocytes of *P. vivax* (Giemsa staining, $\times 1000$)

and cytoplasm separation (Fig. 6.65 a,b,c,d); however, the small trophozoites of *P. vivax* usually present a shape of the nucleus and cytoplasm connection.

A malaria case imported from Pakistan was suspected to be coinfecting with *P. vivax* and *P. ovale* by microscopic examination and confirmed to be *P. vivax* by nested PCR and real-time PCR. In fact, RBCs parasitized by *P. vivax* can also form spiny trailing tails, especially in the immature stage (DEF). However, *P. vivax* is generally large in size and occupies all RBCs, and the typical morphology is also helpful for diagnosis (ABCGHI). The Howell-Jolly body is shown by a black arrow.

The proportion of people with the Duffy blood type in sub-Saharan Africa is 90% of the total population but accounts for less than 30% in the Horn of Africa (northeastern Africa). Therefore, sub-Saharan African populations are protected from *P. vivax* infection or at reduced risk of infection. This is similar to the presence of an immune barrier against *P. vivax*. In addition, epidemiological data of imported malaria from overseas in Wuhan city have shown that *P. ovale* and *P. malariae* are

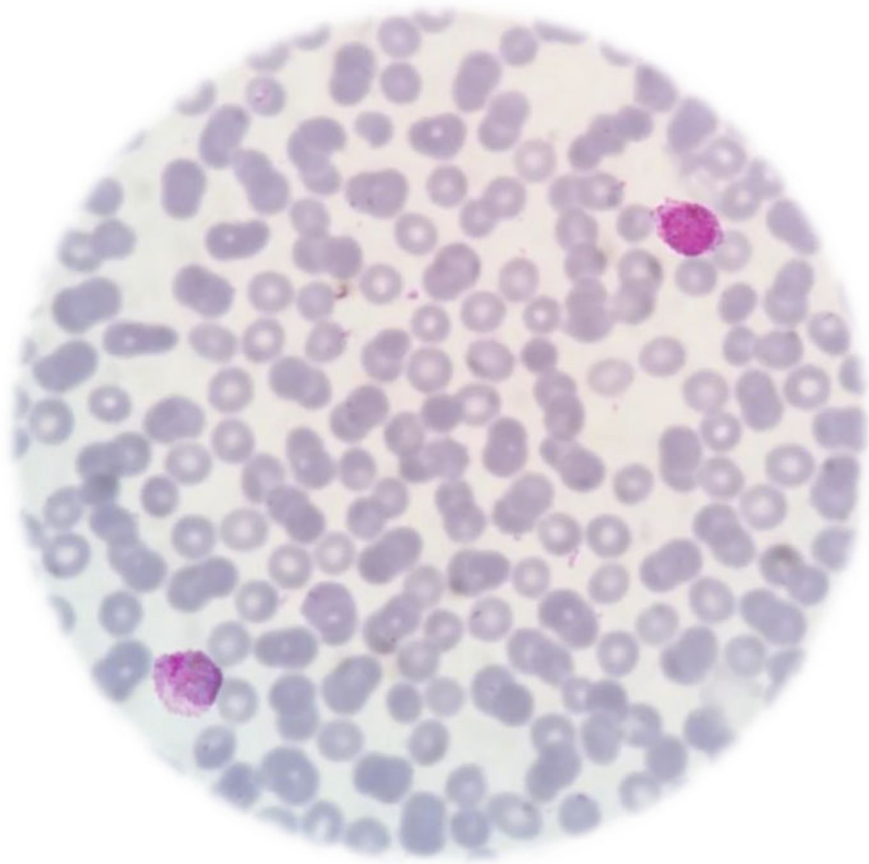


Fig. 6.58 A male gametocyte (upper) and a nearly mature female gametocyte (lower) of *P. vivax* (Giemsa staining, $\times 1000$)

mainly distributed in the tropical rainforest regions of sub-Saharan Africa and are rare in other areas of the world. Thus, it provides a way to distinguish between *P. ovale* and *P. vivax* imported from endemic areas according to the epidemiological history and life cycle of *Plasmodium* species. For example, if the patient returned from the Democratic Republic of the Congo and was detected as “nonfalciparum malaria” by RDT, there is a high probability that the patient was infected with *P. ovale* or *P. malariae*. If the patient returning from Angola for more than 3 months ago develops clinical symptoms related to malaria, “nonfalciparum malaria” is identified by RDT and microscopic examinations identify positive *Plasmodium*, there is a great possibility that is a *P. ovale*. Because *P. vivax* and *P. ovale* have a long dormant period and *P. ovale* are prevalent in sub-Saharan Africa. Geographical distribution characteristics of *P. ovale* and *P. malariae* facilitate the preliminary identification of microscopic morphology.

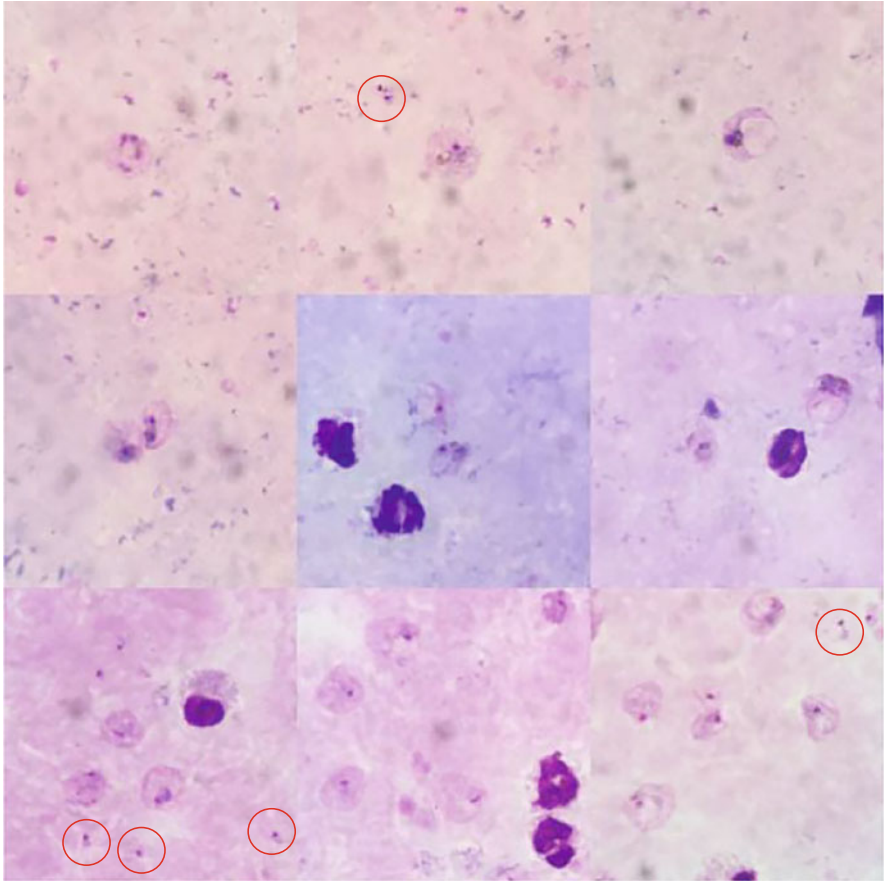


Fig. 6.59 Trophozoites of *P. vivax* on a thick blood smear (Giemsa staining, $\times 1000$)

6.5 Morphology of *Plasmodium malariae*

6.5.1 Small Trophozoites of *P. malariae* in Thin Blood Smears

The morphology of the small trophozoites of *P. malariae* is shown in Fig. 6.80.

When *P. malariae* has just invaded RBCs, small trophozoites are very small, with a red nucleus and blue cytoplasm concentrated together (AB), dense, darkly colored, similar to impurities, and extremely easy to miss detection. As they develop, the cytoplasm gradually becomes larger and changes from round (C) to rectangular-like (DE), with a regular morphology. The dark-brown malarial pigments appear earlier and are granular and arranged along the cytoplasmic edge. At this point, the nucleus and malaria pigments are more visible, while the cytoplasm is masked by malaria

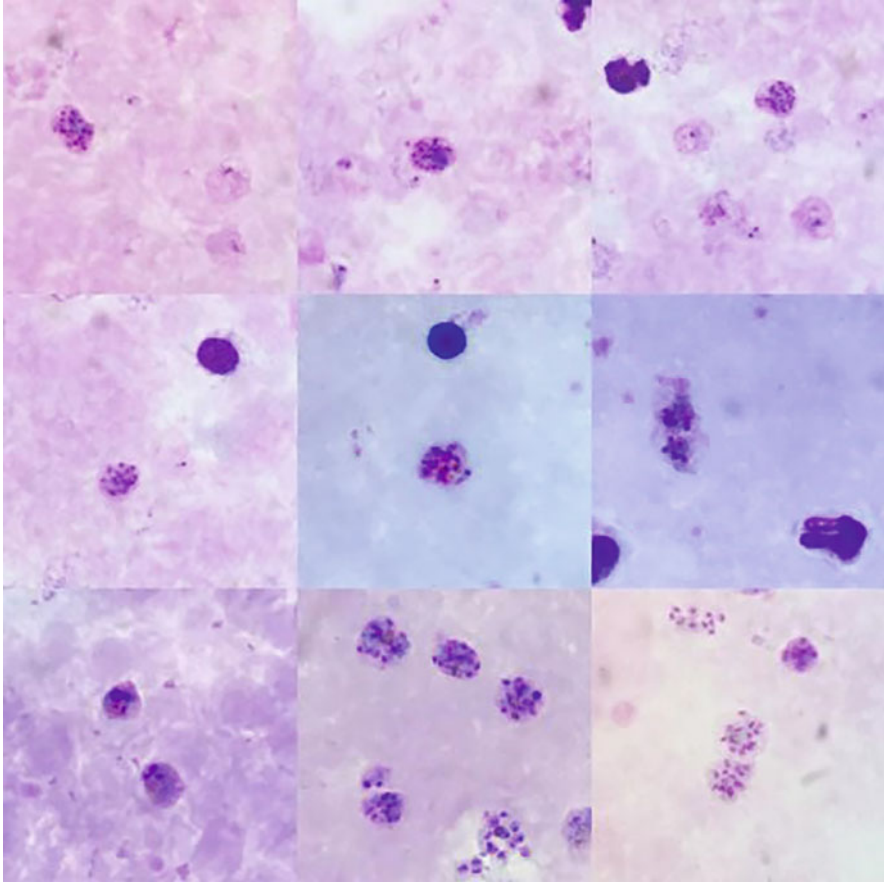


Fig. 6.60 Schizonts and trophozoites of *P. vivax* on a thick blood smear (Giemsa staining, $\times 1000$)

pigments (FGHI). If the staining quality is poor, only the nucleus and the ring-shaped malarial pigments are seen. *P. malariae* parasites aged RBCs, so the pRBCs are slightly smaller than the surrounding RBCs but with a regular morphology. Additionally, the parasitism rate is usually very low, which can lead to misdiagnosis. There are also long periods of asymptomatic peripheral blood carriage of *P. malariae*, and the longest case of *P. malariae* has been observed in Wuhan after returning to China for 6 months.

6.5.2 Large Trophozoites of *P. malariae* in Thin Blood Smears

The morphology of the large trophozoites of *P. malariae* is shown in Figs. 6.81, 6.82, and 6.83.

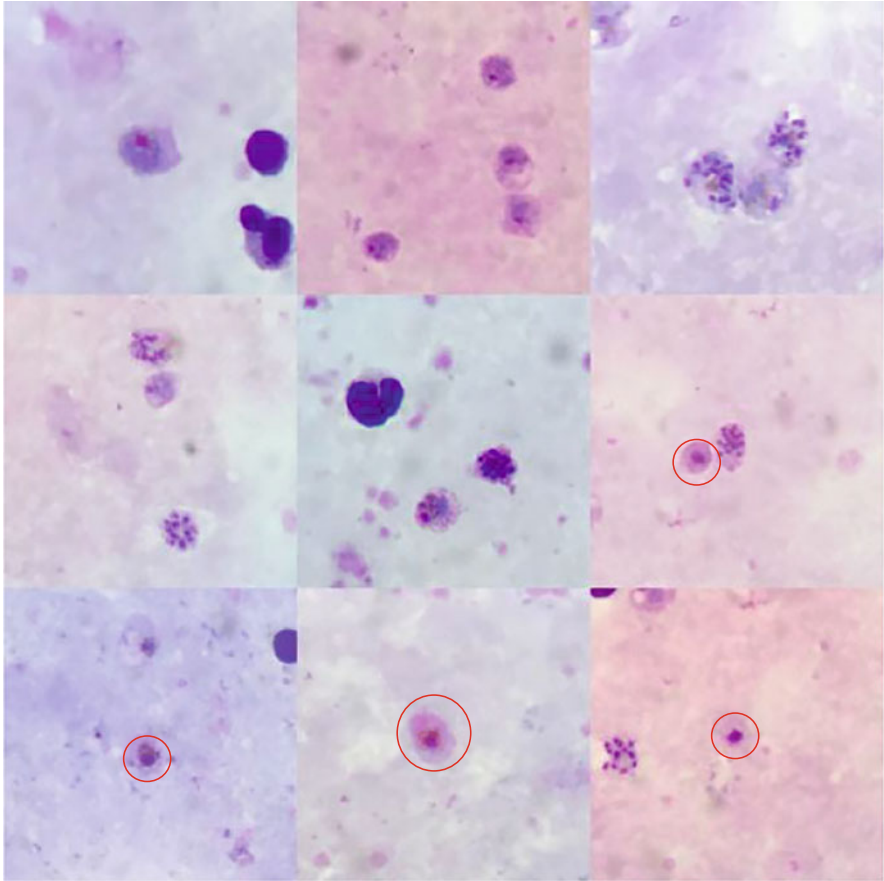


Fig. 6.61 Gametocytes and schizonts of *P. vivax* on a thick blood smear (Giemsa staining, $\times 1000$)

Large trophozoites are critical for the identification of *P. malariae*. When the nucleus becomes larger, the cytoplasm becomes larger and thicker, and the vacuole gradually fills up, indicating development into large trophozoites. The large trophozoites are initially round (AB) and gradually become “ribbon” (FGHI), with the dark-brown malaria pigment granules becoming more remarkable and thicker, which are arranged or accumulated in a pile along the cytoplasmic edge. The banded cytoplasm varies in size and can reach the ends of the pRBCs (GHI) or be slightly twisted (FH). The pRBCs are generally slightly smaller than the surrounding RBCs and have a normal morphology. The yellow arrows point to lymphocytes. If the nucleus and cytoplasm become bigger and circular, early or immature gametocytes may be considered.

There is only one large trophozoite of *P. malariae*. The nucleus and malaria pigments are apparent, and the light-blue cytoplasm is faintly visible. The yellowish-

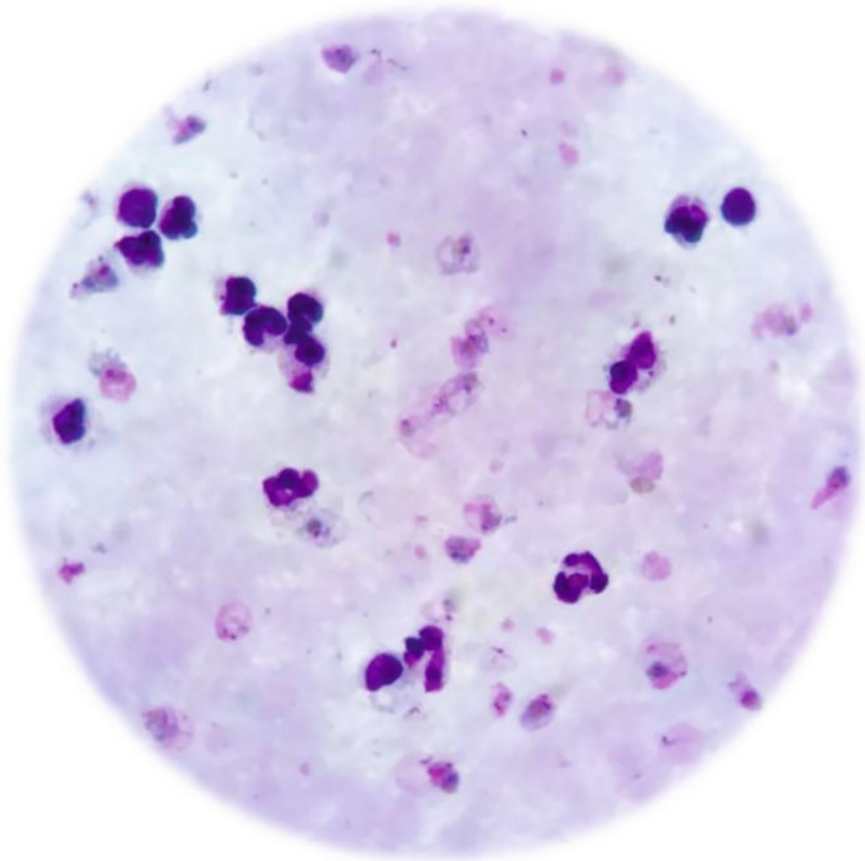


Fig. 6.62 Various trophozoites of *P. vivax* on a thick blood smear (Giemsa staining, $\times 1000$)

brown malaria pigment particles form a rectangle-like band. Lymphocytes are indicated by yellow arrows.

6.5.3 Schizonts of *P. malariae* in Thin Blood Smears

The morphology of the schizonts of *P. malariae* is shown in Figs. 6.84, 6.85, 6.86, and 6.87.

The immature schizonts of *P. malariae* are more common in the peripheral blood at the erythrocytic phase. The pRBCs are smaller than the surrounding RBCs. The size is smaller, with 2–7 merozoites, and dark-brown malaria pigment granules begin to aggregate and are unevenly distributed, often at the edge of the blue cytoplasm or wrapped in the cytoplasm with the nucleus. As the number of merozoites increases,

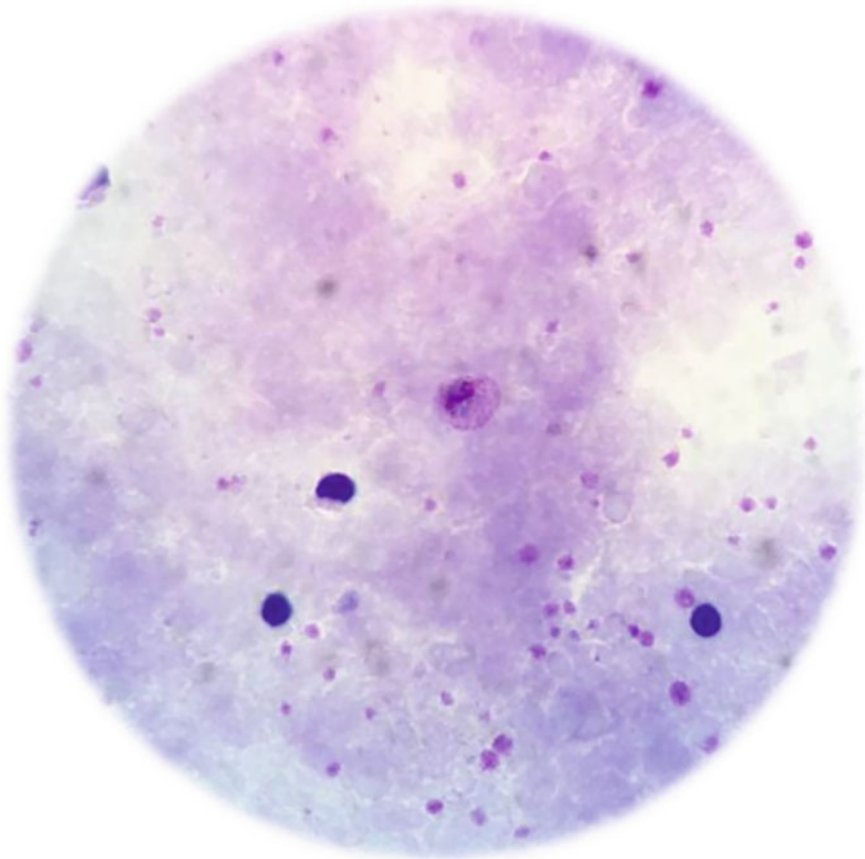


Fig. 6.63 An immature schizont of *P. vivax* on a thick blood smear (Giemsa staining, $\times 1000$)

the cytoplasm changes from rectangular (ABCD) to round or oval (EFGHI). When the cytoplasm tends to divide, this indicates that schizonts tend to mature (HI). The yellow arrows point to lymphocytes.

Mature schizonts are critical for determining *P. malariae*, but they are uncommon in the peripheral blood at the erythrocytic phase. The schizonts present a petal-like shape, which resembles plum blossom or peach blossom. The merozoites are arranged around the stamen-like dark-brown malarial pigments. Generally, there are 6–8 merozoites, more than 10 occasionally (H). The merozoites are small, few, scattered, and often exhibit fission and escape (I).

The blue arrow indicates neutrophils.

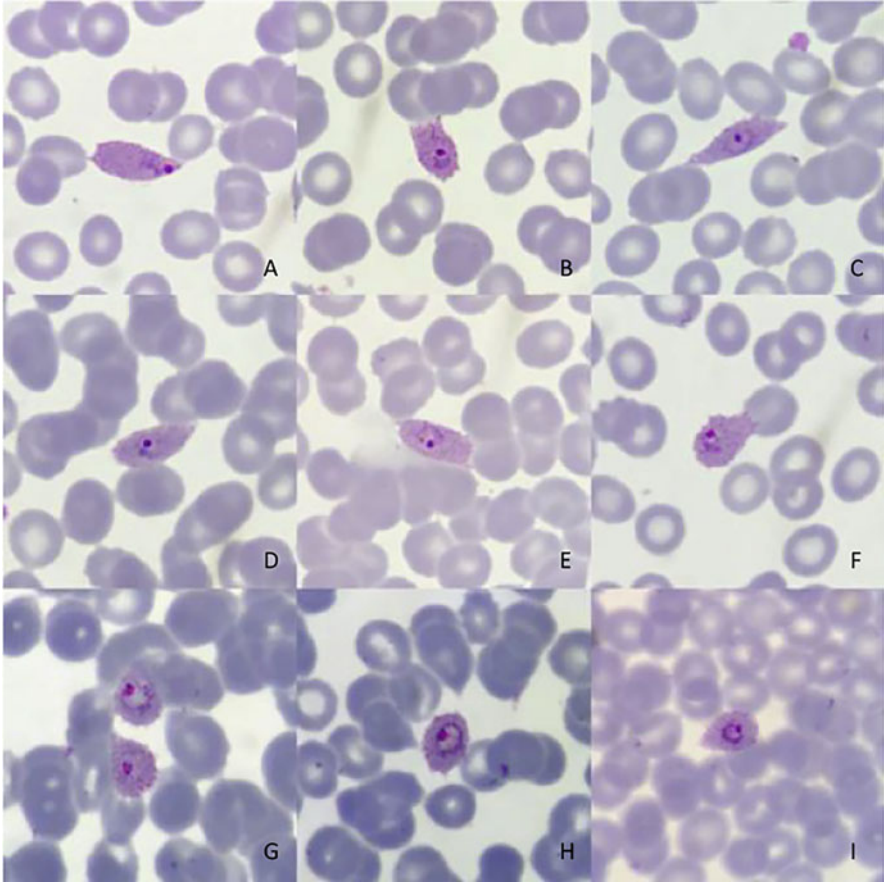


Fig. 6.64 The small trophozoites of *P. ovale* (Giemsa staining, $\times 1000$)

6.5.4 Gametocytes of *P. malariae* in Thin Blood Smears

The morphology of the gametocytes of *P. malariae* is shown in Figs. 6.88, 6.89, 6.90, and 6.91.

Immature female gametocytes (ABCDEs) of *P. malariae* are common in the peripheral blood at the erythrocytic phase. Compared with large or mature trophozoites, the nucleus of immature female gametocytes is larger and circular, and the cytoplasm is thick and gradually filled with pRBCs, indicating that the gametocytes begin to develop. At this moment, the malarial pigments are yellowish-brown or dark-brown and granular. Mature female gametocytes of *P. malariae* (FGHI) are similar to those of *P. vivax* in terms of morphology but smaller than those of *P. vivax*. They have a large bright-red circular nucleus, which is located on one side of the gametocytes, and the cytoplasm is dark blue circular or oval. The

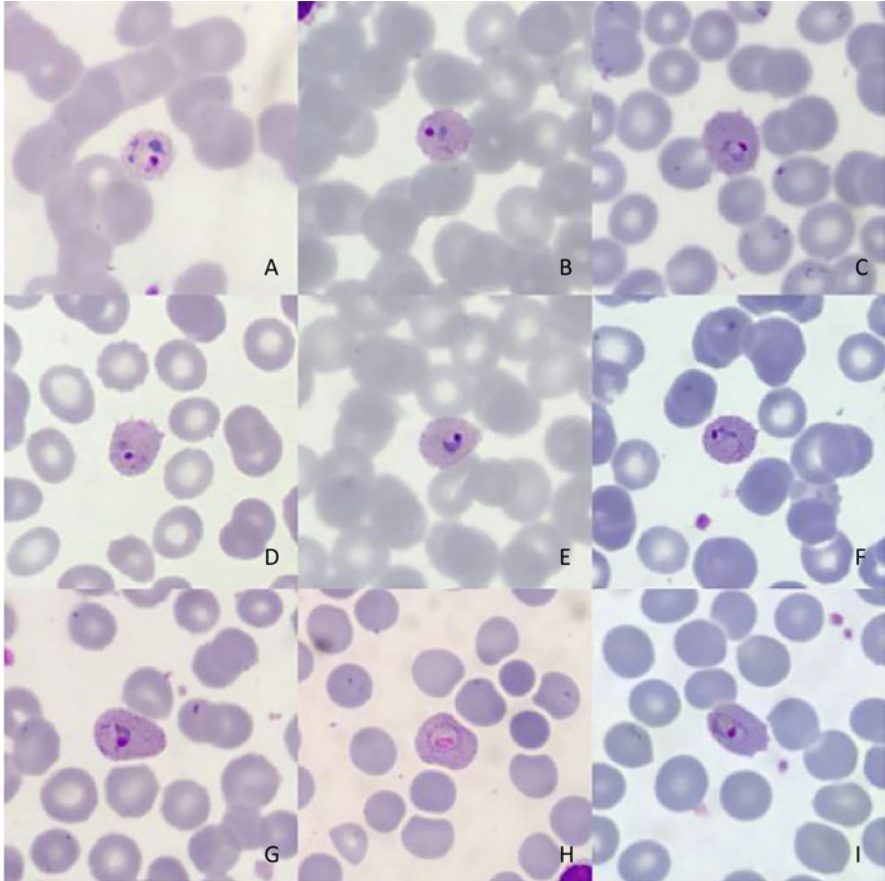


Fig. 6.65 Morphology of atypical small trophozoites of *P. ovale* (Giemsa staining, $\times 1000$)

malarial pigments are arranged along the edge of the gametocytes; however, they may be evenly distributed in the cytoplasm or aggregated into piles. The pRBCs are normal or slightly reduced.

Male gametocytes of *P. malariae* are similar to those of *P. vivax* in terms of morphology; however, the size is significantly smaller, and the pRBCs are normal or slightly reduced. The red nucleus and brownish malarial pigments are obvious, but the light-blue cytoplasm is invisible. The blue arrow indicates neutrophils.

There is only one mature female gametocyte of *P. malariae*. Female gametocytes of *P. malariae* are similar to those of *P. vivax* in terms of morphology; however, their sizes are smaller than those of *P. vivax*. The structure of *P. malariae* gametocytes is overall compact, and the pRBCs are normal or slightly smaller than the surrounding RBCs.

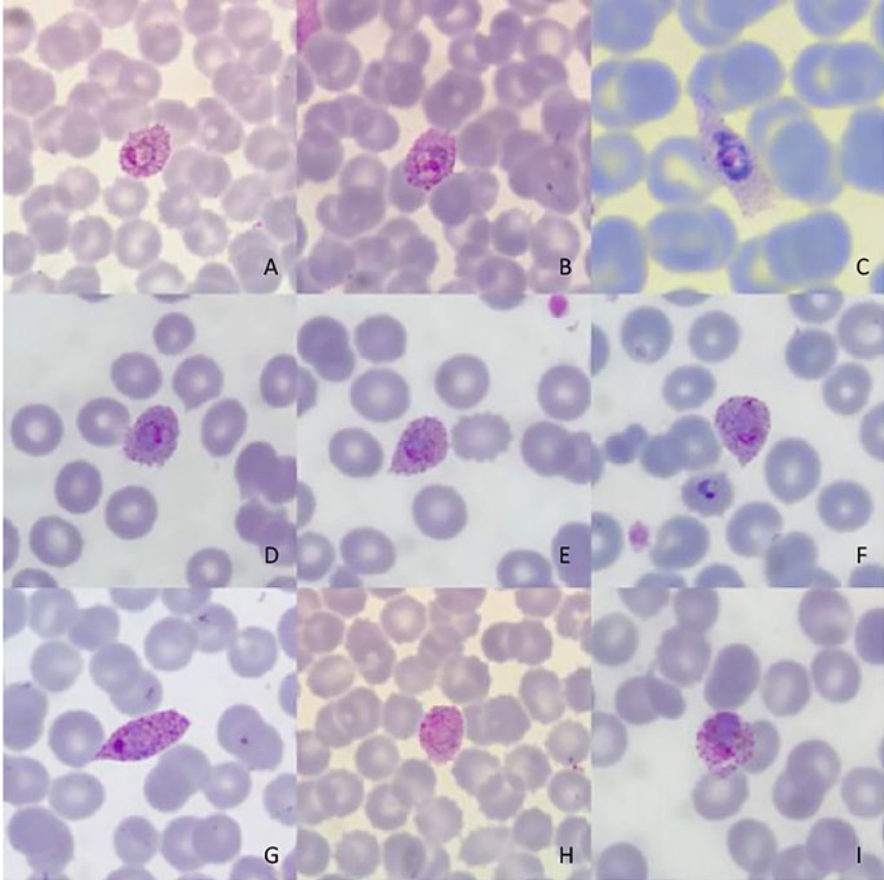


Fig. 6.66 Large trophozoites of *P. ovale* (Giemsa staining, $\times 1000$)

A mature female gametocyte of *P. malariae* is shown in view, with a large, red and round nucleus and rectangular cytoplasm. Lymphocytes are indicated by yellow arrows.

6.5.5 The Morphology of *P. malariae* in Thick Blood Smears

The morphology of *P. malariae* is overall consistent on thick and thin blood smears; however, *P. malariae* is more compact on thick blood smears. It is, therefore, more challenging to identify *P. malariae* due to the development of the small, dense, and dark-staining parasite body. The size of *P. malariae* is approximately 1/4–1/5 of the diameter of the surrounding WBCs on a thick blood smear. A very low density of *P. malariae* is found in the human blood stage, and therefore, the pathogenicity is

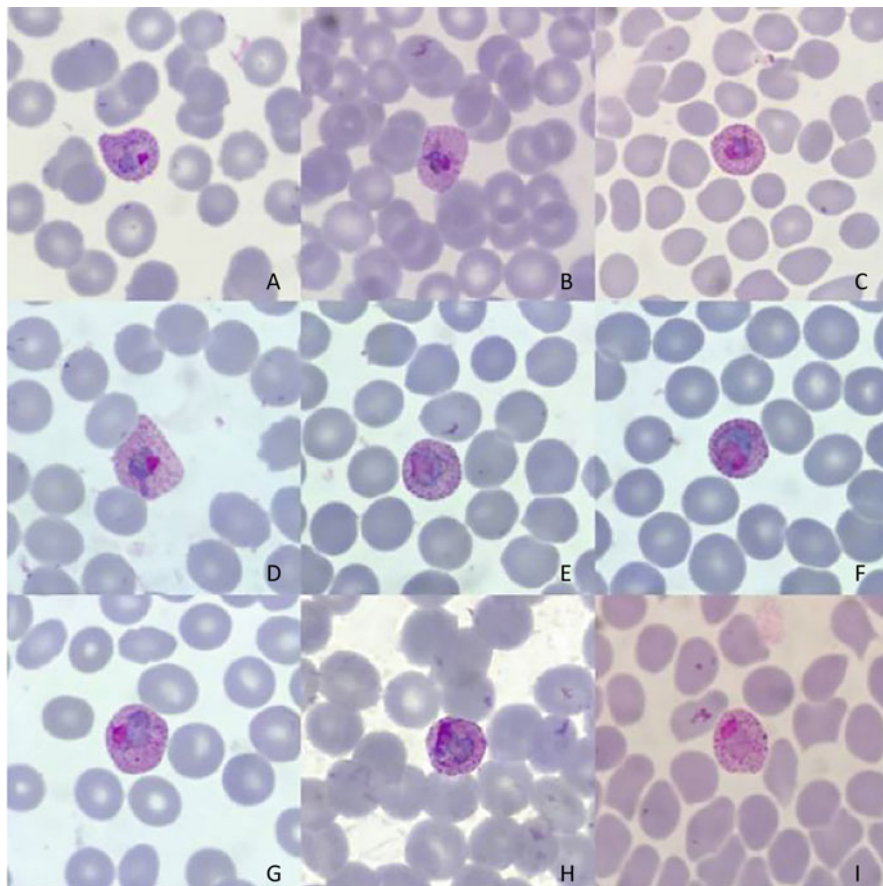


Fig. 6.67 Morphology of atypical large trophozoites of *P. ovale* (Giemsa staining, $\times 1000$)

mild, and asymptomatic parasitism probably occurs. The morphology of *P. malariae* on a thick blood smear is shown in Figs. 6.92, 6.93, 6.94, and 6.95.

In the thick blood smears, the small trophozoites are similar in morphology to the *P. falciparum* rings, but their dark-brown malaria pigments are very remarkable, and because the malaria pigments appear earlier and are distributed along the cytoplasm, they form a cytoplasmic morphology (red circle). The large trophozoites retain a ribbon-like rectangle with a distinct nucleus and malaria pigments and a faintly visible cytoplasm. The malaria pigment characteristic is one of the distinctive features of *P. malariae* in thick blood smears.

Schizonts of *P. malariae* share the same shape on the thin and thick blood smears but are reduced slightly in size. The immature schizonts are rectangular or round, approximately $1/4$ – $1/5$ the size of the surrounding WBCs. Due to the scattered distribution of merozoites, the mature schizonts are relatively large but still petal-

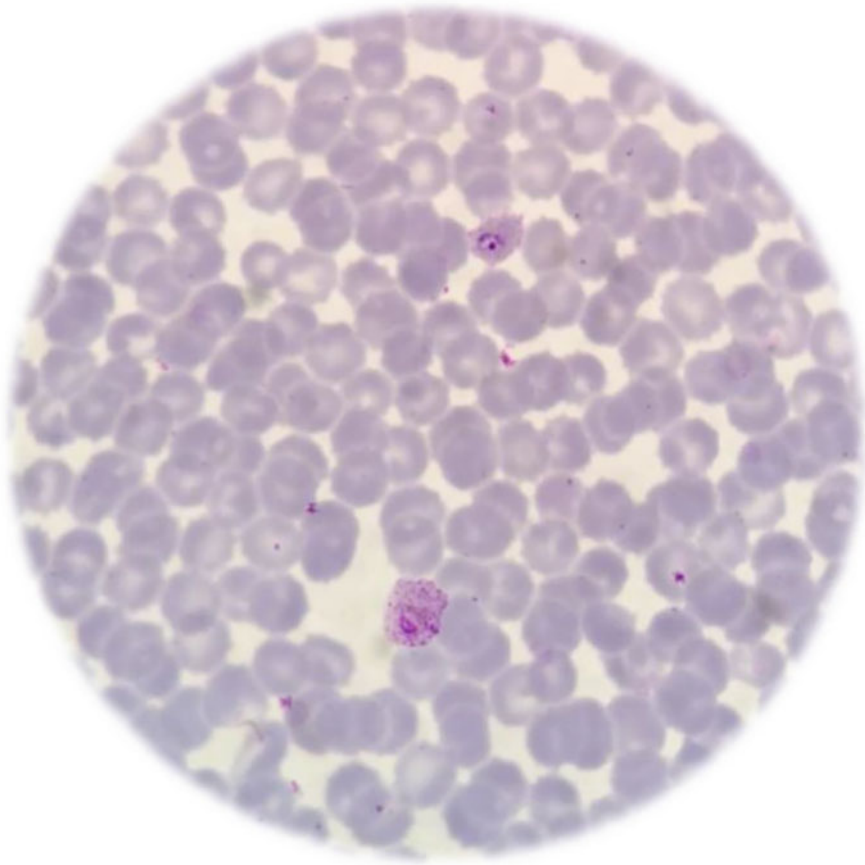


Fig. 6.68 Trophozoites of *P. ovale* (Giemsa staining, $\times 1000$)

like in form and easily recognizable. The red circle shows the trophozoites of *P. malariae*.

In the thick blood smears, the gametophytes of *P. malariae* share the same shape on the thin and thick blood smears but are reduced slightly in size. The gametophytes are a compact body, and a red nucleus and dark-brown granular malaria pigments are obvious, but the cytoplasm is masked by malaria pigments. In thick blood smears, the granular malaria pigments of *P. malariae* are clearly different from those of the other three species and can be used as a basis for differentiation. The trophozoites are in the red circle, the male gametophytes are in the red box, and the platelets are in the blue circle.

The density of *P. malariae* is generally low. Due to their small size and compact structure, they are difficult to identify. *P. malariae* trophozoites are in the red circle, schizonts are in the yellow circle, and the female gametophyte is in the blue circle.

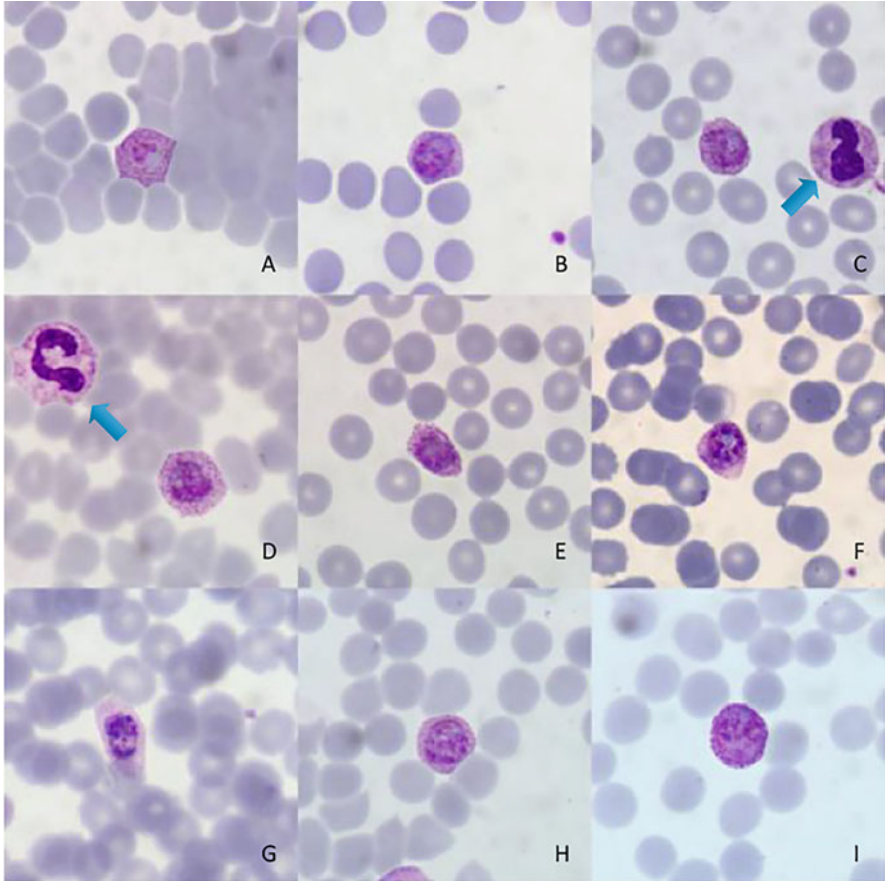


Fig. 6.69 Immature schizonts of *P. ovale* (Giemsa staining, $\times 1000$)

6.6 The Morphological Characteristics of *Plasmodium* Treated with Antimalarial Drugs

In the daily microscopic examination, blood smears after using antimalarial drugs are often encountered. Some are the dynamic *Plasmodium* monitoring and evaluation of hospitalized patients after using antimalarial drugs, and the others are caused by patients taking antimalarial drugs before hospital admission, and it is not uncommon for them to take antimalarial drugs by themselves.

After the use of antimalarial drugs, first, the density of *Plasmodium* decreased greatly, which led to a decrease in the positive rate, so it is very easy to miss detection; second, the original morphological characteristics of *Plasmodium* changed or disappeared, which led to the difficulty of *Plasmodium* species

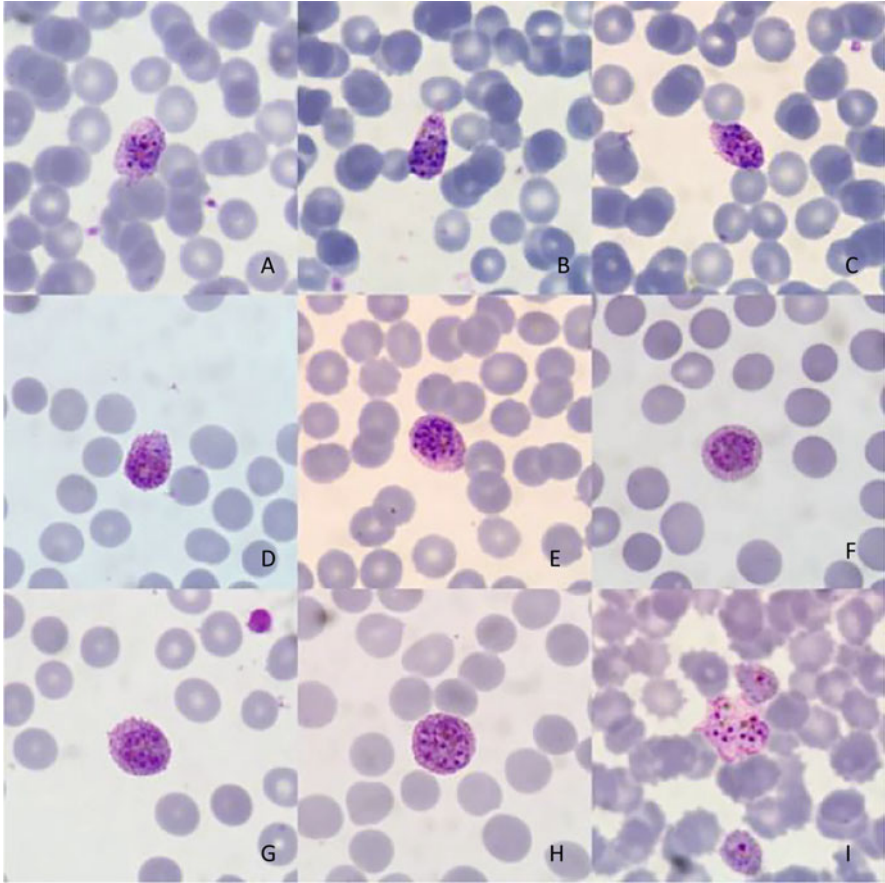


Fig. 6.70 Mature schizonts of *P. ovale* (Giemsa staining, $\times 1000$)

identification and even the failure of effective identification. The killing process of the same type of antimalarial drugs against *Plasmodium* is almost the same. For example, after the use of artemisinin, the *Plasmodium* cytoplasm disappears or breaks into several pieces first, and then the pigment agglutinates and darkens, leaving only the nucleus. With the increase in artemisinin treatment, the nucleus began to be destroyed, deformed, and stained dark, even black. It should be recognized that insufficient use of antimalarial drugs will lead to a decline in drug sensitivity and a delay in *Plasmodium* elimination, eventually leading to treatment failure. At the same time, it is also strongly recommended that a thick blood smear be used to determine the negative or positive in order to ensure the detection rate of low density after medication, sometimes, it is necessary for comprehensive judgment to combine with RDT, molecular biology, and epidemiological results if it is hard for you to make a decision by microscopic examination.

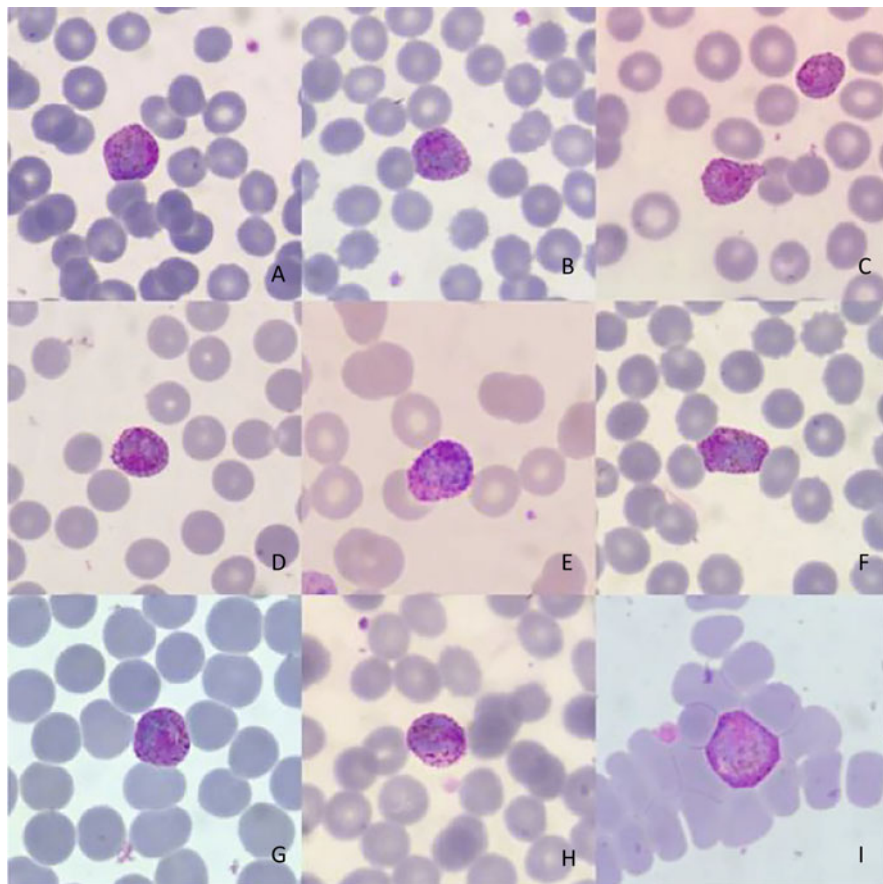


Fig. 6.71 Female gametocytes of *P. ovale* (Giemsa staining, $\times 1000$)

Therefore, the density changes and morphological characteristics of *Plasmodium* after treatment are also the focus of learning and mastering. This section summarizes the characteristics of four kinds of *Plasmodium* species after treatment and interprets them in combination with the form of cases. Mastering the knowledge points in this section will help to avoid missed detection and scientifically evaluate the therapeutic effect of antimalarial drugs.

The morphological characteristics of *Plasmodium* treated with antimalarial drugs are shown in Figs. 6.96, 6.97, 6.98, 6.99, and 6.100.

Currently, *P. falciparum* trophozoites remain sensitive to artemisinins. After treatment with artemisinin drugs, the density decreases dramatically, the cytoplasm becomes concentrated (EF), distorted (AB), and disappears (CD), and the nucleus is not “red, round and bright” but deformed, hollow (HI), and darkened (F). In this case, it is important to capture the typical morphology and observe whether there is a

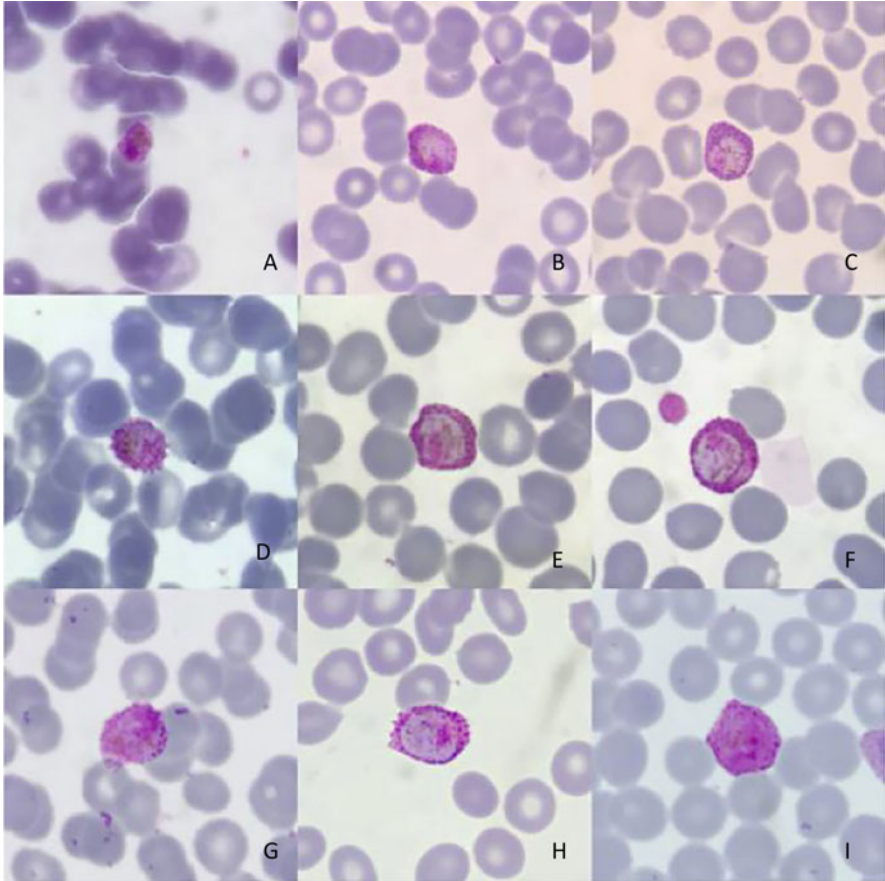


Fig. 6.72 Male gametocytes of *P. ovale* (Giemsa staining, $\times 1000$)

vacuolated area of cytoplasmic occupancy (CD) and to distinguish it from the Howell-Jolly body. In addition, RDT and epidemiological history may help with the identification.

The patient was diagnosed with imported vivax malaria from Ethiopia. Prior to hospital admission, artemisinin-based combinations were self-administered orally, but the name and dosage of these combinations are unknown. Microscopically, the original morphology disappeared, and the appearance was fragmented. The most obvious changes in cytoplasmic morphology are loss of cytoplasm in the early stages (ABCD) and distortion and fragmentation in the late stages (ECGH), with lighter coloration and the presence of large vacuolated areas (E). The nucleus is still evident, but with a distorted morphology, dark-red coloration (C), and the malarial pigments are condensed into coarse granules. However, the overall outline of *Plasmodium* is larger, and the pRBCs are swollen and deformed with Schüffner's dots.

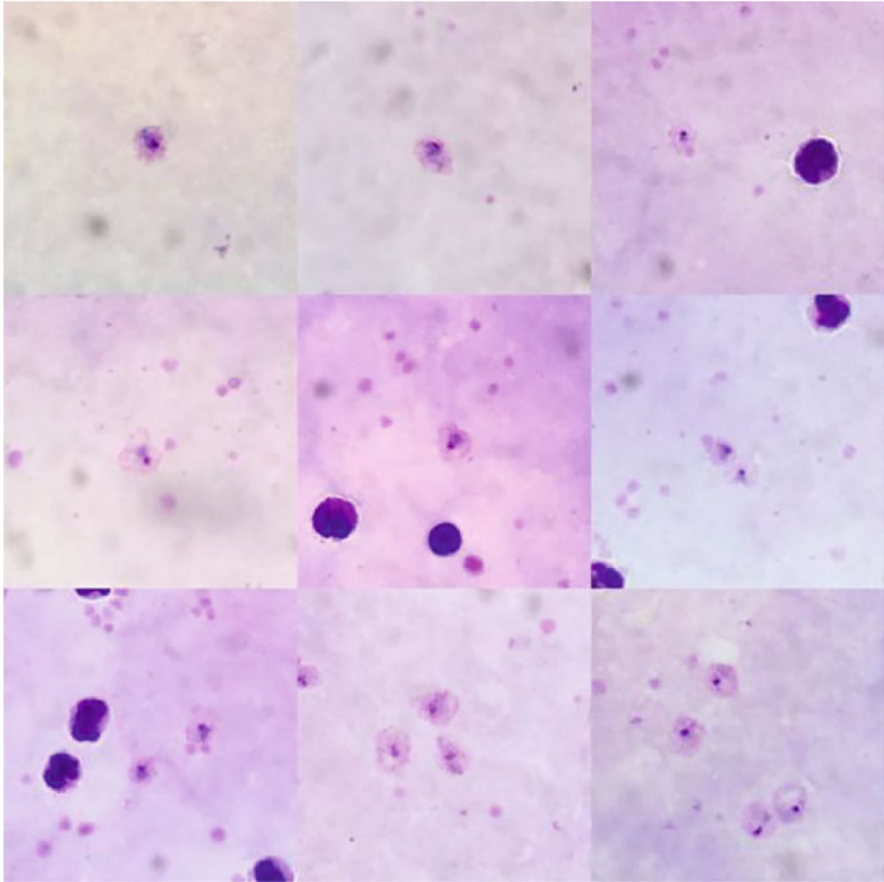


Fig. 6.73 Trophozoites of *P. ovale* on a thick blood smear (Giemsa staining, $\times 1000$)

Identification of a typical morphology (I) and inquiry of the epidemiological history and molecular diagnosis is helpful for the identification of *P. vivax*.

The patient was diagnosed with an imported case of *P. ovale* malaria from Guinea. Prior to admission, he was orally administered artemisinin compounds, but the name and dosage of these compounds are unknown. The nucleus and cytoplasm of the small trophozoites are dark red in color, and the cytoplasm is concentrated and reduced (A), similar in morphology to that of the *P. falciparum* rings. The cytoplasm of large trophozoites is morphologically altered or mutilated, and the malaria pigments are condensed to black-brown (BC). The merozoites of schizonts have partially hollow nuclei and are partially darkened. The malarial pigments are condensed into dark-brown clumps. The cytoplasm of immature schizonts is still evident but broken into pieces, merozoites are unevenly distributed and more scattered, and pRBCs are lysed (DE). The mature schizonts are reduced in size, and merozoites are more scattered, similar to *P. falciparum* schizonts or

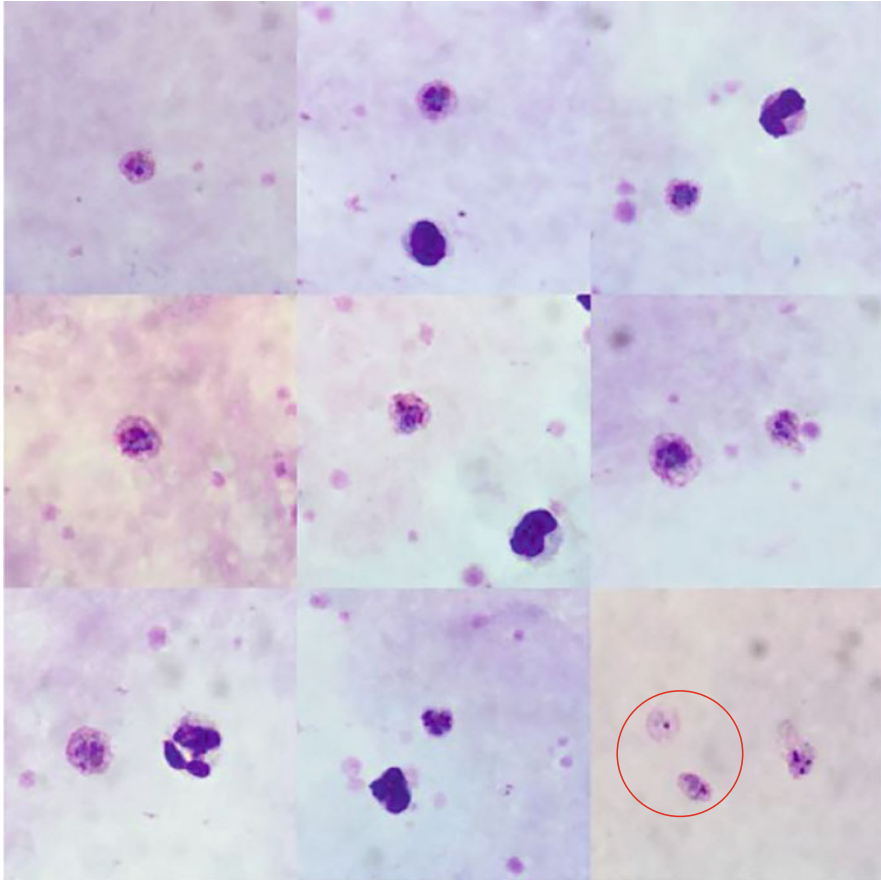


Fig. 6.74 Schizonts of *P. ovale* on a thick blood smear (Giemsa staining, $\times 1000$)

P. malariae schizonts (FGHs). Sometimes, Schüffner's dots can be observed in pRBCs (BI), and the female gametophytes are smaller and make up a part of the pRBCs (I). The geographical distribution of nonfalciparum malaria in Africa (Fig. 6.69) and molecular diagnosis are helpful for identification.

The patient was diagnosed with an imported case of *P. ovale* malaria from South Sudan, and artesunate was injected once prior to admission. Under the microscope, the density of *P. ovale* is extremely low, the size is reduced, and the original morphology of *P. ovale* is destroyed. The cytoplasm disappears or is broken, the nucleus is loose, and the malarial pigments are condensed into granules. The nucleus, cytoplasm, and malarial pigments are fused. Schuffner's dots degenerate into a grid (BCDEF), and the pRBCs are swollen and multiform, which are not distinguished from *P. vivax*. The combination of the geographical distribution of the parasite (Fig. 6.68) and molecular diagnosis is helpful for the identification of *P. ovale*.

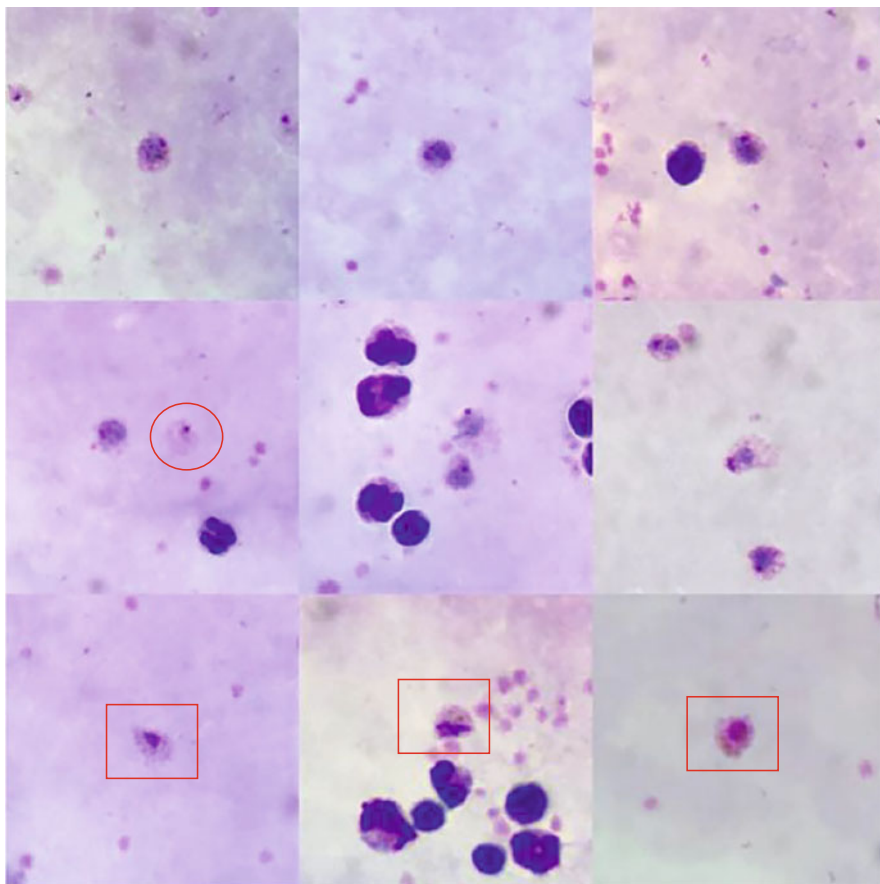


Fig. 6.75 Gametocytes of *P. ovale* on a thick blood smear (Giemsa staining, $\times 1000$)

The patient was diagnosed with an imported case of *P. malariae* malaria from Cameroon. Prior to admission, he was given chloroquine phosphate tablets for three days with unknown dosing. The density of *P. malariae* is low, the cytoplasm gradually disappears or is pierced, and the malarial pigments are condensed into granules. The nucleus of small trophozoites appears hollow and black (AB), the number of merozoites of schizonts decreases, merozoites shrink (FG), malarial pigments are scattered, and the cytoplasm of the gametophyte is fragmentary (HI). However, the size of *Plasmodium* and pRBCs is small. In addition, the trophozoites appear to have an apparent ribbon-like shape (BCDE). These microscopic features may help the identification of *P. malariae*.

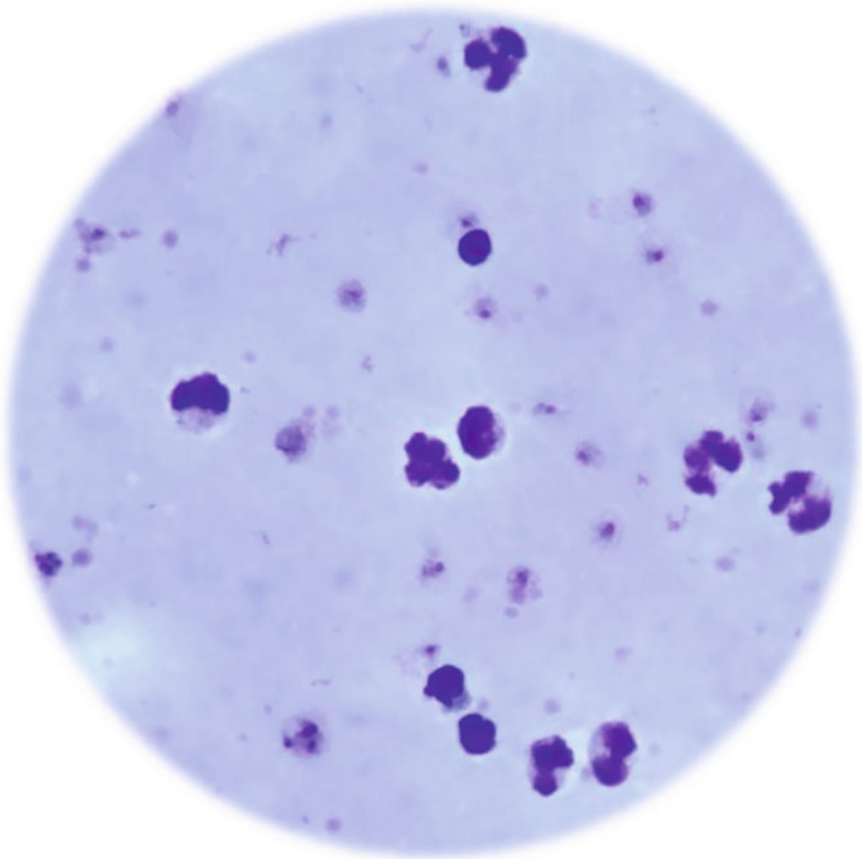


Fig. 6.76 Morphology of *P. ovale* on a thick blood smear (Giemsa staining, $\times 1000$)

6.7 Other Cell Morphologies in Blood Smears of Malaria Cases

Microscopic examination is still the “gold standard” of malaria diagnosis (WHO recommendation), which cannot be replaced temporarily by new technology or automated equipment, resulting in many confounding factors affecting the process and results of microscopic examination. It should also be recognized that the identification of common cell morphology in the blood of malaria patients is conducive to obtaining disease information and providing an important reference for clinical treatment. For example, the appearance of immature RBCs indicates anemia, and an increase in WBC count indicates different types and degrees of infection. Therefore, the microscopic examination of human *Plasmodium* is closely related to the morphological identification of blood cells.

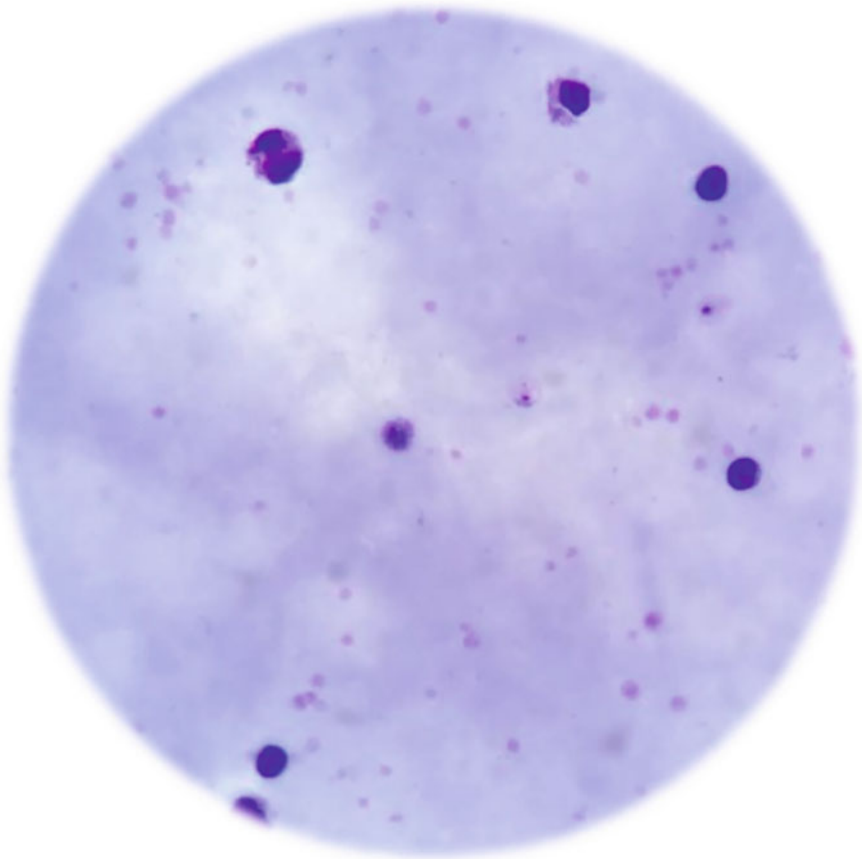


Fig. 6.77 Morphology of *P. ovale* on a thick blood smear (Giemsa staining, $\times 1000$)

Hemocytology examination is a traditional clinical examination technique, and it is difficult to master. Although the new technology can provide great help for the differential diagnosis of blood diseases, the final diagnosis of difficult blood diseases still depends on the traditional morphological examination.

In addition to exogenous impurities, several common blood cell morphologies in the blood smears of malaria cases are summarized and introduced in this section. There are chromatin bodies, some types of immature RBCs, platelets, and various types of WBCs in the blood of malaria patients. Sometimes, they are easily confused with *Plasmodium* if the density of *Plasmodium* is low or the staining is poor, thus affecting the microscopic identification and evaluation of antimalaria treatment effects.

Learning and mastering the content of this chapter is conducive to the development of microscopic malaria examination, improving the diagnostic coincidence

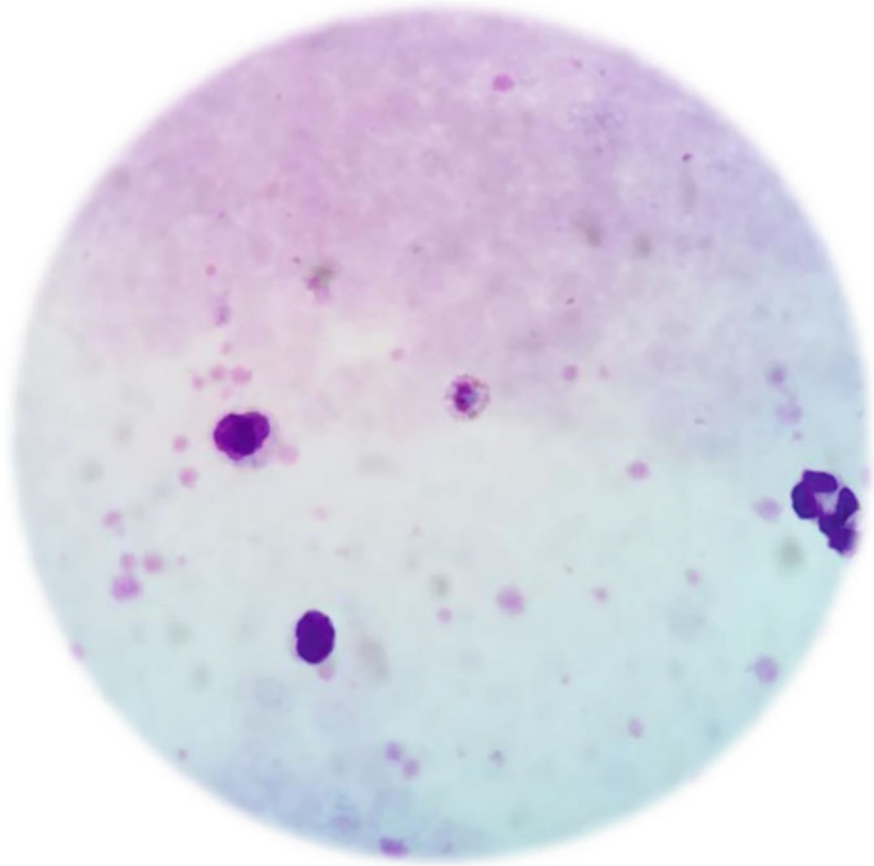


Fig. 6.78 An immature schizont of *P. ovale* on a thick blood smear (Giemsa staining, $\times 1000$)

rate, and preliminarily understanding the condition of the case through microscopic examination (Qian et al. 2008).

6.7.1 Howell-Jolly Body

The Howell-Jolly body is shown in Fig. 6.101.

Malaria cases, notably falciparum malaria cases, often present different degrees of anemia, and Howell-Jolly bodies are frequently seen in RBCs of peripheral blood. The Howell-Jolly body can be found in a variety of proliferative anemias, mostly in early erythrocytes and occasionally in mature erythrocytes, as round particles approximately 1–2 μm in diameter, similar to the nuclear morphology of *P. falciparum* rings. The Howell-Jolly bodies are dark purplish-red, dark blue-purple or blackish in color after Giemsa staining, poorly stereoscopic and refractive,

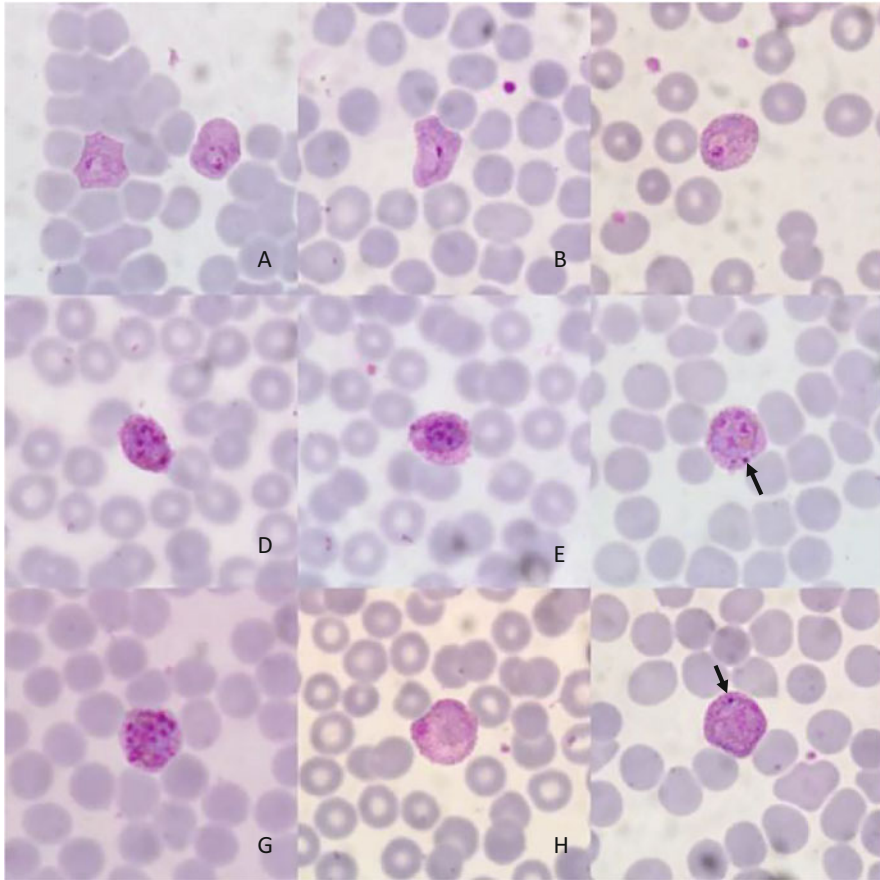


Fig. 6.79 A vivax malaria case imported from Pakistan (Giemsa staining, $\times 1000$)

twisting fine quasi-focal spirals, and do not appear to be on the same plane as RBCs, with no vacuoles formed by the *Plasmodium* cytoplasm or cytoplasmic space-occupying around them. In malaria cases treated with adequate antimalarial drugs, it is very easy to confuse Howell-Jolly bodies with *P. falciparum* rings.

6.7.2 Immature RBCs

The morphology of immature RBCs is shown in Figs. 6.102, 6.103, and 6.104.

Due to hemolytic anemia, basophilic stippling is common in blood smears. The blue-black particles in immature RBCs vary in size and number. The morphological characteristics of these particles are similar to those of Schuffner's dots or Maurer's clefts. However, the particles are widely distributed and stained blue-black. Sometimes, *Plasmodium* parasitizes these particles (GHI), and basophilic dots are also

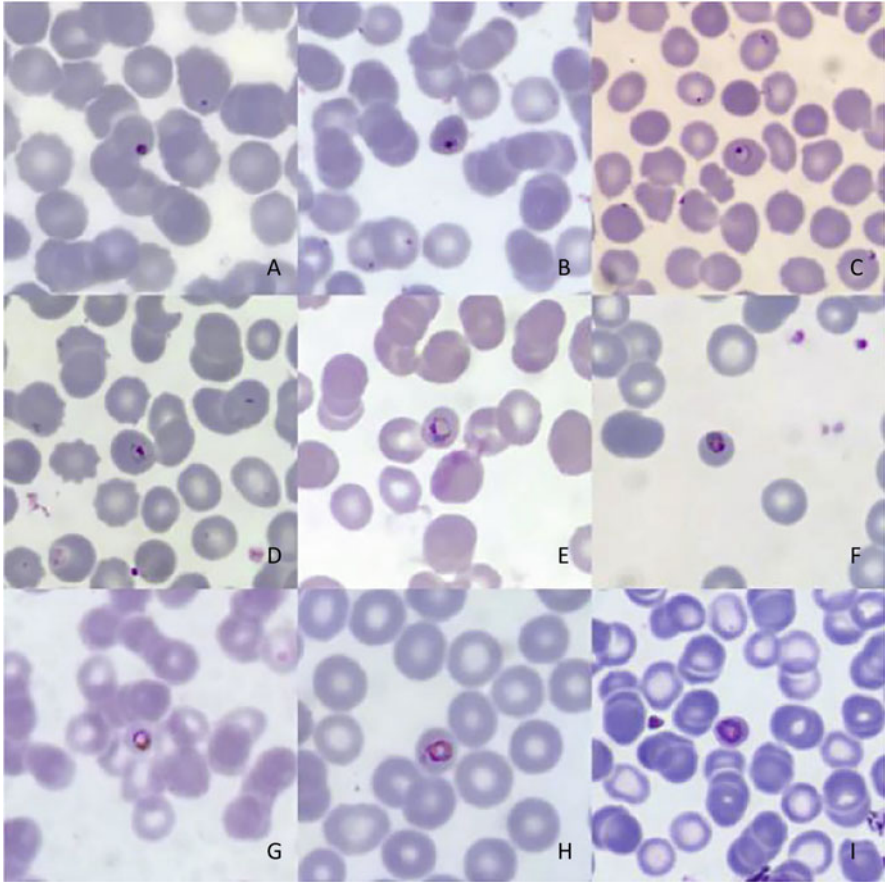


Fig. 6.80 Small trophozoites of *P. malariae* (Giemsa staining, $\times 1000$)

seen in the orthochromic normoblasts (F). Lymphocytes are indicated by yellow arrows. A mature schizont of *P. vivax* is shown in the red circle.

In malaria cases, orthochromic normoblasts are common in peripheral blood smears due to anemia, with diameters ranging from 7 to 10 μm and a nucleus located in the center or on one side. Occasionally, polychromatic normoblasts (HIs) can be checked in the peripheral blood of malaria patients. The diameter is 8–15 μm , the nucleus is round, the nuclear chromatin is dense and condenses into cords or blocks, and the pulp is rich, polychromatic, and light blue. They are easily mistaken as schizonts of *P. ovale* or *P. falciparum* if their nuclei are poorly stained. Lymphocytes are indicated by yellow arrows.

In malaria cases, due to acute hemorrhagic and hemolytic anemia, polychromatic and macrocyte erythrocytes are common in the peripheral blood, and *Plasmodium* can also be parasites (EH). The polychromatic erythrocytes are grayish-blue in color and slightly larger than the surrounding mature erythrocytes due to the presence of

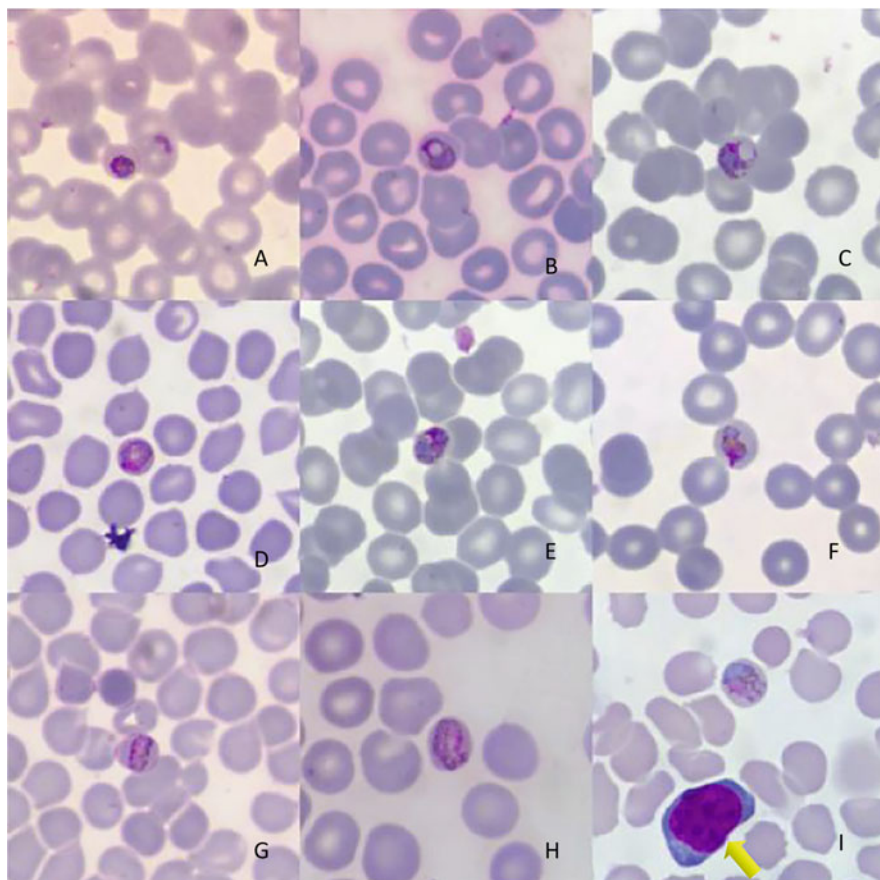


Fig. 6.81 Large trophozoites of *P. malariae* (Giemsa staining, $\times 1000$)

basophilic materials in the cytoplasm (ABCD, blue circle). Macrocyte erythrocytes (DE red circle) are larger than $10\ \mu\text{m}$ in diameter with a reduced central lightly stained area; when the diameter is larger than $15\ \mu\text{m}$, the morphology is irregular, and the lightly stained area disappears. They are called giant erythrocytes (FGHI), which show high pigmentation and are mostly polychromatophilic (FHI). The yellow arrows point to lymphocytes and the blue arrows to neutrophils.

6.7.3 Platelets

The platelets are shown in Fig. 6.105.

The platelets are red or light-pink, and their diameter is commonly $2\text{--}4\ \mu\text{m}$. They are often dispersed and should be distinguished from the nucleus of *Plasmodium* on an anticoagulant blood smear. Giant platelets (ABCD) and aggregated platelets

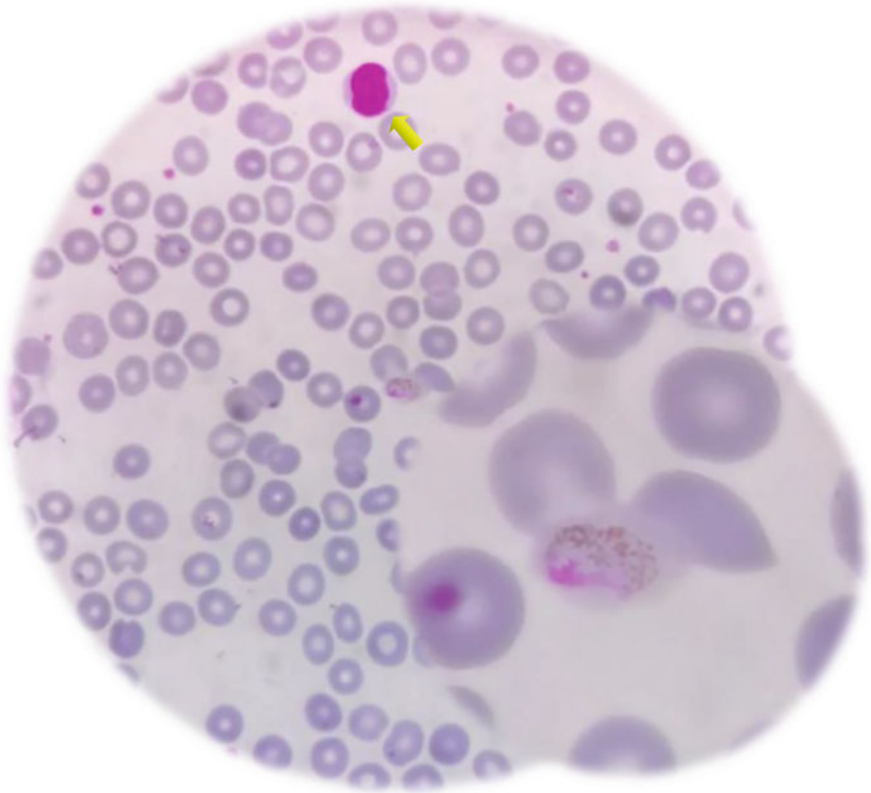


Fig. 6.82 Large trophozoite of *P. malariae* (Giemsa staining, $\times 1000$)

(FGHI) are often observed in blood smears of malaria patients. This suggests bone marrow hyperplasia and a risk of bleeding. Sometimes, the male gametocyte, which looks like a large platelet, is full of pRBCs. However, unlike platelets, its boundaries are clear. The blue arrow indicates neutrophils.

6.7.4 White Blood Cells

WBCs in the blood are shown in Figs. 6.106, 6.107, 6.108, 6.109, and 6.110.

Neutrophils make up the highest proportion of WBCs, approximately 50%–70%, and are the most numerous, relatively uniform in size, with darkly stained curved rod-shaped (horseshoe-shaped) or lobulated nuclei, and the lobulated nuclei usually being 2–5 lobes. It can be used as a reference for the size of the malaria parasites in thick blood smears. Falciparum malaria is often associated with an elevated WBC count, characterized by an elevated neutrophil ratio, and infectious shock can develop within 3 days of onset.

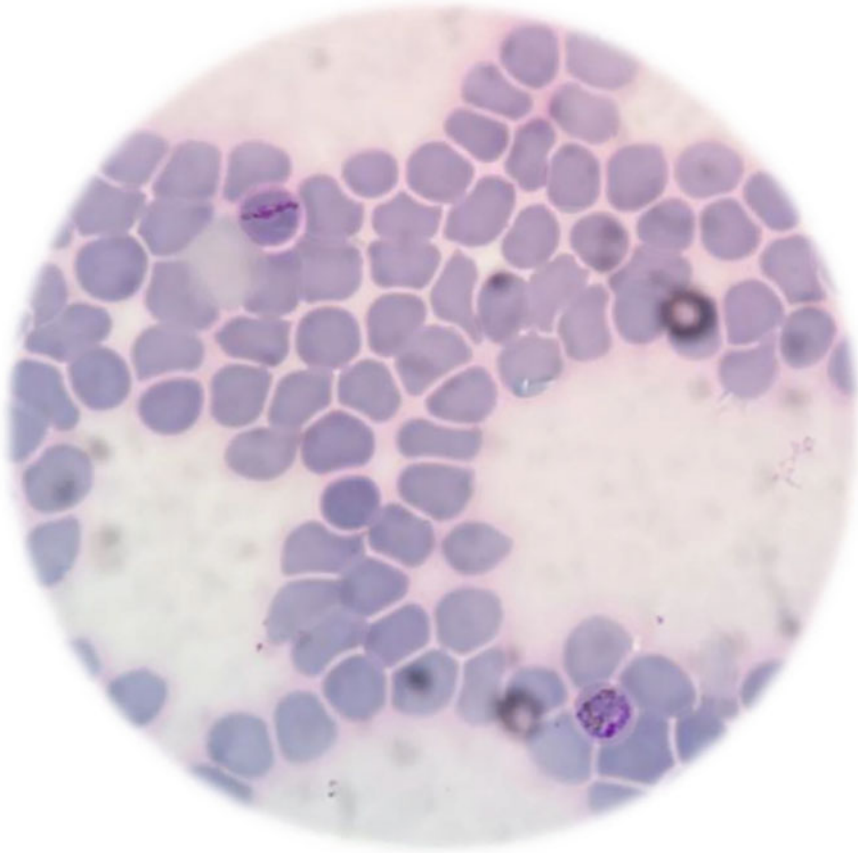


Fig. 6.83 A linear trophozoite (upper left) and a mature trophozoite (lower right) of *P. malariae* (Giemsa staining, $\times 1000$)

The lymphocyte count is the second highest among the WBCs, and its size varies, reference value: 0.19%–0.47%, absolute value $(1.0\text{--}3.3) \times 10^9/\text{L}$. The nuclei of small lymphocytes are round and sometimes similar in shape and color to the male gametocytes of *P. vivax*. However, the nuclei of small lymphocytes have dense, coarse, dark purple-red chromatin, whereas the nuclei of male gametocytes are red or light red, and malaria pigments and Schuffner's dots can be observed.

Monocytes, with a relatively large amount of cytoplasm, are light gray-blue and opaque, with fine dusty purplish-red particles in the pulp. Reference value in blood: 0.03%–0.08%, absolute value $(0.1\text{--}0.8) \times 10^9/\text{L}$. Nonfalciparum malaria cases have normal or elevated WBC counts, generally characterized by an increased proportion of monocytes.

Eosinophils are rare in peripheral blood, with a small proportion of WBCs, approximately 0.005%–0.05%, absolute value $(0.01\text{--}0.5) \times 10^9/\text{L}$. The nuclei are

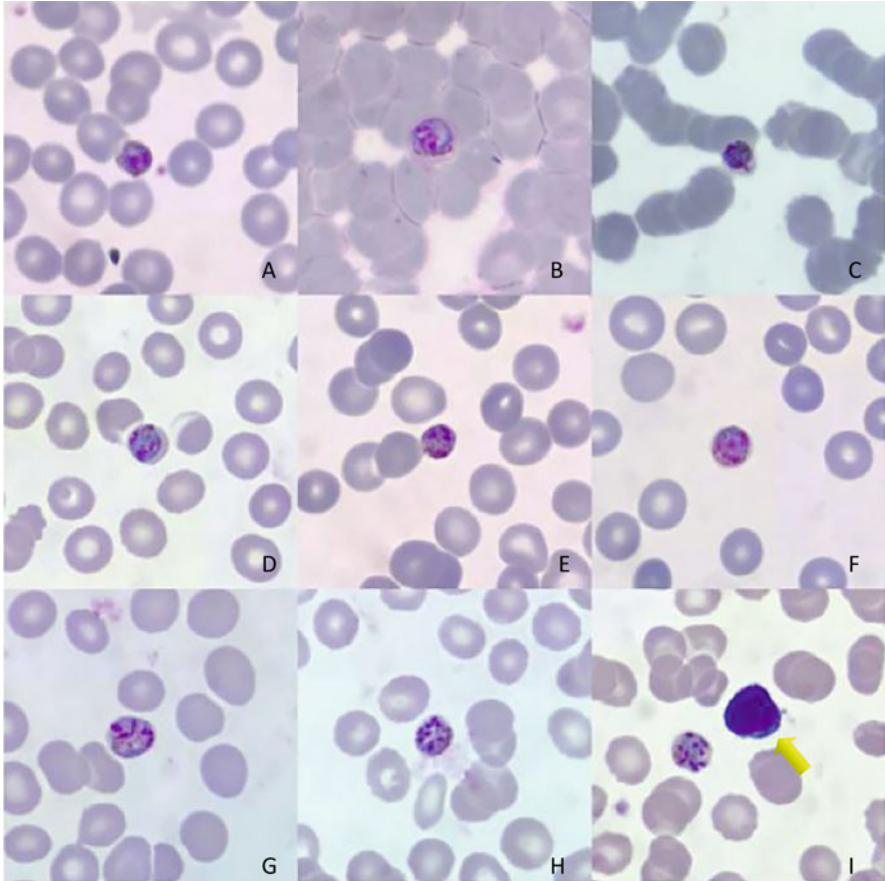


Fig. 6.84 Immature schizonts of *P. malariae* (Giemsa staining, $\times 1000$)

mostly divided into two lobes, and the pulp is filled with coarse, uniform orange-red granules, which are also red dots. The dots are similar to the nucleus of *P. falciparum* rings when they break up and escape. However, the dots are poorly stereoscopic and refractive, lightly colored, and distributed in patches, with no blue cytoplasm, which is similar to that of *P. falciparum*. In malaria cases, the eosinophil count is normal or decreasing or even tends to 0.

The degenerated nucleus of blast cells is smeared to a broom shape and looks like a basket, and it is therefore called basket cells or smear cells. It is common in blood smears of malaria cases. The blue arrow indicates neutrophils.

Unfortunately, no basophils have been found in my nearly 20 years of microscopic examination of *Plasmodium*.

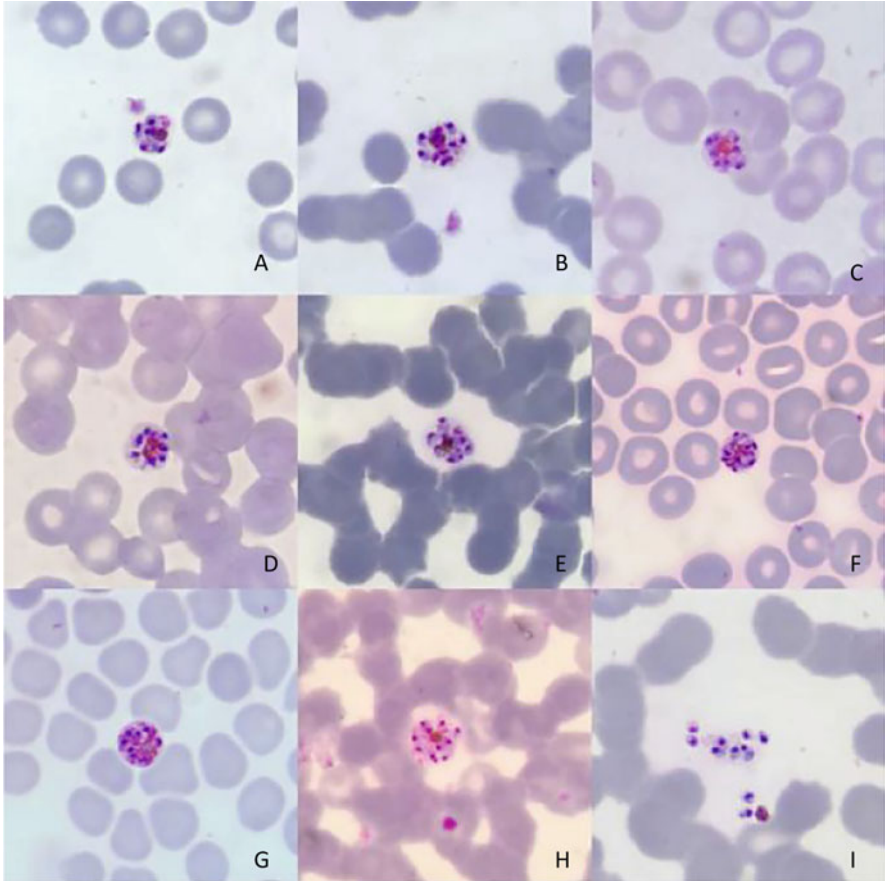


Fig. 6.85 Mature schizonts of *P. malariae* (Giemsa staining, $\times 1000$)

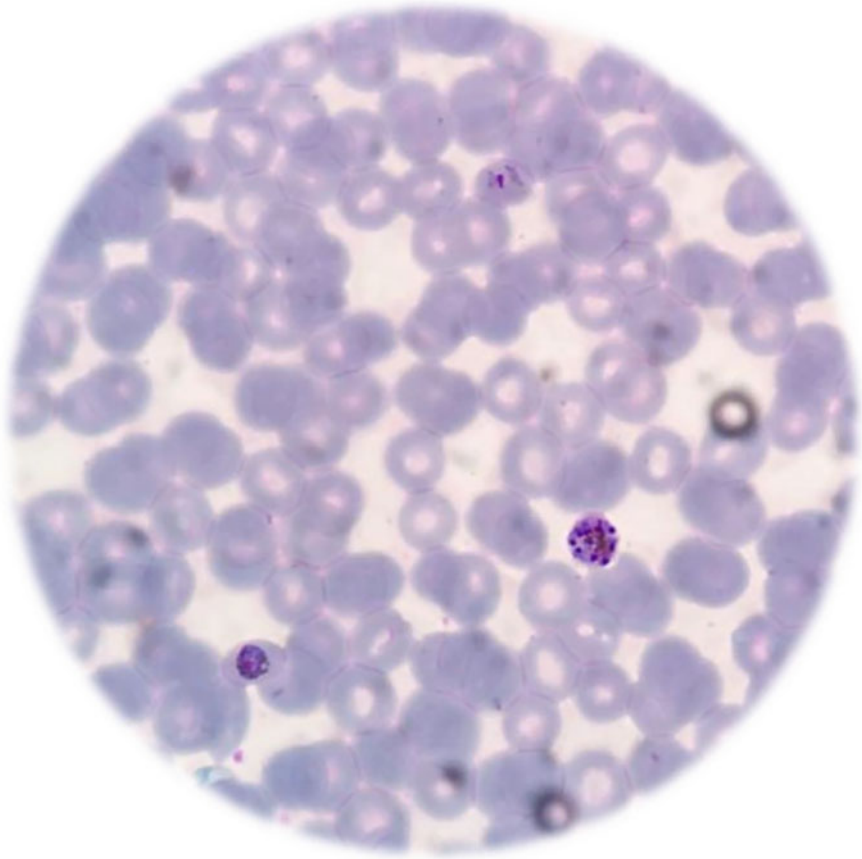


Fig. 6.86 Two trophozoites and a mature schizont of *P. malariae* (Giemsa staining, $\times 1000$)

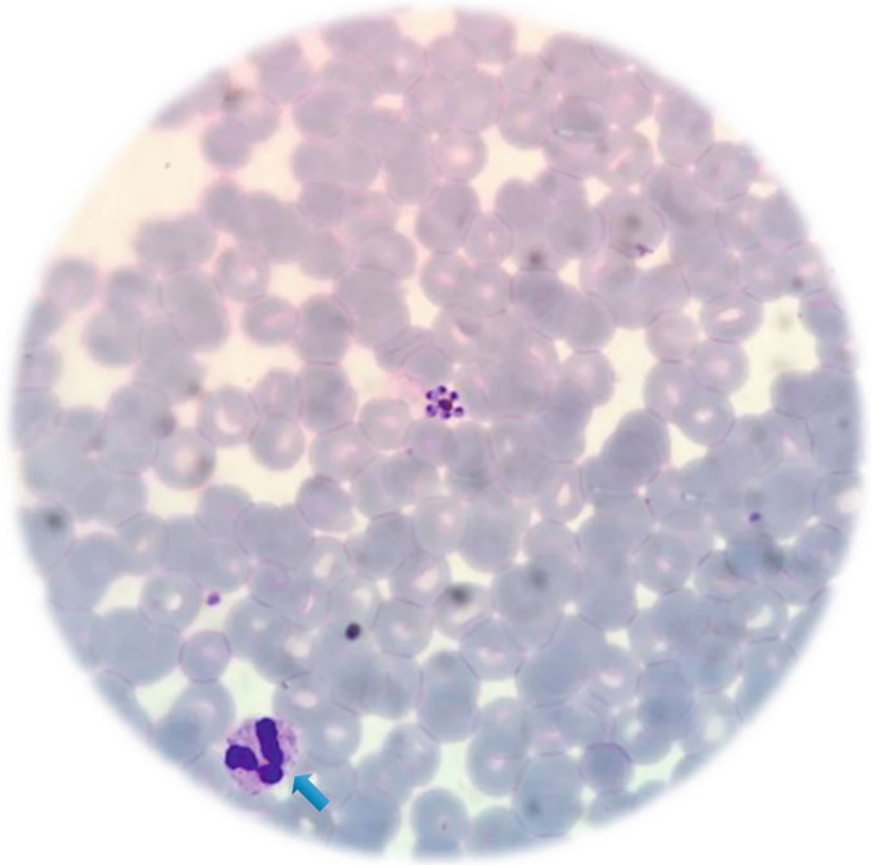


Fig. 6.87 A typical petaloid schizont of *P. malariae* (Giemsa staining, $\times 1000$)

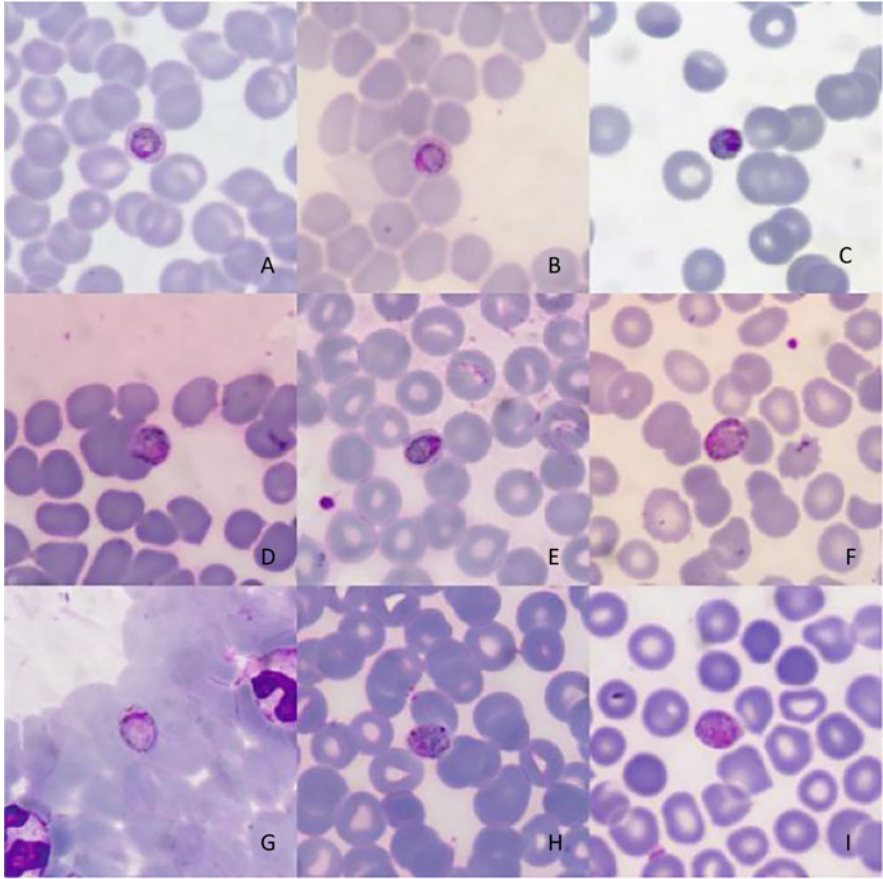


Fig. 6.88 Female gametocytes of *P. malariae* (Giemsa staining, $\times 1000$)

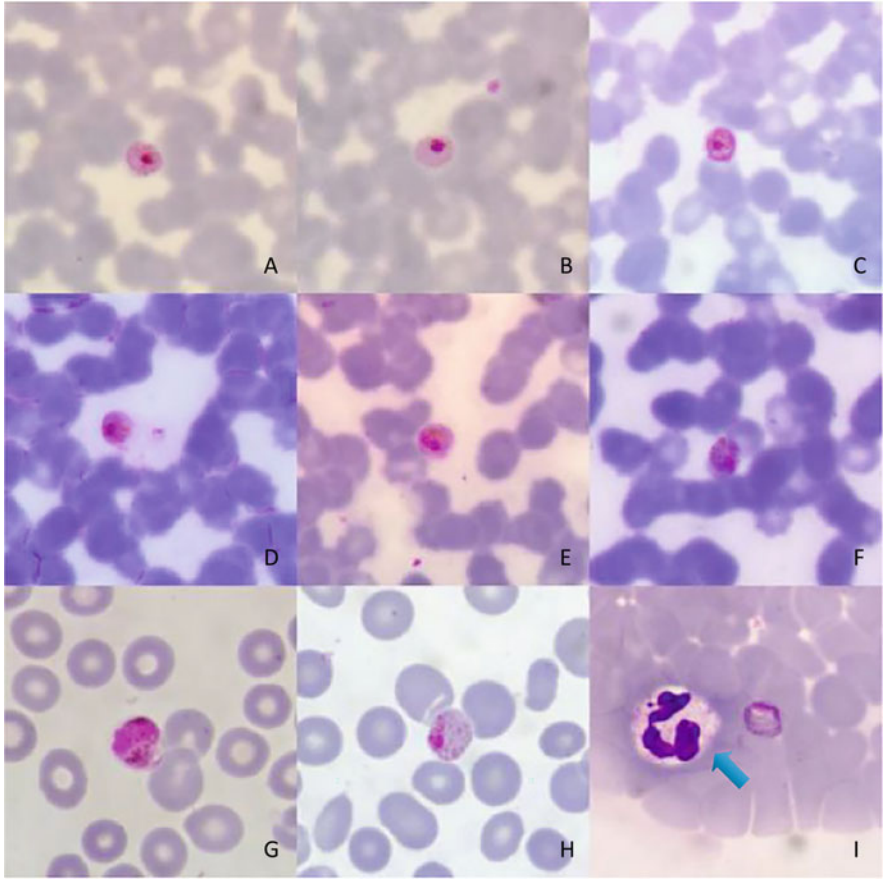


Fig. 6.89 Male gametocytes of *P. malariae* (Giemsa staining, $\times 1000$)

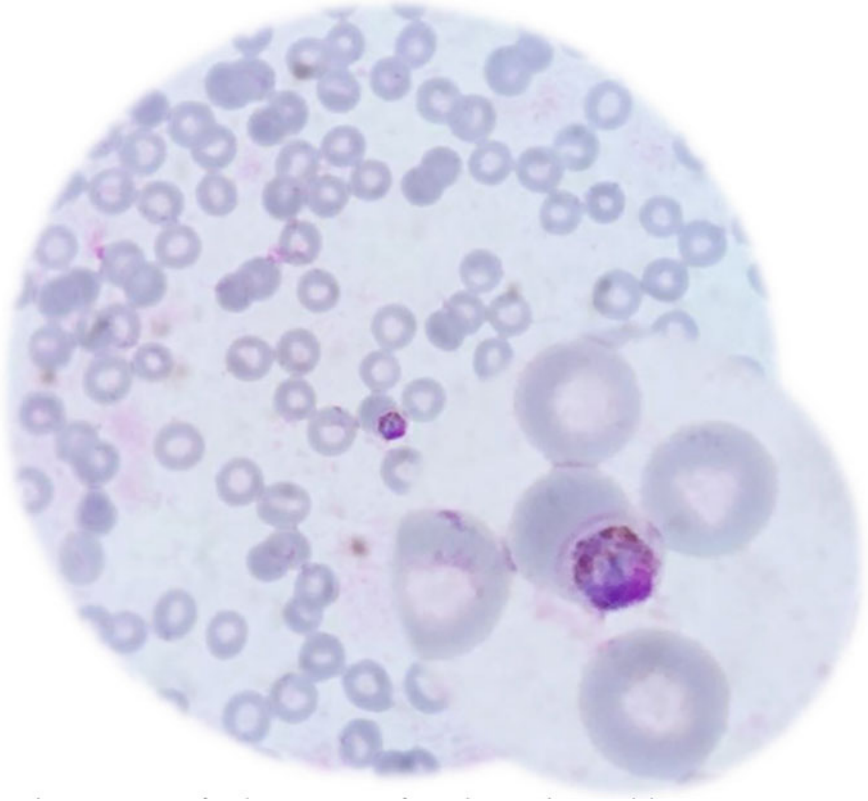


Fig. 6.90 Mature female gametocytes of *P. malariae* (Giemsa staining, ×1000)

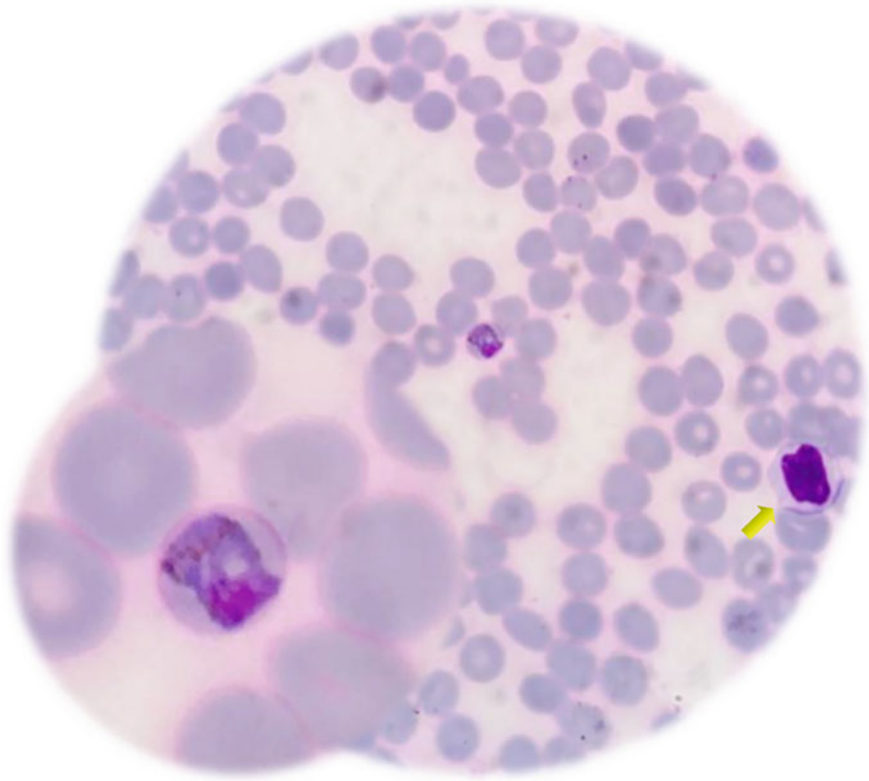


Fig. 6.91 Mature female gametocytes of *P. malariae* (Giemsa staining, $\times 1000$)

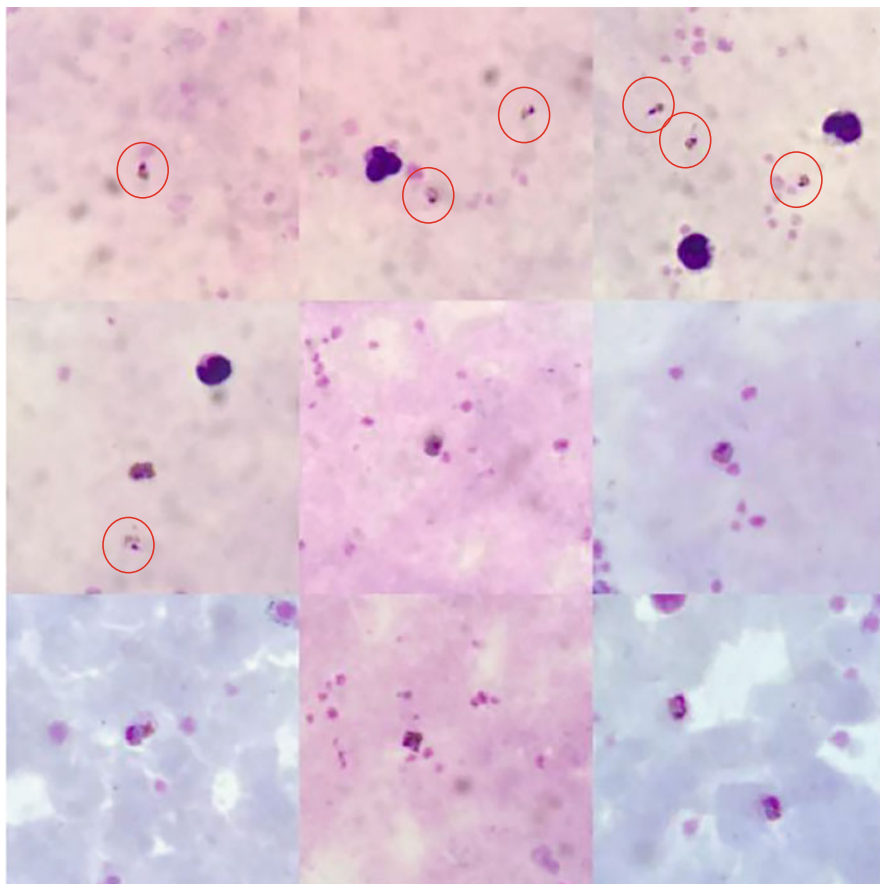


Fig. 6.92 Trophozoites of *P. malariae* on a thick blood smear (Giemsa staining, $\times 1000$)

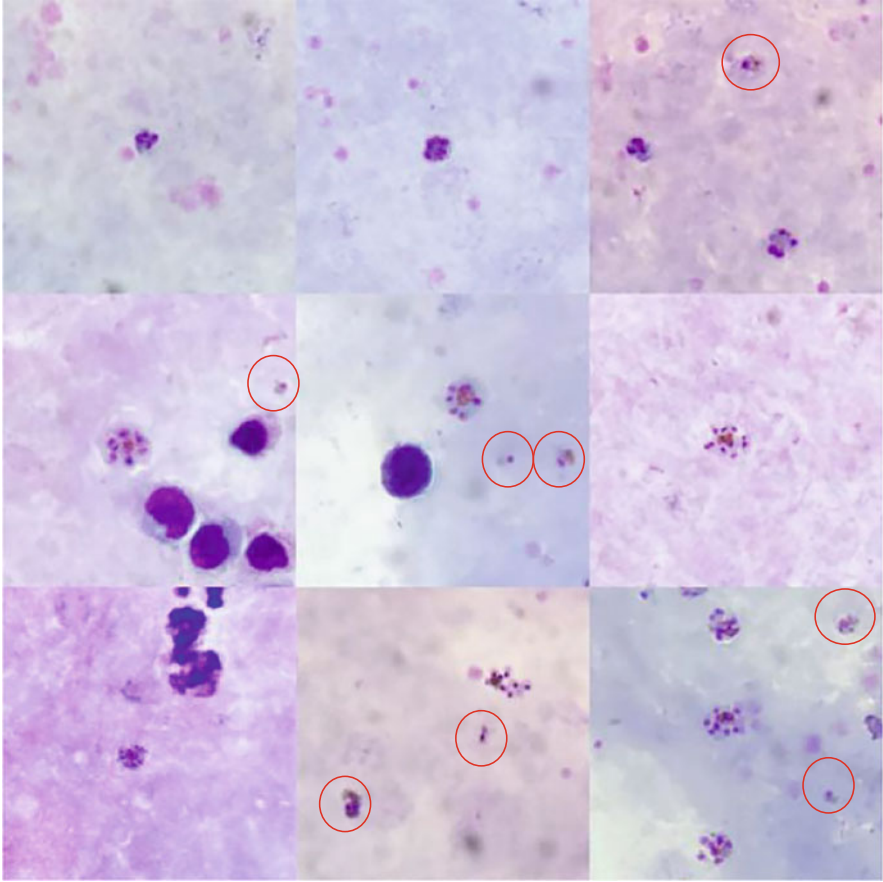


Fig. 6.93 Schizonts of *P. malariae* on a thick blood smear (Giemsa staining, $\times 1000$)

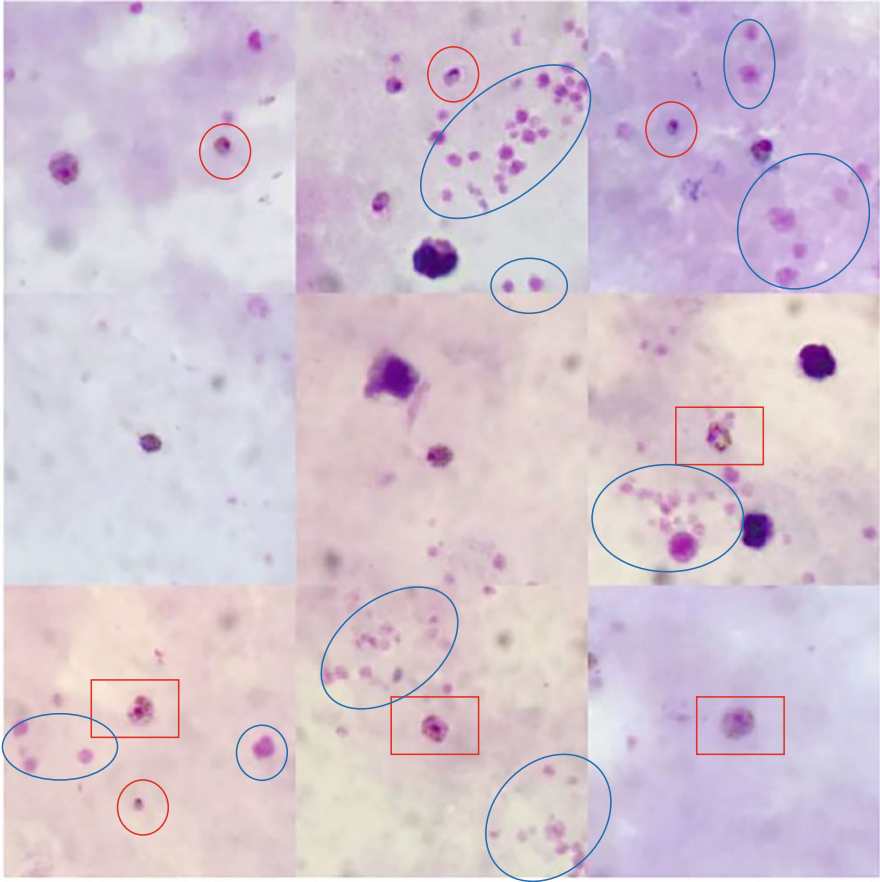


Fig. 6.94 Gametocytes of *P. malariae* on a thick blood smear (Giemsa staining, $\times 1000$)

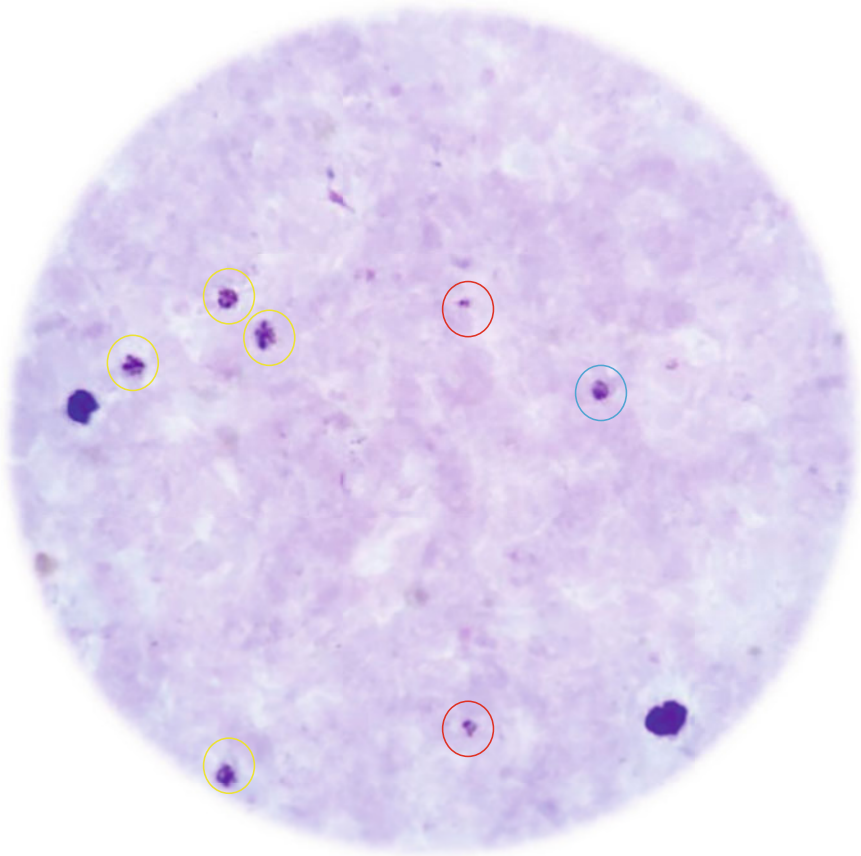


Fig. 6.95 Trophozoites, schizonts, and gametocytes of *P. malariae* on a thick blood smear (Giemsa staining, $\times 1000$)

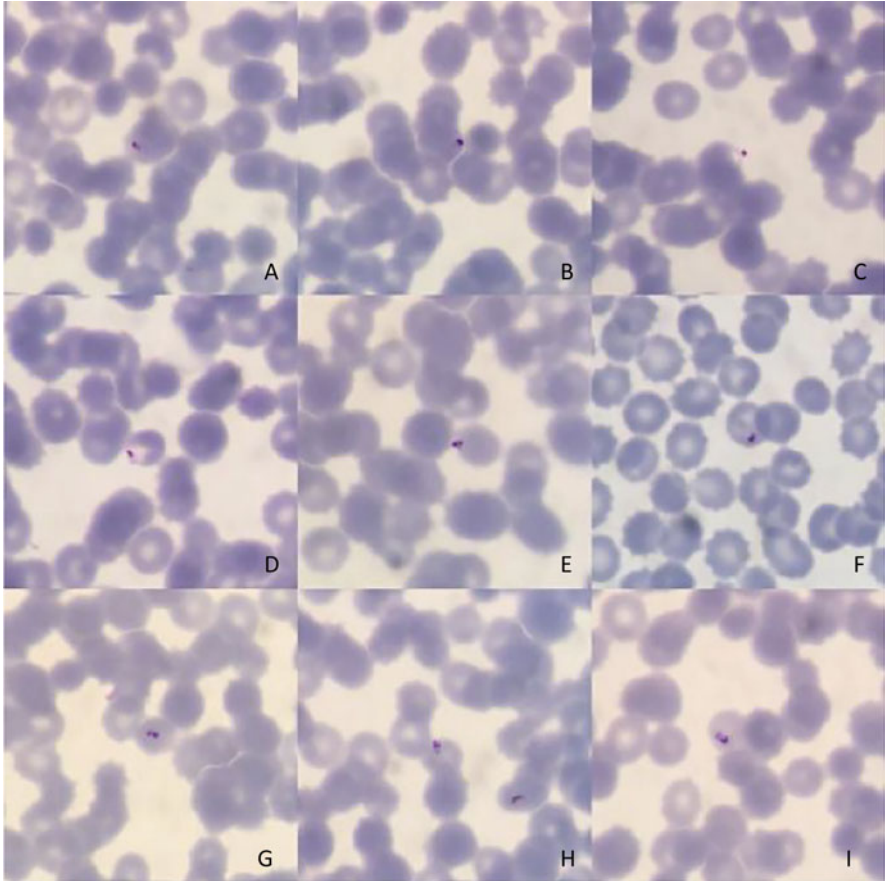


Fig. 6.96 Morphology of *P. falciparum* after treatment (Giemsa staining, $\times 1000$)

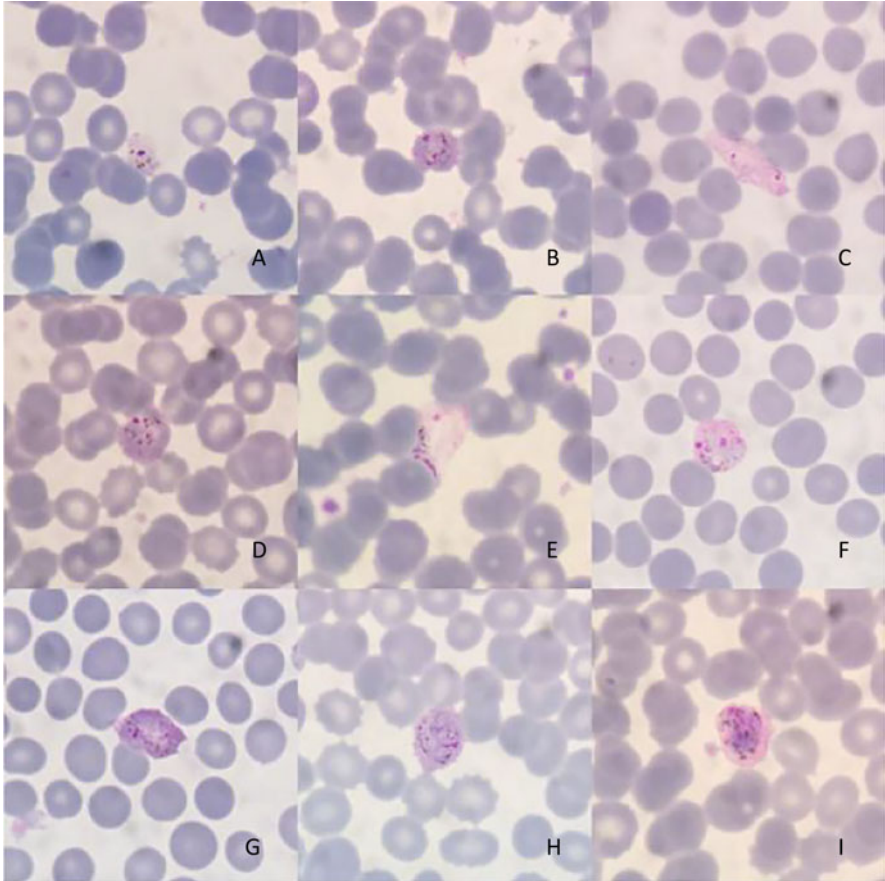


Fig. 6.97 Morphology of *P. vivax* after treatment (Giemsa staining, $\times 1000$)

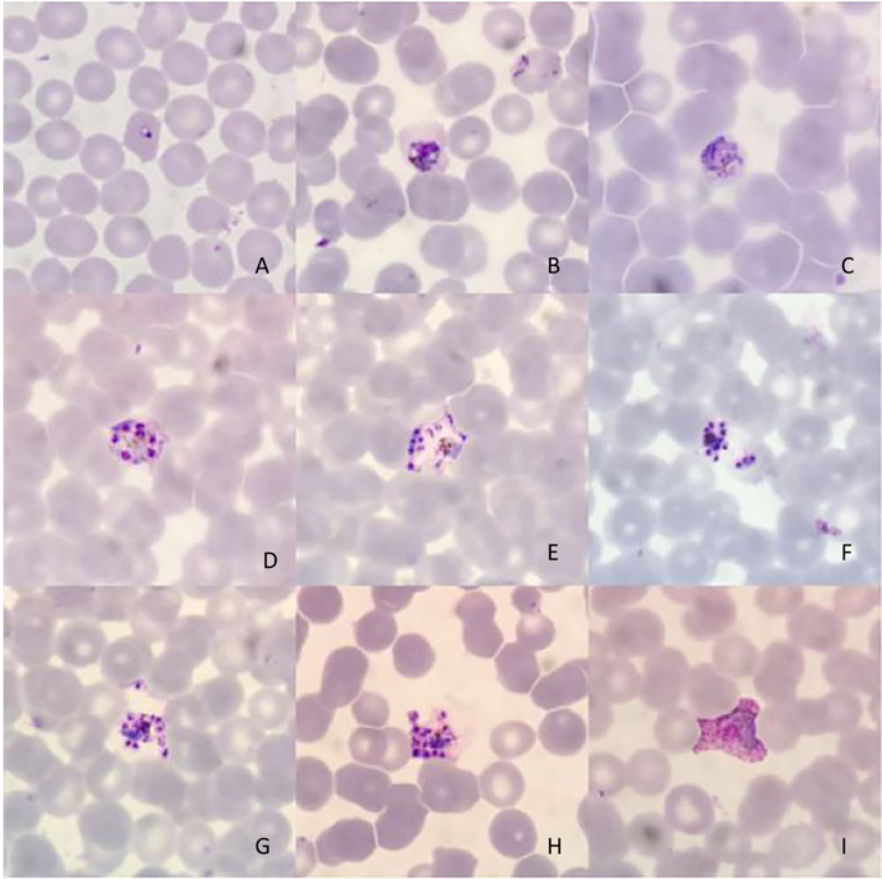


Fig. 6.98 Morphology of *P. ovale* after treatment (Giemsa staining, $\times 1000$)

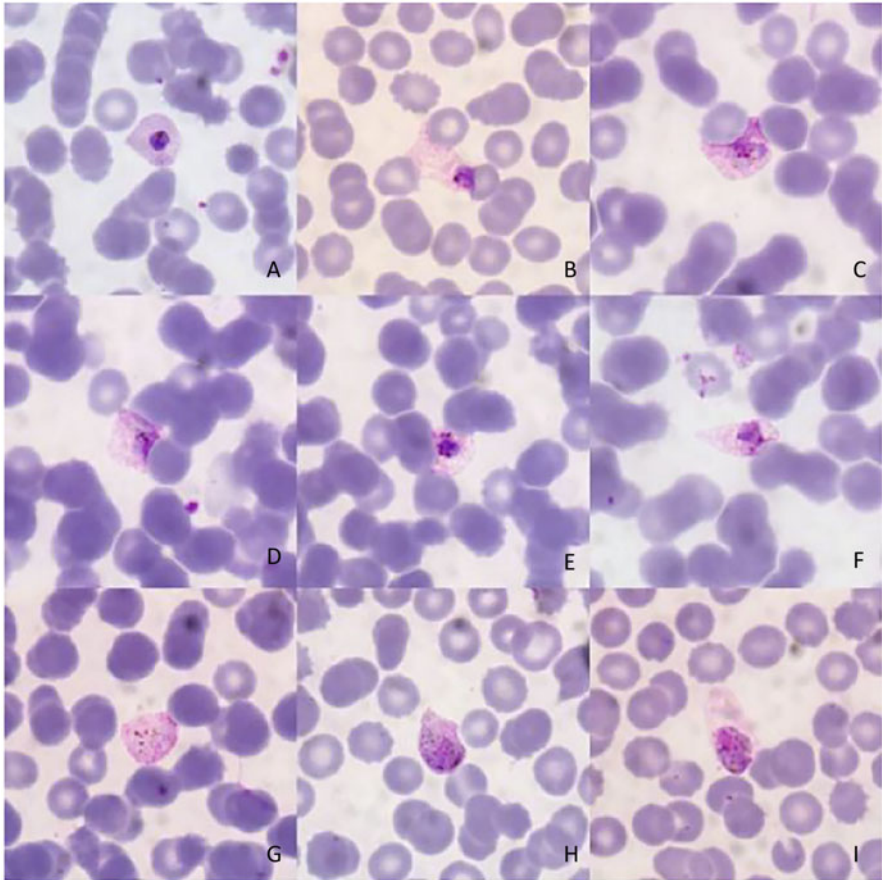


Fig. 6.99 Morphology of *P. ovale* after treatment (Giemsa staining, $\times 1000$)

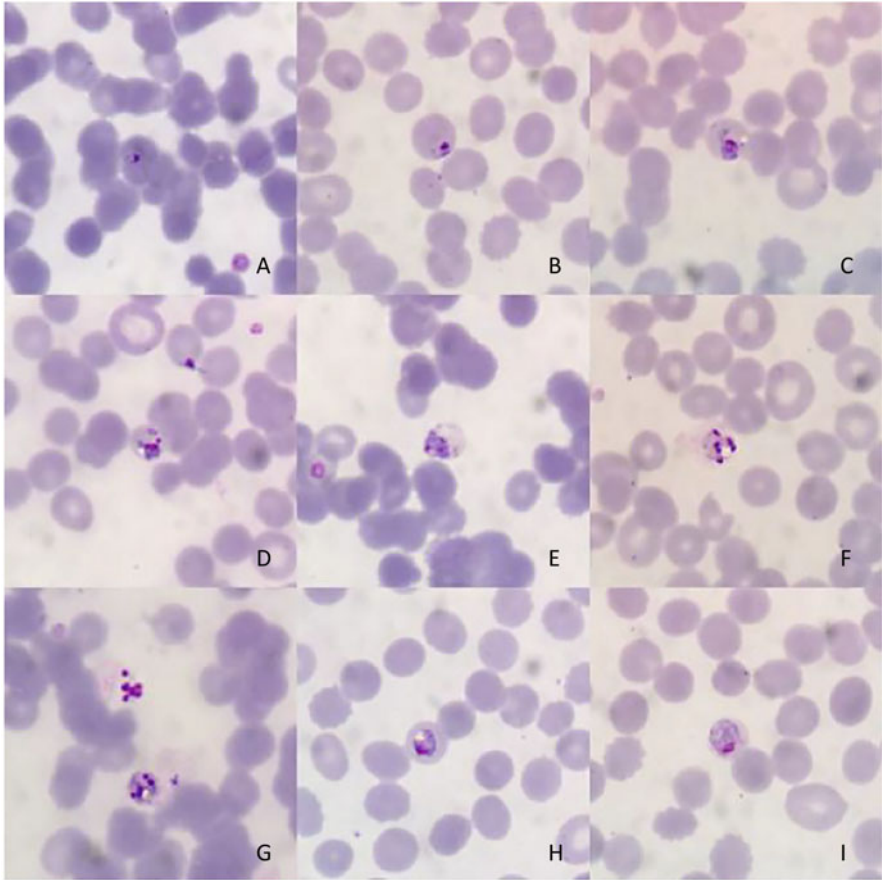


Fig. 6.100 Morphology of *P. malariae* after treatment (Giemsa staining, $\times 1000$)

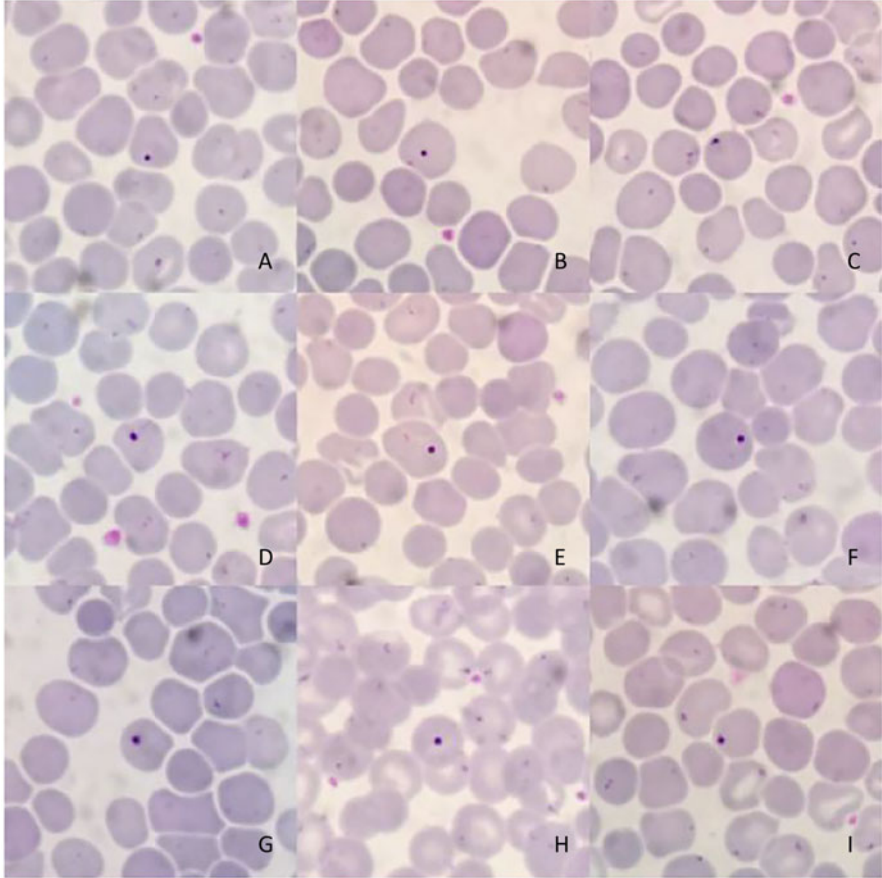


Fig. 6.101 Howell-Jolly body (Giemsa staining, $\times 1000$)

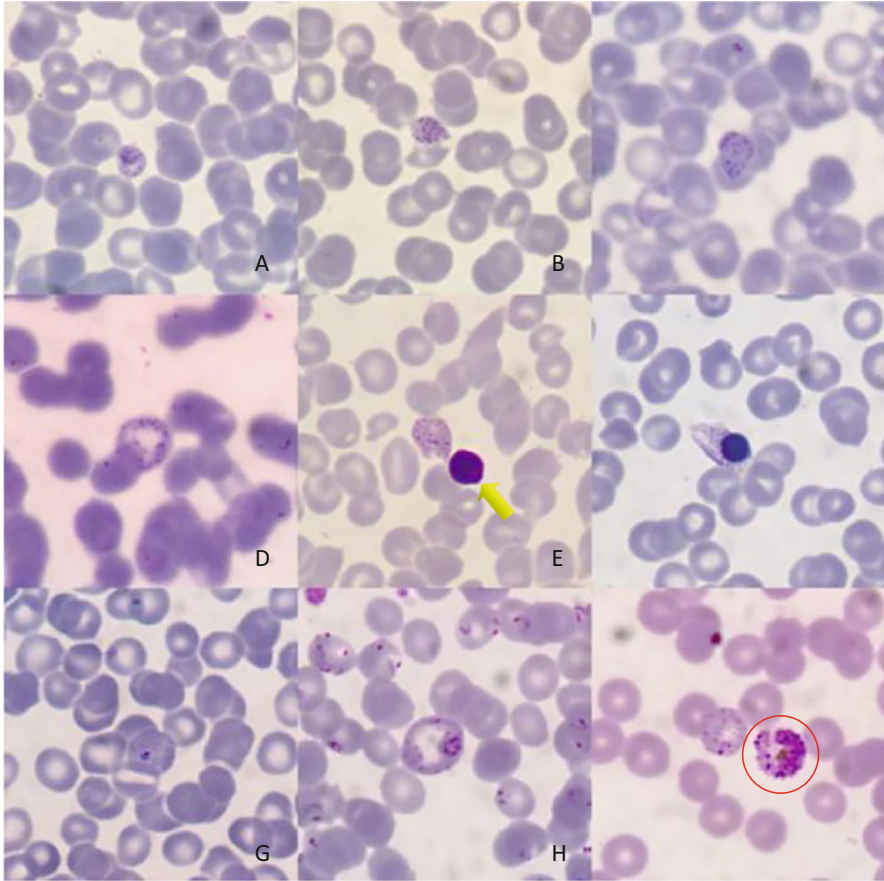


Fig. 6.102 Basophilic stippling (Giemsa staining, $\times 1000$)

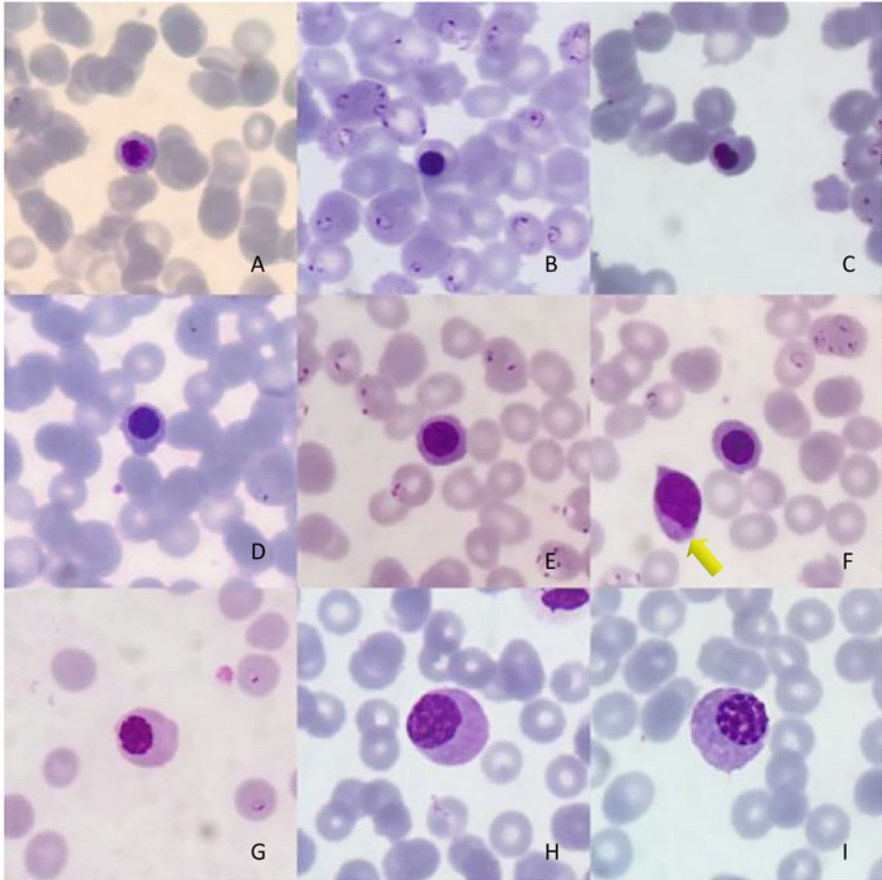


Fig. 6.103 Orthochromatic normoblasts and polychromatic normoblasts (Giemsa staining, $\times 1000$)

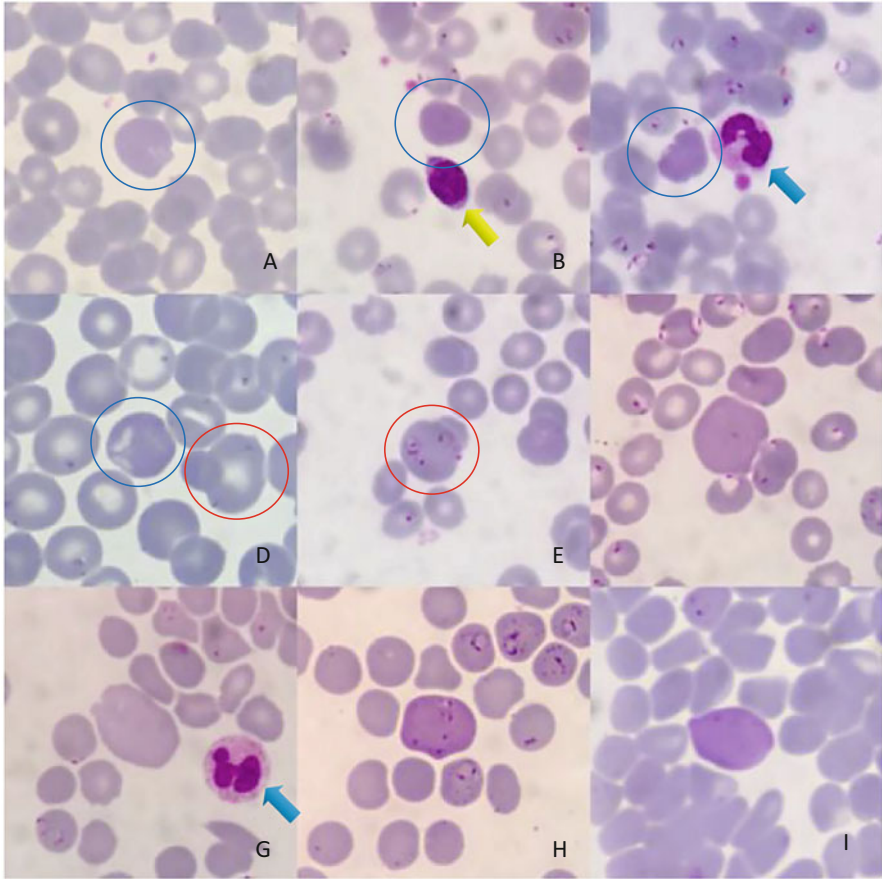


Fig. 6.104 Polychromatic and macrocyte erythrocytes (Giemsa staining, $\times 1000$)

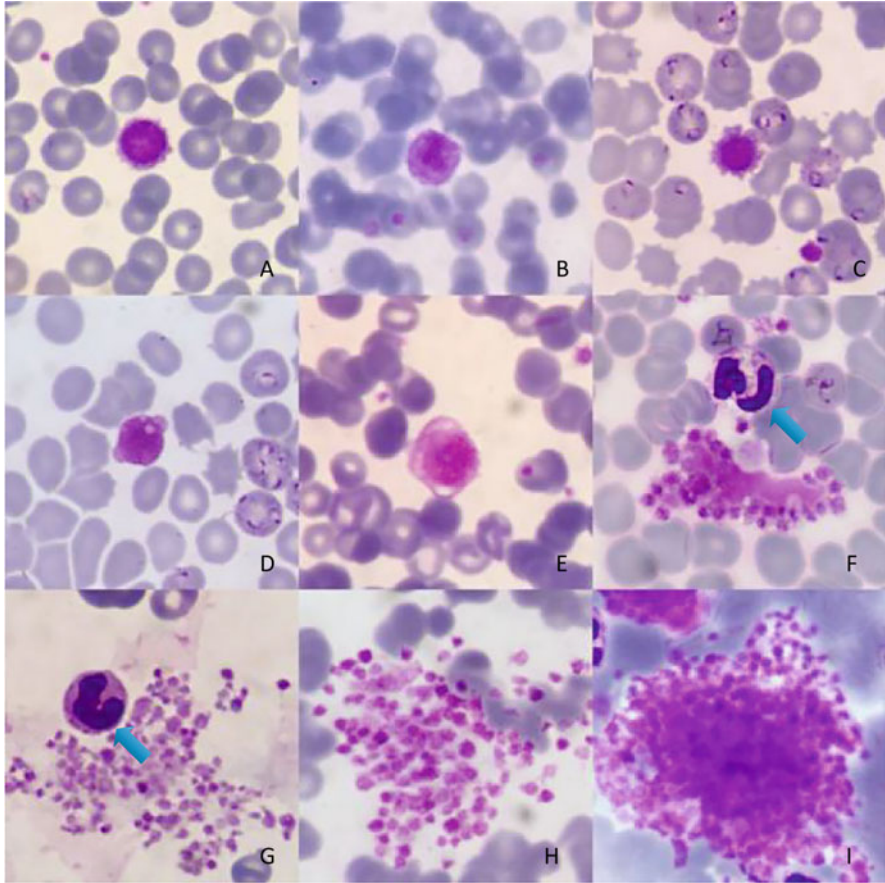


Fig. 6.105 Platelets (Giemsa staining, $\times 1000$)

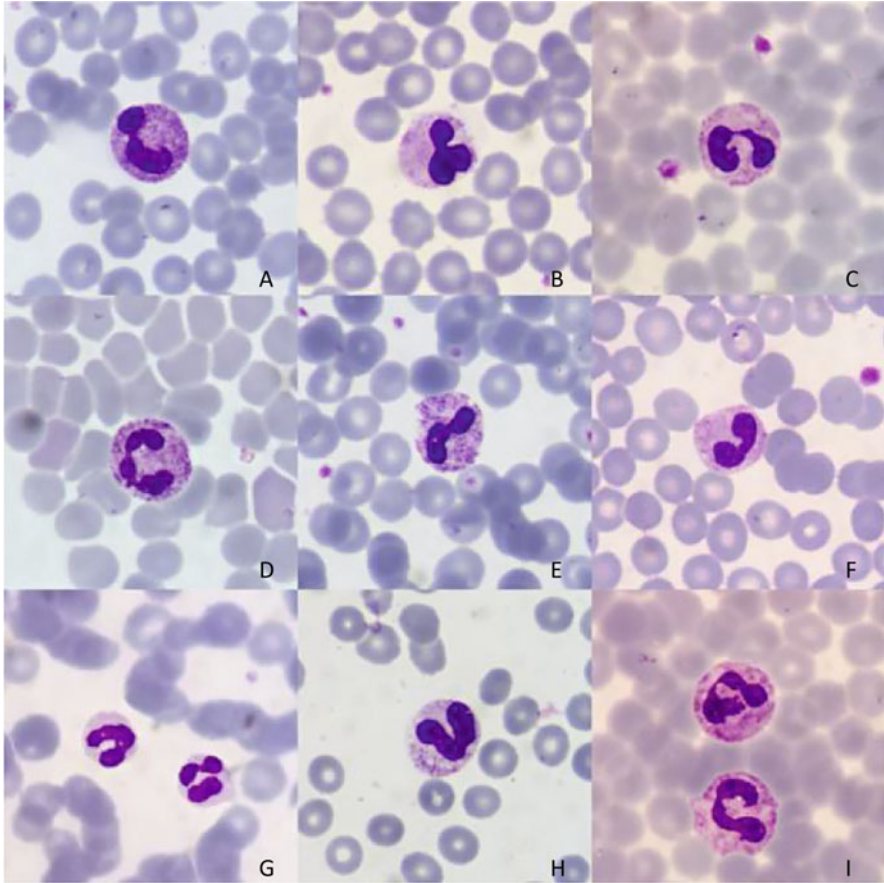


Fig. 6.106 Neutrophils (Giemsa staining, $\times 1000$)

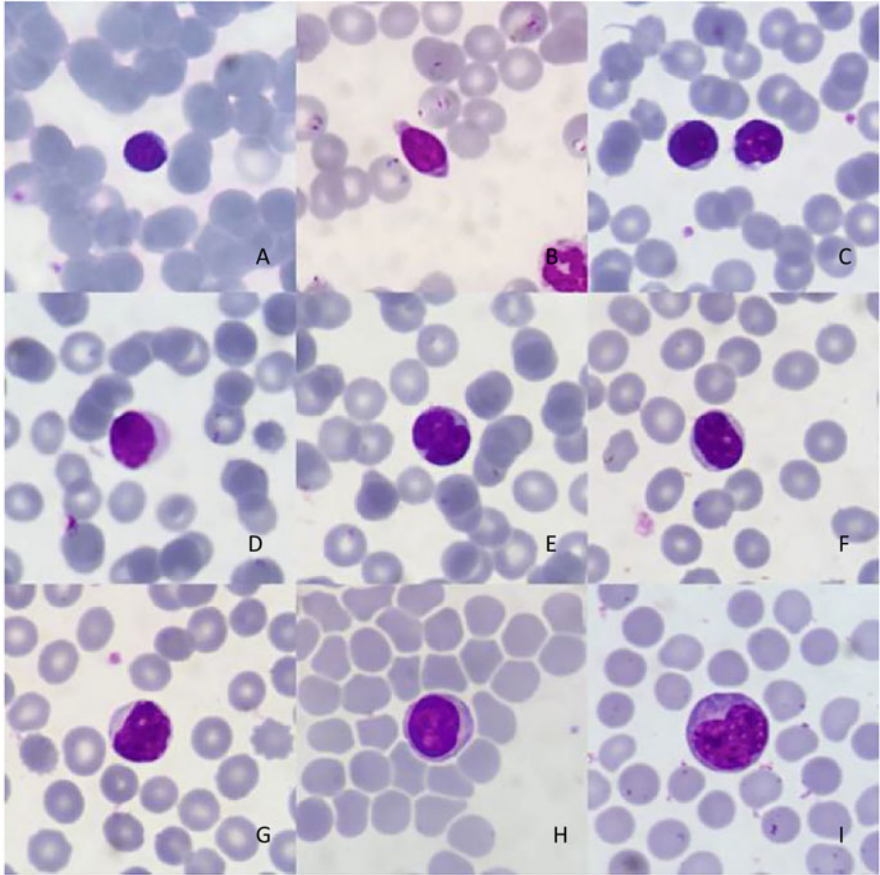


Fig. 6.107 Lymphocytes (Giemsa staining, $\times 1000$)

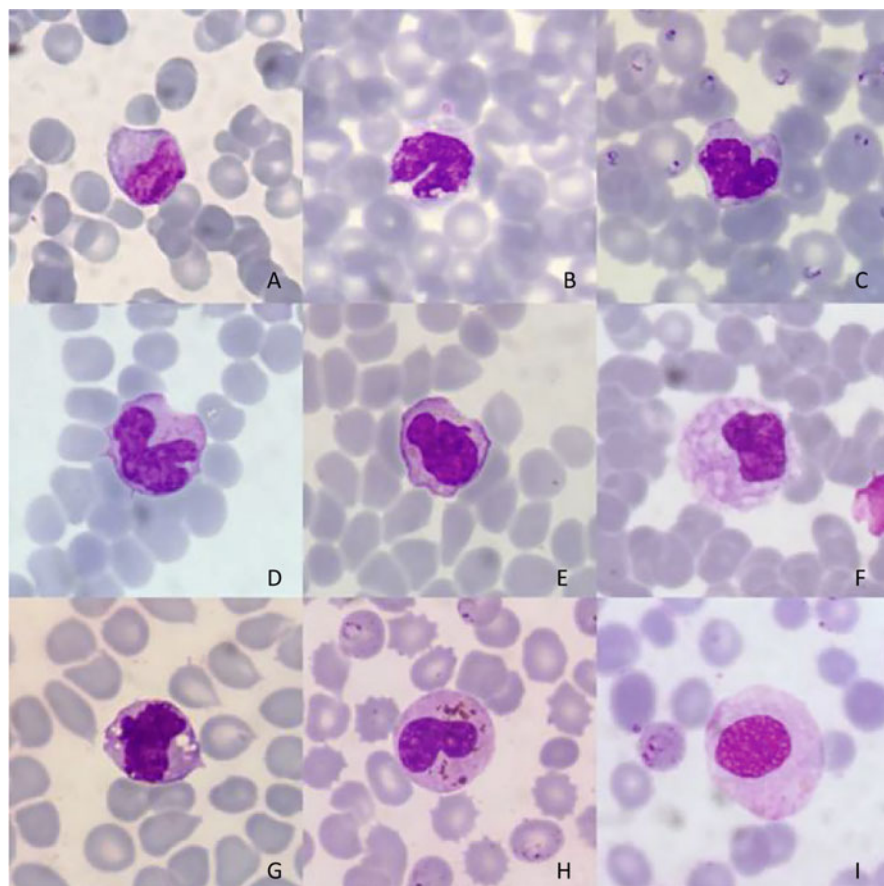


Fig. 6.108 Monocytes (Giemsa staining, $\times 1000$)

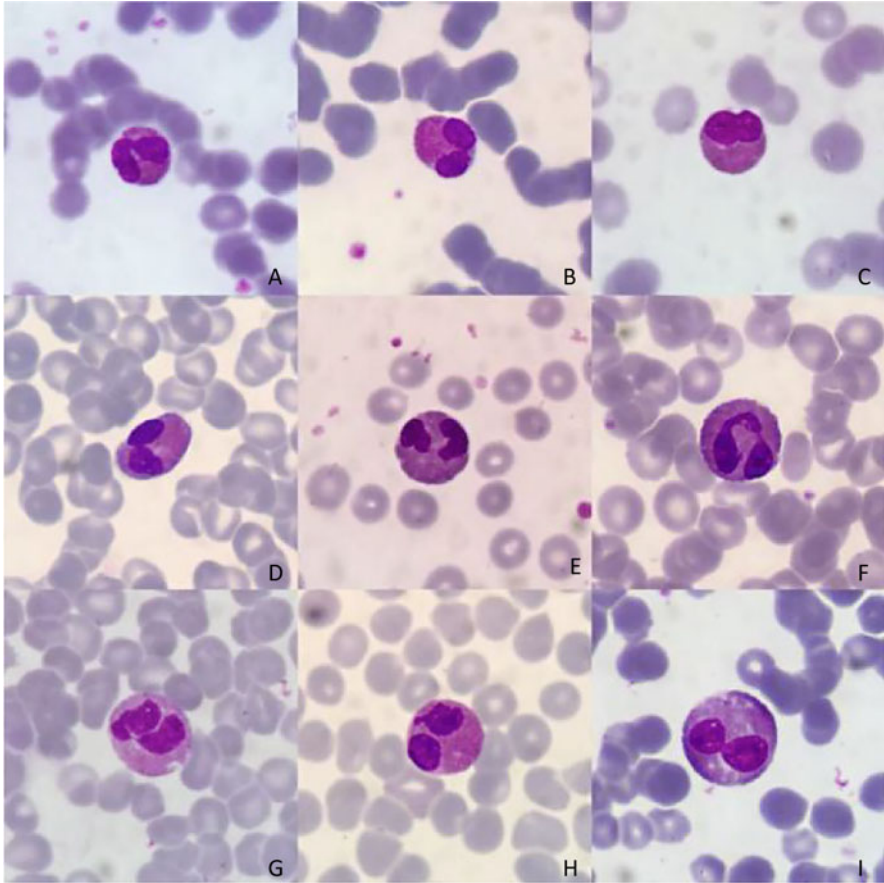


Fig. 6.109 Eosinophils (Giemsa staining, $\times 1000$)

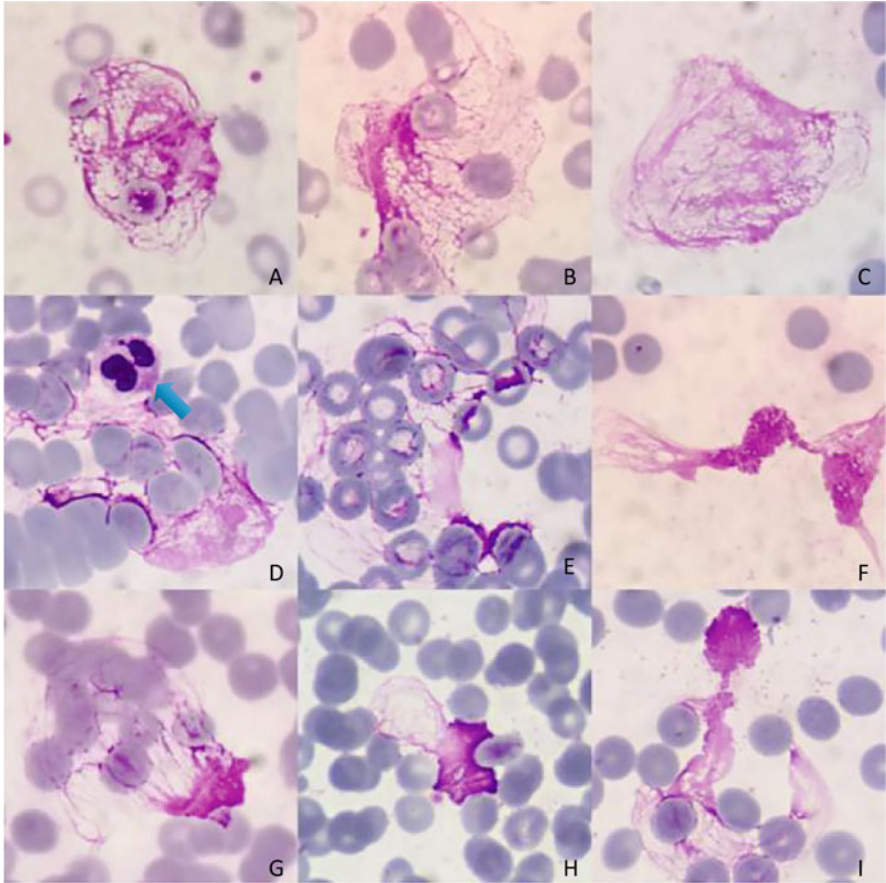


Fig. 6.110 Basket cells (Giemsa staining, $\times 1000$)

References

- Kai W, Jian L, Wei W (2021) Morphology of human malaria parasites: theory and applications [M]. Hubei Science and Technology Press, Wuhan
- Xiaoqiu Q (2007) Malaria control manual (3rd edition) [M]. People's Medical Publishing House, Beijing
- Qian W, Meng-en Z, Yurong Q (2008) Atlas of Hemocytology diagnostics [M]. China Science Publishing House, Beijing



Immunodiagnosis of Malaria

7

Jianhai Yin, He Yan, and Jian Li

Abstract

Malaria remains one of the world's most important public health threats, and prompt, precise diagnosis is still an essential component of malaria control and elimination strategies, even in the postelimination phase. There are many kinds of diagnostic tools used for malaria diagnosis, including microscopy, rapid diagnostic tests, and nucleic acid amplification testing. There are advantages and disadvantages among these methods in practice. In this chapter, we introduce different techniques for the immunodiagnosis of malaria based on malarial antigens and antibodies and provide recommendations for the future research and development of novel technologies for malaria diagnosis and transmission risk evaluation in China after malaria elimination.

Keywords

Malaria · Antigen · Antibody · Immunodiagnosis

J. Yin (✉) · H. Yan

National Institute of Parasitic Diseases, Chinese Center for Disease Control and Prevention (Chinese Center for Tropical Diseases Research), NHC Key Laboratory of Parasite and Vector Biology, WHO Collaborating Center for Tropical Diseases, National Center for International Research on Tropical Diseases, Shanghai, China
e-mail: yinhj@nipd.chinacdc.cn; yanhe@nipd.chinacdc.cn

J. Li

Hubei University of Medicine, Wuhan City, China

7.1 Introduction

With the advancement of the global malaria control process, an increasing number of countries have entered the preelimination stage or the malaria elimination stage (WHO 2021a). However, the trends have been partially stalled by COVID-19, and a significant increase in malaria cases and deaths were reported in 2020 in the World Malaria Report 2021 (WHO 2021b), where the estimated number of cases in 87 endemic countries in the world reached 241 million, and the estimated number of deaths reached 627,000. This was attributed to the disruption of medical services for malaria due to the COVID-19 pandemic. Therefore, there is still a long way to go to achieve the global eradication of malaria.

Prompt, precise diagnosis is an essential component of malaria control and elimination strategies, and parasitological testing is the only way for accurate malaria diagnosis in febrile patients (WHO 2011). It is also critical to the reliability of surveillance data and the understanding of malaria transmission. There are several methods to detect the presence of malaria parasites in the blood. The gold standard method is microscopy, although rapid diagnostic tests (RDTs) have rapidly become a primary diagnostic test in many endemic areas. Furthermore, many kinds of novel serological and molecular methods have been developed and assessed to overcome the limitations of microscopy and RDTs.

In this chapter, immunoassays for malarial antigen or antibody detection are discussed.

7.2 Immunoassays for Antigen Detection

7.2.1 Rapid Diagnostic Tests

Immunochromatographic-based diagnostic tests are already the most common diagnostic methods for malaria that detect antigens, and they are also known as rapid diagnostic tests (RDTs), which are extensively used worldwide (Wilson 2012). These methods are lateral flow assays usually in the format of cassettes, dipsticks, or cards, consisting of capture antibodies against *Plasmodium*-specific antigens immobilized on nitrocellulose membranes and bound to gold particles or other visually detectable markers (labeled antibodies) in the mobile phase. Antigens of the parasite are detected when the blood of a person suspected of having malaria is dropped in a membrane strip, where the liquid sample flows across. As a result, the immobilized complexes “capture antibody–antigen–labeled antibody” will be formed and can be visualized with colored lines when the blood is infected with *Plasmodium* (Gimenez et al. 2021).

RDTs are cost-effective and simple to operate, the results are displayed in less than 30 min and are easy to interpret, and little infrastructure and no electrical equipment are required (Mukkala et al. 2018). They are important alternatives for malaria diagnosis in areas where microscopy or other approaches are used to detect malaria parasites in the blood. Meanwhile, they are the most commonly used method

for malaria diagnosis in resource-limited endemic settings. Not only are they increasingly used in malaria screening and epidemic investigations, but they are also useful tool for malaria self-diagnosis. It was reported that 3.1 billion malaria RDTs were sold globally in 2010–2020, with nearly 81% of these sales going to sub-Saharan African countries (WHO 2021b). Correspondingly, 2.2 billion RDTs were distributed by national malaria programmes, with approximately 88% in sub-Saharan Africa (WHO 2021b).

However, various factors, such as *Plasmodium* species, level of parasitemia, storage conditions, interpretation of the results, and the variability of the parasite antigen tested, may impact the performance of RDTs. First, RDTs are only suitable for the diagnosis of *P. falciparum*- and *P. vivax*-specific infections thus far. Currently, commercial RDTs available on the market are mostly able to detect *P. falciparum*-specific histidine-rich protein 2 (HRP2), *P. vivax*-specific lactate dehydrogenase, *Plasmodium* panspecific lactate dehydrogenase (pLDH), or *Plasmodium* spp. aldolase. However, their sensitivity to detect nonfalciparum spp. is low overall (Yerlikaya et al. 2018), and even for the detection of *P. vivax*, the sensitivity of the most frequently used RDTs was 75–87% compared to microscopy (Abba et al. 2014). Moreover, no RDTs can specifically detect *P. ovale*, *P. malariae*, or *P. knowlesi*, even with high sensitivity. Second, the performance of RDTs is also limited to low parasitemia, and they usually have the capability of detecting >100 parasites/ μ l. It is worth noting that the presence of a low number of parasites is relevant, especially for pregnant women and children under the age of 5 years, who are the most vulnerable populations. Third, humidity and extreme temperatures tend to easily affect RDT performance, and persistence of antigens in the patient's blood circulation after treatment may lead to false positives (Yan et al. 2013). Fourth, interpretation of results can be confusing when testing for combinations of antigens, especially when control and *Plasmodium* panspecific lines are displayed together. Fifth, the emergence and spread of *Pf*HRP2/3-deleted strains in countries where malaria is endemic results in the increasing occurrence of false negativity in symptomatic patients who are infected with variants of *P. falciparum* that do not express HRP2 (Cheng et al. 2014). It was reported that *Pf*LDH-based RDTs could be used for *P. falciparum* detection in *Pf*HRP2-deleted samples at high density but vary greatly at lower densities (Gatton et al. 2020).

Therefore, quality-assured RDTs can be important for case diagnosis and case management, and users such as clinicians and laboratory personnel must be familiar with the RDTs used in their facilities and their associated performance characteristics, while the causes of fever in nonmalarial patients should be followed up and properly managed appropriately. Consequently, the minimum procurement criteria were recommended by the WHO Malaria Policy Advisory Committee, and independent global quality assessment programmes for malaria RDT lots have been carried out by the WHO in collaboration with other Malaria programmes, such as the Foundation for Innovative New Diagnostics (FIND), and coordinated the WHO Malaria RDT Product Testing Programme (Cunningham et al. 2019). In detail, any RDT should be fast and independent of the device, available to those who need it, and require minimal training. Furthermore, their sensitivity and specificity were

recommended to reach at least a 75% “panel detection score” at 200 parasites/ μ L, with a false positive rate of less than 10% and an invalid rate of <5%, for the detection of *P. falciparum* and, if applicable for *P. vivax*, in all transmission settings (<https://www.who.int/teams/global-malaria-programme/case-management/diagnosis/rapid-diagnostic-tests>). To date, eight rounds of WHO product testing of malaria RDTs have been completed since 2008, and the summary results of malaria RDT performance have been published (Malaria Rapid Diagnostic Test Performance Summary results of WHO product testing of malaria RDTs: rounds 1–8 (2008–2018)) (Cunningham et al. 2019).

Given the significantly lower sensitivities for nonfalciparum species mainly due to the lower parasitemia and the importance for the detection of low levels of parasitemia, malaria RDTs used for malaria diagnosis should be confirmed by other laboratory tests (e.g., blood film examination and nucleic acid amplification test). Moreover, high-sensitivity RDTs for *P. falciparum*, such as Alere Malaria Ag *P. f* (Alere) and NxTek Eliminate Malaria *P. f* (Abbott), have been developed and tested for their ability to detect malaria infection in asymptomatic individuals or individuals with very low parasitemia, and this might be a good strategy to better detect malaria parasites in the future, especially in the low-transmission setting or malaria-eliminated areas. In addition, there are also real-world implications for the discovery of new malaria RDT candidate antigens. One is Plasmodium glutamate dehydrogenase (pGDH), which has come to the attention of researchers; it is specific to *Plasmodium*, but the similarity among different species is so high that it is difficult to identify different *Plasmodium* spp. (Ahmad et al. 2019; Krishna et al. 2015). The other is GAPDH, which includes unique regions that make it possible to raise antibodies against pan-*Plasmodium* specificity and to detect *P. falciparum* or rodent malaria parasites specifically, but other species-specific detection for GAPDH has not been reported (Krause et al. 2017). Therefore, more work is needed in the future to determine whether pGDH-based or GAPDH-based RDTs can be used to detect malaria parasites.

7.2.2 Other Laboratory Assays for the Detection of Malaria Parasite Antigens

The development of assays used in the laboratory for malaria antigen testing has greatly benefited from the significant advances in the development of stable hybridomas as sources of monoclonal antibodies and improvements in immunoassay platforms throughout the decades (Plucinski et al. 2021). For example, a colorimetric sandwich ELISA has the capacity to detect HRP2 at levels of <100 pg/ml, with assay wells showing the intensity of color proportional to the amount of antigen in the sample (Jang et al. 2018). Other multiplexed detection systems for malaria diagnosis using different panels of *Pf*HRP2 and panmalarial antigen targets to differentiate species in malaria infection have been developed, such as the Luminex xMAP bead-based assay (Martianez-Vendrell et al. 2020) and the Quansys Q-Plex Human Malaria assay (Jang et al. 2019). For instance, the former assay can screen

P. falciparum with simultaneous analysis of glutamate-rich protein (GLURP) antigens R0 and R2, merozoite surface protein 3 (MSP3), MSP1 hybrid, and apical merozoite antigen 1 (AMA1) in blood from a person suspected of having malaria infection, according to the fluorescence intensity signals for different antigen targets for samples (Rogier et al. 2017). Furthermore, these assays are usually sensitive to detect malaria parasite antigens at low concentrations, plus their operator independence and reliability; thus, they have routine clinical application for malaria diagnosis. In addition, some promising laboratory tests of nontraditional immunoassays and aptamer-based antigen detection systems with good sensitivity and specificity have been developed (Frith et al. 2018; Mu et al. 2017; Hemben et al. 2017; Paul et al. 2017).

7.3 Immunoassays for Antibody Detection

Although serologic testing is generally not recommended for the routine diagnosis of malaria, it is still used for some cases, such as febrile patients traveling to malaria-endemic areas with repeatedly negative blood smears and cases of suspected tropical splenomegaly syndrome. Moreover, it is also used to screen blood donors and evaluate donors with suspected cases of transfusion-transmitted malaria. Additionally, it is used for detecting malarial antibodies in seroepidemiological studies for monitoring malaria control and elimination under specific and predictable requirements. Thus, the ideal test should be high throughput, easy to operate, easy to interpret, and quick to display the results. Most of the tests available are either immunofluorescence assays or enzyme immunoassays and can be performed on serum or plasma.

7.3.1 Complement Fixation Test

The complement fixation test (CFT) is a classical laboratory testing and one of the earliest methods for malarial antibody detection, which is more sensitive than microscopy of peripheral blood smears for detecting current infections (Thomson 1918). The test is based on the capacity of complement, a group of heat-labile proteins present in the plasma, to bind to antigen–antibody complexes. When the complexes are present on the surface of red blood cells, complement causes their lysis, which can be measured photospectroscopically. In practice, heating the serum first leads to the destruction of complement, and then the serum is mixed with the appropriate pathogenic antigen and incubated. Next, exogenous complement is added into the mixture when the antigen–antibody complexes are formed. This complement then binds to the complexes and is “fixed,” no longer able to cause lysis of the added indicator red blood cells. The test measures certain types of antibodies (mainly IgG antibodies) that occur only during the acute phase of pathogenic infection and has been widely used as an alternative for malaria diagnosis. However, this method is less sensitive and more complex, as well as labor

intensive; thus, it has been increasingly replaced by modern immunoassays such as enzyme-linked immunosorbent assay (ELISA) (Wilson et al. 1975; Drakeley and Cook 2009).

7.3.2 Indirect Hemagglutination Assay

Indirect hemagglutination assays (IHAs) have been developed and optimized continuously and used for detecting malarial antibodies. This method initially used tanned formalized sheep red blood cells sensitized with an antigen prepared from erythrocytic *Plasmodium* released from the red blood cells (Bray 1966). For instance, it was reported that soluble antigens prepared from *P. falciparum* and *P. vivax* could attach to aldehyde-fixed type “O” erythrocytes and detect antibodies in more than 91% of infections with homologous *Plasmodium* species and 72–76% of infections caused by heterologous species using the IHA (Mathews et al. 1975). Sera are tested by serial dilution but are difficult to standardize, resulting in limitations of cross-comparison of data from different research groups.

7.3.3 Immunofluorescence Antibody Test

The Immunofluorescence Antibody Test (IFAT) was extensively used for malaria seroepidemiology (Drakeley and Cook 2009). First, the whole parasitized red blood cells with the antigen of interest were fixed on a microscope slide, and then the sera sample was incubated on the slide. Finally, the resulting fluorescence according to the binding of a secondary antibody coupled with a fluorescent compound and the bound antibodies in the serum was examined using a specialized microscope. Compared with other methods, it is easier to prepare whole malarial parasite antigens, and these antigens are more stable than extracts of soluble antigens (Ambroise-Thomas 1976). However, this method is also difficult to standardize, and the fluorescence is subjectively determined by visual examination. Moreover, the sensitivity is limited due to the antigens used not being from the target malarial parasites, although *P. falciparum* culture became available as a stable source of antigen. In addition, it is also labor intensive for slide preparation, and the derived antibody responses are not specific since all parasitized red blood cells are used (Drakeley and Cook 2009).

7.3.4 Enzyme-Linked Immunosorbent Assay

The principle of Enzyme-Linked Immunosorbent Assay (ELISA) is similar to that of IFA, but the antigens of ELISA are coated on the microtiter plate instead of the glass slide of IFA, and the antigens are often single recombinant proteins. The bound antibodies are detected with a secondary antibody linked with an enzyme, and color change or fluorescence is quantified by a spectrophotometer if the bound enzyme is

present in the well. Furthermore, it is relatively cheap and easy to perform and generates objective results. Additionally, it is also a high-throughput, standardizable test that can be compared from different laboratories with robust results (Drakeley and Cook 2009; Esposito et al. 1990).

7.3.5 Protein Microarray

Protein microarray is similar to ELISA, but recombinant proteins are bound to a microarray slide in nanogram quantities and screen thousands of antigens simultaneously and have a greater dynamic detection range than ELISA; thus, it is much more suitable for antigen discovery and broad assessments of the immune response to malaria. However, it is not available for field investigation due to many factors, such as equipment requirements and signal variation between slides (Drakeley and Cook 2009; Doolan et al. 2009; Gray et al. 2007).

7.3.6 Cytometric Bead Array

Flow cytometric bead-based Cytometric Bead Array (CBA) can measure the response to multiple antigens in biological and environmental samples simultaneously. There are several advantages: it allows the assessment of multiple analytes in a single sample, collects data with minimal sample size, is reproducible, and can be compared with results from previous experiments and results from other assays, as well as evaluate multiple samples faster. There were different cytokine/chemokine kits, two flow cytometry-based (eBioscience® FlowCytomix™ and BD™ Cytometric Bead Array Human Enhanced Sensitivity) and four Luminex®-based (Invitrogen™ Human Cytokine 25-Plex Panel, Invitrogen™ Human Cytokine Magnetic 30-Plex Panel, Bio-Rad® Bio-Plex Pro™ Human Cytokine Plex Assay, and Millipore™ MILLIPLEX® MAP Plex Kit) kits used to quantify and compare cytokine and chemokine responses in culture supernatants from *P. falciparum* stimulations (Moncunill et al. 2013). Moreover, the protein levels of the cytokines IL-2, IL-6, IL-10, IL-17, IFN- γ , and TNF in the serum, frontal cortex, and hippocampus of controls and *P. berghei*-infected mice treated or not treated with artesunate were determined using a CBA kit (Miranda et al. 2013).

7.3.7 Engineered Yeast Agglutination Assay

A new agglutination assay named the Engineered Yeast Agglutination Assay (Cruz et al. 2022) was developed using modified *Saccharomyces cerevisiae* cells as antigen-displaying bead-like particles to capture malaria antibodies. The epidermal growth factor-1-like domain (EGF1) of *P. falciparum* merozoite surface protein-1 (PfMSP-119) was displayed on the yeast surface and shown to bind antimalarial antibodies. After mixing with a second yeast strain showing the Z domain of Protein

A from *Staphylococcus aureus* and settling in a round-bottomed well, the yeast produced a visually distinctive agglutination test result. This method is relatively inexpensive and may have the potential for regions seeking malaria surveillance information to guide their elimination programmes.

7.4 Challenges and Perspectives

China officially achieved the elimination of malaria (Zhou 2021), but malaria remains one of the world's most important public health threats, and China also faces numerous challenges in the prevention of malaria re-establishment of transmission (Yin et al. 2022b). For instance, a large number of imported malaria cases continue to be reported per year, including border malaria cases, especially at the China–Myanmar border. Moreover, there are potentially unknown infections, including asymptomatic infections and *P. falciparum* with HRP2/3 gene deletions, which are easily missed. Currently, malaria microscopy and RDTs are still the main methods for malaria diagnosis in the first line, but microscopy competency is difficult to maintain, and there is a shortage of sensitive species-specific RDTs except for *P. falciparum* and *P. vivax* in China (Yin et al. 2022a). Moreover, there are no suitable kits for malaria seroepidemiology for the evaluation of malaria transmission after malaria elimination. Therefore, it is still critical to strengthen the detection capacity to meet the timely detection of these sources of infection in the postelimination phase, which will contribute to the prevention of malaria re-establishment in areas with malaria transmission environments.

First, the research and development of improved diagnostic tools, including antigen detection and antibody detection for malaria diagnosis, need to be accelerated, and they can detect asymptomatic infections of very low parasite densities. Moreover, they should be cost-effective, easy to operate and interpret, and thereby suitable for mass screening and surveillance. Additionally, it is recommended to integrate malaria testing into diagnostics for other febrile diseases in health systems after malaria elimination.

Second, more antigen targets should be identified for rapid malaria diagnosis, especially for species-specific identification, not only for *P. falciparum* and *P. vivax* or pan-Plasmodium. Furthermore, it is best for the new targets to solve the challenge in *P. falciparum* with HRP2/3 gene deletions simultaneously.

Third, serologic methods are valuable tools for the measurement of transmission, especially in the postelimination phase. To date, there are many different serologic methods for the detection of malarial antibodies, but the results from different methods cannot be compared. Therefore, method standardization, including antigen standardization, is an important area for further research.

Fourth, noninvasive testing in samples such as saliva or other bodily fluids rather than currently the most commonly used blood deserves further exploration.

In conclusion, although traditional techniques, such as microscopy and RDTs, are still being used in the field, the exploration and field implementation of advanced technologies, including immunoassays for malaria diagnosis, are still needed in the

postelimination phase in China. Not only for the detection of the presence of malaria parasites in the blood of the suspected individuals but also to evaluate the transmission risk through seroepidemiology. It will continue to maintain and strengthen the surveillance and response of imported malaria and contribute to the prevention of malaria re-establishment of transmission.

References

- Abba K, Kirkham AJ, Olliaro PL, Deeks JJ, Donegan S, Garner P, Takwoingi Y (2014) Rapid diagnostic tests for diagnosing uncomplicated non-falciparum or plasmodium vivax malaria in endemic countries. *Cochrane Database Syst Rev* 12:CD011431
- Ahmad A, Verma AK, Krishna S, Sharma A, Singh N, Bharti PK (2019) Plasmodium falciparum glutamate dehydrogenase is genetically conserved across eight malaria endemic states of India: exploring new avenues of malaria elimination. *PLoS One* 14(6):e0218210
- Ambroise-Thomas P (1976) Immunofluorescence in the diagnosis, therapeutic follow-up and sero-epidemiological studies of some parasitic diseases. *Trans R Soc Trop Med Hyg* 70(2):107–112
- Bray RS (1966) el-Nahal HM: indirect haemagglutination test for malarial antibody. *Nature* 212(5057):83
- Cheng Q, Gatton ML, Barnwell J, Chiodini P, McCarthy J, Bell D, Cunningham J (2014) Plasmodium falciparum parasites lacking histidine-rich protein 2 and 3: a review and recommendations for accurate reporting. *Malar J* 13:283
- Cruz CJG, Kil R, Wong S, Dacquay LC, Mirano-Bascos D, Rivera PT, McMillen DR (2022) Malarial antibody detection with an engineered yeast agglutination assay. *ACS Synth Biol* 11(9):2938–2946
- Cunningham J, Jones S, Gatton ML, Barnwell JW, Cheng Q, Chiodini PL, Glenn J, Incardona S, Kosack C, Luchavez J et al (2019) A review of the WHO malaria rapid diagnostic test product testing programme (2008–2018): performance, procurement and policy. *Malar J* 18(1):387
- Doolan DL, Dobano C, Baird JK (2009) Acquired immunity to malaria. *Clin Microbiol Rev* 22(1):13–36
- Drakeley C, Cook J (2009) Chapter 5. Potential contribution of sero-epidemiological analysis for monitoring malaria control and elimination: historical and current perspectives. *Adv Parasitol* 69:299–352
- Esposito F, Fabrizi P, Proveddi A, Tarli P, Habluetzel A, Lombardi S (1990) Evaluation of an ELISA kit for epidemiological detection of antibodies to plasmodium falciparum sporozoites in human sera and bloodspot eluates. *Acta Trop* 47(1):1–10
- Frith KA, Fogel R, Goldring JPD, Krause RGE, Khati M, Hoppe H, Cromhout ME, Jiwaji M, Limson JL (2018) Towards development of aptamers that specifically bind to lactate dehydrogenase of plasmodium falciparum through epitopic targeting. *Malar J* 17(1):191
- Gatton ML, Chaudhry A, Glenn J, Wilson S, Ah Y, Kong A, Ord RL, Rees-Channer RR, Chiodini P, Incardona S et al (2020) Impact of plasmodium falciparum gene deletions on malaria rapid diagnostic test performance. *Malar J* 19(1):392
- Gimenez AM, Marques RF, Regiart M, Bargieri DY (2021) Diagnostic methods for non-falciparum malaria. *Front Cell Infect Microbiol* 11:681063
- Gray JC, Corran PH, Mangia E, Gaunt MW, Li Q, Tetteh KK, Polley SD, Conway DJ, Holder AA, Bacarese-Hamilton T et al (2007) Profiling the antibody immune response against blood stage malaria vaccine candidates. *Clin Chem* 53(7):1244–1253
- Hemben A, Ashley J, Tohill IE (2017) Development of an immunosensor for PfHRP 2 as a biomarker for malaria detection. *Biosensors* 7(3):28
- Jang IK, Das S, Barney RS, Peck RB, Rashid A, Proux S, Arinaitwe E, Rek J, Murphy M, Bowers K et al (2018) A new highly sensitive enzyme-linked immunosorbent assay for the detection of plasmodium falciparum histidine-rich protein 2 in whole blood. *Malar J* 17(1):403

- Jang IK, Tyler A, Lyman C, Kahn M, Kalnoky M, Rek JC, Arinaitwe E, Adrama H, Murphy M, Imwong M et al (2019) Simultaneous quantification of plasmodium antigens and host factor C-reactive protein in asymptomatic individuals with confirmed malaria by use of a novel multiplex immunoassay. *J Clin Microbiol* 57(1):e00948
- Krause RGE, Hurdal R, Choveaux D, Przyborski JM, Coetzer THT, Goldring JPD (2017) Plasmodium glyceraldehyde-3-phosphate dehydrogenase: a potential malaria diagnostic target. *Exp Parasitol* 179:7–19
- Krishna S, Bharti PK, Chandel HS, Ahmad A, Kumar R, Singh PP, Singh MP, Singh N (2015) Detection of mixed infections with plasmodium spp. by PCR, India, 2014. *Emerg Infect Dis* 21(10):1853–1857
- Martinez-Vendrell X, Jimenez A, Vasquez A, Campillo A, Incardona S, Gonzalez R, Gamboa D, Torres K, Oyibo W, Faye B et al (2020) Quantification of malaria antigens PfHRP2 and pLDH by quantitative suspension array technology in whole blood, dried blood spot and plasma. *Malar J* 19(1):12
- Mathews HM, Fried JA, Kagan IG (1975) The indirect hemagglutination test for malaria. Evaluation of antigens prepared from plasmodium falciparum and plasmodium vivax. *Am J Trop Med Hyg* 24(3):417–421
- Miranda AS, Brant F, Rocha NP, Cisalpino D, Rodrigues DH, Souza DG, Machado FS, Rachid MA, Teixeira AL Jr, Campos AC (2013) Further evidence for an anti-inflammatory role of artesunate in experimental cerebral malaria. *Malar J* 12:388
- Moncunill G, Aponte JJ, Nhabomba AJ, Dobano C (2013) Performance of multiplex commercial kits to quantify cytokine and chemokine responses in culture supernatants from plasmodium falciparum stimulations. *PLoS One* 8(1):e52587
- Mu J, Andersen JF, Valenzuela JG, Welles TE (2017) High-sensitivity assays for plasmodium falciparum infection by Immuno-polymerase chain reaction detection of PfIDEh and PFLDH antigens. *J Infect Dis* 216(6):713–722
- Mukkala AN, Kwan J, Lau R, Harris D, Kain D, Boggild AK (2018) An update on malaria rapid diagnostic tests. *Curr Infect Dis Rep* 20(12):49
- Paul KB, Panigrahi AK, Singh V, Singh SG (2017) A multi-walled carbon nanotube-zinc oxide nanofiber based flexible chemiresistive biosensor for malaria biomarker detection. *Analyst* 142(12):2128–2135
- Plucinski M, Aidoo M, Rogier E (2021) Laboratory detection of malaria antigens: a strong tool for malaria research, diagnosis, and epidemiology. *Clin Microbiol Rev* 34(3):e0025020
- Rogier E, Plucinski M, Lucchi N, Mace K, Chang M, Lemoine JF, Candrinho B, Colborn J, Dimbu R, Fortes F et al (2017) Bead-based immunoassay allows sub-picogram detection of histidine-rich protein 2 from plasmodium falciparum and estimates reliability of malaria rapid diagnostic tests. *PLoS One* 12(2):e0172139
- Thomson JG (1918) Preliminary note on the complement deviation in cases of malaria: a new aid to diagnosis. *Br Med J* 2(3023):628–629
- WHO (2011) Universal access to malaria diagnostic testing: an operational manual: World Health Organization
- WHO (2021a) Zeroing in on malaria elimination: final report of the E-2020 initiative: World Health Organization
- WHO (2021b) World Malaria Report 2021: World Health Organization
- Wilson ML (2012) Malaria rapid diagnostic tests. *Clin Infect Dis* 54(11):1637–1641
- Wilson M, Fife EH Jr, Mathews HM, Sulzer AJ (1975) Comparison of the complement fixation, indirect immunofluorescence, and indirect hemagglutination tests for malaria. *Am J Trop Med Hyg* 24(5):755–759
- Yan J, Li N, Wei X, Li P, Zhao Z, Wang L, Li S, Li X, Wang Y, Li S et al (2013) Performance of two rapid diagnostic tests for malaria diagnosis at the China-Myanmar border area. *Malar J* 12: 73

- Yerlikaya S, Campillo A, Gonzalez IJ (2018) A systematic review: performance of rapid diagnostic tests for the detection of *Plasmodium knowlesi*, *Plasmodium malariae*, and *Plasmodium ovale* Mono-infections in human blood. *J Infect Dis* 218(2):265–276
- Yin J, Li M, Yan H, Zhou S, Xia Z (2022a) Laboratory diagnosis for malaria in the elimination phase in China: efforts and challenges. *Front Med* 16(1):10–16
- Yin J, Yan H, Li M (2022b) Prompt and precise identification of various sources of infection in response to the prevention of malaria re-establishment in China. *Infect Dis Poverty* 11(1):45
- Zhou XN (2021) China declared malaria-free: a milestone in the world malaria eradication and Chinese public health. *Infect Dis Poverty* 10(1):98



Molecular Basis of Malaria Pathogenesis

8

Su-Jin Li, Zhenghui Huang, and Lubin Jiang

Abstract

Blood stage is the most important period for parasite growth, development, and pathogenesis. Studying the transcriptional regulatory mechanism of key pathogenic genes during the growth and development of *Plasmodium falciparum* will provide an important theoretical basis for our targeted vaccine design and new drug development, and provide a solid guarantee for malaria prevention and control both in our country and all over the world. Here, we review the existing research results of the molecular basis and regulatory mechanism of the three important biological processes (RBC invasion, immune escape, and gametocyte differentiation) of *Plasmodium* in the blood stage.

Keywords

Malaria · *Plasmodium falciparum* · Erythrocyte invasion · Immune escape · Sexual differentiation · Transcriptional regulatory

8.1 Introduction

The ancient scourge, malaria, is still one of the most serious infectious diseases endangering human life and health worldwide. Invading into erythrocytes and developing in them is an essential step for the proliferation, development, and transmission of *Plasmodium*. The blood stage is also where individuals experience clinical symptoms and sometimes lethal diseases. Therefore, it is always of great importance to uncover the molecular basis of severe malaria pathogenesis in this stage.

S.-J. Li · Z. Huang · L. Jiang (✉)

Institut Pasteur of Shanghai, Chinese Academy of Sciences, Huangpu, Shanghai, China

e-mail: sjli@ips.ac.cn; zh Huang@ips.ac.cn; lbjiang@ips.ac.cn

Usually, it takes malaria parasites only a few minutes to complete the invasion process from red blood cell recognition and adhesion to final invasion into red blood cells (RBCs) (Cowman and Crabb 2006). Infected individuals readily make many immune effector molecules, including immune cells, cytokines, and antibodies, to disrupt adhesion and destroy the infected erythrocytes. To avoid this fate, parasites have developed a series of precise and perfect immune escape and immune suppression strategies to evade host immune attack during the long run road of evolution with the host.

To cope with changes in the external living environment and maintain the reproduction of species, in each asexual replication cycle, a small number of parasites (5–10%) will undergo sexual development through a process of epigenetic regulation. Mature male and female germ cells (1:5, male-to-female ratio) are released into the blood circulation and can be transmitted back to the mosquito vector. In this chapter, we will combine the existing research results, focusing on the molecular basis and regulatory mechanism of the three important biological processes (RBC invasion, immune escape, and gametocyte differentiation) of *Plasmodium* in the blood stage.

8.2 Molecular Basis of Malaria Parasite Invasion into Host Erythrocytes

Invasion into new host erythrocytes is almost the only function of asexual *Plasmodium* merozoites. The invasion process, which is important for malaria parasite erythrocytic stage growth and rapid reproduction, can be mainly divided into initial attachment, tight binding, tight junction formation, and finally complete invasion into RBCs and completion of RBC membrane repair (Cowman et al. 2017).

The molecular basis for which proteins are involved in the initial stage of merozoite invasion is poorly defined. It is thought that the initial invasion stage may be mediated by *Plasmodium* merozoite surface proteins (MSPs) in earlier studies because merozoite surface protein 1 (MSP1), together with a number of peripheral proteins, can form a large complex on the merozoite surface and is considered to be related to the invasion process of *Plasmodium*. However, the study by Das et al. (2015) identified that even if *Plasmodium* merozoites did not express MSP1 protein, they could invade erythrocytes normally, suggesting that MSP1 might not be necessary in the stage of malaria parasite invasion but rather plays a role in the division of mature merozoites from erythrocytes. While these surface proteins and peripheral proteins may not be directly involved in the invasion of *Plasmodium* merozoites, they play a part in preventing merozoites from being attacked by the host's immune system during the process of release from and invasion into erythrocytes. Thus, these proteins are important targets for the development of new antimalarial drugs and vaccines (Boyle et al. 2015; Kennedy et al. 2016).

Relative to the initial attachment stage, the mechanism of the tight binding stage has been well studied. Significant studies have demonstrated that *Plasmodium*

completes tight attachment through different pathways, which mainly depend on the different ligand–receptor interactions. Based on whether neuraminidase is required to degrade sialic acid during invasion, pathways of tight binding can be mainly divided into sialic acid-dependent and sialic acid-independent pathways (Camus and Hadley 1985). *Plasmodium* merozoite surface proteins involved in the sialic acid-dependent pathway mainly include EBA175, EBL-1, and EBA140. Their corresponding erythrocyte receptors are glycophorin A (GPA), glycophorin B (GPB), and glycophorin C (GPC) (Maier et al. 2003; Mayer et al. 2006; Mayer et al. 2009). It has been suggested that EBA181 and RH1 are also involved in this pathway, but their erythrocyte receptors have not yet been identified (Gilberger et al. 2003; Triglia et al. 2005). Merozoite surface protein involved in the sialic acid-independent pathway is RH4, and its erythrocyte receptor is CD35 (Tham et al. 2010). By applying the epigenetic CRISPR/dCas9 system to precisely regulate the transcription start site regions of EBA175 and RH4, Xiao et al. (2019) achieved the switch of malaria parasite invasion pathways. Moreover, some studies suggested that glycosylphosphatidylinositol (GPI)-anchored micronemal antigen (GAMA), a micronemal antigen of *P. falciparum* binding to erythrocytes, played a part in the sialic acid-independent invasion pathway (Hinds et al. 2009; Arumugam et al. 2011; Cheng et al. 2016). However, the specific erythrocyte membrane receptors that interact with GAMA and the mechanisms behind their interaction remain poorly understood. Recently, by conducting LC-MS analysis on the components of the erythrocyte membrane, Lu et al. (2022) indicated that band 3 membrane protein and ankyrin 1 (ANK1) may be potential receptors for PfGAMA. Antibodies against band 3-P5 can inhibit *P. falciparum* invasion by blocking GAMA binding to the infected erythrocyte membranes. In addition to the surface proteins above, other proteins, such as RH2a, RH2b, and RH5, have been demonstrated to be involved in the process of tight attachment, (Duraisingh et al. 2003; Crosnier et al. 2011) but most of these proteins, except RH5, are not necessary (Lopatnicki et al. 2011). RH5 plays a crucial role in the merozoite invasion process. Compared with other members of the RH protein family, RH5 has a smaller molecular weight and no transmembrane domain. It can form a complex with RIPR and CyRPA and bind to the erythrocyte surface receptor CD147 to complete the process of tight attachment. During tight binding with RBCs, the parasites trigger the flow of calcium ions to produce calcineurin, which strengthens the attachment of *Plasmodium* merozoites and RBCs. The binding of the RH5/RIPR/CYRPA complex to the erythrocyte receptor CD147 is essential in this process (Volz et al. 2016; Weiss et al. 2015). When either protein is knocked out in the complex, the *Plasmodium* merozoites will not be able to invade host erythrocytes.

Following the binding of the RH5/RIPR/CYRPA complex to the receptor CD147, tight junction formation occurs. AMA1 and RON2 are the two most important proteins in this stage. Apical membrane antigen protein 1 (AMA1) is a microfilament protein secreted on the surface of *Plasmodium* merozoites, while rhoptry neck protein 2 (RON2) is one of the earliest proteins to be transported into erythrocytes (Mitchell et al. 2004). Relevant studies in *Toxoplasma gondii* have shown that when RON2 is transported into erythrocytes, it embeds itself into the

erythrocyte membrane. Then, AMA1 binds to RON2 to form tight junctions between merozoites and host erythrocytes, through which merozoites move into erythrocytes (Mital et al. 2005). In addition to AMA1 and RON2, a claudin-like apicomplexan filament protein (CLAMP) may also play an important role in the formation of tight junctions, but aspects of the function of this protein in *P. falciparum* remain difficult to explain (Sidik et al. 2016).

With tight junctions moving from the apical to the posterior, the surface membrane located at the tight junction will be degraded by serine proteases, and adhesion proteins at the tight junction will be degraded by long-standing proteases. The process above will contribute to repairing the membrane of infected RBCs. Finally, the malaria parasites complete the invasion process by producing parasitophorous vacuoles rather than penetrating the cell membrane.

8.3 Precise and Perfect Immune Evasion Strategies of Malaria Parasites

To avoid the host's antibody response and establish chronic infection, many pathogens have formed a well-established system of phenotypic variation during long-term evolution and natural selection. Among them, a coordinated approach of switching gene expression and surface antigen protein variation to evade the clearance of the host immune system, named antigenic variation, is the most classic immune evasion strategy (Guizetti and Scherf 2013). It is through this mechanism that the malaria parasites reproduce indefinitely in the host's erythrocytes without being cleared by the host's immune system.

In general, when infected RBCs travel with the blood to the main immune organs, such as the spleen, the host immune system will eliminate them. However, due to the expression of *P. falciparum* erythrocyte membrane protein 1 (PfEMP1) on the cell surface, (Miller et al. 2002) infected erythrocytes eventually bind to receptors on vascular endothelial cells, avoiding clearance by the host immune system. PfEMP1 is encoded by a multicopy gene family named *var*. This gene family consists of 60 members, and each *var* gene encodes a variant form of PfEMP1. According to the position of its gene sequence on the chromosome, the *var* gene family can be divided into three basic types referred to as the UpsA, UpsB, and UpsC groups (Kraemer and Smith 2003; Lavstsen et al. 2003). Interestingly, a single malaria parasite will only randomly express specific PfEMP1 proteins in an asexual reproduction cycle. Once the protein is recognized by the host immune system and responds to the host's corresponding antibody, the parasite will switch the expression of another *var* gene and manage to evade host immune system attacks.

The pattern of *var* gene expression in *Plasmodium* is referred to as mutually exclusive expression, and several studies have shed significant light on the regulatory mechanism of this expression pattern. The study by Jiang et al. (2013) found that PfSET2, a histone H3K36me3-specific methyltransferase of *P. falciparum*, plays an important role in maintaining the mutually exclusive expression of the *var* gene. PfSET2 is mainly responsible for silencing the promoter region and the

intergenic region between exons of the *var* gene, making these regions maintain high levels of H3K36me3. When PfSET2 was knocked out, H3K36me3 decreased in these regions, while the levels of H3K4me3 increased, and the expression of all 60 *var* genes in *P. falciparum* was activated. Other studies by Bradley Coleman and Nicolas Brancucci et al. (Brancucci et al. 2014; Coleman et al. 2014) identified that heterochromatin protein (HP1) and histone deacetylase (HDA2) both played important roles in the mutually exclusive expression of the *var* gene of *P. falciparum*, since conditional knockout of either gene could activate the expression of all *var* genes. Recently, by applying chromosome conformation capture coupled with high-throughput sequencing (Hi-C seq), analyzing the three-dimensional (3D) genome organization, and conducting other experimental studies, Lu et al. (2021) identified that high-mobility group B 1 (HMGB1), a nonhistone architectural chromosomal protein, was critical in maintaining the integrity of centromere/telomere-based chromosome organization of *P. falciparum*. The entire repertoire of the *var* gene family was completely silenced in the absence of PfHMGB1. Once HMGB1 is complemented, the mutually exclusive expression of the *var* gene will be rescued. In addition, Li et al. (2019) in 2019 provided further data suggesting that the *P. falciparum* DNA helicase (RecQ1) also makes a difference in maintaining the mutually exclusive expression strategy of the *var* gene. A study conducted by Jing et al. (2018) found that antisense long noncoding RNA (aslncRNA) derived from *var* introns is an activator of the corresponding *var* gene. Moreover, significant work by Zhang et al. (2014) has demonstrated that *P. falciparum* RNase II (PfrNaseII) can silence UpsA *var* gene expression by specifically degrading the mRNA of UpsA *var*, and the expression of UpsA *var* will be specifically activated when PfrNaseII is conditionally knocked out. Further identification of RNA deep sequencing in clinical severe malaria samples found that the expression of PfrNase II in severe malaria clinical samples with high expression of UpsA *var* genes was significantly lower than that in other samples, leading to a philosophy: The severity of malaria is usually closely associated with the expression of UpsA-like genes in the *var* gene family.

In addition to the PfEMP1 protein, *P. falciparum* expresses 27–45 kDa repetitive interspersed repeats (RIFINs), encoded by the *rif* genes, on the infected erythrocyte surface for pathogenesis. RIFINs are the largest known family of variable antigens in *P. falciparum*, and each parasite genome encodes 150–200 *rif* genes (Kyes et al. 2001). In recent years, scientists have isolated human broadly reactive antibodies containing extracellular LAIR1 motif insertion from malaria patients (Pieper et al. 2017; Tan et al. 2016). These antibodies recognize the RIFIN protein through the inserted LAIR1 motifs. Another study found that parasites could achieve their immune evasion by binding RIFINs and another immunosuppressive receptor, LILRB1 (Saito et al. 2017). To clarify the host immune response mechanisms behind the interactions between the immune inhibitory receptor LAIR1 and RIFINs, Yijia Xie et al. (2021) solved the monomeric structure of RIFIN and the complex structures of two RIFINs bound to similar sites of LAIR1 in different patterns. Members of the RIFIN family use different binding sites to bind to LAIR1 or LILRB1, indicating the diversity of the RIFIN family. They also found that the binding site of RIFINs and LAIR1 partially overlaps with that of LAIR1 and its

natural ligand collagens. The RIFIN–LAIR1 interaction can induce LAIR1-mediated signal activation downstream, while broadly reactive antibodies inserted with LAIR1 mutants block signal activation. The authors revealed that *P. falciparum* used the RIFIN protein on the surface of infected RBCs to facilitate escape from the host immune system, whereas the host blocked the interactions by producing antibodies inserted with LAIR1 mutants in response.

In addition to antigenic variation, other strategies by which malaria parasites escape host innate immunity, such as secreting TatD-like DNases to degrade the molecular DNA of host neutrophil extracellular traps (NETs), were reported by Zhiguang Chang et al. (2016) NETs were found in the peripheral blood of a *P. falciparum*-infected child (Baker et al. 2008) and have been demonstrated to be related to the innate immune response. Zhiguang Chang et al. identified that TatD-like DNases of *P. falciparum* were associated with malaria parasite virulence and could be a potential candidate for the development of malaria vaccines.

Overall, proteins in diverse mechanisms have been reported to be responsible for malaria parasite immune evasion. However, due to their special expression mechanism, research on developing a malaria vaccine targeting them remains difficult to put forward. More research to clarify the mystery of the regulation of *Plasmodium* antigenic variation and other related molecules is needed to provide a solid theoretical basis for malaria pathogenesis and the development of novel strategies for antimalarial vaccines, antibodies, and drugs.

8.4 Molecular Mechanisms of Sexual Differentiation of Malaria Parasites

From the invasion of sporozoites into the host liver to the release of merozoites from the liver and infecting the host erythrocytes to the release of new merozoites and the reinvasion of new erythrocytes, this series of processes can be classified as the asexual growth cycle of malarial parasites. Although the growth and development of the asexual stage is closely related to the clinical symptoms and death of malaria, what truly plays a decisive role in the incidence of malaria is the sexual development of the *Plasmodium*, that is, the growth and development of the gametocyte. Sexual development ensures that *Plasmodium* can transmit from a vertebrate host to a mosquito-borne host and to the next vertebrate host again by the mosquito. Gametocytes thus play a decisive role in the spread of malaria (Baker 2010). The development of *Plasmodium* gametocytes is controlled by a unique mechanism that is different from the regulation of asexual growth and development. It usually takes 10–12 days to mature and form male and female gametocytes at the same time (Josling et al. 2018).

In laboratory cultures, sexual differentiation of *P. falciparum* is largely dependent on genetic background and culture conditions. There are many factors that alter the balance of asexual and gametophytic reproduction in *Plasmodium* as well as the ratio of male to female gametocytes (Henry et al. 2019). Next, we will discuss recent

advances in the regulation of sexual differentiation in *Plasmodium* and the mechanisms by which the parasite senses and integrates these environmental signals.

8.4.1 Molecular Regulation of Sexual Differentiation

Actually, it is still an unsolved mystery when *Plasmodium* begins to generate gametocytes, and this has always been a hot spot in *Plasmodium* research. In 2014, scientists found that the production of gametocytes is closely related to the expression of a DNA-binding protein, AP2-gametocyte (AP2-G), a member of the largest family of transcription factors known as *Apetala 2* (AP2) in *Plasmodium* (Kafsack et al. 2014; Sinha et al. 2014). It was found that after mutating AP2-G in *Plasmodium berghei*, the parasite would not be able to produce gametocytes, but if we reverted the mutation, the parasite could produce gametocytes normally. This means that robust expression of AP2-G is necessary and sufficient for sexual differentiation in asexually replicating parasites. Subsequent studies found that the transcription of *Pfap2-g* is silenced by heterochromatin. This silencing requires trimethylation on lysine 9 of histone H3 (H3K9me3), which is a typical marker of heterochromatin, as well as other factors required for the maintenance of general heterochromatin, including the histone deacetylase Hda2 (Coleman et al. 2014) and recognition of H3K9me3 by heterochromatin protein 1 (HP1) (Brancucci et al. 2014). Since the upstream region of AP2-G contains multiple AP2-G binding sites, if the AP2-G promoter cannot be effectively silenced, it will lead to high-level expression of AP2-G. Once AP2-G begins to be expressed, it forms a transcriptional positive feedback loop (Josling et al. 2020). In addition, Qingfeng Zhang et al. also discovered a core regulator PfAP2-G5 as a transcriptional repressor that can inhibit the transcriptional activity of *Pfap2-g*, which is also a heterochromatin structure-related factor that can participate in local heterochromatin formation at target gene loci and inhibit the expression of target genes. As a result, PfAP2-G5 can prevent the onset of sexual transition of the malaria parasite and continue to remain in the human body for asexual reproduction when there is no suitable opportunity for transmission (Shang et al. 2021). The same research team also found that the m5C level was relatively high in gamete cells in both rodent parasites and *P. falciparum*. This means that m5C modification may play an important role in sexual development and transmission. Both parasite species carry a homolog of NSUN2 (PyNSUN2; PfNSUN2), which acts as a methyltransferase and plays a major role in these m5C modifications of the transcriptome (Liu et al. 2022).

In *Plasmodium falciparum*, the activation of AP2-G expression and sexual differentiation is dependent on the gametocyte development-related gene (GDV1) (Eksi et al. 2012; Usui et al. 2019; Filarsky et al. 2018). Similar to AP2-G, GDV1 is only expressed in a subset of asexual blood stages; it localizes to heterochromatin regions and decreases the overall level of HP1 in these regions to increase the proportion of sexual differentiation by upregulating the expression of *Pfap2-g*. Conditional overexpression of GDV1 can significantly increase the ratio of sexual differentiation, and similar to ap2-g, GDV1 is also prone to loss-of-function

mutations during long-term in vitro culture. Unlike *ap2-g*, the expression of *gdv1* is not directly regulated by heterochromatin but by complementary noncoding RNAs, but the specific regulatory mechanism is unclear. The *gdv1* antisense RNA is transcribed from a large downstream region that encodes multiple noncoding RNAs. Interestingly, a large part of this downstream region also has the H3K9me3 silencing mark, which further leads us to believe that a second regulatory circuit involving heterochromatin plays a very important role in the regulation of sexual differentiation (Filarsky et al. 2018). Although GDV1 plays a very important role in the sexual differentiation of *P. falciparum*, the gene *gdv1* is not found in rodent *Plasmodium*, so the regulatory mechanism of gametocyte production in different species of *Plasmodium* may be very different.

Based on PfAP2-G, Kafsack et al. further analyzed its function in the sexual differentiation of *Plasmodium falciparum* by single-cell transcriptome sequencing of 12,800 parasites in different growth stages combined with bioinformatics analysis and finally established a regulatory model of PfAP2-G on the sexual development of Plasmodium; that is, PfAP2-G regulates the expression of AP2 (PF3D7_1224000), AP2 (PF3D7_1139300), ISWI, LSD2, SNF2, and HDA1 and other proteins to prepare for Plasmodium sexual growth and development (Poran et al. 2017).

8.4.2 Impact of External Signals on Sexual Differentiation

It has long been noted that the sexual differentiation rate of *Plasmodium falciparum* during culture increases with the increase in the infection rate of *Plasmodium* (Carter et al. 1993; Carter and Miller 1979) or the use of conditioned and spent media (Brancucci et al. 2015; Fivelman et al. 2007; Williams 1999). This tight dependence clearly indicates that external environmental stimuli have an important effect on the rate of sexual differentiation of the parasite, but it is unclear whether this is mediated by increased factors produced during parasite growth, fast nutrient consumption in the medium, or both. Extracellular vesicles from conditioned media were also associated with sexual differentiation rates (Mantel et al. 2013; Regev-Rudzki et al. 2013), which only increased sexual differentiation rates at high concentrations, and conditioned media retained their promised promoting effects even when extracellular vesicles were depleted (Brancucci et al. 2017). In addition, culturing under serum starvation conditions also significantly increased the rate of sexual differentiation (Brancucci et al. 2017; Gulati et al. 2015).

In addition to changes in medium composition or serum starvation culture increasing the rate of sexual differentiation, studies have also found that many metabolites may also affect the sexual differentiation rate of *Plasmodium*. For example, treatment with DTT or thapsigargin increases the rate of sexual differentiation. In addition, preaddition of erythrocyte homocysteine or other ER stress triggers also increases the rate of sexual differentiation (Tehlivets et al. 1832; Chaubey et al. 2014; Beri et al. 2017), as does adding too much serine to the medium (Gulati et al. 2015). Finally, Brancucci et al. identified lysophospholipid (LysoPC) as an active serum component that regulates sexual differentiation. Studies have shown that

adding LysoPC can inhibit sexual differentiation by inhibiting the transcription of *Pfap2-g*. Studies have shown that in vitro culture of *Plasmodium falciparum* in medium without human serum can greatly increase the production of gametocytes, and LysoPC can effectively inhibit the gametocyte production of Pf2004 (derived from NF54) and PfHB3 in vitro (50% effective inhibitory concentration was 1.7 μ M) (Brancucci et al. 2017). However, it could not inhibit the gametocyte generation of rodent *Plasmodium*, which once again proved that the regulatory mechanism of gametocyte generation among different species of Plasmodium is different. Furthermore, they found that the choline head group of LysoPC is a key component in inhibiting differentiation. Recently, the patatin-like phospholipase PNPLA1 has also been suggested to promote sexual differentiation (Flammersfeld et al. 2020). Conditional knockdown of PNPLA1 effectively suppressed the increase in sexual differentiation induced by serum starvation cultures, whereas overexpression of PNPLA1 with an asexual stage-specific promoter promoted sexual differentiation, while using a gametophytic stage-specific promoter did not. Since deletion of this phospholipase is identical to the phenotype in the presence of LysoPC, whereas overexpression is consistent with the phenotype of LysoPC depletion, this suggests that PNPLA1 may counteract the inhibitory effect of LysoPC by degrading LysoPC.

8.5 Conclusion

Blood stage is the most important period for parasite growth, development and pathogenesis. Due to the rapid asexual reproduction of the malaria parasite, the host has clinical symptoms, and the malaria parasite also develops from asexual development to sexual differentiation to cope with the harsh living environment during this stage. Understanding the molecular basis of the growth and development of *Plasmodium* during this stage is crucial for us to finish the research and development of antimalarial drugs or vaccines. However, there is still a large number of works that need to be further explored and improved, such as the transcriptional regulation mechanism of the invasion-related genes in this stage, the selection mechanism of the invasion pathway, and the regulation mechanism of sexual differentiation. Related research results are expected to provide more potential targets for the development of malaria drugs and vaccines.

References

- Arumugam TU et al (2011) Discovery of GAMA, a plasmodium falciparum merozoite micronemal protein, as a novel blood-stage vaccine candidate antigen. *Infect Immun* 79:4523–4532. <https://doi.org/10.1128/IAI.05412-11>
- Baker DA (2010) Malaria gametocytogenesis. *Mol Biochem Parasitol* 172:57–65. <https://doi.org/10.1016/j.molbiopara.2010.03.019>
- Baker VS et al (2008) Cytokine-associated neutrophil extracellular traps and antinuclear antibodies in plasmodium falciparum infected children under six years of age. *Malar J* 7:41. <https://doi.org/10.1186/1475-2875-7-41>

- Beri D et al (2017) A disrupted transsulphuration pathway results in accumulation of redox metabolites and induction of gametocytogenesis in malaria. *Sci Rep* 7:40213. <https://doi.org/10.1038/srep40213>
- Boyle MJ et al (2015) Human antibodies fix complement to inhibit plasmodium falciparum invasion of erythrocytes and are associated with protection against malaria. *Immunity* 42:580–590. <https://doi.org/10.1016/j.immuni.2015.02.012>
- Brancucci NM, Goldowitz I, Buchholz K, Werling K, Marti M (2015) An assay to probe plasmodium falciparum growth, transmission stage formation and early gametocyte development. *Nat Protoc* 10:1131–1142. <https://doi.org/10.1038/nprot.2015.072>
- Brancucci NMB et al (2014) Heterochromatin protein 1 secures survival and transmission of malaria parasites. *Cell Host Microbe* 16:165–176. <https://doi.org/10.1016/j.chom.2014.07.004>
- Brancucci NMB et al (2017) Lysophosphatidylcholine regulates sexual stage differentiation in the human malaria parasite plasmodium falciparum. *Cell* 171:1532–1544 e1515. <https://doi.org/10.1016/j.cell.2017.10.020>
- Camus D, Hadley TJ (1985) A plasmodium falciparum antigen that binds to host erythrocytes and merozoites. *Science* 230:553–556. <https://doi.org/10.1126/science.3901257>
- Carter R, Miller LH (1979) Evidence for environmental modulation of gametocytogenesis in plasmodium falciparum in continuous culture. *Bull World Health Organ* 57(Suppl 1):37–52
- Carter R, Ranford-Cartwright L, Alano P (1993) The culture and preparation of gametocytes of plasmodium falciparum for immunochemical, molecular, and mosquito infectivity studies. *Methods Mol Biol* 21:67–88. <https://doi.org/10.1385/0-89603-239-6:67>
- Chang Z et al (2016) The TatD-like DNase of plasmodium is a virulence factor and a potential malaria vaccine candidate. *Nat Commun* 7:11537. <https://doi.org/10.1038/ncomms11537>
- Chaubey S, Grover M, Tatu U (2014) Endoplasmic reticulum stress triggers gametocytogenesis in the malaria parasite. *J Biol Chem* 289:16662–16674. <https://doi.org/10.1074/jbc.M114.551549>
- Cheng Y et al (2016) Plasmodium vivax GPI-anchored micronemal antigen (PvGAMA) binds human erythrocytes independent of Duffy antigen status. *Sci Rep* 6:35581. <https://doi.org/10.1038/srep35581>
- Coleman BI et al (2014) A plasmodium falciparum histone deacetylase regulates antigenic variation and gametocyte conversion. *Cell Host Microbe* 16:177–186. <https://doi.org/10.1016/j.chom.2014.06.014>
- Cowman AF, Crabb BS (2006) Invasion of red blood cells by malaria parasites. *Cell* 124:755–766. <https://doi.org/10.1016/j.cell.2006.02.006>
- Cowman AF, Tonkin CJ, Tham WH, Duraisingh MT (2017) The molecular basis of erythrocyte invasion by malaria parasites. *Cell Host Microbe* 22:232–245. <https://doi.org/10.1016/j.chom.2017.07.003>
- Crosnier C et al (2011) Basigin is a receptor essential for erythrocyte invasion by plasmodium falciparum. *Nature* 480:534–537. <https://doi.org/10.1038/nature10606>
- Das S et al (2015) Processing of plasmodium falciparum merozoite surface protein MSP1 activates a Spectrin-binding function enabling parasite egress from RBCs. *Cell Host Microbe* 18:433–444. <https://doi.org/10.1016/j.chom.2015.09.007>
- Duraisingh MT et al (2003) Phenotypic variation of plasmodium falciparum merozoite proteins directs receptor targeting for invasion of human erythrocytes. *EMBO J* 22:1047–1057. <https://doi.org/10.1093/emboj/cdg096>
- Eksi S et al (2012) Plasmodium falciparum gametocyte development 1 (Pfgdv1) and gametocytogenesis early gene identification and commitment to sexual development. *PLoS Pathog* 8:e1002964. <https://doi.org/10.1371/journal.ppat.1002964>
- Filarsky M et al (2018) GDV1 induces sexual commitment of malaria parasites by antagonizing HP1-dependent gene silencing. *Science* 359:1259–1263. <https://doi.org/10.1126/science.aan6042>
- Fivelman QL et al (2007) Improved synchronous production of plasmodium falciparum gametocytes in vitro. *Mol Biochem Parasitol* 154:119–123. <https://doi.org/10.1016/j.molbiopara.2007.04.008>

- Flammersfeld A et al (2020) A patatin-like phospholipase functions during gametocyte induction in the malaria parasite *Plasmodium falciparum*. *Cell Microbiol* 22:e13146. <https://doi.org/10.1111/cmi.13146>
- Gilberger TW et al (2003) A novel erythrocyte binding antigen-175 paralogue from *Plasmodium falciparum* defines a new trypsin-resistant receptor on human erythrocytes. *J Biol Chem* 278: 14480–14486. <https://doi.org/10.1074/jbc.M211446200>
- Guizetti J, Scherf A (2013) Silence, activate, poise and switch! Mechanisms of antigenic variation in *Plasmodium falciparum*. *Cell Microbiol* 15:718–726. <https://doi.org/10.1111/cmi.12115>
- Gulati S et al (2015) Profiling the essential nature of lipid metabolism in asexual blood and gametocyte stages of *Plasmodium falciparum*. *Cell Host Microbe* 18:371–381. <https://doi.org/10.1016/j.chom.2015.08.003>
- Henry NB et al (2019) Biology of *Plasmodium falciparum* gametocyte sex ratio and implications in malaria parasite transmission. *Malar J* 18:70. <https://doi.org/10.1186/s12936-019-2707-0>
- Hinds L, Green JL, Knuepfer E, Grainger M, Holder AA (2009) Novel putative glycosylphosphatidylinositol-anchored micronemal antigen of *Plasmodium falciparum* that binds to erythrocytes. *Eukaryot Cell* 8:1869–1879. <https://doi.org/10.1128/EC.00218-09>
- Jiang L et al (2013) PfSETvs methylation of histone H3K36 represses virulence genes in *Plasmodium falciparum*. *Nature* 499:223–227. <https://doi.org/10.1038/nature12361>
- Jing Q et al (2018) *Plasmodium falciparum* var gene is activated by its antisense long noncoding RNA. *Front Microbiol* 9:3117. <https://doi.org/10.3389/fmicb.2018.03117>
- Josling GA, Williamson KC, Llinas M (2018) Regulation of sexual commitment and gametocytogenesis in malaria parasites. *Annu Rev Microbiol* 72:501–519. <https://doi.org/10.1146/annurev-micro-090817-062712>
- Josling GA et al (2020) Dissecting the role of PfAP2-G in malaria gametocytogenesis. *Nat Commun* 11:1503. <https://doi.org/10.1038/s41467-020-15026-0>
- Kafsack BF et al (2014) A transcriptional switch underlies commitment to sexual development in malaria parasites. *Nature* 507:248–252. <https://doi.org/10.1038/nature12920>
- Kennedy AT et al (2016) Recruitment of factor H as a novel complement evasion strategy for blood-stage *Plasmodium falciparum* infection. *J Immunol* 196:1239–1248. <https://doi.org/10.4049/jimmunol.1501581>
- Kraemer SM, Smith JD (2003) Evidence for the importance of genetic structuring to the structural and functional specialization of the *Plasmodium falciparum* var gene family. *Mol Microbiol* 50: 1527–1538. <https://doi.org/10.1046/j.1365-2958.2003.03814.x>
- Kyes S, Horrocks P, Newbold C (2001) Antigenic variation at the infected red cell surface in malaria. *Annu Rev Microbiol* 55:673–707. <https://doi.org/10.1146/annurev.micro.55.1.673>
- Lavstsen T, Salanti A, Jensen AT, Arnot DE, Theander TG (2003) Sub-grouping of *Plasmodium falciparum* 3D7 var genes based on sequence analysis of coding and non-coding regions. *Malar J* 2:27. <https://doi.org/10.1186/1475-2875-2-27>
- Li Z et al (2019) DNA helicase RecQ1 regulates mutually exclusive expression of virulence genes in *Plasmodium falciparum* via heterochromatin alteration. *Proc Natl Acad Sci U S A* 116:3177–3182. <https://doi.org/10.1073/pnas.1811766116>
- Liu M et al (2022) 5-methylcytosine modification by *Plasmodium* NSUN2 stabilizes mRNA and mediates the development of gametocytes. *Proc Natl Acad Sci U S A* 119. <https://doi.org/10.1073/pnas.2110713119>
- Lopatnicki S et al (2011) Reticulocyte and erythrocyte binding-like proteins function cooperatively in invasion of human erythrocytes by malaria parasites. *Infect Immun* 79:1107–1117. <https://doi.org/10.1128/IAI.01021-10>
- Lu B et al (2021) The architectural factor HMGB1 is involved in genome organization in the Human Malaria Parasite *Plasmodium falciparum*. *mBio* 12. <https://doi.org/10.1128/mBio.00148-21>
- Lu J et al (2022) Glycosylphosphatidylinositol-anchored micronemal antigen (GAMA) interacts with the band 3 receptor to promote erythrocyte invasion by malaria parasites. *J Biol Chem* 298: 101765. <https://doi.org/10.1016/j.jbc.2022.101765>

- Maier AG et al (2003) Plasmodium falciparum erythrocyte invasion through glycophorin C and selection for Gerbich negativity in human populations. *Nat Med* 9:87–92. <https://doi.org/10.1038/nm807>
- Mantel PY et al (2013) Malaria-infected erythrocyte-derived microvesicles mediate cellular communication within the parasite population and with the host immune system. *Cell Host Microbe* 13:521–534. <https://doi.org/10.1016/j.chom.2013.04.009>
- Mayer DC et al (2006) The glycophorin C N-linked glycan is a critical component of the ligand for the plasmodium falciparum erythrocyte receptor BAEBL. *Proc Natl Acad Sci U S A* 103:2358–2362. <https://doi.org/10.1073/pnas.0510648103>
- Mayer DC et al (2009) Glycophorin B is the erythrocyte receptor of plasmodium falciparum erythrocyte-binding ligand, EBL-1. *Proc Natl Acad Sci U S A* 106:5348–5352. <https://doi.org/10.1073/pnas.0900878106>
- Miller LH, Baruch DI, Marsh K, Doumbo OK (2002) The pathogenic basis of malaria. *Nature* 415: 673–679. <https://doi.org/10.1038/415673a>
- Mital J, Meissner M, Soldati D, Ward GE (2005) Conditional expression of toxoplasma gondii apical membrane antigen-1 (TgAMA1) demonstrates that TgAMA1 plays a critical role in host cell invasion. *Mol Biol Cell* 16:4341–4349. <https://doi.org/10.1091/mbc.e05-04-0281>
- Mitchell GH, Thomas AW, Margos G, Dluzewski AR, Bannister LH (2004) Apical membrane antigen 1, a major malaria vaccine candidate, mediates the close attachment of invasive merozoites to host red blood cells. *Infect Immun* 72:154–158. <https://doi.org/10.1128/IAI.72.1.154-158.2004>
- Pieper K et al (2017) Public antibodies to malaria antigens generated by two LAIR1 insertion modalities. *Nature* 548:597–601. <https://doi.org/10.1038/nature23670>
- Poran A et al (2017) Single-cell RNA sequencing reveals a signature of sexual commitment in malaria parasites. *Nature* 551:95–99. <https://doi.org/10.1038/nature24280>
- Regev-Rudzki N et al (2013) Cell-cell communication between malaria-infected red blood cells via exosome-like vesicles. *Cell* 153:1120–1133. <https://doi.org/10.1016/j.cell.2013.04.029>
- Saito F et al (2017) Immune evasion of plasmodium falciparum by RIFIN via inhibitory receptors. *Nature* 552:101–105. <https://doi.org/10.1038/nature24994>
- Shang X et al (2021) A cascade of transcriptional repression determines sexual commitment and development in plasmodium falciparum. *Nucleic Acids Res* 49:9264–9279. <https://doi.org/10.1093/nar/gkab683>
- Sidik SM et al (2016) A genome-wide CRISPR screen in toxoplasma identifies essential apicomplexan genes. *Cell* 166:1423–1435 e1412. <https://doi.org/10.1016/j.cell.2016.08.019>
- Sinha A et al (2014) A cascade of DNA-binding proteins for sexual commitment and development in plasmodium. *Nature* 507:253–257. <https://doi.org/10.1038/nature12970>
- Tan J et al (2016) A LAIR1 insertion generates broadly reactive antibodies against malaria variant antigens. *Nature* 529:105–109. <https://doi.org/10.1038/nature16450>
- Tehlivets O, Malanovic N, Visram M, Pavkov-Keller T, Keller W (1832) S-adenosyl-L-homocysteine hydrolase and methylation disorders: yeast as a model system. *Biochim Biophys Acta* 204-215:2013. <https://doi.org/10.1016/j.bbadis.2012.09.007>
- Tham WH et al (2010) Complement receptor 1 is the host erythrocyte receptor for plasmodium falciparum Pfrh4 invasion ligand. *Proc Natl Acad Sci U S A* 107:17327–17332. <https://doi.org/10.1073/pnas.1008151107>
- Triglia T, Duraisingh MT, Good RT, Cowman AF (2005) Reticulocyte-binding protein homologue 1 is required for sialic acid-dependent invasion into human erythrocytes by plasmodium falciparum. *Mol Microbiol* 55:162–174. <https://doi.org/10.1111/j.1365-2958.2004.04388.x>
- Usui M et al (2019) Plasmodium falciparum sexual differentiation in malaria patients is associated with host factors and GDV1-dependent genes. *Nat Commun* 10:2140. <https://doi.org/10.1038/s41467-019-10172-6>
- Volz JC et al (2016) Essential role of the Pfrh5/Pfripr/CyRPA complex during plasmodium falciparum invasion of erythrocytes. *Cell Host Microbe* 20:60–71. <https://doi.org/10.1016/j.chom.2016.06.004>

- Weiss GE et al (2015) Revealing the sequence and resulting cellular morphology of receptor-ligand interactions during plasmodium falciparum invasion of erythrocytes. *PLoS Pathog* 11: e1004670. <https://doi.org/10.1371/journal.ppat.1004670>
- Williams JL (1999) Stimulation of plasmodium falciparum gametocytogenesis by conditioned medium from parasite cultures. *The American journal of tropical medicine and hygiene* 60:7–13. <https://doi.org/10.4269/ajtmh.1999.60.7>
- Xiao B et al (2019) Epigenetic editing by CRISPR/dCas9 in plasmodium falciparum. *Proc Natl Acad Sci U S A* 116:255–260. <https://doi.org/10.1073/pnas.1813542116>
- Xie Y et al (2021) Structural basis of malarial parasite RIFIN-mediated immune escape against LAIR1. *Cell Rep* 36:109600. <https://doi.org/10.1016/j.celrep.2021.109600>
- Zhang Q et al (2014) Exonuclease-mediated degradation of nascent RNA silences genes linked to severe malaria. *Nature* 513:431–435. <https://doi.org/10.1038/nature13468>



Artificial Intelligence and Deep Learning in Malaria Diagnosis

9

Min Fu and Zuodong Li

Abstract

Microscopic examination is the gold standard for malaria diagnosis. However, microscopic diagnosis of malaria relies heavily on pathologists or technicians with specialized knowledge and expertise, and manual microscopic screening is an unreliable method in nonexpert situations. In addition, diagnosing malaria requires considerable time and effort, overwhelming experts when too many cases need to be tested, and for the same test, different results can occur due to different testers. The same test can yield different results for different testers. Therefore, automated image analysis systems can break the dependence of accurate *Plasmodium* detection on specialized technicians, improve the accuracy and efficiency of detection and reduce the cost of *Plasmodium* detection. Traditional methods use image-based algorithms for extracting features (e.g., color, shape, texture, and gradient changes) for image detection, image segmentation, feature extraction, and classification. However, the accuracy rate of traditional methods is 80–90%, which cannot meet clinical requirements. With the re-emergence of artificial neural networks, deep learning algorithms based on convolutional neural networks and other deep learning algorithms driven by massive data have gained tremendous development in the direction of computer vision, such as image classification, target localization, target detection, and image segmentation, which has led to an increasing interest in the applicability of deep learning methods based on convolutional neural networks in medical image analysis. After applying the deep learning algorithm, compared with the traditional algorithm, the accuracy can be increased by 10–20%, which has

M. Fu (✉)

School of Aerospace Engineering, Xiamen University, Xiamen, Fujian, China

Z. Li

Wuhan Foreland Intelligent Technology Co., Ltd., Xiamen, Fujian, China

reached the level of human doctors. It has become a reality that the detection of malaria parasites can be replaced by machines in the clinic.

Keywords

Microscopic diagnosis · Malaria diagnosis · Traditional methods · Deep learning · Feature extraction · Artificial intelligence

9.1 The Inevitability of Computer-Aided Diagnosis

Since the latter part of the last century, various attempts and studies have been made on the self-detection and classification of malaria, and remarkable results have been achieved. In the twenty-first century, information technology is becoming increasingly developed, and machine vision, machine learning, and image processing technologies are increasingly widely used in scientific research. These technologies are also widely used in disease detection, and the traditional methods of malaria detection have also changed. The use of computer vision for malaria diagnosis is considered to be a method to simplify the diagnostic process by increasing diagnostic accuracy, saving diagnostic time, reducing the required manpower, and minimizing human error (Tek et al. 2009; Díaz et al. 2009; Mandal et al. 2010; Kumarasamy et al. 2011; Jan et al. 2018).

Microscopic examination is the gold standard for malaria diagnosis, with thin blood smears identifying the species; thick blood smears, which are slide samples with large amounts of blood, are most useful for characterization. Thick blood films are primarily used to detect the presence of malaria parasite infection and to assess malaria parasitemia but not to detect which species the infection belongs to. In contrast, thin blood smears are 1–2 microliters of blood spread over most of the slide, dried and fixed in methanol, and when fixing thin blood smears, care should be taken to avoid exposing thick smears to methanol. Thin blood smears help physicians detect which *Plasmodium* species are causing the infection. Table 9.1 discusses the

Table 9.1 Variation in blood smears

Thick smears	Thin smears
Suitable for detecting the presence of malaria parasites	Beneficial for <i>plasmodium</i> species
The sample requirement is blood for no less than 4–5 microliters	No more than 1–2 microliters of blood spread over a larger area of the slide
RBCs must be ruptured but WBCs, platelets, and malaria parasites must be visible before or during the staining	Observation of <i>plasmodium</i> in RBCs and analysis of the differences between infected and normal RBCs
Improving the detection efficiency of malaria parasites	Low detection efficiency and easy to miss at low density
No methanol fixation required	Requires methanol fixation prior to staining
For confirming the diagnosis	Able to identify <i>plasmodium</i> species

differences between thick and thin blood smears in the evaluation of malaria parasite detection. The advantages of microscopic examination are the ability to differentiate between malaria parasite species, quantify parasitemia, observe the different stages of parasite characteristics, and have a low material cost. However, microscopic diagnosis of malaria relies heavily on pathologists or technicians with specialized knowledge and expertise, and manual microscopic screening is an unreliable method in nonexpert situations. In addition, diagnosing malaria requires considerable time and effort, overwhelming experts when too many cases need to be tested, and for the same test, different results can occur due to different testers. The same test can yield different results for different testers. Therefore, automated image analysis systems can break the dependence of accurate *Plasmodium* detection on specialized technicians, improve the accuracy and efficiency of detection and reduce the cost of *Plasmodium* detection. Computers are playing an increasingly important role in the medical field, and without computer technology, medical proficiency and productivity would be significantly reduced. Computers already play an important role in various medical diagnostic applications, such as digital X-ray, magnetic resonance imaging (MRI), computed tomography (CT), and ultrasound. Computer-aided diagnosis of malaria is a microscopic diagnostic technique through the use of computer vision and machine learning algorithms. It can replace manual microscopic detection for semiautomatic or fully automatic detection of *Plasmodium*. With the development of picture technology and vision technology, malaria detection has gradually evolved from purely manual to semiautomated or even fully automated. Screening for malaria parasites by light microscopy is still considered the main method of malaria detection in health testing laboratories and hospitals worldwide, and incorrect diagnostic cutoffs will lead to patients infected with malaria not receiving timely and effective treatment, resulting in serious consequences. In recent years, malaria self-testing systems have been shown to be systematic, and the steps are more uniform. The main steps to acquire images are image preprocessing, image segmentation, feature extraction, and detection and classification.

9.2 Introduction of Traditional Methods to Assist in the Intelligent Diagnosis of Malaria

Traditional methods use image-based algorithms for extracting features (e.g., color, shape, texture, and gradient changes) for image detection, image segmentation, feature extraction, and classification. Makkapati and Rao (2009) proposed a method to segment red blood cells and stained masses from Leishmania-stained blood smears by detecting the primary color range and calculating the optimal saturation threshold to segment erythrocytes and parasites. The method is performed in HSV space, where the background in the image is first determined by detecting the primary color range and the remaining pixels are the erythrocytes and chromatin dots to be segmented. Then, a method is proposed to determine the optimal saturation threshold to segment the erythrocytes and chromatin dots. This work illustrates the potential of color image processing techniques in providing diagnostic solutions

for severe infectious diseases. Ross et al. (2006) proposed an automated image processing and classification technique to detect red blood cells infected with malaria parasites and to differentiate the species of infected *Plasmodium*. The authors used morphological techniques combined with a new threshold selection technique with local and global thresholds to segment potentially infected red blood cells from thin blood smears and then designed tree classifiers with two nodes based on thin blood smear image features such as texture, color, and geometry of the image, using feedback feedforward neural networks to identify whether a red blood cell is infected and, if infected, to determine the malaria species, eliminating the reliance on technician skills and experience. Panchbhai et al. (2012) proposed a model based on RGB color space to achieve segmentation of erythrocytes and parasites by first dividing the thin blood smear RGB image into three different layers, R, G, and B. Then, the G layer was further processed, and the Otsu algorithm was used to determine the optimal threshold value to segment all infected erythrocytes, reducing the detection time and the chance of human error in malaria. May and Aziz (2013) proposed a method for the automatic quantification and classification of *P. falciparum*-infected erythrocytes. This method uses the Otsu method to find local thresholds to segment out infected erythrocytes. Since each parasite infects one erythrocyte, the thin blood smear images are classified according to the number of infected cells detected. This method finally obtained a good classification result, but the limitation of this study is that it only targets *Plasmodium interrogans* in the trophozoite stage, so the results are relatively poor for other parasite species. Somasekar and Reddy (2015) proposed an edge-based segmentation method to segment erythrocytes infected with *Plasmodium*. First, the brightness difference of the image was corrected by reducing the effect of image color through color space transformation and γ homogenization, and then the infected erythrocytes were extracted using the fuzzy C-mean clustering method, and the infected erythrocytes were segmented using the minimum perimeter polygon algorithm. This work provides a consistent and robust method for edge segmentation of infected erythrocytes in microscopic images. In 2017, Somasekar and Reddy (2017) also proposed a two-stage threshold segmentation method for segmenting malaria-infected cells in microscopy images. The method performs segmentation in two stages, where the first stage maximizes the interclass variance of the original image and then iterative threshold selection is performed on the thresholded image of the first stage to segment malaria parasites according to suitable stopping conditions. This work was able to successfully detect *Plasmodium* without prior knowledge of the image content, without parameter adjustment, and to extract malaria-infected cells in both thick blood smears and thin blood smears.

9.3 Introduction of Deep Learning in the Assisted Intelligent Diagnosis of Malaria

With the re-emergence of artificial neural networks, deep learning algorithms based on convolutional neural networks and other deep learning algorithms driven by massive data have gained tremendous development in the direction of computer

vision, such as image classification, target localization, target detection, and image segmentation (Krizhevsky et al. 2012; He et al. 2016), which has led to an increasing interest in the applicability of deep learning methods based on convolutional neural networks in medical image analysis. Meanwhile, an increasing number of deep learning models have been applied to malaria diagnosis for automatic classification, detection, and segmentation tasks of cells in malaria microscopy images.

The essence of deep learning is to build deep networks with multiple hidden layers based on large-scale sample data sets and powerful computing power and train the networks through multiple iterations to learn the effective features in the data to obtain higher prediction or classification accuracy. Compared with traditional machine learning, the most important feature of deep learning is its network structure with multiple hidden layers, which can automatically learn the features in the data without human involvement.

Deep learning is the latest trend in machine learning, and it has already achieved outstanding performance in many nonmedical fields. In addition to using more network layers, deep learning is seen as an extension of the well-known multilayer neural network classifier trained using backpropagation, using different kinds of layers in a typical succession. Deep learning usually requires a large training set, which is one of the reasons why the medical field has been slower to introduce deep learning methods, as is by the difficulty in harvesting annotated training images in terms of expert knowledge requirements and considering privacy issues.

Hung and Carpenter (2017) applied for the first time a target detection model previously used for natural images on blood smear images of *Plasmodium* infection to identify *Plasmodium* cells and recognize the growth stage they are in based on Faster R-CNN for malaria detection, which avoids the segmentation task and does not rely on general features for classification. Rajaraman et al. (2018) evaluated the use of convolutional neural network-based pretrained models to extract image features for the classification of infected and uninfected cells. The paper evaluated the performance of pretrained convolutional neural networks, including AlexNet, VGG16, ResNet-50, and DenseNet-121, in extracting features of infected and uninfected cells and experimentally determined the optimal layer for feature extraction for each model to help improve the classification. The results showed that the pretrained convolutional neural network exhibited good performance for extracting image features. Subsequently, Rajaraman et al. (2019) built on the literature to detect infected cells in blood smears by constructing an integration of multiple deep learning models. The performance of custom and pretrained convolutional neural networks was first evaluated, and an optimal integration model was constructed for the challenge of classifying infected and normal cells in thin blood smear images. The integration by VGG-19 and SqueezeNet outperformed the classification performance of a single model.

9.3.1 Introduction of Neural Network

Artificial neural networks (ANNs), abbreviated as neural networks, are mathematical models based on the principle of biological neural networks, which use the network topology principle to simulate the response mechanism of the human brain nervous system to various information by analyzing and studying the structure of the human brain and the feedback mechanism of external stimuli. ANNs have successfully solved many real-world problems in many fields, such as video detection, smart driving, and smart medical care, and have shown good performance. In ANN, a neuron is the smallest unit of operation, which receives input parameters from other neurons and outputs the final result after computation. Figure 9.1 shows an example diagram of the neuron structure.

x_1, x_2, \dots, x_n are the inputs of this neuron, w_1, w_2, \dots, w_n are the weights and b is the bias. The output of this neuron can be expressed by the mathematical formula as:

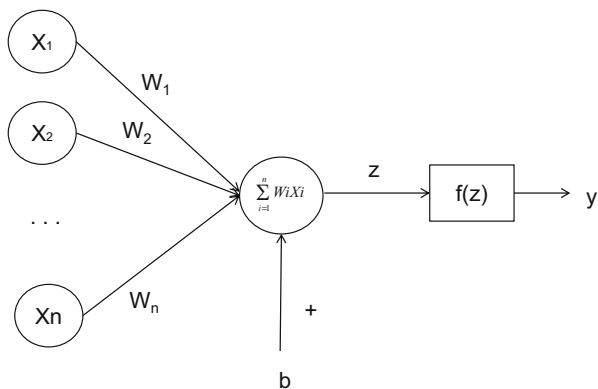
$$y = f\left(\sum_{i=1}^n x_i w_i + b\right) \quad (9.1)$$

where $f(x)$ denotes the activation function.

A neural network consists of multiple neurons and neural layers, and Fig. 9.2 shows a basic neural network structure.

For each neuron in the n th layer of the ANN, its input is the output of the neuron in the n th-first layer, and the output of that neuron will continue to be the input of the neuron in the n th + first layer. In an ANN containing multiple intermediate hidden layers, the output of the n th layer neuron and the input of the n th + first layer neuron are interconnected by an activation function. Since many real-world problems are very complex nonlinear problems and the activation function can introduce nonlinear properties to form a nonlinear mapping between the input and output of neurons as a way to increase the nonlinearity of the network, enhance the expressiveness of

Fig. 9.1 Neuron structure diagram



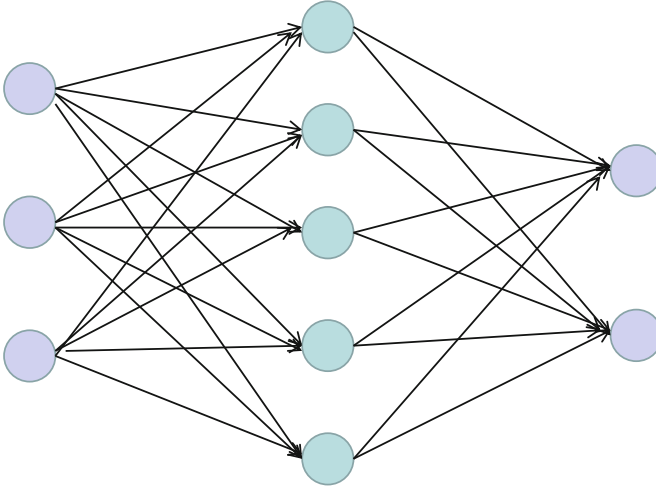


Fig. 9.2 Structure diagram of the Neural Network

the network, and make the network more powerful, the selection of the correct and suitable activation function is crucial to build the ANN model.

The following describes the characteristics and mathematical formulas of several more commonly used activation functions.

9.3.1.1 Activation Function

Sigmoid Function

Sigmoid is the most common nonlinear activation function, and its main role is to map arbitrary real numbers between (0,1), which is usually used for binary classification tasks. Its mathematical formula is:

$$\sigma(x) = \frac{1}{1 + e^x} \quad (9.2)$$

Tanh Function

Tanh is similar to the function curve of a sigmoid. When the input of both functions is small or large, their outputs are close to smooth when the gradient is infinitely close to 0, which will not be conducive to the update of parameters, resulting in the training of the network not proceeding. The output interval of Tanh is (-1,1), and its mathematical formula is expressed as:

$$\tanh(x) = \frac{e^x - e^{-x}}{e^x + e^{-x}} \quad (9.3)$$

ReLU Function

Commonly used in the output of the hidden layer of the network, this function avoids the problem of gradient disappearance that occurs in the sigmoid function and the tanh function, but as the network continues to be trained iteratively, there may be neuron death, which results in parameters that cannot be updated. Its mathematical formula is:

$$f(x) = \max(0, x) \quad (9.4)$$

LeakyReLU Function

From Eqs. (9.4), it can be seen that when the input of the ReLU function is negative, its function values are all zero, which may lead to neuron death. In the LeakyReLU function, when the input is negative, it sets a nonzero slope to the input so that its function value is no longer 0 as a way to correct the data distribution and avoid the problem of neuron death caused by the ReLU function, whose mathematical formula is:

$$f(x) = \begin{cases} x, & x \geq 0 \\ \alpha x, & x < 0 \end{cases} \quad (9.5)$$

where α is a very small constant, taken between 0 and 1.

9.3.1.2 Backpropagation Algorithm

Currently, the most commonly used and effective network training method in neural networks is the backpropagation algorithm. 10 (Back propagation Algorithm, BP algorithm), whose core technique is the chain derivation rule. The BP algorithm consists of two processes, namely, forward propagation of data and backpropagation of errors.

1. Forward propagation: Mainly used for the transmission of data feature information, the data are first input to the neural network from the input layer and then transmitted toward the output layer by layer. In the neural network, forward propagation can be expressed by the following equation:

$$x^l = f(u^l) \quad (9.6)$$

$$u^l = w^l x^{l-1} + b^l \quad (9.7)$$

where l is the current layer, x^l is the output of layer l , b^l and w^l denote the bias and weight of the l th layer, respectively, and $f(x)$ is the activation function. Then, the forward propagation of the j th neuron in the l th layer can be expressed as:

$$z_j^l = \sum_i a_i^{l-1} * w_{jk}^l + b_j^l \tag{9.8}$$

$$a_j^l = f\left(\sum_i a_i^{l-1} * w_{jk}^l + b_j^l\right) \tag{9.9}$$

where z_j^l and a_j^l denote the input and output of the j th neuron in the l th layer, respectively, w_{jk}^l denotes the weight of the k th neuron in the $(l-1)$ layer connected to the j th neuron in the l th layer, and b_j^l denotes the bias of the j th neuron in the l th layer.

2. Backpropagation: Since there is a certain error between the desired result and the actual result, backpropagation passes the error back from the output layer of the network toward the input layer in the opposite direction while updating the values of the parameters in the neural network according to the error value to minimize the error, and backpropagation reflects the correction and fine-tuning of the model based on the error information.

Suppose that the neural network loss function is defined in the form of a squared error function:

$$J(w, b, x, y) = \frac{1}{2} \|h_{w, b}(x) - y\|^2 \tag{9.10}$$

where x is the input to the network, y is the corresponding desired output result of input x , $h_{w, b}(x)$ is the actual output result of the neural network, and the weights W and bias b are the parameters of the neural network. For a training set containing m data, the overall loss function is defined as:

$$J(W, b) = \frac{1}{m} \sum_{i=1}^m J(w, b, x^i, y^i) = \frac{1}{m} \sum_{i=1}^m \left(\frac{1}{2} \|h_{w, b}(x^i) - y^i\|^2\right) \tag{9.11}$$

The final training objective of a neural network is to minimize the error between the desired and actual output results of the network by continuously updating the optimization parameter vector W, b , i.e., minimizing the loss function $J(W, b)$ of the network. Usually, the gradient descent algorithm is used to update W and b with the following update formula:

$$W_{ij}^l = W_{ij}^l - \alpha \frac{\partial}{\partial W_{ij}^l} J(W, b) \tag{9.12}$$

$$b_i^l = b_i^l - \alpha \frac{\partial}{\partial b_i^l} J(W, b) \tag{9.13}$$

where α is the learning rate and $\frac{\partial}{\partial W_{ij}^l} J(W, b)$ and $\frac{\partial}{\partial b_i^l} J(W, b)$ denote the loss function to the parameters to W and b bias derivatives, respectively. The steps of the

backpropagation algorithm are as follows: first, the error value of the j th neuron in the l th layer is calculated according to Eqs. (9.9), (9.10), and (9.12) as follows:

$$\begin{aligned}\delta_j^l &= \frac{\partial J}{\partial z_j^l} = \sum_k \frac{\partial J}{\partial z_k^{l+1}} \cdot \frac{\partial z_k^{l+1}}{\partial a_j^l} \cdot \frac{\partial a_j^l}{\partial z_j^l} \\ &= \sum_k \delta z_k^{l+1} \cdot \frac{\partial (w_{jk}^{l+1} a_j^l + b_j^{l+1})}{\partial a_j^l} \cdot f' \left(z_j^l \right) \\ &= \sum_k \delta z_k^{l+1} \cdot w_{jk}^{l+1} \cdot f \left(z_j^l \right)\end{aligned}\quad (9.14)$$

The partial derivatives of the weights are then calculated as follows:

$$\frac{\partial J}{\partial w_{jk}^l} = \frac{\partial J}{\partial z_j^l} \cdot \frac{\partial z_j^l}{\partial w_{jk}^l} = \delta_j^l \cdot \frac{\partial (w_{jk}^l a_k^{l-1} + b_j^l)}{\partial w_{jk}^l} = a_k^{l-1} \delta_j^l \quad (9.15)$$

Next, the partial derivatives of the bias are calculated as follows:

$$\frac{\partial J}{\partial b_j^l} = \frac{\partial J}{\partial z_j^l} \cdot \frac{\partial z_j^l}{\partial b_j^l} = \delta_j^l \cdot \frac{\partial (w_{jk}^l a_k^{l-1} + b_j^l)}{\partial b_j^l} = \delta_j^l \quad (9.16)$$

Finally, the parameter vectors W and b are updated according to Eqs. (9.13) and (9.14).

9.3.1.3 Neural Network Model Optimization Algorithm

The goal of neural network learning is to find suitable parameter values that make the value of the loss function as small as possible, and optimization algorithms are a class of algorithms that address this problem. The gradient descent algorithm is the most basic and common optimization algorithm. The gradient descent algorithm continuously updates the parameters in the neural network according to certain rules until the value of the loss function no longer changes significantly, i.e., it converges to a minimum value to achieve the training purpose of the neural network. In a function, the direction of the fastest decrease in the value of the function is the negative gradient direction of the function, so the gradient descent algorithm gradually iteratively updates the parameters along the negative gradient direction, which allows the value of the loss function to converge to the minimum value at the fastest speed. Equations (9.13) and (9.14) are the iterative formulas of the gradient descent algorithm. The condition of using the gradient descent algorithm to obtain the global optimal solution is limited to the loss function being a convex function, but in practical applications, the loss function is relatively complex and not always convex, so there will be saddle points and local minima. In addition, the computation time of the gradient descent method is relatively long; in the actual training data, it is usually a lot, and the loss function is the sum of the losses on all the training set data. In

addition, the whole training process is quite time consuming. In view of the above problems, the following will introduce several improved optimization algorithms based on gradient descent, which can make the network converge more stably and faster than the gradient descent method and have better optimization effects in applications.

1. Stochastic gradient descent algorithm

Stochastic Gradient Descent (SGD) can speed up the update of parameters in each round. The improvement over the gradient descent algorithm is that the algorithm randomly selects the loss function on training data for parameter optimization in each iteration round instead of directly optimizing the loss function on all 12 training data. For large linear models that need to be trained on large-scale data, SGD is a necessary optimization algorithm, but SGD also has the shortcoming that a small value of the loss function on a certain training data does not mean a small value of the loss function on all training data, which means that SGD only considers the gradient of a single data, which can easily lead to a locally optimal result for the network. To balance the performance of both the above gradient descent algorithm and the stochastic gradient descent algorithm, in practice, each iteration usually selects a small portion of the loss function on the training data for optimization, and this small portion of the training data is treated as a batch, so the method is also known as the small batch gradient descent algorithm.

2. Gradient descent algorithm with Momentum. The principle of the gradient descent algorithm with Momentum is to calculate the exponentially weighted average of the gradients and then use this value to update the parameter optimization network, and the parameter update formula is as follows:

$$v_t = \beta v_{t-1} + (1 - \beta) g_t \quad (9.17)$$

$$w_t = w_{t-1} - \alpha v_t \quad (9.18)$$

where α and β are two hyperparameters, α denotes the learning rate, which controls the exponentially weighted average, and β denotes the effect of the previous gradient on the present, the larger β means the greater the effect of the previous gradient on the present. g_t denotes the original gradient of a parameter in a certain iteration, v_t is the gradient calculated by the exponentially weighted average, and the initial value of v_t is 0. The above formula can be interpreted as speeding up the update rate when the gradient direction is constant, which reduces the oscillation and speeds up the convergence of the network.

3. Adaptive learning rate algorithm

If the learning rate is set too small, the convergence speed will be very slow for parameters with large gradients; if the learning rate is set too large, the parameters that will be optimized may be unstable. Adagrad is the most classic adaptive learning rate algorithm, which automatically adjusts the learning rate of each parameter by calculating the sum of squares of historical gradients, and its adjustment law is such that parameters that are updated more frequently have a smaller learning rate and parameters that are updated rarely have a larger learning rate. The updated formula of the Adagrad algorithm is:

$$V_t = V_{t-1} + g_t^2 \quad (9.19)$$

$$w_t = w_{t-1} - \frac{\alpha}{\sqrt{V_t + \epsilon}} g_t \quad (9.20)$$

where g_t is synonymous with Eq. (9.18), V_t is the cumulative squared gradient sum with an initial value of 0. α is the global learning rate, and ϵ is a tiny quantity used to prevent the denominator from being zero.

One drawback of the Adagrad algorithm is that as V_t gradually increases cumulatively, the learning rate decreases, eventually leading to the cessation of updates. Therefore, an improved RMSprop algorithm is proposed. The RMSprop algorithm introduces a decay factor β that makes V_t decay at each iterative update, similar to the approach in Momentum. Its updated equation is as follows:

$$V_t = \beta V_{t-1} + (1 - \beta) g_t^2 \quad (9.21)$$

$$w_t = w_{t-1} - \frac{\alpha}{\sqrt{V_t + \epsilon}} g_t \quad (9.22)$$

Adam's algorithm combines the RMSprop and Momentum algorithms, considering both the sum of squares of historical gradients to achieve adaptive adjustment of the learning rate of each parameter and retaining the average of historical gradients as momentum, so that the update of each parameter is more independent during the training process of the network, which speeds up the training speed of the network and improves the stability of the network training at the same time. Its update equation is as follows:

$$v_t = \beta_1 v_{t-1} + (1 - \beta_1) g_t \quad (9.23)$$

$$V_t = \beta_2 V_{t-1} + (1 - \beta_2) g_t^2 \quad (9.24)$$

$$w_t = w_{t-1} - \frac{\alpha}{\sqrt{V_t + \epsilon}} v_t w_t = w_{t-1} - \frac{\alpha}{\sqrt{V_t + \epsilon}} v_t$$

$$w_t = w_{t-1} - \frac{\alpha}{\sqrt{V_t + \epsilon}} v_t \quad (9.25)$$

9.3.1.4 Convolutional Neural Networks

Convolutional neural networks (CNNs) are one of the most classical and commonly used neural networks, and they have made many breakthroughs in image analysis and processing. Since convolutional neural networks were proposed, many models based on convolutional neural networks have also been successively proposed for solving image-related problems, such as image denoising, action recognition, and target detection, and all of these models have shown good performance. Compared with previous image processing algorithms, the main advantage of CNN is that it reduces the complicated preprocessing steps, especially the image preprocessing that requires human involvement, and CNN can directly input the image to be processed into the network for subsequent work, which has been widely used in various fields of image-related applications. In 1959, Hubel and Wiesel, in their study of how the cat brain processes visual information, discovered a complex structure of cells that responded to localized areas of visual information, thus introducing the “receptive field.” Inspired by this research and based on it, Fukushima proposed the neurocognitive machine, which is called the predecessor of CNN, which uses an alternating structure of local feature extraction and feature exchange layers to maintain the ability to recognize targets even when they are deformed or displaced. Although the neurocognitive machine model did not use error backpropagation for supervised learning, it is still considered the first discovery of convolutional neural networks. Later, based on the neurocognitive machine, YannLeCun et al. proposed the convolutional neural network model, the famous LeNet-5 network, using the error backpropagation method, and numerous CNN models proposed since then have been improved on this basis. 14 Compared with the ordinary ANN, the hidden layer of CNN usually consists of a convolutional layer, an activation layer, a pooling layer, and a fully connected layer. From input to output, the layers of CNN create connections between each other through different neuron nodes and transfer the input data along the network structure layer by layer; successive convolutional and pooling layers are used to extract the features of the input data and compress the features, and the final fully connected layer will classify the data based on the extracted features.

1. Convolutional layer

The convolutional layer is mainly used for extracting image features. Two techniques are applied in the convolutional operation, namely, local perceptual field and weight sharing, which allow the network to better utilize the local features of the image and significantly reduce the number of parameters to be optimized in the network.

2. Local perceptual field: In convolutional neural networks, the neuron nodes in each layer are no longer connected to each other in a fully connected manner, but the neurons in the n th layer are only connected to some neurons in the $n-1$ th layer,

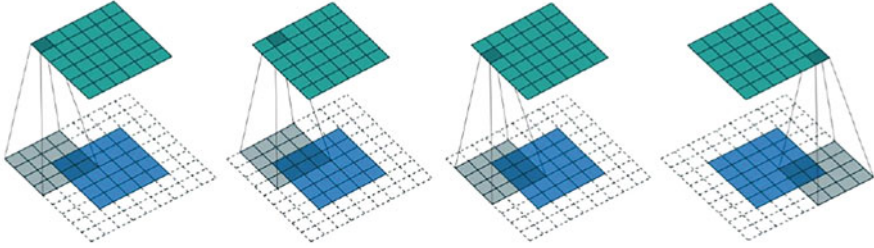


Fig. 9.3 Example of the convolution operation process

i.e., locally connected, thus reducing the number of parameters in the network training. Fig. 2.4 shows an example of the local connection of neurons, in which each neuron in layer $n + 1$ is connected to only 3 neurons in layer n instead of all neurons in layer n . This connection method reduces the number of parameters for network training from $5 \times 5 = 15$ to $3 \times 3 = 9$, which is a 40% reduction in the number of parameters, and the same connection method is used for neurons in layers $n + 2$ and $n + 1$. The use of local connections in CNN greatly reduces the number of parameters, speeds up the learning rate of the network, and reduces the possibility of overfitting to a certain extent.

3. **Weight sharing:** During the convolutional operation, each convolutional kernel is repeatedly applied to the whole perceptual field, i.e., weight sharing, which can also reduce the number of parameters. As shown in Fig. 9.3, there are three different sets of weights 1, 2, and 3. If only local connectivity is applied, the network needs a total of 9 parameters.

4. Convolution operation

The convolution operation is the core operation of the convolution layer. Figure 9.3 shows part of the process of a convolution operation. There are several important parameters in the convolution operation process.

5. Pooling layer.

The pooling layer is usually found between successive convolutional layers and is mainly used to compress the feature map to extract important features of the image on the one hand and reduce the size of the feature map on the other hand, thus simplifying the complexity of computation. The pooling operation can ignore the influence of the target due to rotation, tilt, and other relative position changes, which can reduce the dimensionality of the feature map while improving the accuracy of the feature mapping and, to a certain extent, can also avoid overfitting.

The pooling operation is usually calculated in two ways: maximum value pooling and mean value pooling. Figure 9.4 shows two examples of the pooling operation process. The basic idea of maximum value pooling is to take the maximum value in each subregion of the feature map as the mapping result; only one of the weights of the convolution kernel is 1, and the rest are 0. The position

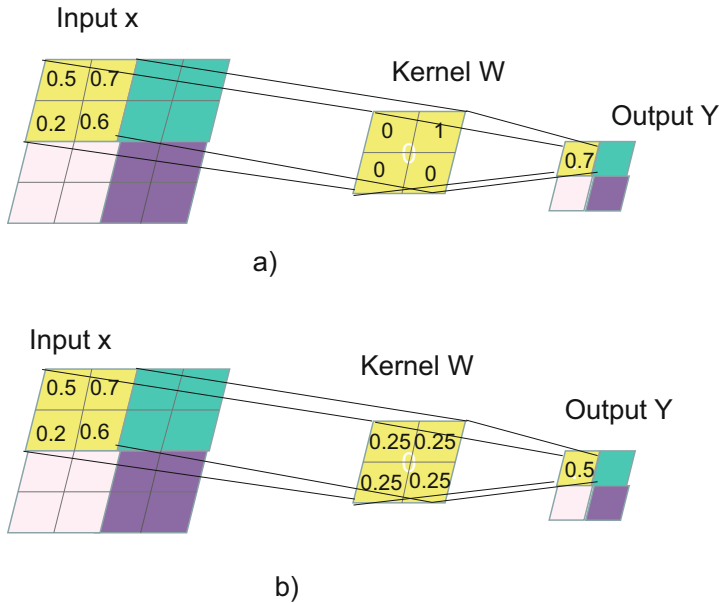


Fig. 9.4 Example of the pooling operation process. (a) Maximum pooling. (b) Mean pooling

with the weight of 1 in the convolution kernel corresponds to the position with the largest value in the overlap region between the input image and the convolution kernel. In the above figure, the size of the convolution kernel is 2×2 , and its moving step on the input image Input X is 2. The result of maximum pooling is to reduce the input image to $1/4$ of the original size and to obtain the maximum value feature in each 2×2 region. Mean pooling takes the average value of the subregions as the mapping result. In Fig. 9.4b, the weights of the convolutional kernels are all 0.25, and the moving step of the convolutional kernels on the input image Input X is 2. Then, the result of the mean pooling is to shrink the input image to $1/4$ of the original size, and at the same time, the input image is blurred.

9.4 Steps of Deep Learning Intelligent-Assisted Malaria Detection Algorithms

Most computer-aided malaria detection techniques include four main image processing stages, as follows:

- (a) Image preprocessing, where image processing is performed for brightness, sharpness, and size of the image.
- (b) Image detection, where the location of red blood cells or the location of the malaria parasite is detected.

- (c) Image segmentation to obtain the size of red blood cells and the size and shape of the abnormal region.
- (d) Image classification to determine whether it is a worm and the type of worm.

9.4.1 Image Preprocessing

The main purpose of the image preprocessing step is to generate images with low noise and high contrast for further processing. Due to the variable stainability of blood smears and camera adjustments, the light brightness of the microscope capturing the image can also change; this particular problem makes it difficult to classify blood cells and find malaria, as it is difficult to accurately segment and classify things with very similar colors for processing. Many researchers have proposed different preprocessing methods, such as illumination, noise reduction, and image enhancement. Different combinations of filters can be used to reduce the light brightness problems from microscope and camera movements; nevertheless, the production of blood slides due to the nonuniform and nonstandard staining concentration and appearance still requires human involvement.

9.4.2 Image Detection

Image detection is the second step in malaria identification and generally involves the detection of two regions:

1. Detection of areas of red blood cells and then determining whether there are worms inside the red blood cells.

Detecting the abnormal region and then judging whether it is a worm.

9.4.2.1 YOLO

YOLO uses a convolutional network to extract the features and then uses fully connected layers to obtain the predicted values. The network structure refers to the GooLeNet model, which contains 24 convolutional layers and 2 fully connected layers, as shown in Fig. 9.5. For the convolutional layers, 1×1 convolution is mainly used to perform channel reduction, and then 3×3 convolution is immediately followed. For the convolutional and fully connected layers, the leaky ReLU activation function is used. However, the last layer uses a linear activation function (Fig. 9.5). The network structure shows that the final output of the network is a tensor of size. This is consistent with the previous discussion. The specific meaning represented by this tensor is shown in Fig. 9.6. For each cell, the first 20 elements are the category probability values, then 2 elements are the bounding box confidence, which can be multiplied to obtain the category confidence, and the last 8 elements are the bounding box. You may wonder why the confidence and the bounding box are arranged separately instead of in this way, but it is purely for the convenience of calculation, because in fact the 30 elements are corresponding to a cell, and their arrangement is arbitrary. However, separating the arrangement makes it easy to

extract each part. Here, to explain, first, the predicted value of the network is a two-dimensional tensor whose shape is. Using slicing, the category probability part is the confidence part, and the last remaining part is the prediction result of the bounding box. In this way, it is very convenient to extract each part, which will facilitate the computation during training and prediction later.

9.4.3 Image Segmentation

Segmentation is an important task in image processing and computer vision research; the other is defined as the process of segmenting a graph into a set of regions that do not overlap. The most important and difficult stage in the automatic classification procedure for analyzing malaria parasites is the accurate segmentation of blood smear images into various elements, such as red blood cells and white blood cells. The purpose of image segmentation is to better segment the different regions and allow us to focus more on the determination of worms. The classical image segmentation algorithms are as follows:

9.4.3.1 FCN (Fully Convolutional Networks)

In general, the last few layers of CNN consist of fully connected layers, and the main function is to transform the feature map output from the convolution layer into a feature vector of specific length and then complete the classification task by the softmax function. In this way, a category prediction can be generated for each pixel in the feature map while preserving the details of the input image, i.e., the feature map can be classified pixel by pixel to complete the segmentation of the image. In short, the fundamental difference between FCN and CNN is that FCN replaces the fully connected layer at the end of CNN with a convolutional layer, and the output of FCN is an image that finely segments the target object, i.e., an image with a target segmentation mask, rather than a probability value. Figure 9.5 shows the comparison

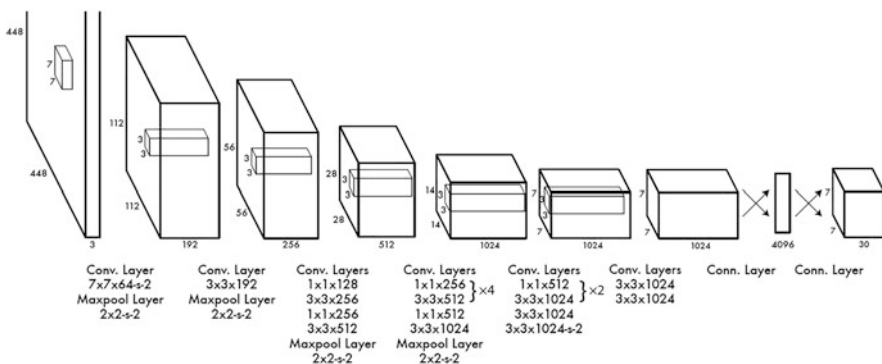


Fig. 9.5 YOLO Network Architecture

of the CNN and FCN network structures. The upper part of the figure is the CNN network structure, and the lower part is the FCN network structure.

The first 5 layers are convolutional layers, and after the convolutional layers, 3 fully connected layers are connected, which is a typical AlexNet network. The output of the 3 fully connected layers is a one-dimensional vector of fixed length, where the length of the last output one-dimensional vector corresponds to the number of categories contained in the data set. The FCN replaces layers 6, 7, and 8 of the CNN with convolutional layers with kernel sizes of (4096,1,1), (4096,1,1), and 21 (1000,1,1), respectively. Successive convolution and pooling of the images generate feature maps with continuously smaller sizes, where the last layer of convolution outputs a feature map called a heatmap. To restore the low-resolution heatmap to the original image size and thus classify each pixel point, a deconvolution operation, or upsampling, is performed on the heatmap. After upsampling, 1000 images of the same size as the original image are obtained. Finally, to perform class prediction for each pixel point, the approach taken in FCN is to find the class with the maximum probability of the location of that pixel point on these 1000 images pixel by pixel and use it as the classification result for that pixel.

Since the feature map is too small, if the original size image is segmented by upsampling the feature map directly, many image details will be lost, making the final segmentation result not fine, so FCN introduces a hopping structure to fuse the prediction with more global information in the last layer and the prediction with more local details in the shallow layer so that both global information and local details can be taken into account when making classification prediction. In this way, both global information and local details can be taken into account in classification prediction to improve segmentation accuracy. Figure 9.6 shows the hopping structure of FCN, in which five successive convolution and pooling operations are performed on the original image to reduce the image to 1/2, 1/4, 1/8, 1/16, and 1/32 of the original image, and then the feature maps of 1/8, 1/16, and 1/32 size of the original image are retained, and finally the fully connected layers in the original CNN are replaced with convolution layers conv6 and conv7. The generated feature map is still 1/32 of the original image, and the feature map is the heatmap. At this time, the network has a 1/32 size heatmap, 1/16 size, and 1/8 size feature map of the original image, and the 1/32 size feature map is directly reduced to the original image size by the deconvolution operation, which will lose some image details, so here we continue to iterate forward, and the 1/16 size and 1/8 size feature maps are also deconvolved in turn to supplement the image details. Finally, the result images of these three deconvolution operations are fused to improve the segmentation accuracy.

FCN is a representative work of deep learning technology applied to image segmentation, which can realize end-to-end image segmentation, although there are some drawbacks of FCN, such as the segmentation results are not fine enough; not sensitive enough to the details in the image; when classifying the image pixel by pixel, the connection between each pixel is not fully considered and lacks spatial consistency. However, since its proposal, FCN has become the basic network

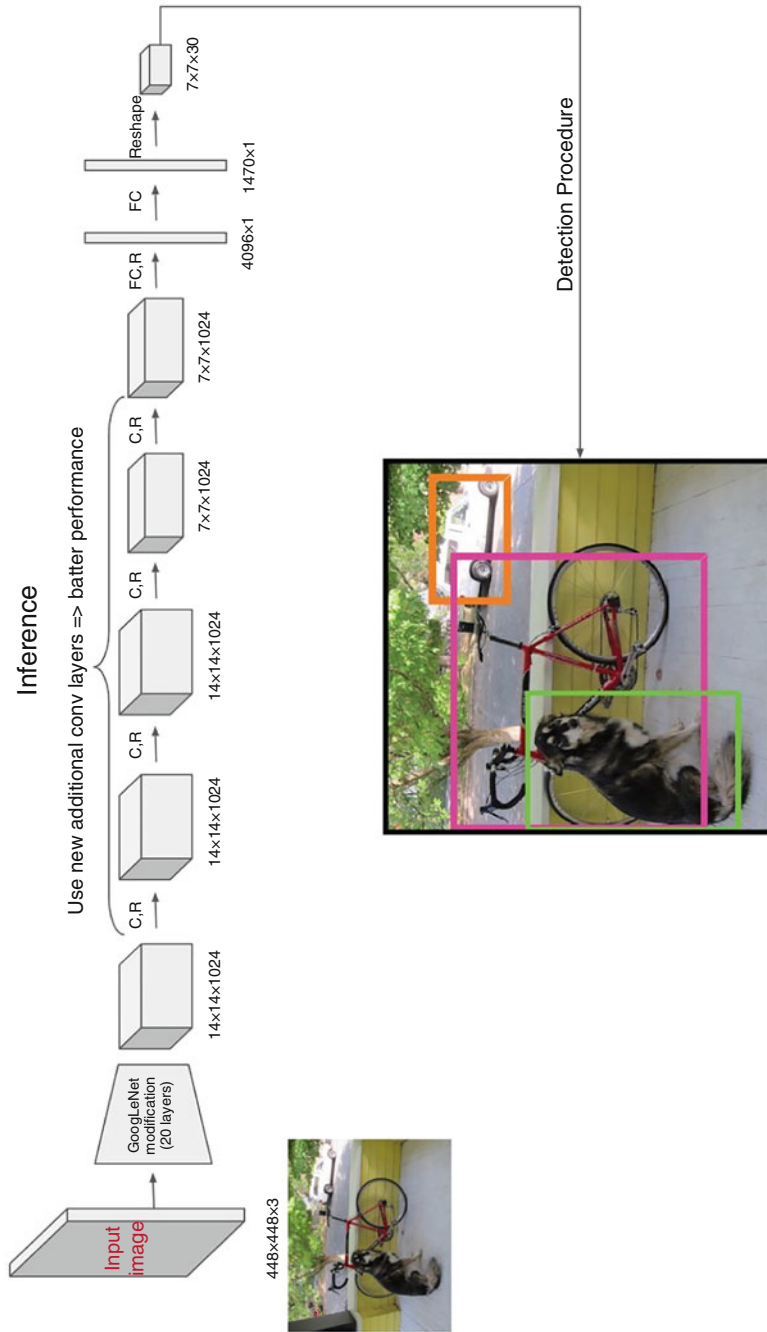


Fig. 9.6 YOLO process

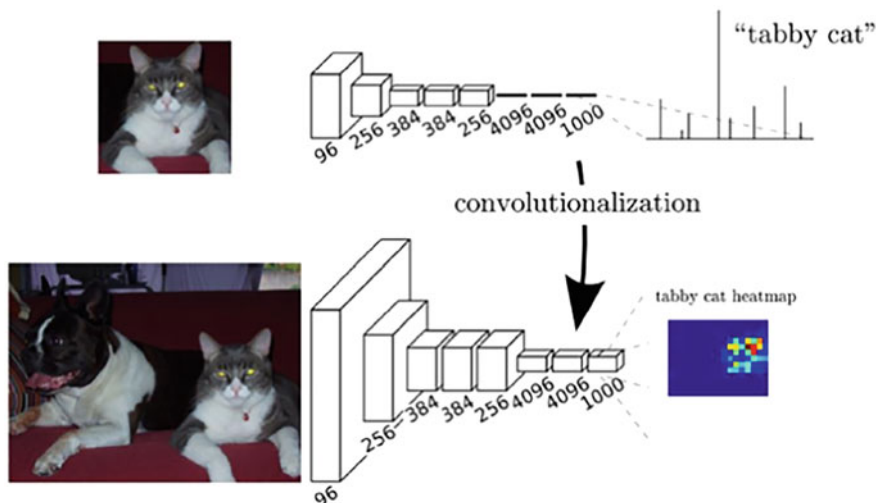


Fig. 9.7 Network structure of the CNN and FCN

framework for semantic segmentation, and many subsequent segmentation algorithms are actually improved on the basis of this framework.

9.4.3.2 U-Net

U-Net was proposed in 2015 and belongs to an improvement of FCN, which can realize end-to-end segmentation. The structure of U-Net is simple but effective and can be regarded as an encoding-decoding structure, where the encoding process gradually reduces the structural information of the image through convolutional and pooling layers while extracting feature information, while the decoding process gradually recovers the structural information of the image through upsampling. The U-Net network structure is shown in Fig. 9.7.

As shown in Fig. 9.7, the network structure of U-Net is symmetrical and shaped like the letter “U”, hence the name U-Net. pooling for feature map compression; green arrows represent upsampling for image size recovery; cyan arrows represent 1×1 convolution, based on RU-Net’s cell segmentation²⁴ for outputting results; gray numbers on the left side of blue and white rectangles indicate image size, and gray numbers on the top indicate the number of channels.

U-Net is a classical fully convolutional network, and the left side of the network (the green rectangular box part in Fig. 9.9) is a CNN architecture consisting of convolutional and pooling layers, i.e., the encoding process, also known as contracting path. Each block consists of two convolutional layers and one pooling layer, where the convolutional layers use a 3×3 convolutional kernel with a ReLU activation function, and the pooling layer uses a maximum pooling of size 2×2 with a step size of 2 for downsampling, increasing the number of feature channels to twice the original number after each downsampling. The right side of the network (the red rectangular box in Fig. 9.7) is the decoding process, also called Expansive path, which

also consists of 4 blocks, each of which first increases the size of the feature map to twice the original size by deconvolution and reduces the number of feature channels to half the original size, and then connects the result of deconvolution with the symmetric feature map in the encoding process to form a new feature map. The result of the deconvolution is then connected with the symmetric feature map in the encoding process to form a new feature map. Since the size of the feature map is slightly larger in the encoding process, it is first cropped and then connected, and then the connected feature map is convolved twice in 3×3 , and the last layer is convolved in 1×1 . The purpose is to convert the feature map of multiple channels into a fixed depth (number of categories, e.g., 2 for binary classification).

The two most important features of the U-Net network are the symmetric “U” structure and hopping connection. The encoding process of U-Net is downsampled 4 times, and symmetrically, its decoding process is also upsampled 4 times to restore the high-level semantic feature map obtained from the encoding process to the resolution of the original image. In addition, U-Net uses jump connections to construct more feature channels in the symmetric phase of encoding and decoding so that the network can fuse the information of the lower-level feature maps with that of the higher-level feature maps through the feature channels to improve the accuracy of image segmentation.

9.4.4 Image Classification

Image classification refers to the classification of unknown images based on the extracted features. In malaria recognition tasks, it is usually the ROI images after image detection and image segmentation, and occasionally the images are classified directly. The classical image classification algorithms are as follows.

Since the breakthrough of the convolutional neural network AlexNet in image classification competition in 2012, some classical convolutional neural network models have been proposed successively and widely used in the field of computer vision in the next 17 years, and several classical convolutional neural network models are introduced below.

9.4.4.1 AlexNet

AlexNet is the first convolutional neural network that has been widely used in the field of computer vision, especially AlexNet, which won the ILSVRC (Image Large Scale Visual Recognition Challenge) in 2012.

In particular, AlexNet won first place in image classification of the ILSVRC (Image Large Scale Visual Recognition Challenge) competition in 2012 and surpassed second place by 10.9%, which has caused a research boom of CNN in the field of computer vision since then.

AlexNet consists of five convolutional layers and three fully connected layers, and the model was initially used to classify images on a data set containing 1000 categories. The AlexNet model architecture is shown in Fig. 9.8.

The AlexNet network has the following features:

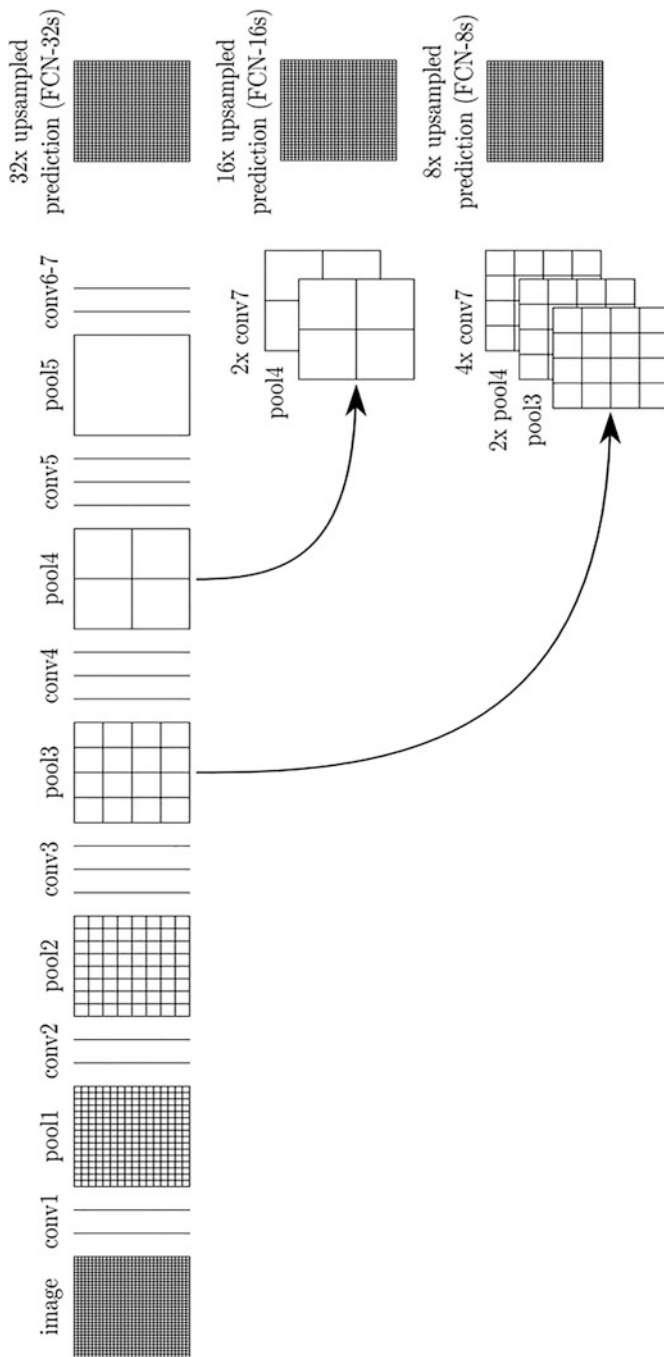


Fig. 9.8 Schematic diagram of the FCN skip structure

1. Successful application of the ReLU function as the activation function avoids the problem of gradient disappearance when the sigmoid function is deeper in the network.
2. proposed LocalResponseNormalization (LRN): increase the weights of neurons that contribute more to the classification, while suppressing other neurons that contribute less to the classification, to further improve the generalization ability of the model.
3. Use dropout in the fully connected layer to randomly discard some neurons to avoid overfitting to some extent.
4. Maximum pooling is used to overcome the blurring results caused by mean pooling. In addition, the step size of pooling is smaller than the size of the pooling kernel, which makes the feature maps that have undergone the pooling operation have overlapping parts with each other, thus increasing the feature richness.

9.4.4.2 VGG-Net

VGG-Net, proposed by the Visual Geometry Group, a research group at the University of Oxford, is the underlying network in the model of the winner of the target localization event and the runner-up of the image classification event in the 2014 ILSVRC competition. VGG-Net focuses on the relationship between the network depth of a convolutional neural network and its performance, and it uses a convolutional layer with repeatedly superimposed 3×3 small convolutional kernels. It uses the method of repeatedly stacking 3×3 convolutional layers with small convolutional kernels and 2×2 maximum pooling layers to construct convolutional neural networks with different numbers of layers from 16 to 19.

The whole VGG-Net can be divided into five parts. Each part is connected with multiple 3×3 convolutional layers in series, each part is followed by a 2×2 maximum pooling, and finally 3 fully connected layers with a softmax layer. There are various structures of VGG-Net; the more common ones are VGG16 and VGG19, among which the VGG16 network is simpler and has good performance. The VGG16 network is simpler, has good performance and is the most widely used. Figure 9.9 shows the network structure of VGG16.

Network structure features:

1. More convolutional layers, deeper network, simpler and more regular structure.
2. The size of the convolutional kernels of VGG-Net is 3×3 . Its main innovation is to use multiple convolutional layers with 3×3 small convolutional kernels instead of one convolutional layer with larger convolutional kernels, which increases the depth of the network and reduces the number of parameters of the network. Because each convolutional layer will be followed by an activation layer, using multiple convolutional layers with small convolutional kernels is equivalent to the network performing more nonlinear mapping, thus improving the nonlinear representation of the network.
3. The LRN layer proposed in AlexNet is discarded. vGG-Net proves that a deeper network can extract features better; VGG-Net also becomes the base network for many subsequent models.

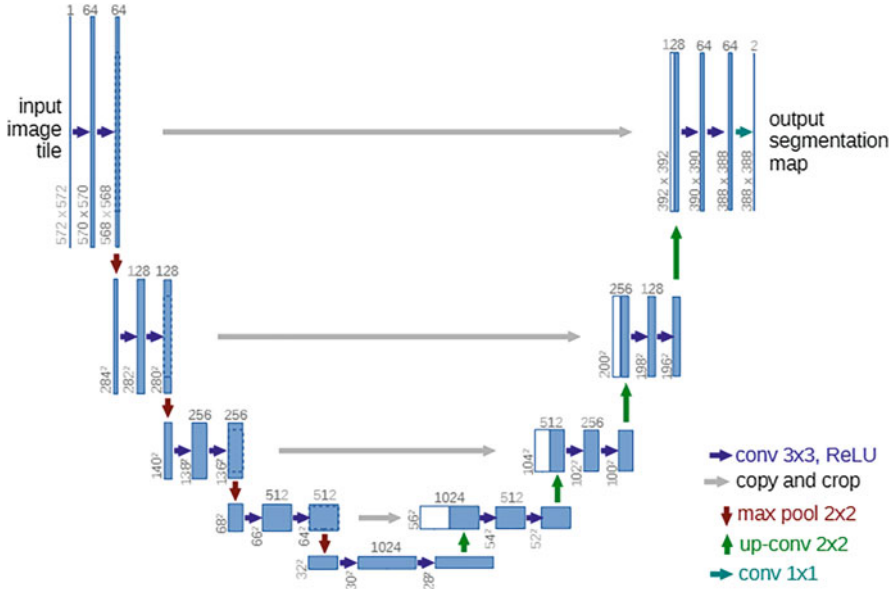


Fig. 9.9 U-Net network structure

9.4.4.3 GoogLeNet

GoogLeNet is a “deep” and “wide” model with 22 layers. Unlike AlexNet and VGG-Net, which only rely on deepening the network to improve its performance, it takes a different approach by considering not only the depth but also the width of the network, introducing the inception module, which uses convolutional kernels of different sizes on the same layer to convolve the input image side by side to generate different feature maps and combine these different feature maps in the depth direction. The structure of the inception module network is shown in Fig. 9.10.

There are four parallel branches in the module. The first three branches use convolutional layers with kernel sizes of 1×1 , 3×3 , and 5×5 to extract information at different spatial scales, where the middle two branches first perform a 1×1 convolution on the input to reduce the number of channels of the input and thus reduce the model complexity. The fourth branch uses a 3×3 maximum pooling layer and then takes a 1×1 convolution to change the number of channels. Appropriate padding is used in all four branches to keep the input and output sizes consistent in height and width. Finally, the output of each branch is concatenated and fed into the next layer. The inception module extracts semantic features at different levels by different branches, thus maximizing the expressiveness of the network.

GoogLeNet is suitable for processing large amounts of data, especially in the case of limited computational resources or memory, and it has the advantages of high computational efficiency and high classification accuracy (Figs. 9.11, 9.12, and 9.13).

Fig. 9.10 Network structure of AlexNet

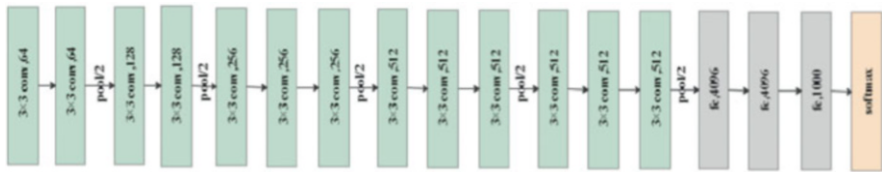
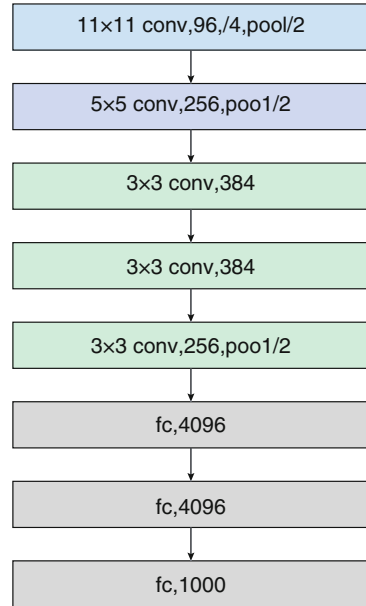


Fig. 9.11 Network structure of VGG16 VGG-Net

9.4.4.4 ResNet

ResNet, proposed by Kaiming He et al. in 2015, was the winner of the ILSVRC competition for the classification task in 2015. The largest contribution of ResNet is the introduction of the residual block to prevent the problem of gradient disappearance due to the increase in network depth, thus further deepening the network depth.

The basic idea of the residual block is to add a constant mapping to the network that allows the input information to be transferred directly to the next layer of the network, and it changes the learning goal of ResNet. Suppose the input of one segment of the network is x and the expected output is $H(x)$. If the output of x is directly transferred to the next segment of the network, then the learning objective becomes $F(x)=H(x)-x$, the residual at that point.

When $F(x) = 0$, the input and expected output are equal, i.e., a constant mapping, so the training objective of ResNet is to make $F(x)$ infinitely close to 0, making the network depth increase without the final accuracy decrease.

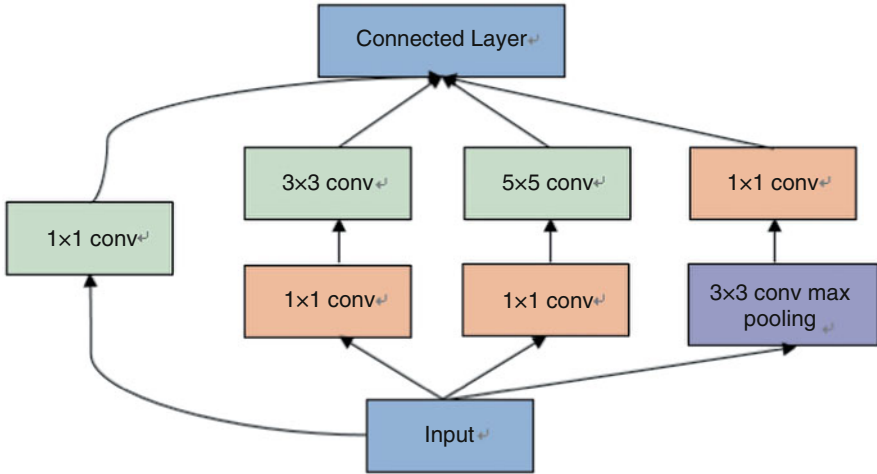
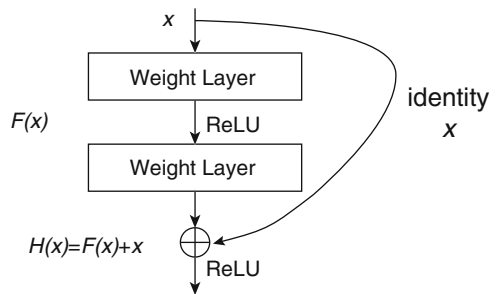


Fig. 9.12 Inception module structure Inception

Fig. 9.13 Residual block structure



9.5 Conclusion

Most of the current segmentation and classification of malaria microscope image cells are based on traditional machine learning or a combination of machine learning and deep learning; both segmentation and classification are carried out in stages, and their classification is generally carried out on the basis of segmentation. For classification, traditional methods require manual participation, human refinement and cleaning of data, and manual construction of features; similarly, for segmentation, traditional image segmentation methods are affected by subjective human operations such as manual selection of initial seed points and initial contours.

References

- Díaz G, González FA, Romero E (2009) A semiautomatic method for quantification and classification of erythrocytes infected with malaria parasites in microscopic images[J]. *J Biomed Inform* 42(2):296–307
- He K, Zhang X, Ren S et al (2016) Deep residual learning for image recognition[C]. In: *Proceedings of the IEEE Conference On Computer Vision And Pattern Recognition*, pp 770–778
- Hung J, Carpenter A (2017) Applying faster r-cnn for object detection on malaria images[C]. In: *Proceedings of the IEEE Conference on Computer Vision and Pattern Recognition Workshops*, pp 56–61
- Jan Z, Khan A, Sajjad M et al (2018) A review on automated diagnosis of malaria parasite in microscopic blood smears images[J]. *Multimed Tools Appl* 77(8):9801–9826
- Krizhevsky A, Sutskever I, Hinton GE (2012) Imagenet classification with deep convolutional neural networks[C]. *Adv Neural Inf Proces Syst* 60:1097–1105
- Kumarasamy SK, Ong SH, Tan KSW (2011) Robust contour reconstruction of red blood cells and parasites in the automated identification of the stages of malarial infection[J]. *Mach Vis Appl* 22(3):461–469
- Makkapati VV, Rao RM (2009) Segmentation of malaria parasites in peripheral blood smear images[C]//2009. In: *IEEE International Conference on Acoustics, Speech and Signal Processing*. IEEE, pp 1361–1364
- Mandal S, Kumar A, Chatterjee J et al (2010) Segmentation of blood smear images using normalized cuts for detection of malarial parasites[C]//2010. In: *Annual IEEE India Conference*. IEEE, pp 1–4
- May Z, Aziz S S A M. Automated quantification and classification of malaria parasites in thin blood smears[C]//2013 *IEEE International Conference on Signal and Image Processing Applications*. IEEE, 2013: 369-373
- Panchbhai VV, Damahe LB, Nagpure AV et al (2012) RBCs and parasites segmentation from thin smear blood cell images[J]. *Int J Image Graphics Signal Proc* 4(10):54
- Rajaraman S, Antani SK, Poostchi M et al (2018) Pretrained convolutional neural networks as feature extractors toward improved malaria parasite detection in thin blood smear images [J]. *PeerJ* 6:e4568
- Rajaraman S, Jaeger S, Antani SK (2019) Performance evaluation of deep neural ensembles toward malaria parasite detection in thin-blood smear images[J]. *PeerJ* 7:e6977
- Ross NE, Pritchard CJ, Rubin DM et al (2006) Automated image processing method for the diagnosis and classification of malaria on thin blood smears[J]. *Med Biol Eng Comput* 44(5): 427–436
- Somasekar J, Reddy BE (2015) Segmentation of erythrocytes infected with malaria parasites for the diagnosis using microscopy imaging[J]. *Computers & Electrical Engineering* 45:336–351
- Somasekar J, Reddy BE (2017) A novel two-stage thresholding method for segmentation of malaria parasites in microscopic blood images[J]. *Journal of Biomedical Engineering and Medical Imaging* 4(2):31–31
- Tek FB, Dempster AG, Kale I (2009) Computer vision for microscopy diagnosis of malaria [J]. *Malar J* 8(1):153



Xiaonan Song and Jian Li

Abstract

Antimalarial drug therapy is the recommended measure for malaria patients. In the chapter, the treatment for uncomplicated malaria, severe and cerebral malaria, and drug-resistant plasmodium parasites was described. Meanwhile, population prophylaxis for malaria is also reviewed.

Keywords

Malaria · *Plasmodium* · Antimalarial drug · Treatment · Drug resistant · Artemisinin-based combination therapies

At present, there is a wide range of antimalarial drugs available for the clinical treatment of malaria, and the effectiveness of drug treatment is gradually improving, but the situation of malaria treatment and prevention and control still has a relatively prominent seriousness. Effective malaria management is based on early and accurate diagnosis and treatment. The discovery of artemisinin changed the challenge of malaria treatment from quinoline-based therapies to artemisinin-based combination therapies (ACTs) (Su and Miller 2015). Currently, ACTs are recognized as the most effective drug for the treatment of malaria worldwide, whether for the treatment of uncomplicated malaria or severe falciparum malaria. Artemisinin and its derivatives, including dihydroartemisinin (DHA), artesunate (AS), and artemether, have shown outstanding therapeutic efficacy and research value in the treatment given their speed, potency, and safety.

X. Song · J. Li (✉)

Hubei University of Medicine, Shiyan City, China

10.1 Management of Uncomplicated Malaria

All signs and symptoms of uncomplicated malaria, like other febrile symptoms, are nonspecific and can appear early or late in the course of the disease. Hepatosplenomegaly, thrombocytopenia, and anemia are clearly associated with malaria in endemic areas, especially in children. Fever, cephalgias, fatigue, malaise, and musculoskeletal pain are the most common clinical features of malaria (Grobusch and Kremsner 2005). The main objectives of the treatment of uncomplicated malaria are to prevent progression to severe disease and death, reduce clinical symptoms and cure the infection as quickly as possible. The main advance in the treatment of uncomplicated falciparum malaria has been the replacement of the failed monotherapies chloroquine (CQ) and sulfadoxine-pyrimethamine (SP) with ACTs, a change that has significantly reduced malaria morbidity and mortality worldwide. Current recommendations state that children and adults with uncomplicated *Plasmodium falciparum* malaria (except pregnant women in the first trimester) should be treated with one of the following ACTs: artemether-lumefantrine (AL), artesunate+amodiaquine (AS+AQ), artesunate+mefloquine (AS+MQ), artesunate+sulfadoxine-pyrimethamine (AS+SP), or dihydroartemisinin+piperazine (DHA + PPQ). The advantage of ACTs is that they combine two active drugs with different mechanisms of action and different half-lives. Two or more drugs with different modes of action make the probability of parasite resistance at the same time much lower than that of parasite resistance to a single drug. ACTs are administered orally in regimens that must in all cases cover a 3-day full course (World Health Organization 2015).

The choice of malaria treatment depends on the infected species, drug resistance, severity of the disease, whether the patient can take oral drugs, and whether he or she belongs to a special risk group (e.g., pregnant women and children) (World Health Organization 2015). If the species of infection is not known or if the infection is caused by more than one species, *P. falciparum* should be treated first, as this parasite causes disease is likely to develop rapidly and have the highest mortality (Lalloo et al. 2007). The patient's travel history provides useful clues for selecting an effective antimalarial drug in terms of the risk of drug resistance. Parenteral treatment is indicated for all patients with severe or complicated malaria, those at high risk of developing the severe disease (e.g., those with over 2% of infected red blood cells; pregnant women), or those unable to take oral medicines.

The use of different treatment options for different species of infections. For *P. ovale*, *P. vivax*, and *P. malariae* infections, CQ is a recommended treatment to kill the intraerythrocytic stage of the parasite and reduce the fever rapidly, which should be followed by a radical cure with a drug with a specific effect on the liver hypnozoites. Thus, the combination of CQ and primaquine (PQ) is commonly used (Chu and White 2016). ACTs are currently recommended as first-line treatment for all patients with *P. falciparum* infection, including in pregnant women (Hanboonkunupakarn and White 2022). They are an alternative to CQ for infections caused by other malaria species, allowing a single treatment to be deployed for all malaria infections.

For *P. vivax* and *P. ovale* infections, CQ plus PQ is preferred. If CQ treatment is ineffective, PPQ, pyronaridine, or ACTs plus PQ can be used. For *P. malariae* infection, CQ is the first choice. When CQ does not respond to treatment, PPQ, pyronaridine or ACTs can be used. For infection with *P. falciparum*, ACTs or pyronaridine are used. PPQ was used in pregnant women suffering from *P. falciparum* within 3 months of pregnancy. Patients with multiple mixed plasmodium parasite infections, such as *P. falciparum* and *P. vivax*, *P. falciparum* and *P. ovale*, are ACTs or pyronaridine plus PQ. Patients with *P. falciparum* and *P. malariae* coinfection should receive ACTs or pyronaridine (Epelboin et al. 2020; Laloo et al. 2016; Imbert and Laurent 2002) (Table 10.1).

10.2 Management of Severe and Cerebral Malaria

In 2011, the WHO recommended Artesunate (AS) instead of quinine (QN) as the first-line treatment for severe malaria (Le et al. 2018). The largest random clinical trial of severe malaria to date has shown that intravenous or intramuscular AS significantly reduces mortality compared to parenteral QN, in addition to being simpler and safer to administer (Checkley and Whitty 2007). As of April 1, 2019, patients who meet one or more of the following criteria for severe malaria should receive treatment with intravenous AS according to the Centers for Disease Control and Prevention's (CDC's): impairment of consciousness/coma, severe normocytic anemia (hemoglobin < 7), renal failure, acute respiratory distress syndrome, hypotension, disseminated intravascular coagulation, spontaneous bleeding, acidosis, hemoglobinuria, jaundice, repeated generalized convulsions, and/or parasitemia exceeding 5% (CDC's). Considering the relative effectiveness of AS as a substitute for QN in the treatment of severe malaria, based on evidence from current practice, the WHO recommends a second-line therapy: AS plus tetracycline, doxycycline, or clindamycin and recommends that artemisinin and its derivatives should not be used as monotherapy in the treatment of malaria (World Health Organization 2015). If intravenous artesunate is not available, use artemether in preference to QN in adults and children (Table 10.2). Parenteral treatment must be shifted to oral treatment when the patient improves and is able to eat and drink. AS is also indicated in its rectal form as a prereferral option for children under 6 years of age living in remote areas waiting for immediate transfer to a higher level (Okebe and Eisenhut 2014).

Cerebral malaria (CM) is the most common severe malaria with a high mortality rate. There are currently no effective therapeutic drugs available for the eradication of CM. The two types of treatments are available for CM include antimalarial chemotherapy, QN, and adjuvant therapy (Purohit et al. 2021). Treatment options for CM were studied, and it was found that intravenous AS was superior to intravenous QN in the treatment of CM, but antimalarial drugs alone are insufficient to prevent death and neurological deficits in patients with severe malaria. The currently available antimalarial drugs lack lipophilicity and are thus unable to reach the brain tissue. Therefore, safe, cost-effective agents with improved lipophilicity possessing the potential to target brain tissues are needed to fight CM worldwide. Among

Table 10.1 Main regimens for the drug treatment of malaria (Ashley and Poespoprodjo 2020; D'Alessandro et al. 2018; Plewes et al. 2019)

Species of plasmodium	Drug	Administration of drugs	Adult dosage	Pediatric dosage
<i>P. vivax</i> <i>P. ovale</i>	Non-ACTs regimens-8-day regimens			
	Chloroquine (CQ) plus primaquine (PQ)	The total dose of CQ was 1200 mg, divided into 3 oral days; the total dose of PQ was 180 mg, divided into 8 oral days	CQ 600 mg (4 tablets) daily divided 2 times oral doses on the first day; CQ 300 mg (2 tablets) by oral once daily on the second and third day; in parallel PQ 22.5 mg (3 tablets) oral once daily for 8 days	CQ (10 mg/kg) divided 2 times oral daily on the first day; CQ once oral daily on the second and third day, once 5 mg/kg body weight; in parallel, PQ (0.375 mg/kg) oral once daily for 8 days
	Piperaquine (PPQ) plus primaquine (PQ)	The total dose of PPQ was 1200 mg, divided into 3 oral days; the total dose of PQ was 180 mg, divided into 8 oral days	PPQ 600 mg (4 tablets) daily divided 2 times oral doses on the first day; PPQ 300 mg (2 tablets) by oral once daily on the second and third day; in parallel PQ 22.5 mg (3 tablets) oral once daily for 8 days	PPQ (10 mg/kg) divided 2 times oral daily on the first day and once oral daily on the second and third day; in parallel PQ (0.375 mg/kg) oral once daily for 8 days
	Artemisinin-based combination therapies (ACTs)- 8-day regimens			
	Dihydroartemisinin-piperaquine (DHA-PPQ) plus PQ	The total dose of DHA-PPQ 8 tablets, divided into 2 oral days; the total dose of PQ was 180 mg, divided into 8 oral days	The first dose of DHA-PPQ is 2 tablets orally; continue oral drug 2 tablets at 8 h, 24 h, and 32 h. PQ 3 tablets per dose oral once daily for 8 days	According to the age and first dose, 8 h, 24 h, 32 h oral, respectively 7–10 years old: The 1 tablet per dose at first dose, 8 h, 24 h, 32 h oral, respectively 11–15 years old: The 1.5 tablets per dose at first dose, 8 h, 24 h, 32 h oral, respectively PQ: 4–10 years old: 7.5 mg (1 tablet) per dose one time daily for 8 days 11–15 years old: 15 mg (2 tablets) per dose one time daily for 8 days

	Artesunate-amodiaquine (AS-AQ) plus PQ	The total dose of AS-AQ 4 tablets, divided into 2 oral days; the total dose of PQ was 180 mg, divided into 8 oral days	AS-AQ 2 tablets per dose oral once daily for 3 days; PQ 3 tablets per dose oral one time daily for 8 days	AS-AQ: According to the age and take orally on the first, second, third day, respectively 2–11 months: 1/4 tablets on the first, second, and third day 1–5 years old: 1/2 tablets on the first, second, and third day 6–13 years old: 1 tablet on the first, second, and third day PQ: 4–10 years old: 7.5 mg (1 tablet) per dose one time daily for 8 days; 11–15 years old: 15 mg (2 tablets) per dose one time daily for 8 days
	Artemisinin-piperazine (ART-PPQ) plus PQ	The total dose of ART-PPQ 4 tablets, divided into 2 oral days; the total dose of PQ was 180 mg, divided into 8 oral days	ART-PPQ 2 tablets per dose oral once daily for 2 days. PQ 3 tablets per dose oral once daily for 8 days	ART-PPQ: According to the age 2–3 years old: 1/2 tablets on the first and second day 4–6 years old: 3/4 tablets on the first and second day 7–10 years old: 1 tablet on the first and second day 11–15 years old: 1 + 1/2 tablets on the first and second day PQ: 4–10 years old: 7.5 mg (1 tablet) per dose one time daily for 8 days 11–15 years old: 15 mg (2 tablets) per dose one time daily for 8 days

(continued)

Table 10.1 (continued)

Species of plasmodium	Drug	Administration of drugs	Adult dosage	Pediatric dosage
	Pyronaridine phosphate plus PQ	The total dose of pyronaridine phosphate was 1200 mg, divided into 3 oral days; the total dose of PQ was 180 mg, divided into 8 oral days	Pyronaridine phosphate 3 tablets per dose twice per day on the first, interval 4–6 h; 3 tablets per dose oral once daily on the second and third day. PQ 3 tablets per dose oral once daily for 8 days	Pyronaridine phosphate: 6 mg/kg weight oral twice daily on the first day, interval 4–6 h, 6 mg/kg weight oral once daily on the second and third day; PQ: 4–10 years old: 7.5 mg (1 tablet) per dose once daily for 8 days; 11–15 years old: 15 mg (2 tablets) per dose once daily for 8 days
<i>P. malariae</i>	Non-ACTs regimens-3-day regimens			
	CQ	Total dose 1200 mg, divided into 3 oral days	CQ 600 mg (4 tablets) daily divided 2 times oral doses on the first day; CQ 300 mg (2 tablets) by oral once daily on the second and third day; in parallel PQ 22.5 mg (3 tablets) oral once daily for 8 days	CQ (10 mg/kg) divided 2 times oral daily on the first day; CQ once oral daily on the second and third day, once 5 mg/kg body weight
	PPQ	Total dose 1200 mg, divided into 3 oral days	PPQ 600 mg (4 tablets) daily divided 2 times oral doses on the first day; PPQ 300 mg (2 tablets) by oral once daily on the second and third day	PPQ (10 mg/kg) divided twice oral daily on the first day and once oral daily on the second and third day
	Pyronaridine phosphate	Total dose 1200 mg, divided into 3 oral days	Pyronaridine phosphate 3 tablets per dose twice per day on the first, interval 4–6 h; 3 tablets per dose oral once daily on the second and third day	Pyronaridine phosphate: 6 mg/kg weight oral twice daily on the first day, interval 4–6 h, 6 mg/kg weight oral once daily on the second and third day

ACTs	DHA + PPQ	The total dose 8 tablets, divided into 2 oral days	The first dose is 2 tablets orally; continue oral drug 2 tablets at 8 h, 24 h and 32 h	According to the age and first dose, 8 h, 24 h, 32 h oral, respectively 7–10 years old: The 1 tablet per dose at first dose, 8 h, 24 h, 32 h oral, respectively 11–15 years old: The 1.5 tablets per dose at first dose, 8 h, 24 h, 32 h oral, respectively
AS+AQ	The total dose 6 tablets, divided into 3 oral days	AS-AQ 2 tablets per dose oral once daily for 3 days	AS-AQ: According to the age and take orally on the first, second, and third day, respectively 2–11 months: 1/4 tablets on the first, second, and third day 1–5 years old: 1/2 tablets on the first, second, and third day 6–13 years old: 1 tablet on the first, second, and third day	
ART+PPQ	The total dose 4 tablets, divided into 2 oral days	ART-PPQ 2 tablets per dose oral once daily for 2 days	ART-PPQ: According to the age 2–3 years old: 1/2 tablets on the first and second day 4–6 years old: 3/4 tablets on the first and second day 7–10 years old: 1 tablet on the first and second day 11–15 years old: 1 + 1/2 tablets on the first and second day	
<i>P. Falciparum</i>	Non-ACTs regimens-3-day regimens Pyronaridine phosphate	Pyronaridine phosphate total dose 1200 mg, divided into 3 oral days	Pyronaridine phosphate 3 tablets per dose twice per day on the first, interval 4–6 h; 3 tablets per dose oral once daily on the second and third day	Pyronaridine phosphate: 6 mg/kg weight oral twice daily on the first day, interval 4–6 h, 6 mg/kg weight oral once daily on the second and third day

(continued)

Table 10.1 (continued)

Species of plasmodium	Drug	Administration of drugs	Adult dosage	Pediatric dosage
	ACTs			
	DHA-PPQ	The total dose of DHA-PPQ 8 tablets, divided into 2 oral days	The first dose is 2 tablets orally; continue oral drug 2 tablets at 8 h, 24 h, and 32 h	According to the age and first dose, 8 h, 24 h, and 32 h oral, respectively 7–10 years old: The 1 tablet per dose at first dose, 8 h, 24 h, 32 h oral, respectively 11–15 years old: The 1.5 tablets per dose at first dose, 8 h, 24 h, 32 h oral, respectively
	AS+AQ	The total dose of AS-AQ 6 tablets, divided into 3 oral days	AS-AQ 2 tablets per dose oral once daily for 3 days	AS-AQ: According to the age and take orally on the first, second, and third day, respectively. 2–11 months: 1/4 tablets on the first, second, and third day 1–5 years old: 1/2 tablets on the first, second, and third day 6–13 years old: 1 tablet on the first, second, and third day
	ART+PPQ	The total dose of ART-PPQ 4 tablets, divided into 2 oral days	ART-PPQ 2 tablets per dose oral once daily for 2 days	ART-PPQ: According to the age 2–3 years old: 1/2 tablets on the first and second day 4–6 years old: 3/4 tablets on the first and second day 7–10 years old: 1 tablet on the first and second day 11–15 years old: 1 + 1/2 tablets on the first and second day

Table 10.2 Antimalarial treatment regimens in severe malaria (Varo et al. 2020; Plewes et al. 2019; Severe malaria 2014)

Drug	Administration of drugs	Adult dosage	Pediatric dosage
First-line initial therapy			
Artesunate	Intravenous (i.v.) or intramuscular (i.m.) injection of artesunate. The course of treatment is not less than 7 days. If the patient's clinical symptoms and physical symptoms are relieved and can eat within 7 days, the use of artesunate injection can be discontinued and changed to oral ACTs a course of treatment to continue.	Artesunate (i.v. or i.m.) 2.4 mg/kg immediately, then at 12, 24 h, and daily until oral medication can be taken reliably.	For children ≥ 20 kg: Give 2.4 mg/kg per dose; for children < 20 kg: Give 3 mg/kg per dose. Dose at 0, 12, and 24 h for a total of seven doses.
Alternative initial therapy			
Artemether	The course of artemether (i.m.) treatment is not less than 7 days. If the patient's clinical symptoms and physical symptoms are relieved and can eat within 7 days, the use of artemether injection can be discontinued and changed to oral ACTs a course of treatment to continue	Artemether (i.m.) 3.2 mg/kg initial dose followed by 1.6 mg/kg daily once daily for 7 days until oral medication can be taken reliably.	
Quinine dihydrochloride	Intravenous infusion	Quinine dihydrochloride (20 mg salt/kg) by slow intravenous infusion over 4 h or by i.m. injection split to both anterior thighs, followed by 10 mg salt/kg 8 h until the patient is able to swallow	
Once the patient can tolerate oral therapy. The previously recommended options for follow-on oral treatment are as follows			
Artemether plus lumefantrine			
Artesunate plus amodiaquine			
Dihydroartemisinin plus piperazine			
Artesunate plus sulfadoxine-pyrimethamine			
Artesunate plus clindamycin or doxycycline			
Quinine plus clindamycin or doxycycline			

survivors, further development of adjuvant therapy in combination with antimalarial therapy is needed to compensate for the inadequacy of existing drugs to improve clinical outcomes and/or reduce mortality and prevent long-term neurocognitive deficits. Various other adjunctive treatments targeting the underlying pathophysiology of malaria (Varo et al. 2018), such as corticosteroids, immunoglobulin (rosiglitazone), levamisole, anti-TNF therapies, antiepileptic drugs, agonists peroxisome proliferator-activated receptor- γ (PPAR- γ), mannitol, nitric oxide or exchange blood transfusions (EBTs), and erythrocytapheresis, have been evaluated clinically, but most attempts have failed. Treatments tested in preclinical models are still a potential direction for adjunctive therapy. Through the establishment of an experimental cerebral malaria mouse model, it was found that rapamycin (Gordon et al. 2015; Mejia et al. 2017), HMG-COA reductase inhibitor (statins) (Kumar et al. 2016; Reis et al. 2012), doxycycline (Beeson et al. 2013), Trichoderma matrix (Cariaco et al. 2018), and curcumin (Shikani et al. 2012) could be used as adjuvant treatment strategies for CM to reduce induced death and neurological damage.

10.3 Treatment of Drug-Resistant Plasmodium

Despite the remarkable efficacy of artemisinin and its derivatives in the treatment of malaria, difficulties and challenges remain for the effective treatment of malaria. ACTs are currently the gold standard for antimalarial treatment, in which artemisinin derivatives are commonly used in combination with MQ, PQ, PPQ, and AQ in ACT therapy. The current standard 3-day ACT course is designed to allow pharmacologically distinct drugs to complement each other while reducing the risk of drug resistance. Even though ACTs address most of the shortcomings associated with monotherapies, resistance to antimalarial drugs is a recurring problem. At present, there are ACT treatment failures in the Greater Mekong Subregion. The effective remedy for treatment failure of ACTs is through exchange of partner drugs. The effective remedy for treatment failure of ACTs is through exchange of partner drugs. An effective remedy for the failure of ACT treatment is through the exchange of companion drugs, but this can easily lead to drug resistance to alternative drugs again, so adding more companion drugs to treatment should be considered without other adjustments, perhaps reducing the risk of resistance (Xu et al. 2022; Wang et al. 2021). An interesting new strategy is triple artemisinin-based combination therapies (TACTs), which combine existing combination formulations of ACTs with a second partner drug that is slowly eliminated, could provide effective treatment and delay the emergence of resistance to antimalarial drugs. Based on this idea, van der Pluijm and colleagues (van der Pluijm et al. 2020) conducted an open randomized controlled trial in which uncomplicated patients with *P. falciparum* malaria were recruited from eight countries, and patients were assigned to take DHA + PPQ, DHA + PPQ plus MQ, AS+MQ, AL, and AL plus AQ. The results show that DHA + PPQ plus MQ and AL plus AQ are highly efficacious, well tolerated, and safe treatments for uncomplicated *P. falciparum* malaria. With the increasing failure of conventional ACTs, TACTs may become a new option for the

treatment of uncomplicated falciparum malaria in the Greater Mekong subregion or other drug-resistant regions in the near future. Hamaluba and colleagues conducted a single-center, open-label, randomized, noninferiority trial using arterolane-based TACTs in treating uncomplicated *P. falciparum* malaria in Kenyan children (Hamaluba et al. 2021). This study demonstrates that arterolane–piperazine–mefloquine is an efficacious and safe treatment for uncomplicated falciparum malaria in children and may be used to prevent or delay the emergence of resistance to antimalarial drugs.

10.4 Prevention of Malaria

The most important measure to eliminate malaria episodes is to prevent them. Infection can be prevented through vector control or bite prevention, chemoprophylaxis, vaccines, and other interventions to minimize the harm caused by malaria (Varo et al. 2020; Ashley and Poespoprodjo 2020).

Vector control measures included the distribution of long-lasting insecticide-impregnated bed nets and indoor residual spraying. Mosquito nets should be used properly during the mosquito season, and mosquito repellents and equipment should be used during outdoor duty. In addition to the large-scale application of insecticides, the most important anti-mosquito measures are the elimination of stagnant water and the eradication of mosquito breeding sites.

The two main chemoprevention strategies in malaria-endemic countries are seasonal malaria chemoprevention and intermittent preventive treatment. Malaria is highly seasonal, with transmission occurring only in consecutive months of the year. A full treatment course is administered a monthly dose of an artemisinin-free antimalarial (SP + AQ) during malaria-transmission season (usually 3–4 months long), up to four times (Varo et al. 2020; Ashley and Poespoprodjo 2020). Due to concerns about its resistance, DHA + PPQ has been proposed as an alternative to seasonal chemoprophylaxis with a dosing interval of once weekly to maximize protective efficacy (Zongo et al. 2015; Sundell et al. 2015; Chotsiri et al. 2019). Intermittent preventive therapy with SP is recommended by WHO 3,4, provided resistance to SP is not established (<50% prevalence of the Pfdhps 540 mutation). This is a recommendation for many African countries with high *P. falciparum* prevalence and has clear health benefits for pregnant women and newborns. WHO currently proposes a minimum of three doses (one month apart) during pregnancy, and infants are given at 10, 14 weeks, and 9 months of age.

Malaria vaccines hold great promise for life-saving benefits, especially for children who bear the brunt of malaria mortality. RTS, S/AS01 is a preerythrocytic vaccine (Draper et al. 2018) that has been shown to give partial protection against falciparum malaria in a large, multicenter trial and has received a favorable opinion from the European Medicines Agency (Efficacy and safety of RTS 2015) and is currently being tested in implementation studies. In parallel, multiple strategies are being advanced to test next-generation malaria vaccines (Laurens 2021), including novel approaches that build on principles learned from RTS, S development,

vaccination with radiation-attenuated sporozoites, and development of monoclonal antibodies targeting immunogenic peptides. Novel vaccine delivery approaches are also being advanced, including self-amplifying RNA vaccine delivery, self-assembling protein nanoparticle methods, circumsporozoite protein-based approaches, whole organism vaccination, and transmission-blocking vaccines. Techniques employed for COVID-19 vaccine development should also be considered for malaria vaccination, including sustained release polymer nanoparticle hydrogel vaccination (Gale et al. 2021) and charge-altering releasable transporters (Haabeth et al. 2021). As vaccine science advances and new approaches optimize knowledge gained, highly effective malaria vaccines that provide sustained protection are within reach.

References

- Ashley EA, Poespoprodjo JR (2020) Treatment and prevention of malaria in children. *Lancet Child Adolesc Health* 4:775–789. [https://doi.org/10.1016/s2352-4642\(20\)30127-9](https://doi.org/10.1016/s2352-4642(20)30127-9)
- Beeson JG, Chan JA, Fowkes FJ (2013) PfEMP1 as a target of human immunity and a vaccine candidate against malaria. *Expert Rev Vaccines* 12:105–108. <https://doi.org/10.1586/erv.12.144>
- Cariaco Y et al (2018) Ethanolic extract of the fungus *Trichoderma stromaticum* decreases inflammation and ameliorates experimental cerebral malaria in C57BL/6 mice. *Sci Rep* 8: 1547. <https://doi.org/10.1038/s41598-018-19840-x>
- Checkley AM, Whitty CJ (2007) Artesunate, artemether or quinine in severe *Plasmodium falciparum* malaria? *Expert Rev Anti-Infect Ther* 5:199–204. <https://doi.org/10.1586/14787210.5.2.199>
- Chotsiri P et al (2019) Optimal dosing of dihydroartemisinin-piperaquine for seasonal malaria chemoprevention in young children. *Nat Commun* 10:480. <https://doi.org/10.1038/s41467-019-08297-9>
- Chu CS, White NJ (2016) Management of relapsing *plasmodium vivax* malaria. *Expert Rev Anti-Infect Ther* 14:885–900. <https://doi.org/10.1080/14787210.2016.1220304>
- D'Alessandro U et al (2018) Treatment of uncomplicated and severe malaria during pregnancy. *Lancet Infect Dis* 18:e133–e146. [https://doi.org/10.1016/s1473-3099\(18\)30065-3](https://doi.org/10.1016/s1473-3099(18)30065-3)
- Draper SJ et al (2018) Malaria vaccines: recent advances and new horizons. *Cell Host Microbe* 24: 43–56. <https://doi.org/10.1016/j.chom.2018.06.008>
- Efficacy and safety of RTS (2015) S/AS01 malaria vaccine with or without a booster dose in infants and children in Africa: final results of a phase 3, individually randomised, controlled trial. *Lancet* 386:31–45. [https://doi.org/10.1016/s0140-6736\(15\)60721-8](https://doi.org/10.1016/s0140-6736(15)60721-8)
- Epelboin L et al (2020) Management and treatment of uncomplicated imported malaria in adults. Update of the French malaria clinical guidelines. *Med Mal Infect* 50:194–212. <https://doi.org/10.1016/j.medmal.2019.07.011>
- Gale EC et al (2021) Hydrogel-based slow release of a receptor-binding domain subunit vaccine elicits neutralizing antibody responses against SARS-CoV-2. *Adv Mater* 33:e2104362. <https://doi.org/10.1002/adma.202104362>
- Gordon EB et al (2015) Inhibiting the mammalian target of rapamycin blocks the development of experimental cerebral malaria. *MBio* 6:e00725. <https://doi.org/10.1128/mBio.00725-15>
- Grobusch MP, Kremsner PG (2005) Uncomplicated malaria. *Curr Top Microbiol Immunol* 295:83–104
- Haabeth OAW et al (2021) An mRNA SARS-CoV-2 vaccine employing charge-altering releasable transporters with a TLR-9 agonist induces neutralizing antibodies and T cell memory. *ACS Cent Sci* 7:1191–1204. <https://doi.org/10.1021/acscentsci.1c00361>

- Hamaluba M et al (2021) Arterolane-piperazine-mefloquine versus arterolane-piperazine and artemether-lumefantrine in the treatment of uncomplicated plasmodium falciparum malaria in Kenyan children: a single-Centre, open-label, randomised, non-inferiority trial. *Lancet Infect Dis* 21:1395–1406. [https://doi.org/10.1016/s1473-3099\(20\)30929-4](https://doi.org/10.1016/s1473-3099(20)30929-4)
- Hanboonkunupakarn B, White NJ (2022) Advances and roadblocks in the treatment of malaria. *Br J Clin Pharmacol* 88:374–382. <https://doi.org/10.1111/bcp.14474>
- Imbert P, Laurent C (2002) Treatment of malaria in children: 1. Uncomplicated malaria. *Med Trop (Mars)* 62:554–560
- Kumar S, Singh RK, Patial B, Goyal S, Bhardwaj TR (2016) Recent advances in novel heterocyclic scaffolds for the treatment of drug-resistant malaria. *J Enzyme Inhib Med Chem* 31:173–186. <https://doi.org/10.3109/14756366.2015.1016513>
- Laloo DG et al (2007) UK malaria treatment guidelines. *J Infect* 54:111–121. <https://doi.org/10.1016/j.jinf.2006.12.003>
- Laloo DG et al (2016) UK malaria treatment guidelines 2016. *J Infect* 72:635–649. <https://doi.org/10.1016/j.jinf.2016.02.001>
- Laurens MB (2021) Novel malaria vaccines. *Hum Vaccin Immunother* 17:4549–4552. <https://doi.org/10.1080/21645515.2021.1947762>
- Le HG et al (2018) Genetic polymorphism and natural selection of circumsporozoite surface protein in plasmodium falciparum field isolates from Myanmar. *Malar J* 17:361. <https://doi.org/10.1186/s12936-018-2513-0>
- Mejia P et al (2017) A single rapamycin dose protects against late-stage experimental cerebral malaria via modulation of host immunity, endothelial activation and parasite sequestration. *Malar J* 16:455. <https://doi.org/10.1186/s12936-017-2092-5>
- Okebe J, Eisenhut M (2014) Pre-referral rectal artesunate for severe malaria. *Cochrane Database Syst Rev* 2014:Cd009964. <https://doi.org/10.1002/14651858.CD009964.pub2>
- Plewes K, Leopold SJ, Kingston HWF, Dondorp AM (2019) Malaria: What's new in the Management of Malaria? *Infect Dis Clin N Am* 33:39–60. <https://doi.org/10.1016/j.idc.2018.10.002>
- Purohit D, Kumar S, Dutt R, Bhardwaj TR (2021) An update on recent advances for the treatment of cerebral malaria. *Mini Rev Med Chem* 22(12):1607–1618. <https://doi.org/10.2174/1389557521666211124143117>
- Reis PA et al (2012) Statins decrease neuroinflammation and prevent cognitive impairment after cerebral malaria. *PLoS Pathog* 8:e1003099. <https://doi.org/10.1371/journal.ppat.1003099>
- Severe malaria (2014) *Tropical Med Int Health* 19(Suppl 1):7–131. https://doi.org/10.1111/tmi.12313_2
- Shikani HJ et al (2012) Cerebral malaria: we have come a long way. *Am J Pathol* 181:1484–1492. <https://doi.org/10.1016/j.ajpath.2012.08.010>
- Su XZ, Miller LH (2015) The discovery of artemisinin and the Nobel prize in physiology or medicine. *Sci China Life Sci* 58:1175–1179. <https://doi.org/10.1007/s11427-015-4948-7>
- Sundell K et al (2015) Variable piperazine exposure significantly impacts protective efficacy of monthly dihydroartemisinin-piperazine for the prevention of malaria in Ugandan children. *Malar J* 14:368. <https://doi.org/10.1186/s12936-015-0908-8>
- van der Pluijm RW et al (2020) Triple artemisinin-based combination therapies versus artemisinin-based combination therapies for uncomplicated plasmodium falciparum malaria: a multicentre, open-label, randomised clinical trial. *Lancet* 395:1345–1360. [https://doi.org/10.1016/s0140-6736\(20\)30552-3](https://doi.org/10.1016/s0140-6736(20)30552-3)
- Varo R, Chaccour C, Bassat Q (2020) Update on malaria. *Med Clin (Barc)* 155:395–402. <https://doi.org/10.1016/j.medcli.2020.05.010>
- Varo R et al (2018) Adjunctive therapy for severe malaria: a review and critical appraisal. *Malar J* 17:47. <https://doi.org/10.1186/s12936-018-2195-7>

- Wang J et al (2021) Triple artemisinin-based combination therapies for malaria: proceed with caution. *Lancet* 396:1976. [https://doi.org/10.1016/s0140-6736\(20\)32400-4](https://doi.org/10.1016/s0140-6736(20)32400-4)
- World Health Organization (2015) Guidelines for the treatment of malaria[M]. World Health Organization, Geneva, p 1355. <https://doi.org/10.1136/dtb.2010.11.0057>
- Xu C et al (2022) Is triple artemisinin-based combination therapy necessary for uncomplicated malaria? *Lancet Infect Dis* 22:585–586. [https://doi.org/10.1016/s1473-3099\(22\)00208-0](https://doi.org/10.1016/s1473-3099(22)00208-0)
- Zongo I et al (2015) Randomized noninferiority trial of Dihydroartemisinin-piperaquine compared with Sulfadoxine-pyrimethamine plus amodiaquine for seasonal malaria chemoprevention in Burkina Faso. *Antimicrob Agents Chemother* 59:4387–4396. <https://doi.org/10.1128/aac.04923-14>



Artemisinin Resistance in *Plasmodium falciparum* Malaria

11

Xiaoxing Wang, Bo Xiao, and Lubin Jiang

Abstract

The worldwide use of artemisinin-based combination therapies (ACTs) has contributed in recent years to a substantial reduction in deaths resulting from *Plasmodium falciparum* malaria. However, resistance to artemisinin and its derivatives (ARTs) has emerged worldwide, which is a threat to the global malaria elimination campaign. In this chapter, we will summarize the emergence of ARTs resistance, the molecular mechanisms of action of ARTs, and measures to slow down or prevent the emergence and spread of ARTs resistance. Combined efforts in strengthened surveillance, resistance detection, molecular mechanism elucidation of artemisinin resistance, and the development of novel targets and antimalarial drugs will help us to apply more effective antimalarial drug policies, putting us ahead of the curve in the fight against artemisinin resistance.

Keywords

Artemisinin resistance · ACT · kelch13 mutations · *Plasmodium falciparum*

11.1 Background

Malaria remains a major public health problem and is prevalent in tropical and subtropical regions worldwide. Globally, an estimated 1.7 billion malaria cases and 10.6 million malaria deaths were averted in the period 2000–2020. Most of the cases (82%) and deaths (95%) averted were in the World Health Organization (WHO) African Region, followed by the WHO Southeast Asia Region (cases 10% and deaths 2%) (WHO, 2021). In the World Malaria Report 2021, the WHO

X. Wang · B. Xiao · L. Jiang (✉)

Institut Pasteur of Shanghai, Chinese Academy of Sciences, Huangpu, Shanghai, China

e-mail: xxwang@ips.ac.cn; bxiao@ips.ac.cn; lbjiang@ips.ac.cn

recommends the broad use of the RTS,S/AS01 (RTS,S) malaria vaccine, which can save tens of thousands of children's lives every year (WHO, 2021). Before the WHO recommended the use of malaria vaccines, malaria control was mainly through antimalarial drugs (chloroquine, sulfadoxine-pyrimethamine, artemisinin, etc.), the spraying of insecticides, and insecticide-treated mosquito nets. With the prolonged use of antimalarial drugs, chloroquine resistance has emerged in the Greater Mekong Subregion (GMS). In 2006, the WHO mandated that artemisinin and its derivatives (ART) be used only in combination with other drugs to avoid the development of chloroquine and sulfadoxine-pyrimethamine resistance in GMS, which are applied in combination with partner drugs, so-called ART combination therapies (ACTs). Unfortunately, some ACTs are unable to rapidly clear *Plasmodium falciparum* parasites from the bloodstream and fail to cure malaria patients, which is a major concern. There is a fear of resistant *Plasmodium falciparum* emerging in the world. In this chapter, we will summarize the emergence of artemisinin resistance, the molecular mechanisms of artemisinin resistance, and measures to slow down or prevent the emergence and spread of ART resistance.

11.2 Emergence of Artemisinin Resistance

In 2006, Afonso et al. first found that *Plasmodium chabaudi* can develop stable resistance to artemisinin in the laboratory but lacks mutations in the candidate genes *atp6* (encoding the sarcoplasmic and endoplasmic reticulum Ca^{2+} ATPase), *tctp*, *mdr1*, and *cg10* (Afonso et al. 2006). In 2008, clinical artemisinin resistance was first reported in Cambodia, which manifested as delayed parasite clearance, with a higher parasitemia by microscopy on day 3 after artemisinin treatment (Noedl et al. 2008). Subsequently, artemisinin resistance is redefined by a delayed parasite clearance half-life ($\text{PC}_{t_{1/2}} > 5 \text{ h}$) in vivo after ART treatment compared to approximately 2 h for sensitive parasites or by an increased parasite survival rate following brief exposure to a high dose of dihydroartemisinin (DHA) in the ring-stage survival assay ($\text{RSA}^{0-3\text{h}}$) in vitro (Noedl et al. 2008; Witkowski et al. 2013). In this assay, parasite clinical isolates are adapted to culture for several weeks, synchronized at the early-ring stage (0–3 h after invasion of RBCs), treated with a pharmacologically relevant dose of DHA for 6 hours, and then cultured for 66 hours (Witkowski et al. 2013). The percentage of parasites surviving DHA exposure was then calculated as the ratio of parasites surviving exposure to DHA versus those surviving exposure to DMSO. $\text{RSA}^{0-3\text{h}}$ discriminates two groups of parasites, one with $< 1\%$ survival and another with $\geq 1\%$ survival, which are generally defined to be artemisinin-sensitive and artemisinin-resistant, respectively (Witkowski et al. 2013).

In 2014, Ariey et al. found mutations in the PF3D7_1343700 kelch propeller domain (“K13-propeller”) associated with artemisinin resistance both the longer $\text{PC}_{t_{1/2}}$ in vivo and higher RSA values in vitro by whole-genome sequencing of an artemisinin-resistant parasite line from Africa and clinical parasite isolates from Cambodia (Ariey et al. 2014). The K13 gene comprises a *Plasmodium*-specific N-terminal domain followed by a CCC (coiled coil-containing) domain, a BTB/POZ

(Broad complex Tramtrack Bric-a-brack/Pox virus Zinc finger) domain, and a Kelch propeller domain. The six-bladed β -propeller domain consists of six Kelch motifs, each folding into a four-stranded antiparallel β -sheet (Coppée et al. 2019). Single nucleotide polymorphisms (SNPs) have been identified throughout the K13 gene, but only nonsynonymous mutations in the propeller domain (K13PDmut, K13 propeller domain mutant) are associated with delayed parasite clearance (Ashley et al. 2014). In 2017, a Chinese researcher found that a 43-year-old man was diagnosed with malaria (*P. falciparum*) in Jiangsu Province and had worked in Equatorial Guinea for approximately 2 years. Importantly, parasites of this patient were still detected on day three with dihydroartemisinin and piperazine treatment, and RSA resulted in a 2.29% survival rate and the mutation M579I in K13, which indicated that artemisinin-resistant strains have emerged in Africa (Lu et al. 2017). Mutations in the K13 propeller domain are recommended for conducting molecular surveillance as an assistant tool for monitoring resistance to artemisinin. To date, the mutations P441L, F446I, S449A, N458Y, M476I, P553L, V568G, P574L, M579I, D584V, and L675V in K13 have been reported to be associated with delayed parasite clearance from global parasite populations. In addition, a list of validated K13 mutations associated with decreased sensitivity to artemisinin has been issued, including F446I, N458Y, Y493H, I543T, R539T, R561H, P574 L, and C580Y (WHO, 2020). By 2022, some K13 mutations were found in Thailand, Vietnam, Myanmar, southern Pakistan, China, Laos, Nigeria, India, Papua New Guinea, South Africa, and Rwanda, which are also markers of slow parasite clearance (Ajogbasile et al. 2022; Ashley et al. 2014; Lautu-Gumal et al. 2021; Lu et al. 2017; Mishra et al. 2016; Na-Bangchang and Karbwang 2013; Thanh et al. 2017; Tun et al. 2015; Wang et al. 2015b). ART resistance was first reported in the GMS, and there are different geographical distributions of K13 mutations. C580Y is most prevalent in the Cambodia-Thailand and Thailand-Myanmar borders (eastern Thailand, Laos, Cambodia, and Vietnam) (Boullé et al. 2016), whereas F446I predominates along the China-Myanmar and Myanmar-India borders (Myanmar, China, and western Thailand) (Wang et al. 2015a, b; Zhang et al. 2019). This difference may result from different drug uses, demographic histories, vectors, genetic backgrounds, and antimalarial policies in these regions.

Recently, Tang et al. found that only the C580Y mutation in K13 with low frequency was associated with artemisinin resistance in the China-Myanmar border region and detected some other high mutation sites of K13 (Tang et al. 2021). Additionally, it has been reported that the S522C mutation in K13 from Kenya was associated with delayed parasite clearance (Schmedes et al. 2021). A low frequency of M476I and C469Y mutations in K13 was found in Pakistan, which is significantly associated with artemisinin resistance (Ghanchi et al. 2021). One study reported that 13 patients from Northern Uganda were infected with *P. falciparum* parasites with mutations in the A675V or C469Y allele in the K13 gene, which were associated with prolonged parasite clearance half-lives, and the RSA also showed a higher frequency of parasite survival among organisms with the A675V allele than among those with the wild-type allele (Balikagala et al. 2021). K13 resistance mutations (including P574L and A675V) in southern Rwanda have been found,

which are common in Southeast Asia and associated with delayed parasite clearance (Tacoli et al. 2016). In 2022, Nima et al. reported that there was no association with artemisinin resistance and K13 mutation in Bangladesh but with a long parasite clearance half-life (8 h) and 2.01% survival in RSA^{0-3 h} (Nima et al. 2022). An interesting discovery has been reported that the P413A mutation in the BTB/POZ domain of K13 also conferred artemisinin resistance *in vitro*, which suggested the importance of monitoring for K13 mutations (Paloque et al. 2022). The emergence and spread of artemisinin-resistant strains have aroused widespread concern. Once these resistant strains spread and become popular, they will pose a serious threat to global malaria control.

11.3 Molecular Mechanisms of Artemisinin Resistance

Artemisinin resistance is primarily associated with point mutations in the parasite's K13 protein. At present, the mechanism of ART resistance has been connected to increased cellular stress, altered DNA replication, an activated unfolded protein response, reduced protein translation, and increased levels of phosphatidylinositol 3-phosphate (Gibbons et al. 2018; Mbengue et al. 2015; Mok et al. 2015; Rocamora et al. 2018).

The location and interactomes of K13 are involved in multiple cellular processes. Some studies have identified the location and interactomes of K13 to understand the functions of K13 using immunoprecipitation (IP) or dimerization-induced quantitative BioID (DiQ-BioID) (Birnbaum et al. 2020; Gnädig et al. 2020; Siddiqui et al. 2020). These results showed that K13 localized to the endoplasmic reticulum, food vacuole markers, Rab-positive vesicles, and the adaptor protein complex 2 μ subunit (AP-2 μ) (Birnbaum et al. 2020; Gnädig et al. 2020; Siddiqui et al. 2020). Birnbaum et al. found that the resulting list of associated proteins of K13 contained 10 uncharacterized proteins (designated K13 interaction candidates, KIC1–10), PFK9, MCA2, epidermal growth factor receptor substrate 15 (Eps15), ubiquitin-binding protein 1 (UBP1), CHDP, FKBP35, HSP90, GTPase-activating protein, MyosinC (MyoC), IMC protein and VPS52. Eps15 is involved in endocytosis in other organisms, which suggests that K13 may play a role in endocytosis (Birnbaum et al. 2020). The study also showed that K13 colocalizes with AP-2 μ but is distinct from clathrin. Disruption of the K13-compartment proteins AP-2 μ , KIC4, UBP1, KIC7, KIC5, Eps15, and MCA2 also resulted in ART resistance in RSAs. Other researchers also identified that Eps15, UBP1, KIC7 and AP-2 μ contribute to the endocytic transport of hemoglobin to the food vacuole in trophozoites using a food vacuole bloating assay (Birnbaum et al. 2020; Jonscher et al. 2019). These findings indicated that K13-compartment proteins influence endocytosis in all asexual life cycle stages, whereas K13 is only required for endocytosis in ring stages. Siddiqui et al. also identified some proteins associated with K13 by IP and liquid chromatography-tandem mass spectrometry analysis, and these proteins are involved in translation, transcription, and the unfolded protein response pathway. Among these proteins, putative endoplasmic reticulum chaperone (GRP94), heat shock protein 70 (BiP),

and protein disulfide isomerase (ERp72) may be involved in the reactive oxidative stress pathway in *Plasmodium* (Siddiqui et al. 2020). Gnädig et al. also identified many putative K13-interacting proteins, including S-adenosylmethionine synthetase, adenosylhomocysteinase, phosphoglycerate mutase 1 (PGM1), phosphoglucomutase 2 (PGM2), the Rab family of GTPases, the Rieske protein, a putative dynamin (involved in mitochondrial fission), ATP synthase F1 alpha subunit (involved in mitochondrial energy metabolism), mitochondrial matrix protein 33, and several proteins involved in the mitochondrial antioxidant system. These proteins are involved in the methionine metabolism pathway, parasite glycolysis, vesicular trafficking and endocytosis, proteasome-mediated degradation, mitochondrial fission, energy, and the antioxidant system (Gnädig et al. 2020). The resulting data sets of interacting proteins of K13 suggest that it is involved in multiple cellular processes (Gnädig et al. 2020; Mok et al. 2021; Siddiqui et al. 2020).

One study demonstrated that the resistance of *Plasmodium* to artemisinin-based compounds depends on alterations of heme metabolism and on a loss of hemozoin formation linked to the downregulation of the recently identified heme detoxification protein (HDP). These artemisinin-resistant strains could detoxify free heme by an alternative catabolism pathway involving glutathione (GSH) mediation (Witkowski et al. 2012). Henriques et al. found that an increased artemisinin-resistant phenotype of *Plasmodium chabaudi* is accompanied by a mutation in a functional element of the AP2 adaptor protein complex, which also suggests that artemisinin resistance may be associated with endocytosis and trafficking of membrane proteins (Henriques et al. 2013). An additional study was reported by Mbengue et al. (Mbengue et al. 2015), who suggested that artemisinin targets *P. falciparum* phosphatidylinositol-3-kinase (PI3K) and that PI3K is the binding partner of K13. Since these parasites have low basal levels of PI3-phosphate (PI3P), the product of PI3K activity, they are highly sensitive to artemisinin-induced inhibition of PI3K. Without a functional PI3K, parasites cannot generate the high PI3P levels they need for growth (PI3P is involved in membrane biogenesis and fusion events and increases in amount as parasites develop from rings to schizonts). This study speculates that K13 mutations fail to bind PI3K, and PI3K accumulates and produces high basal levels of PI3P. When subsequently exposed to artemisinin, high basal levels of PI3P enable the continuous PI3P-dependent growth of artemisinin-resistant parasites while they recover from the effects of PI3K inhibition. PI3P is located in the FV membrane and RBC cytoplasm vesicles. A membrane-bound glutathione S-transferase (PfEXP1, PF3D7_1121600), found on the parasitophorous vacuole membrane, was upregulated twofold in the DHA-tolerant 3b1 parasite strain compared to the parental Dd2 strain and was further upregulated twofold in 3b1 upon DHA exposure (Lisewski et al. 2014). In cell-free systems, PfEXP1 can conjugate reduced GSH to hemozoin, accelerating the degradation of the toxic hemozoin digestion byproduct (Lisewski et al. 2014). Artesunate inhibits PfEXP1 glutathione transferase activity, likely by alkylation, as endoperoxide-containing antimalarials alkylate PfEXP1 (Ismail et al. 2016), which could functionally inactivate this protein. PfEXP1 was also among the antioxidant response genes upregulated in 3D7 parasites pressured with artemisinin in a separate study (Rocamora et al. 2018).

Some studies have found that K13 can act as an adaptor to bring E3 ligase(s) and their substrate(s) into proximity. Ubiquitin moieties are attached to substrates via an ATP-dependent cascade of E1 ubiquitin-activating enzymes, E2 ubiquitin-conjugating enzymes, and E3 ubiquitin ligases (Varshavsky 2017). K13 is hypothesized to bind a Cullin 3 RING E3 ligase complex (CRL3) via the BTB domain and bind a yet-to-be-identified substrate(s) via the kelch propeller domains (Coppée et al. 2019; Tilley et al. 2016). In this proposed scenario, wild-type K13 binds substrate(s) and allows for CRL3-mediated ubiquitination. In contrast, the K13 propeller domain mutant would be unable to bind substrate(s), preventing CRL3-mediated ubiquitination. Depending on the nature of ubiquitin chain linkages, ubiquitination of substrate(s) can act as a signal for localization, downstream signaling, or proteasome-mediated degradation (Varshavsky 2017).

Mok et al. have provided some evidence to suggest that they were able to link artemisinin resistance to an upregulated “unfolded protein response” pathway involving two major chaperone complexes: *Plasmodium* reactive oxidative stress complex (PROSC) and TCP-1 ring complex (TRiC) (Mok et al. 2015). Recently, mutation of ferredoxin (D97Y) was reported to be strongly associated with artemisinin resistance. Research has shown that ferredoxin is not a direct target of artemisinin, but its mutation may be involved in the protective response against the oxidative stress caused by artemisinin (Kimata-Arigo and Morihisa 2022). It has been shown that nutrient-permeable channels are important for nutrient and drug access and reveal amino acid deprivation as a critical constraint in artemisinin-resistant parasites (Mesén-Ramírez et al. 2021). Some findings elucidate the role of PfGCN5 as a global chromatin regulator of stress responses with a potential role in modulating artemisinin drug resistance and identify PfGCN5 as an important target against artemisinin-resistant parasites (Rawat et al. 2021). Additionally, it has been shown that the autophagy-related gene 18 (ATG18) T38I polymorphism may provide additional resistance against artemisinin derivatives but not partner drugs, even in the absence of kelch13 mutations, and may also be important in parasite survival during nutrient deprivation (Breglio et al. 2018).

11.4 Responding to Artemisinin Resistance

To monitor the occurrence and spread of artemisinin resistance and drug or treatment efficacy, surveillance for artemisinin resistance should combine parasite clearance half-life in vivo, RSA in vitro, and molecular monitoring of resistance gene markers. K13 mutations have been demonstrated to be a useful marker gene for surveillance of resistant parasites in Cambodia by Ariet et al. Artemisinin partial resistance is monitored using an established list of validated and candidate K13 markers associated with decreased sensitivity to artemisinin. Recently, the detection of K13 mutations in Africa, South America, and Oceania suggests the importance of further monitoring K13 mutations to understand artemisinin resistance globally. The proteins that interact with K13 may also be candidate marker genes for new resistance-conferring mutations (Birnbaum et al. 2020; Xie et al. 2016). Several

reports have found that parasites with delayed parasite clearance in Africa were not associated with K13 mutations, which may be due to mutations in other K13 pathway genes (Henriques et al. 2014; Kone et al. 2020; Li et al. 2019; Madamet et al. 2017; Sutherland et al. 2017). Specifically, it would be important to monitor the occurrence of SNPs in EPS15, UBPI, coronin, AP-2 μ , MCA2, KIC7, KIC4, KIC5, ATG18, and possibly PI3K in isolates from patients who present with delayed parasite clearance. Therefore, molecular monitoring of artemisinin resistance could play an important role in providing early warning of the emergence of resistance and could also help us map the spread of ART resistance.

Interventions that decrease the selective advantage of parasites with reduced sensitivity to a drug will slow the spread of drug resistance. Consequently, interventions can be done by using combinations of different drugs, which ensure that drug pressure on a parasite population is not from one drug only and that minimizes the risk that parasites from recrudescence cases are transmitted. It is critical that the right partner drugs were selected, which gives the relatively short window of action of artemisinin. The first-line treatments for *P. falciparum* include artemether lumefantrine (AL), artesunate-pyronaridine (AS-PY), artesunate-amodiaquine (AS-AQ), and dihydroartemisinin-piperaquine (DHA-PPQ) in the WHO African Region. The first-line treatment drugs were AL, artesunate mefloquine (AS-MQ), and chloroquine (CQ) in the WHO Region of the Americas. In the Southeast Asia Region, the first-line treatments were AL, AS-PY, AS-MQ, DHA-PPQ, and artesunate plus sulfadoxine-pyrimethamine (AS+SP). In 2015–2020, AL found high efficacy with all treatments in India, Bangladesh, Brazil, Myanmar, and Columbia. In India, although treatment failure rates with AS+SP remained low, one study from Chhattisgarh State detected a high prevalence of dhfr and dhps, which indicated decreased sensitivity to SP. DHA-PPQ conducted in Indonesia and Myanmar showed high rates of efficacy, with failure rates of less than 5%. In Thailand, where drug efficacy is assessed with integrated drug efficacy surveillance, treatment failure rates with DHA-PPQ plus primaquine in 2018, 2019 and 2020 were all less than 10%, whereas failure rates were high in Sisaket Province, which led the province to change its first-line therapy to AS-PY in 2020. In the Eastern Mediterranean Region, AL and AS+SP remain more efficacious and are the first-line treatments. In the WHO Western Pacific Region, AL, AS-MQ, AS-PY, and DHA-PPQ were the first-line treatments. The first-line treatment of DHA-PPQ was replaced with AS-PY in provinces where high treatment failure rates were observed in Vietnam (WHO, 2021). In addition, optimizing the course of therapy (for example, from 3 to 7 days) may also help us maintain the effect of the drugs (Wang et al. 2019). Triple artemisinin-based combination therapies (TACTs), combining artemisinin with two partner drugs, could be an effective therapy for treating multidrug-resistant malaria, which can prevent the global emergence and spread of artemisinin resistance (van der Pluijm et al. 2021). Furthermore, the use of the gametocytocidal drug (primaquine) might interrupt the transmission of artemisinin-resistant parasites.

Since the number of antimalarial drugs is limited and resistance is emerging, seeking to lower transmission and stop the resistance spread with interventions is

important. Malaria preventive measures must first manage the source of infection, improve epidemic reporting, and eradicate malaria patients and those with malaria parasites. In terms of cutting off the route of transmission, it is mainly to eliminate *Anopheles* mosquitoes, including preventing being bitten by *Anopheles* mosquitoes, using insecticides to remove places where *Anopheles* mosquito larvae breed, using mosquito nets or applying mosquito repellents to avoid being bitten. Currently, new intervention strategies are urgently needed to fight against malaria. Some *Plasmodium*-blocking symbiotic bacteria and their secretion products were identified from *Anopheles sinensis* and could confer mosquito resistance to malarial infection, which might provide a novel vector control tool for blocking the transmission of malaria (Gao et al. 2021; Wang et al. 2017). Drug resistance is a continuing challenge to control and eradicate malaria worldwide, and this scientific question remains a hot research topic. Studies on artemisinin resistance have contributed to a comprehensive understanding of the molecular mechanisms of ART resistance, which are involved in endocytosis, the cellular stress response, and multiple cellular processes (Ross and Fidock 2019). The identification of artemisinin targets and resistance markers offers convenient molecular surveillance tools to detect the emergence and forestall the spread of ART resistance. With the rapid emergence and spread of artemisinin resistance, there is also an urgent need to discover antimalarial drugs with new modes of action and activity against the malaria parasite. Recently, the innovative antimalarial drugs JX21108, compound 11 and JX₃₅ were reported, which are histone deacetylase inhibitors developed from the clinical anticancer drug candidate quisinostat and could cure multiple life-stage and multidrug-resistant *Plasmodium*, indicating that these novel drugs could be used to cure artemisinin-resistant parasites and block malaria transmission in the future (Huang et al. 2020; Li et al. 2021; Wang et al. 2022). Additionally, a new antimalarial drug ASP3026 was developed based on the lysyl-tRNA synthetase (LysRS) novel drug targets of *P. falciparum* (Zhou et al. 2020). Combined efforts in strengthened surveillance, resistance detection, molecular mechanism elucidation of artemisinin resistance, and the development of novel targets and antimalarial drugs will help us to apply more effective antimalarial drug policies, putting us ahead of the curve in the fight against artemisinin resistance.

References

- Afonso A, Hunt P, Cheesman S, Alves AC, Cunha CV, do Rosário V, Cravo P (2006) Malaria parasites can develop stable resistance to artemisinin but lack mutations in candidate genes *atp6* (encoding the sarcoplasmic and endoplasmic reticulum Ca²⁺ ATPase), *tctp*, *mdr1*, and *cg10*. *Antimicrob Agents Chemother* 50:480–489
- Ajogbasile FV, Oluniyi PE, Kayode AT, Akano KO, Adegboyega BB, Philip C, Ogbulafor N, Okafor HU, Oguche S, Wammanda RD, Mokuolu OA, Folarin OA, Happi CT (2022) Molecular profiling of the artemisinin resistance Kelch 13 gene in *plasmodium falciparum* from Nigeria. *PLoS One* 17:e0264548
- Ariey F, Witkowski B, Amaratunga C, Beghain J, Langlois AC, Khim N, Kim S, Duru V, Bouchier C, Ma L, Lim P, Leang R, Duong S, Sreng S, Suon S, Chhor CM, Bout DM,

- Ménard S, Rogers WO, Genton B, Fandeur T, Miotto O, Ringwald P, Le Bras J, Berry A, Barale JC, Fairhurst RM, Benoit-Vical F, Mercereau-Puijalon O, Ménard D (2014) A molecular marker of artemisinin-resistant plasmodium falciparum malaria. *Nature* 505:50–55
- Ashley EA, Dhorda M, Fairhurst RM, Amaratunga C, Lim P, Suon S, Sreng S, Anderson JM, Mao S, Sam B, Sopha C, Chuor CM, Nguon C, Sovannaroeth S, Pukrittayakamee S, Jittamala P, Chotivanich K, Chutasmit K, Suchatsoonthorn C, Runcharoen R, Hien TT, Thuy-Nhien NT, Thanh NV, Phu NH, Htut Y, Han KT, Aye KH, Mokuolu OA, Olaosebikan RR, Folaranmi OO, Mayxay M, Khanthavong M, Hongvanthong B, Newton PN, Onyamboko MA, Fanello CI, Tshefu AK, Mishra N, Valecha N, Phyo AP, Nosten F, Yi P, Tripura R, Borrmann S, Bashraheil M, Peshu J, Faiz MA, Ghose A, Hossain MA, Samad R, Rahman MR, Hasan MM, Islam A, Miotto O, Amato R, MacInnis B, Stalker J, Kwiatkowski DP, Bozdech Z, Jeeyapant A, Cheah PY, Sakulthaew T, Chalk J, Intharabut B, Silamut K, Lee SJ, Vihokhern B, Kunasol C, Imwong M, Tarning J, Taylor WJ, Yeung S, Woodrow CJ, Flegg JA, Das D, Smith J, Venkatesan M, Plowe CV, Stepniewska K, Guerin PJ, Dondorp AM, Day NP, White NJ (2014) Spread of artemisinin resistance in plasmodium falciparum malaria. *N Engl J Med* 371:411–423
- Balikagala B, Fukuda N, Ikeda M, Katuru OT, Tachibana SI, Yamauchi M, Opio W, Emoto S, Anywar DA, Kimura E, Palacpac NMQ, Odongo-Aginya EI, Ogwang M, Horii T, Mita T (2021) Evidence of artemisinin-resistant malaria in Africa. *N Engl J Med* 385:1163–1171
- Birnbaum J, Scharf S, Schmidt S, Jonscher E, Hoeijmakers WAM, Flemming S, Toenhake CG, Schmitt M, Sabitzki R, Bergmann B, Fröhlke U, Mesén-Ramírez P, Blanche Soares A, Herrmann H, Bártfai R, Spielmann T (2020) A Kelch13-defined endocytosis pathway mediates artemisinin resistance in malaria parasites. *Science* 367:51–59
- Boullé M, Witkowski B, Duru V, Sriprawat K, Nair SK, McDew-White M, Anderson TJ, Phyo AP, Menard D, Nosten F (2016) Artemisinin-resistant plasmodium falciparum K13 mutant alleles, Thailand-Myanmar border. *Emerg Infect Dis* 22:1503–1505
- Breglio KF, Amato R, Eastman R, Lim P, Sa JM, Guha R, Ganesan S, Dorward DW, Klumpp-Thomas C, McKnight C, Fairhurst RM, Roberts D, Thomas C, Simon AK (2018) A single nucleotide polymorphism in the Plasmodium falciparum atg18 gene associates with artemisinin resistance and confers enhanced parasite survival under nutrient deprivation. *Malar J* 17:391
- Coppée R, Jeffares DC, Miteva MA, Sabbagh A, Clain J (2019) Comparative structural and evolutionary analyses predict functional sites in the artemisinin resistance malaria protein K13. *Sci Rep* 9:10675
- Gao H, Bai L, Jiang Y, Huang W, Wang L, Li S, Zhu G, Wang D, Huang Z, Li X, Cao J, Jiang L, Jacobs-Lorena M, Zhan S, Wang S (2021) A natural symbiotic bacterium drives mosquito refractoriness to Plasmodium infection via secretion of an antimalarial lipase. *Nat Microbiol* 6: 806–817
- Ghanchi NK, Qurashi B, Raees H, Beg MA (2021) Molecular surveillance of drug resistance: Plasmodium falciparum artemisinin resistance single nucleotide polymorphisms in Kelch protein propeller (K13) domain from Southern Pakistan. *Malar J* 20:176
- Gibbons J, Button-Simons KA, Adapa SR, Li S, Pietsch M, Zhang M, Liao X, Adams JH, Ferdig MT, Jiang RHY (2018) Altered expression of K13 disrupts DNA replication and repair in Plasmodium falciparum. *BMC Genomics* 19:849
- Gnädig NF, Stokes BH, Edwards RL, Kalantarov GF, Heimsch KC, Kuderjavy M, Crane A, Lee MCS, Straimer J, Becker K, Trakht IN, Odom John AR, Mok S, Fidock DA (2020) Insights into the intracellular localization, protein associations and artemisinin resistance properties of Plasmodium falciparum K13. *PLoS Pathog* 16:e1008482
- Henriques G, Hallett RL, Beshir KB, Gadalla NB, Johnson RE, Burrow R, van Schalkwyk DA, Sawa P, Omar SA, Clark TG, Bousema T, Sutherland CJ (2014) Directional selection at the pfmdr1, pfprt, pfubp1, and pfap2mu loci of Plasmodium falciparum in Kenyan children treated with ACT. *J Infect Dis* 210:2001–2008
- Henriques G, Martinelli A, Rodrigues L, Modrzyńska K, Fawcett R, Houston DR, Borges ST, d'Alessandro U, Tinto H, Karema C, Hunt P, Cravo P (2013) Artemisinin resistance in rodent

- malaria—mutation in the AP2 adaptor μ -chain suggests involvement of endocytosis and membrane protein trafficking. *Malar J* 12:118
- Huang Z, Li R, Tang T, Ling D, Wang M, Xu D, Sun M, Zheng L, Zhu F, Min H, Boonhok R, Ding Y, Wen Y, Chen Y, Li X, Chen Y, Liu T, Han J, Miao J, Fang Q, Cao Y, Tang Y, Cui J, Xu W, Cui L, Zhu J, Wong G, Li J, Jiang L (2020) A novel multistage antiparasitic inhibitor targeting plasmodium falciparum histone deacetylase 1. *Cell Discov* 6:93
- Ismail HM, Barton VE, Panchana M, Charoensuthivararakul S, Biagini GA, Ward SA, O'Neill PM (2016) A click chemistry-based proteomic approach reveals that 1,2,4-trioxolane and artemisinin antimalarials share a common protein alkylation profile. *Angew Chem Int Ed Engl* 55:6401–6405
- Jonscher E, Flemming S, Schmitt M, Sabitzki R, Reichard N, Birnbaum J, Bergmann B, Höhn K, Spielmann T (2019) PfVPS45 is required for host cell cytosol uptake by malaria blood stage parasites. *Cell Host Microbe* 25:166–173.e165
- Kimata-Arigo Y, Morihisa R (2022) Effect of artemisinin on the redox system of NADPH/FNR/ferredoxin from malaria parasites. *Antioxidants* (Basel) 11
- Kone A, Sissoko S, Fofana B, Sangare CO, Dembele D, Haidara AS, Diallo N, Coulibaly A, Traore A, Toure S, Haidara K, Sanogo K, Sagara I, Beshir KB, Gil JP, Doumbo OK, Djimde AA (2020) Different Plasmodium falciparum clearance times in two Malian villages following artesunate monotherapy. *Int J Infect Dis* 95:399–405
- Lautu-Gumal D, Razook Z, Koleala T, Nate E, McEwen S, Timbi D, Hetzel MW, Lavu E, Tefuarani N, Makita L, Kazura J, Mueller I, Pomat W, Laman M, Robinson LJ, Barry AE (2021) Surveillance of molecular markers of Plasmodium falciparum artemisinin resistance (kelch13 mutations) in Papua New Guinea between 2016 and 2018. *Int J Parasitol Drugs Drug Resist* 16:188–193
- Li J, Shi Y, Zhang W, Yan H, Lin K, Wei S, Wei H, Yang Y, Huang S, Lu Y, Ma A, Qin J (2019) K13-propeller gene polymorphisms of plasmodium falciparum and the therapeutic effect of artesunate among migrant workers returning to Guangxi, China (2014–2017). *Malar J* 18:349
- Li R, Ling D, Tang T, Huang Z, Wang M, Ding Y, Liu T, Wei H, Xu W, Mao F, Zhu J, Li X, Jiang L, Li J (2021) Discovery of novel Plasmodium falciparum HDAC1 inhibitors with dual-stage antimalarial potency and improved safety based on the clinical anticancer drug candidate Quisinostat. *J Med Chem* 64:2254–2271
- Lisewski AM, Quiros JP, Ng CL, Adikesavan AK, Miura K, Putluri N, Eastman RT, Scandfeld D, Regenbogen SJ, Altenhofen L, Llinás M, Sreekumar A, Long C, Fidock DA, Lichtarge O (2014) Supergenomic network compression and the discovery of EXP1 as a glutathione transferase inhibited by artesunate. *Cell* 158:916–928
- Lu F, Culleton R, Zhang M, Ramaprasad A, von Seidlein L, Zhou H, Zhu G, Tang J, Liu Y, Wang W, Cao Y, Xu S, Gu Y, Li J, Zhang C, Gao Q, Menard D, Pain A, Yang H, Zhang Q, Cao J (2017) Emergence of indigenous artemisinin-resistant plasmodium falciparum in Africa. *N Engl J Med* 376:991–993
- Madamet M, Kounta MB, Wade KA, Lo G, Diawara S, Fall M, Bercion R, Nakoulima A, Fall KB, Benoit N, Gueye MW, Fall B, Diatta B, Pradines B (2017) Absence of association between polymorphisms in the K13 gene and the presence of Plasmodium falciparum parasites at day 3 after treatment with artemisinin derivatives in Senegal. *Int J Antimicrob Agents* 49:754–756
- Mbengue A, Bhattacharjee S, Pandharkar T, Liu H, Estiu G, Stahelin RV, Rizk SS, Njimoh DL, Ryan Y, Chotivanich K, Nguon C, Ghorbal M, Lopez-Rubio JJ, Pfrender M, Emrich S, Mohandas N, Dondorp AM, Wiest O, Haldar K (2015) A molecular mechanism of artemisinin resistance in Plasmodium falciparum malaria. *Nature* 520:683–687
- Mesén-Ramírez P, Bergmann B, Elhabiri M, Zhu L, von Thien H, Castro-Peña C, Gilberger TW, Davioud-Charvet E, Bozdech Z, Bachmann A, Spielmann T (2021) The parasitophorous vacuole nutrient channel is critical for drug access in malaria parasites and modulates the artemisinin resistance fitness cost. *Cell Host Microbe* 29:1774–1787.e1779
- Mishra N, Bharti RS, Mallick P, Singh OP, Srivastava B, Rana R, Phookan S, Gupta HP, Ringwald P, Valecha N (2016) Emerging polymorphisms in falciparum Kelch 13 gene in Northeastern region of India. *Malar J* 15:583

- Mok S, Ashley EA, Ferreira PE, Zhu L, Lin Z, Yeo T, Chotivanich K, Imwong M, Pukrittayakamee S, Dhorda M, Nguon C, Lim P, Amaratunga C, Suon S, Hien TT, Htut Y, Faiz MA, Onyamboko MA, Mayxay M, Newton PN, Tripura R, Woodrow CJ, Miotto O, Kwiatkowski DP, Nosten F, Day NP, Preiser PR, White NJ, Dondorp AM, Fairhurst RM, Bozdech Z (2015) Drug resistance. Population transcriptomics of human malaria parasites reveals the mechanism of artemisinin resistance. *Science* 347:431–435
- Mok S, Stokes BH, Gnädig NF, Ross LS, Yeo T, Amaratunga C, Allman E, Solyakov L, Bottrill AR, Tripathi J, Fairhurst RM, Llinás M, Bozdech Z, Tobin AB, Fidock DA (2021) Artemisinin-resistant K13 mutations rewire *Plasmodium falciparum*'s intra-erythrocytic metabolic program to enhance survival. *Nat Commun* 12:530
- Na-Bangchang K, Karbwang J (2013) Emerging artemisinin resistance in the border areas of Thailand. *Expert Rev Clin Pharmacol* 6:307–322
- Nima MK, Mukherjee A, Sazed SA, Hossainey MRH, Phru CS, Johora FT, Safeukui I, Saha A, Khan AA, Marma ASP, Ware RE, Mohandas N, Calhoun B, Haque R, Khan WA, Alam MS, Haldar K (2022) Assessment of *plasmodium falciparum* artemisinin resistance independent of kelch13 polymorphisms and with escalating malaria in Bangladesh. *MBio* 13:e0344421
- Noeld H, Se Y, Schaecher K, Smith BL, Socheat D, Fukuda MM (2008) Evidence of artemisinin-resistant malaria in western Cambodia. *N Engl J Med* 359:2619–2620
- Paloque L, Coppée R, Stokes BH, Gnädig NF, Niaré K, Augereau JM, Fidock DA, Clain J, Benoit-Vical F (2022) Mutation in the *plasmodium falciparum* BTB/POZ domain of K13 protein confers artemisinin resistance. *Antimicrob Agents Chemother* 66:e0132021
- van der Pluijm RW, Amaratunga C, Dhorda M, Dondorp AM (2021) Triple artemisinin-based combination therapies for malaria—a new paradigm? *Trends Parasitol* 37:15–24
- Rawat M, Kanyal A, Sahasrabudhe A, Vembar SS, Lopez-Rubio JJ, Karmodiya K (2021) Histone acetyltransferase PfGCN5 regulates stress responsive and artemisinin resistance related genes in *Plasmodium falciparum*. *Sci Rep* 11:852
- Rocamora F, Zhu L, Liang KY, Dondorp A, Miotto O, Mok S, Bozdech Z (2018) Oxidative stress and protein damage responses mediate artemisinin resistance in malaria parasites. *PLoS Pathog* 14:e1006930
- Ross LS, Fidock DA (2019) Elucidating mechanisms of drug-resistant *plasmodium falciparum*. *Cell Host Microbe* 26:35–47
- Schmedes SE, Patel D, Dhal S, Kelley J, Savigel SS, Dimbu PR, Adeothy AL, Kahunu GM, Nkoli PM, Beavogui AH, Kariuki S, Mathanga DP, Koita O, Ishengoma D, Mohamad A, Hawela M, Moriarty LF, Samuels AM, Gutman J, Plucinski MM, Udhayakumar V, Zhou Z, Lucchi NW, Venkatesan M, Halsey ES, Talundzic E (2021) *Plasmodium falciparum* kelch 13 mutations, 9 countries in Africa, 2014–2018. *Emerg Infect Dis* 27:1902–1908
- Siddiqui FA, Boonhok R, Cabrera M, Mbenda HGN, Wang M, Min H, Liang X, Qin J, Zhu X, Miao J, Cao Y, Cui L (2020) Role of *plasmodium falciparum* Kelch 13 protein mutations in *P. falciparum* populations from Northeastern Myanmar in mediating artemisinin resistance. *MBio*:11
- Sutherland CJ, Lansdell P, Sanders M, Muwanguzi J, van Schalkwyk DA, Kaur H, Nolder D, Tucker J, Bennett HM, Otto TD, Berriman M, Patel TA, Lynn R, Gkrania-Klotsas E, Chiodini PL (2017) pfk13-independent treatment failure in four imported cases of *plasmodium falciparum* malaria treated with artemether-lumefantrine in the United Kingdom. *Antimicrob Agents Chemother*:61
- Tacoli C, Gai PP, Bayingana C, Sift K, Geus D, Ndoli J, Sendegeya A, Gahutu JB, Mockenhaupt FP (2016) Artemisinin resistance-associated K13 polymorphisms of *plasmodium falciparum* in southern Rwanda, 2010–2015. *Am J Trop Med Hyg* 95:1090–1093
- Tang T, Xu Y, Cao L, Tian P, Shao J, Deng Y, Zhou H, Xiao B (2021) Ten-year molecular surveillance of drug-resistant *plasmodium* spp. isolated from the China-Myanmar border. *Front Cell Infect Microbiol* 11:733788
- Thanh NV, Thuy-Nhien N, Tuyen NT, Tong NT, Nha-Ca NT, Dong LT, Quang HH, Farrar J, Thwaites G, White NJ, Wolbers M, Hien TT (2017) Rapid decline in the susceptibility of

- plasmodium falciparum to dihydroartemisinin-piperaquine in the south of Vietnam. *Malar J* 16:27
- Tilley L, Straimer J, Gnädig NF, Ralph SA, Fidock DA (2016) Artemisinin action and resistance in *Plasmodium falciparum*. *Trends Parasitol* 32:682–696
- Tun KM, Imwong M, Lwin KM, Win AA, Hlaing TM, Hlaing T, Lin K, Kyaw MP, Plewes K, Faiz MA, Dhorda M, Cheah PY, Pukrittayakamee S, Ashley EA, Anderson TJ, Nair S, McDew-White M, Flegg JA, Grist EP, Guerin P, Maude RJ, Smithuis F, Dondorp AM, Day NP, Nosten F, White NJ, Woodrow CJ (2015) Spread of artemisinin-resistant *Plasmodium falciparum* in Myanmar: a cross-sectional survey of the K13 molecular marker. *Lancet Infect Dis* 15:415–421
- Varshavsky A (2017) The ubiquitin system, autophagy, and regulated protein degradation. *Annu Rev Biochem* 86:123–128
- Wang J, Xu C, Liao FL, Jiang T, Krishna S, Tu Y (2019) A temporizing solution to "artemisinin resistance". *N Engl J Med* 380:2087–2089
- Wang M, Tang T, Li R, Huang Z, Ling D, Zheng L, Ding Y, Liu T, Xu W, Zhu F, Min H, Boonhok R, Mao F, Zhu J, Li X, Jiang L, Li J (2022) Drug repurposing of Quisinostat to discover novel *plasmodium falciparum* HDAC1 inhibitors with enhanced triple-stage antimalarial activity and improved safety. *J Med Chem* 65:4156–4181
- Wang S, Dos-Santos ALA, Huang W, Liu KC, Oshaghi MA, Wei G, Agre P, Jacobs-Lorena M (2017) Driving mosquito refractoriness to *Plasmodium falciparum* with engineered symbiotic bacteria. *Science* 357:1399–1402
- Wang Z, Shrestha S, Li X, Miao J, Yuan L, Cabrera M, Grube C, Yang Z, Cui L (2015a) Prevalence of K13-propeller polymorphisms in *plasmodium falciparum* from China-Myanmar border in 2007–2012. *Malar J* 14:168
- Wang Z, Wang Y, Cabrera M, Zhang Y, Gupta B, Wu Y, Kemirembe K, Hu Y, Liang X, Brashear A, Shrestha S, Li X, Miao J, Sun X, Yang Z, Cui L (2015b) Artemisinin resistance at the China-Myanmar border and association with mutations in the K13 propeller gene. *Antimicrob Agents Chemother* 59:6952–6959
- Witkowski B, Amaratunga C, Khim N, Sreng S, Chim P, Kim S, Lim P, Mao S, Sopha C, Sam B, Anderson JM, Duong S, Chuor CM, Taylor WR, Suon S, Mercereau-Pujalon O, Fairhurst RM, Menard D (2013) Novel phenotypic assays for the detection of artemisinin-resistant *plasmodium falciparum* malaria in Cambodia: in-vitro and ex-vivo drug-response studies. *Lancet Infect Dis* 13:1043–1049
- WHO (2020) World Malaria Report 2020
- WHO (2021) World Malaria Report 2021
- Witkowski B, Lelièvre J, Nicolau-Travers ML, Iriart X, Njomnang Soh P, Bousejra-Elgarah F, Meunier B, Berry A, Benoit-Vical F (2012) Evidence for the contribution of the hemozoin synthesis pathway of the murine *Plasmodium yoelii* to the resistance to artemisinin-related drugs. *PLoS One* 7:e32620
- Xie SC, Dogovski C, Hanssen E, Chiu F, Yang T, Crespo MP, Stafford C, Batinovic S, Teguh S, Charman S, Klonis N, Tilley L (2016) Haemoglobin degradation underpins the sensitivity of early ring stage *Plasmodium falciparum* to artemisinins. *J Cell Sci* 129:406–416
- Zhang J, Li N, Siddiqui FA, Xu S, Geng J, Zhang J, He X, Zhao L, Pi L, Zhang Y, Li C, Chen X, Wu Y, Miao J, Cao Y, Cui L, Yang Z (2019) In vitro susceptibility of *Plasmodium falciparum* isolates from the China-Myanmar border area to artemisinins and correlation with K13 mutations. *Int J Parasitol Drugs Drug Resist* 10:20–27
- Zhou J, Huang Z, Zheng L, Hei Z, Wang Z, Yu B, Jiang L, Wang J, Fang P (2020) Inhibition of *plasmodium falciparum* Lysyl-tRNA synthetase via an anaplastic lymphoma kinase inhibitor. *Nucleic Acids Res* 48:11566–11576



Traditional Chinese Medicines for Malaria Therapy

12

Changhua Lu, Lilei Wang, and Wei Wang

Abstract

Malaria, one of the “big three” killer diseases, is a major public health problem as well as a major cause of mortality and morbidity worldwide. The goals of the global malaria elimination program mainly include (1) to reduce malaria case incidence by at least 90% by 2030; (2) to reduce malaria mortality rates by at least 90% by 2030; (3) to eliminate malaria in at least 35 countries by 2030; and (4) to prevent a resurgence of malaria in all malaria-free countries. Currently, the malaria elimination strategy mainly depends on chemotherapy, and the currently available antimalarials are mainly divided into four categories according to the chemical structure and mechanism of drug actions, including arylamino alcohol compounds, 8-aminoquinolines, antifolate compounds, artemisinins, and other agents. Artemisinin, a sesquiterpene lactone extracted from the Chinese medicinal herb *A. annua*, has been recommended as the first-choice treatment for malaria by the World Health Organization. However, the rapid emergence of artemisinin resistance in malaria parasites urges the development of novel treatments during the stage toward malaria elimination in the world. Previous studies have shown the effectiveness and safety of traditional Chinese medicines for the treatment of parasitic diseases, including malaria. In this chapter, we

C. Lu

Yixing Hospital of Traditional Chinese Medicine, Yixing City, Jiangsu Province, China

L. Wang

Shandong Institute of Parasitic Diseases, Shandong First Medical University & Shandong Academy of Medical Sciences, Jining City, Shandong Province, China

W. Wang (✉)

National Health Commission Key Laboratory of Parasitic Disease Prevention and Control, Jiangsu Provincial Key Laboratory of Parasite and Vector Control Technology, Jiangsu Institute of Parasitic Diseases, Wuxi City, Jiangsu Province, China

e-mail: wangwei@jjpd.com

discuss other traditional Chinese medicines that show potential value for malaria treatment except artemisinins. The crude extracts and pure compounds from ginger, garlic, the Asteraceae family, *Bupleuri radix* and *Daphne* spp. have shown in vitro and in vivo anti-*Plasmodium* activities, and some have been tested for their antimalarial actions in malaria patients. Further randomized, controlled clinical trials to examine the efficacy and safety of traditional Chinese medicine for the treatment of malaria and to unravel the underlying mechanisms seem justified.

Keywords

Malaria · Traditional Chinese medicine · Artemisinin · Ginger · Garlic · Asteraceae · *Bupleuri radix* · *Daphne* · Antimalarial activity

12.1 Introduction

Malaria is an acute, febrile, life-threatening, mosquito-borne parasitic disease caused by infection with the genus *Plasmodium*, which is transmitted to humans through the bites of *Plasmodium*-infected female *Anopheles* mosquitoes (Ashley et al. 2018). Although more than 200 species of *Plasmodium* have been identified, there are only five *Plasmodium* species that may naturally infect humans and cause human malaria, with *P. falciparum* as the deadliest malaria parasite and the most prevalent on the African continent, *P. vivax* as the most widespread malaria parasite and the dominant malaria parasite outside of sub-Saharan Africa (Sato 2021). Malaria, together with human immunodeficiency virus (HIV)/AIDS and tuberculosis (TB), has been recognized as the “big three” killer diseases in the world (Parola 2013), which is a major public health problem as well as a major cause of mortality and morbidity in the world (Phillips et al. 2017). According to the World Malaria Report 2021 released by the World Health Organization (WHO), approximately 241 million cases were estimated to have malaria, and 627,000 deaths occurred due to malaria in the world in 2020, with 95% of malaria cases and 96% of mortality due to malaria reported in sub-Saharan Africa; more importantly, almost half of the world’s population was estimated to be at risk of malaria infections in 2020 (WHO 2021a).

The global decline in malaria morbidity and mortality during the 20-year period between 2000 and 2019 led to ambitious targets set for the global malaria elimination program by the WHO, including (1) to reduce malaria case incidence by at least 90% by 2030; (2) to reduce malaria mortality rates by at least 90% by 2030; (3) to eliminate malaria in at least 35 countries by 2030; and (4) to prevent a resurgence of malaria in all countries that are malaria-free (WHO 2021b). However, the global COVID-19 pandemic (Hogan et al. 2020; Rogerson et al. 2020; Sherrard-Smith et al. 2020) and the spread of insecticide resistance and antimalarial drug resistance pose great threats to the agenda for malaria elimination (Achan et al. 2018; Lindsay et al. 2021).

Currently, the malaria elimination strategy mainly depends on chemotherapy, and the primary goal of malaria therapy is to achieve rapid, complete removal of malaria parasites to prevent an uncomplicated malaria case from progressing to severe disease or death (Shrivastava et al. 2021). The currently available antimalarials are mainly divided into four categories according to the chemical structure and mechanism of drug actions, including arylamino alcohol compounds (quinine, quinidine, chloroquine, amodiaquine, mefloquine, halofantrine, piperazine, and lumefantrine), 8-aminoquinolines (primaquine and tafenoquine), antifolate compounds (sulfadoxine, pyrimethamine, proguanil, chlorproguanil, and trimethoprim), artemisinins (artemisinin, artesunate, artemether, β -arteether, and dihydroartemisinin), and other agents (atovaquone and antibacterial drugs such as tetracycline, doxycycline, and clindamycin) (Na-Bangchang and Karbwang 2019).

Artemisinins, also known as Qinghaosu, are sesquiterpene lactones that are extracted from the dried leaves or flower clusters of the sweet wormwood plant *Artemisia annua* (Qinghao), a Chinese herb used for traditional Chinese medicines (Li 2012). The antipyretic action of the plant was first documented in “A Handbook of Prescriptions for Emergencies” by a Chinese physician Hong Ge in the fourth century CE (Hsu 2006). In the early 1970s, artemisinin, the active ingredient of *A. annua*, was identified by Youyou Tu, who shared the 2015 Nobel Prize in Physiology or Medicine (Ma et al. 2020), and the discovery of artemisinin was considered a great contribution to traditional Chinese medicine to the world (Tu 2016). Currently, artemisinin is the most common agent used for malaria control and plays a critical role in the treatment of malaria throughout the world (Martino et al. 2019), and artemisinin-based combination therapy (ACT) has been recommended by the WHO as the first-line treatment for uncomplicated falciparum malaria worldwide (Sinclair et al. 2009). The efficacy and safety of artemisinins against malaria have been extensively tested, and the description of artemisinin treatments for malaria and artemisinin resistance in malaria parasites has been detailed in Chaps. 10 and 11. Hereby, we discuss other traditional Chinese medicines that show potential value for malaria treatment.

12.2 Ginger

Ginger, rhizomes of *Zingiber officinale*, an herbal medicinal plant of the family Zingiberaceae, has been widely used as a spice, flavoring, food, and medicine (Anh et al. 2020). Previous studies have shown that ginger exhibits a variety of pharmacological actions, including antioxidant, antiparasitic, anti-inflammatory, antiemetic, pesticidal, and antimicrobial activities (Ali et al. 2008). The ethyl acetate extract from *Z. officinale* presented 10 and 10 $\mu\text{g/mL}$ IC_{50} values against chloroquine-sensitive and chloroquine-resistant strains of *P. falciparum*, respectively, with a 50% cytotoxic concentration (TC_{50}) of 35 $\mu\text{g/mL}$ against HeLa cells (Kaushik et al. 2013). Administration of the methanol crude extract of *Zingiber officinale* at doses of 250, 500, and 1000 mg/kg resulted in $(80.03 \pm 0.84)\%$, $(76.31 \pm 1.49)\%$, and $(67.06 \pm 1.03)\%$ parasitemia percentages, $(19.87 \pm 0.84)\%$,

(23.49 ± 1.47)%, and (32.83 ± 1.03)% chemosuppression percentages, and (6.28 ± 0.2), (6.38 ± 0.24), and (7.33 ± 0.51) days of survival in mice infected with the chloroquine-sensitive *P. berghei* strain ANKA, indicating that *Zingiber officinale* shows activities against *P. berghei* in a dose-dependent manner (Biruksew et al. 2018). *C. xanthorrhiza* rhizome extracts displayed 100% inhibitory activity against *P. falciparum* (Murnigsih et al. 2005). Administration of ginger-partitioned moxibustion given once every 3 days for five treatments achieved cure in 31 cases and improvements in 8 cases, showing an overall effective rate of 92.9% among malaria patients in the Republic of Congo (Li 2011). In addition, ginger is one of the most commonly used Chinese herbs for the self-treat of malaria in Ethiopia (Kovalev and Wells 2020).

12.3 Garlic

Garlic (*Allium sativum*), an edible perennial plant of the family Amaryllis, is one of the most important bulb vegetables that has a pungent flavor and has been widely used as a spice and flavoring agent all over the world and has been used for the treatment of diseases for thousands of years (Bayan et al. 2014). Previous studies have shown that garlic exhibits a variety of pharmacological actions, including antibacterial, antifungal, anti-protozoal, antiviral, antioxidant and anti-inflammatory, anticancer, anti-Alzheimer's disease, anti-metabolic, and antihypertensive activities (El-Saber Batiha et al. 2020). Administration of ajoene (4,5,9-trithiadodeca-1,6,11-triene 9-oxide), a product initially isolated from extracts of garlic at a single dose of 50 mg/kg, suppressed the development of parasitemia in a murine model of *P. berghei* with no obvious acute toxic effects tested, and combined treatment with ajoene at a dose of 50 mg/kg and chloroquine at a dose of 4.5 mg/kg completely prevented the development of parasitemia (Perez et al. 1994). Oral administration of the ethanol solution of allicin, a major active principle of garlic, given at a dose of 3 or 9 mg/kg on days 0–2 postinfection resulted in a clear-cut reduction in the 5-day parasitemia (27.1% for the 3 mg/kg dose group and 32.6% for the 9 mg/kg dose group), and a further decline of the 7-day parasitemia in BALB/c mice infected with the *P. yoelii* 17XL strain, and treatment with the ethanol solution of allicin at a dose of 3 ($P < 0.05$ vs. infected but untreated controls) or 9 mg/kg ($P < 0.01$ vs. infected but untreated controls) significantly prolonged the survival period of infected mice (Feng et al. 2012). Injection of aqueous allicin solutions decreased *P. yoelii* infections in mice, and treatment of sporozoites with aqueous allicin solutions prior to injection completely prevented malaria infections, while a 4-day treatment with allicin resulted in a remarkable reduction in parasitemias and extension of the survival period in infected mice (Coppi et al. 2006). In addition, the combination of garlic and artemisinin derivatives achieved a higher antimalarial activity and longer survival period than garlic or artemisinin derivatives in parasite-infected mice (Ounjaijean and Somsak 2022; Palakkod Govindan et al. 2016; Vathsala and Krishna Murthy 2020).

In addition, there are clinical reports showing the potential of garlic for malaria treatment. Among 447 Ethiopian children under the age of 5 years who had had a recent episode of fever, 95 (22.2%) had used medicinal plants as their first-choice treatment, and garlic decoction was the most commonly used herbal medicine; in addition, the administration of garlic decoction resulted in cure in 51.4% of children (18/35) and improvements in 48.6% of children (17/35) (Gurmu et al. 2018). Following treatment with garlic ointment 2 hours prior to the disease episode and removal after the episode, the clinical episode of *P. vivax* malaria ceased on the day of treatment, and 1-month follow-up showed no more episodes (Feng 1972). In the Nsukka Local Government Area, southeastern Nigeria, 0.94% of the study subjects (2/213) used cold maceration with garlic for malaria treatment (Odoh et al. 2018). Further randomized, controlled clinical trials to test the efficacy and safety of garlic for malaria treatment are warranted.

12.4 Asteraceae

The Asteraceae family is one of the largest angiosperm families and contains more than 1620 genera and 23,600 species of herbaceous plants, shrubs, and trees in the world (Carvalho Jr et al. 2018). The Asteraceae family members, which have been used for ornamentals, diet, and folk medicine for centuries, have shown potent antioxidant, anti-inflammatory, antimicrobial, diuretic, and wound-healing properties (Rolnik and Olas 2021). A recent systematic review of published articles retrieved from electronic databases, including PubMed, Web of Knowledge, ScienceDirect, and Saudi Digital Library and MSc/PhD. These results revealed that the medicinal plants of the Asteraceae family are the most abundant for use in laboratory tests for antimalarial activity against murine blood-stage malaria (Dkhil et al. 2021). Treatment with the ethyl acetate extract from *Chrysanthemum morifolium* at a dose of 100 mg/mL was found to inhibit the growth of *P. falciparum* in erythrocytes (Wu et al. 1995). Intraperitoneal injection of ethanol and chloroform extracts of *Chrysanthemum morifolium* at doses of 0.6 and 1.4 g/kg was found to achieve 6.25%, 12.05%, 4.25%, 2.11% and 1.56% and 2.52%, 5.64%, 2.08%, 2.17% and 0.68% parasitemias on days 1, 2, 3, 4, and 5 at the erythrocytic stage of *P. berghei* in infected mice (Zhao et al. 1996a), and intraperitoneal injection of the chloroform extract of *C. morifolium* at a dose of 1.4 g/kg was found to inhibit the development of *P. berghei* gametocytes into oocysts and infected sporozoites in *Anopheles stephensi* (Zhao et al. 1996b). Intraperitoneal injection of the chloroform extract of *C. morifolium* at a dose of 700 mg/kg resulted in inhibition of the development of exoerythrocytic stage *P. yoelii* in rats (Zhao et al. 1996c, 1996d). In addition, intraperitoneal injection of the alcohol extract from *C. morifolium* inhibited the development of erythrocytic stage *P. yoelii* (Zhao et al. 1997a), and intraperitoneal injection of the chloroform extract from *C. morifolium* inhibited the development of exoerythrocytic stage *P. yoelii* (Zhao et al. 1997b). The leaf extract of *C. indicum* showed 20 and 19 $\mu\text{g/mL}$ IC_{50} values against chloroquine-sensitive and chloroquine-resistant strains of *P. falciparum*, a TC_{50} of >100 $\mu\text{g/mL}$ against

HeLa cells and a TC_{50}/IC_{50} ratio of >5 , indicating that *C. indicum* may serve as an antimalarial agent even in its crude form (Kamaraj et al. 2012). In Ethiopia, the Asteraceae family is the most commonly used traditional herbal medicine for antimalarial uses (Suleman et al. 2018).

12.5 *Daphne* spp.

Daphne, a genus containing 70–95 species of deciduous and evergreen shrubs in the family Thymelaeaceae, is noted for its scented flowers and often brightly colored berries (Moshiashvili et al. 2020). Daphnetin (7,8-dihydroxycoumarin), a coumarin derivative extracted from and one of the major bioactive components isolated from the genus *Daphne*, such as *D. giraldii*, *D. marginate*, and *D. odora*, has shown a wide range of pharmacological actions, including anti-inflammatory, antioxidative, anticancer, depigmenting, analgesic, anti-arthritic, antipyretic, neuroprotective, and antimalarial properties (Du et al. 2014; Javed et al. 2022; Wang et al. 2019).

The antimalarial activity of daphnetin was first documented in 1992 (Yang et al. 1992). An in vitro assay showed that treatment with daphnetin at concentrations of 25–40 $\mu\text{mol/L}$ resulted in 50% inhibition of ^3H -hypoxanthine incorporation by *P. falciparum*, with its antimalarial activity suppressed by the addition of iron, and administration of daphnetin was found to significantly prolong the survival period of *P. yoelii*-infected mice (Yang et al. 1992). Treatment with daphnetin at concentrations of 1, 2, 4, 8, and 10 $\mu\text{mol/L}$ showed in vitro activity against *P. falciparum* schistocytes in a dose-dependent manner, which was comparable to chloroquine treatment, and oral administration of daphnetin at doses of 1, 10, 50, and 100 mg/kg 4 hours postinfection once daily for four consecutive days resulted in 15%, 31%, 74%, and 72% reductions in parasitemias and prolonged the survival period from (8.1 ± 2.8) days in controls to (8.7 ± 4.3) , (8.9 ± 2.9) , (24.9 ± 8.4) , and (22.2 ± 10.2) days in *P. yoelii*-infected mice, while intraperitoneal injection of daphnetin at doses of 1, 10, 50, and 100 mg/kg 4 hours postinfection once daily for four consecutive days resulted in 15%, 73%, 88%, and 91% reductions in parasitemias and prolonged the survival period from (8.8 ± 5.2) days in controls to (11.5 ± 8.1) , (23.6 ± 10.5) , (24.7 ± 11.2) and (27.4 ± 8.2) days in *P. yoelii*-infected mice (Wang et al. 2000). Following oral administration of daphnetin at doses of 10, 50, and 100 mg/kg 0.5 h postinfection for four consecutive days, no *P. yoelii* infection was detected in mice 7 days posttreatment, and there were $(9.16 \pm 7.35)\%$, $(10.98 \pm 6.71)\%$, and $(9.4 \pm 10.84)\%$ of erythrocytes infected with *P. yoelii* compared with $(13.08 \pm 11.91)\%$ of erythrocytes infected with *P. yoelii* in controls, indicating that treatment with daphnetin alone presents no activity against the exo-erythrocytic stage *P. yoelii*; however, the combination of daphnetin at a dose of 50 mg/kg and primaquine at a dose of 5 mg/kg achieved a comparable activity against the exo-erythrocytic stage *P. yoelii* with treatment with primaquine alone at a dose of 10 mg/kg (Liu et al. 2001). Treatment with daphnetin at doses of 1, 4, 8, and 12 $\mu\text{mol/L}$ resulted in 45.2%, 67.7%, 80%, and 88.5% reductions in the numbers of *P. falciparum*-infected erythrocytes, showing dose-dependent

schizontocidal activity; however, this activity was inhibited by Fe^{2+} (Mu et al. 2002), while exposure to daphnetin at a concentration of 4 $\mu\text{mol/L}$ resulted in a significant reduction in the total superoxide dismutase (SOD) activity in *P. falciparum* (13.73 ± 2.23 vs. 34.26 ± 3.33 U/mg protein in the control, $P < 0.01$), which was reversed by desferrioxamine B, and daphnetin treatment caused a reduction in the DNA synthesis rate 1 ($18.6\% \pm 2.8\%$ vs. $20\% \pm 4.5\%$), 6 ($27.4\% \pm 4.8\%$ vs. $28.5\% \pm 1.9\%$), 15 ($41.8\% \pm 1.9\%$ vs. $50\% \pm 2.4\%$), 21 ($54.1\% \pm 5.2\%$ vs. $85.8\% \pm 6\%$), and 26 hours posttreatment ($65\% \pm 2.9\%$ vs. 100%) relative to controls (Mu et al. 2003). Similar antimalarial activity of daphnetin was observed in subsequent in vitro and in vivo assays (Wang et al. 2004a), and the daphnetin-artemether combination was found to result in a higher antimalarial activity against *P. berghei* than daphnetin and artemether alone in mice (Guo et al. 2004). The recrystallized and crude daphnetins showed median effective doses (ED_{50} values) of 18.36 mg/kg (95% CI: 5.96–56.54 mg/kg) and 11.46 mg/kg (95% CI: 8.63–15.22 mg/kg) against *P. berghei* schizonts (Wang et al. 2004b), and two daphnetin derivatives, DA79 and DA78, both showed potent in vitro activity against *P. falciparum* (Huang et al. 2006a, 2008a). In addition, daphnetin treatment resulted in the suppression of cytochrome C oxidase and ribonucleotide reductase activity in *P. falciparum* (Huang et al. 2006b, 2008b). Further randomized, controlled clinical trials to test the clinical efficacy and safety of daphnetin against malaria are encouraged.

12.6 Bupleuri Radix

Bupleuri radix, also known as Chaihu, a large genus of annual or perennial herbs or woody shrubs belonging to the family Apiaceae, is one of the most commonly used herbs in Chinese herbal medicine, and the crude extracts and pure compounds from *B. radix* have shown a wide range of pharmacological actions, such as anti-inflammatory, anticancer, antipyretic, antimicrobial, antiviral, hepatoprotective, neuroprotective, and immunomodulatory activities (Yang et al. 2017). As a traditional Chinese medicinal herb for more than 2000 years in China and other Asian countries, *B. radix* has been used as an antipyretic agent for thousands of years (Yuan et al. 2017), and *B. radix* prescribed in decoction formulations has been used for malaria therapy for decades (Chen 1959; Li 1954; Ruo and Sui 1956). Among 44 malaria cases (39 cases with *P. vivax* malaria and 5 cases with *P. malariae* malaria), administration of Chaihu decoctions was found to result in fever abatement among 36 cases within 3 days and 8 cases within 4–6 days posttreatment, and 25% malaria recurrence was observed during the follow-up period 26–75 days posttreatment, with no adverse events reported (Li 1960). Oral administration of Xiaochaihu Decoction 4–5 hours prior to the episode for two consecutive days resulted in a complete cure of 13 cases with *P. vivax* malaria and one case with *P. malariae* malaria, and no recurrence was found during the 16-year follow-up (Liu 1976). In a pregnant woman in the second trimester, malaria parasites were not detected in blood following four doses of Xiaochaihu Decoction, with a healthy female child delivered

4 months posttreatment, and no recurrence was observed during the 2-year follow-up period (Yong 1994). In addition, the results from a randomized, controlled clinical trial showed that the mean duration of fever abatement (25.8 ± 8.6 vs. 48.8 ± 16.3 h, $P < 0.05$), mean duration of malaria-associated symptoms (5.2 ± 1.2 vs. 7.7 ± 2 days, $P < 0.05$) and mean duration of hospital stay (7.8 ± 1.9 vs. 11.3 ± 2.8 days, $P < 0.05$) were all significantly shorter among severe malaria patients in the artesunate-Xiaochaihu combination group than in the artesunate group, while a significantly higher overall response rate was observed in the combination group than in the artesunate group (95.7% vs. 87.8%, $P < 0.05$) (Gao et al. 2019).

12.7 Concluding Remarks

Artemisinin, a sesquiterpene lactone extracted from the Chinese medicinal herb *A. annua*, has been widely accepted as a miracle of traditional Chinese medicine (Kong and Tan 2015; Wang and Liang 2016) since it presents a variety of pharmacological actions beyond antimalarials, including antiviral, antiparasitic, antifungal, anti-inflammatory, anticancer, and immunoregulatory activities (Ho et al. 2014; Meng et al. 2021). Since 2006, the WHO has recommended artemisinin as the first-choice treatment for malaria; however, the rapid emergence of artemisinin resistance in malaria parasites urges the development of novel treatments during the stage toward malaria elimination in the world (Martino et al. 2019).

Previous studies have shown the effectiveness and safety of traditional Chinese medicines for the treatment of parasitic diseases, including malaria (Mehlhorn et al. 2014). The crude extracts and pure compounds from ginger, garlic, the Asteraceae family, *Bupleuri radix* and *Daphne* spp. have shown in vitro and in vivo anti-*Plasmodium* activities, and some have been tested for their antimalarial actions in malaria patients. In addition, *Piper tuberculatum* (Oliveira et al. 2018) and *Dichroa febrifuga* (Zhao 1986) were reported to be active against *Plasmodium* species. Further randomized, controlled clinical trials to examine the efficacy and safety of traditional Chinese medicine for the treatment of malaria and to unravel the underlying mechanisms seem justified.

Acknowledgments The study was supported by Wuxi Municipal Health Commission.

Conflicts of Interest The authors declare no conflicts of interest.

References

- Achan J, Mwesigwa J, Edwin CP, D'alessandro U (2018) Malaria medicines to address drug resistance and support malaria elimination efforts. *Expert Rev Clin Pharmacol* 11:61–70
- Ali BH, Blunden G, Tanira MO, Nemmar A (2008) Some phytochemical, pharmacological and toxicological properties of ginger (*Zingiber officinale* Roscoe): a review of recent research. *Food Chem Toxicol* 46:409–420

- Anh NH, Kim SJ, Long NP, Min JE, Yoon YC, Lee EG, Kim M, Kim TJ, Yang YY, Son EY, Yoon SJ, Diem NC, Kim HM, Kwon SW (2020) Ginger on human health: a comprehensive systematic review of 109 randomized controlled trials. *Nutrients* 12:157
- Ashley EA, Pyae Phyo A, Woodrow CJ (2018) Malaria. *Lancet* 391:1608–1621
- Bayan L, Koulivand PH, Gorji A (2014) Garlic: a review of potential therapeutic effects. *Avicenna J Phytomed* 4:1–14
- Biruksew A, Zeynudin A, Alemu Y, Golassa L, Yohannes M, Debella A, Urge G, De Spiegeleer B, Suleman S (2018) *Zingiber officinale* Roscoe and *Echinops kebericho* Mesfin showed antiplasmodial activities against *Plasmodium berghei* in a dose-dependent manner in Ethiopia. *Ethiop J Health Sci* 28:655–664
- Carvalho AR Jr, Diniz RM, Suarez MAM, Figueiredo CSSES, Zagnignan A, Grisotto MAG, Fernandes ES, da Silva LCN (2018) Use of some Asteraceae plants for the treatment of wounds: from ethnopharmacological studies to scientific evidence. *Front Pharmacol* 9:784
- Chen YH (1959) Wang Mengying's use of Jiajian Xiaochaihu Decoction for malaria treatment: a case study. *J Trad Chi Med* 9:43–44
- Coppi A, Cabinian M, Mirelman D, Sennis P (2006) Antimalarial activity of allicin, a biologically active compound from garlic cloves. *Antimicrobial Agents Chemother* 50:1731–1737
- Dkhil MA, Al-Quraishy S, Al-Shaebi EM, Abdel-Gaber R, Thagfan FA, Qasem MAA (2021) Medicinal plants as a fight against murine blood-stage malaria. *Saudi J Biol Sci* 28:1723–1738
- Du G, Tu H, Li X, Pei A, Chen J, Miao Z, Li J, Wang C, Xie H, Xu X, Zhao H (2014) Daphnetin, a natural coumarin derivative, provides the neuroprotection against glutamate-induced toxicity in HT22 cells and ischemic brain injury. *Neurochem Res* 39:269–275
- El-Saber Batiha G, Magdy Beshbishy A, Wasef GL, Elewa YHA, Al-Sagan A, Abd El-Hack ME, Taha AE, Abd-Elhakim YM, Prasad Devkota H (2020) Chemical constituents and pharmacological activities of garlic (*Allium sativum* L.): a review. *Nutrients* 12:872
- Feng XY (1972) Clinical observation of garlic ointment for treatment of malaria. *J New Med* 4:42
- Feng Y, Zhu X, Wang Q, Jiang Y, Shang H, Cui L, Cao Y (2012) Allicin enhances host pro-inflammatory immune responses and protects against acute murine malaria infection. *Malar J* 11:268
- Gao C, Liu YT, Zhou JM, Guo Y (2019) Clinical observation on the efficacy of artesunate combined with Xiaochaihu granule for treatment of malaria in a peace-keeping second hospital by China. *J Prev Med Chin PLA* 37:95–96
- Guo J, Ni YC, Wu JT, Wang QM (2004) Additive therapeutic effect of a combination of artemether and daphnetin against *plasmodium berghei* in mice. *Chin J Parasitol Parasit Dis* 22:164–166
- Gurmu AE, Kisi T, Shibru H, Graz B, Willcox M (2018) Treatments used for malaria in young Ethiopian children: a retrospective study. *Malar J* 17:451
- Ho WE, Peh HY, Chan TK, Wong WS (2014) Artemisinins: pharmacological actions beyond anti-malarial. *Pharmacol Ther* 142:126–139
- Hogan AB, Jewell BL, Sherrard-Smith E, Vesga JF, Watson OJ, Whittaker C, Hamlet A, Smith JA, Winskill P, Verity R, Baguelin M, Lees JA, Whittles LK, Ainslie KEC, Bhatt S, Boonyasiri A, Brazeau NF, Cattarino L, Cooper LV, Coupland H, Cuomo-Dannenburg G, Dighe A, Djaafara BA, Donnelly CA, Eaton JW, van Elsland SL, FitzJohn RG, Fu H, Gaythorpe KAM, Green W, Haw DJ, Hayes S, Hinsley W, Imai N, Laydon DJ, Mangal TD, Mellan TA, Mishra S, Nedjati-Gilani G, Parag KV, Thompson HA, Unwin HJT, Vollmer MAC, Walters CE, Wang H, Wang Y, Xi X, Ferguson NM, Okell LC, Churcher TS, Arinaminpathy N, Ghani AC, Walker PGT, Hallett TB (2020) Potential impact of the COVID-19 pandemic on HIV, tuberculosis, and malaria in low-income and middle-income countries: a modeling study. *Lancet Glob Health* 8:e1132–e1141
- Hsu E (2006) The history of qing hao in the Chinese materia medica. *Trans R Soc Trop Med Hyg* 100:505–508
- Huang F, Tang LH, Chen B, Ni YC, Wang QM (2006b) *In vitro* effect of daphnetin on cytochrome C oxidase and ribonucleotide reductase of *Plasmodium falciparum*. *Chin J Parasitol Parasit Dis* 24:179–182

- Huang F, Tang LH, Chen B, Zhou SS, Wang QM (2008b) The potentiation of antimalarial activities by daphnetin derivatives against malaria parasites *in vitro* and *in vivo*. *J Pathog Biol* 3:288–291
- Huang F, Tang LH, Yu LQ, Ni YC, Wang QM, Nan FJ (2006a) *In vitro* potentiation of antimalarial activities by daphnetin derivatives against *Plasmodium falciparum*. *Biomed Environ Sci* 19: 367–370
- Huang F, Tang LH, Yu LQ, Ni YC, Wang QM, Zhou SS (2008a) The potentiation of antimalarial activities by daphnetin derivatives against malaria parasites *in vitro* and *in vivo*. *J Pathog Biol* 3: 35–38
- Javed M, Saleem A, Xaveria A, Akhtar MF (2022) Daphnetin: a bioactive natural coumarin with diverse therapeutic potentials. *Front Pharmacol* 13:993562
- Kamaraj C, Kaushik NK, Mohanakrishnan D, Elango G, Bagavan A, Zahir AA, Rahuman AA, Sahal D (2012) Antiplasmodial potential of medicinal plant extracts from Malaiyur and Javadhur hills of South India. *Parasitol Res* 111:703–715
- Kaushik NK, Bagavan A, Rahuman AA, Mohanakrishnan D, Kamaraj C, Elango G, Zahir AA, Sahal D (2013) Antiplasmodial potential of selected medicinal plants from eastern Ghats of South India. *Exp Parasitol* 134:26–32
- Kong LY, Tan RX (2015) Artemisinin, a miracle of traditional Chinese medicine. *Nat Prod Rep* 32: 1617–1621
- Kovalev V, Wells ML (2020) Self-treatment practices for perceived symptoms of malaria in Ethiopia. *Cureus* 12:e9359
- Li FC (1960) Therapeutic efficacy of Chaihu against malaria: a report of 44 cases. *Chin J Intern Med* 8:560
- Li J (2011) Forty-two cases of malaria treated with ginger-partitioned moxibustion in the republic of Congo. *Zhongguo Zhen Jiu* 31:559–561
- Li WP (1954) Thinking of Xiaochaihu for malaria treatment. *Jiangxi J Tradit Chin Med* 4:18–22
- Li Y (2012) Qinghaosu (artemisinin): chemistry and pharmacology. *Acta Pharmacol Sin* 33:1141–1146
- Lindsay SW, Thomas MB, Kleinschmidt I (2021) Threats to the effectiveness of insecticide-treated bednets for malaria control: thinking beyond insecticide resistance. *Lancet Glob Health* 9: e1325–e1331
- Liu GH (1976) Treatment of malaria with Xiaochaihu Decoction: a report of 14 cases Shaanxi. *Med J* 5:60
- Liu YG, Wang QM, Xu YQ, Ni QZ, Ni YC (2001) Effect of daphnetin on the exo-erythrocytic stage of rodent malaria. *Chin J Parasitol Parasit Dis* 19:30–32
- Ma N, Zhang Z, Liao F, Jiang T, Tu Y (2020) The birth of artemisinin. *Pharmacol Ther* 216:107658
- Martino E, Tarantino M, Bergamini M, Castelluccio V, Coricello A, Falcicchio M, Lorusso E, Collina S (2019) Artemisinin and its derivatives; ancient tradition inspiring the latest therapeutic approaches against malaria. *Future Med Chem* 11:1443–1459
- Mehlhorn H, Wu ZD, Ye B (2014) Treatment of human parasitosis in traditional Chinese medicine. Springer, Berlin
- Meng Y, Ma N, Lyu H, Wong YK, Zhang X, Zhu Y, Gao P, Sun P, Song Y, Lin L, Wang J (2021) Recent pharmacological advances in the repurposing of artemisinin drugs. *Med Res Rev* 41: 3156–3181
- Moshiashvili G, Tabatadze N, Mshvildadze V (2020) The genus *Daphne*: a review of its traditional uses, phytochemistry and pharmacology. *Fitoterapia* 143:104540
- Mu LY, Wang QM, Ni YC (2002) *In vitro* antimalarial effect of daphnetin relating to its iron-chelating activity. *Chin J Parasitol Parasit Dis* 20(2):83–85
- Mu LY, Wang QM, Ni YC (2003) Effect of daphnetin on SOD activity and DNA synthesis of *Plasmodium falciparum in vitro*. *Chin J Parasitol Parasit Dis* 21:157–159
- Murnigsih T, Subeki MH, Takahashi K, Yamasaki M, Yamato O, Maede Y, Katakura K, Suzuki M, Kobayashi S, Chairul YT (2005) Evaluation of the inhibitory activities of the extracts of Indonesian traditional medicinal plants against *Plasmodium falciparum* and *Babesia gibsoni*. *J Vet Med Sci* 67:829–831

- Na-Bangchang K, Karbwang J (2019) Pharmacology of antimalarial drugs, current anti-malarials.- In: Kremsner P, Krishna S (eds) Encyclopedia of malaria. Springer, New York
- Odoh UE, Uzor PF, Eze CL, Akunne TC, Onyegbulam CM, Osadebe PO (2018) Medicinal plants used by the people of Nsukka local government area, southeastern Nigeria for the treatment of malaria: an ethnobotanical survey. *J Ethnopharmacol* 218:1–15
- Oliveira FAS, Passarini GM, Medeiros DSS, Santos APA, Fialho SN, Gouveia AJ, Latorre M, Freitag EM, Medeiros PSM, Teles CBG, Facundo VA (2018) Antiplasmodial and antileishmanial activities of compounds from *Piper tuberculatum* Jacq fruits. *Rev Soc Bras Med Trop* 51:382–386
- Ounjaijean S, Somsak V (2022) Effect of allicin and artesunate combination treatment on experimental mice infected with *Plasmodium berghei*. *Vet Med Int* 2022:7626618
- Palakkod Govindan V, Panduranga AN, Krishna Murthy P (2016) Assessment of *in vivo* antimalarial activity of arteether and garlic oil combination therapy. *Biochem Biophys Rep* 5:359–364
- Parola P (2013) The return of the big three killers. *Clin Microbiol Infect* 19:887–888
- Perez HA, De la Rosa M, Apitz R (1994) *In vivo* activity of ajoene against rodent malaria. *Antimicrob Agents Chemother* 38:337–339
- Phillips MA, Burrows JN, Manyando C, van Huijsduijnen RH, Van Voorhis WC, Wells TNC (2017) Malaria. *Nat Rev Dis Primers* 3:17050
- Rogerson SJ, Beeson JG, Laman M, Poespoprodjo JR, William T, Simpson JA, Price RN, ACREME Investigators (2020) Identifying and combating the impacts of COVID-19 on malaria. *BMC Med* 18:239
- Rolnik A, Olas B (2021) The plants of the Asteraceae family as agents in the protection of human health. *Int J Mol Sci* 22:3009
- Ruo X, Sui L (1956) Malaria: Clinical treatment II. *Jiangxi J Tradit Chin Med* 6:44–47
- Sato S (2021) *Plasmodium*-a brief introduction to the parasites causing human malaria and their basic biology. *J Physiol Anthropol* 40:1
- Sherrard-Smith E, Hogan AB, Hamlet A, Watson OJ, Whittaker C, Winskill P, Ali F, Mohammad AB, Uhomoihibi P, Maikore I, Ogbulafor N, Nikau J, Kont MD, Challenger JD, Verity R, Lambert B, Cairns M, Rao B, Baguelin M, Whittles LK, Lees JA, Bhatia S, Knock ES, Okell L, Slater HC, Ghani AC, Walker PGT, Okoko OO, Churcher TS (2020) The potential public health consequences of COVID-19 on malaria in Africa. *Nat Med* 26:1411–1416
- Shrivastava N, Khan SA, Ahmad S, Al-Balushi K, Husain A (2021) Recent advances in the development of chemotherapeutic agents for malaria. *Mini Rev Med Chem* 21:1487–1508
- Sinclair D, Zani B, Donegan S, Olliaro P, Garner P (2009) Artemisinin-based combination therapy for treating uncomplicated malaria. *Cochrane Database Syst Rev* 3:CD007483
- Suleman S, Beyene Tufa T, Kebebe D, Belew S, Mekonnen Y, Gashe F, Mussa S, Wynendaele E, Duchateau L, De Spiegeleer B (2018) Treatment of malaria and related symptoms using traditional herbal medicine in Ethiopia. *J Ethnopharmacol* 213:262–279
- Tu Y (2016) Artemisinin-A gift from traditional Chinese medicine to the world (Nobel Lecture). *Angew Chem Int Ed Engl* 55:10210–10226
- Vathsala PG, Krishna Murthy P (2020) Immunomodulatory and antiparasitic effects of garlic-artether combination via nitric oxide pathway in *Plasmodium berghei*-infected mice. *J Parasit Dis* 44:49–61
- Wang G, Pang J, Hu X, Nie T, Lu X, Li X, Wang X, Lu Y, Yang X, Jiang J, Li C, Xiong YQ, You X (2019) Daphnetin: a novel anti-*Helicobacter pylori* agent. *Int J Mol Sci* 20:850
- Wang QM, Liu YG, Tao Y, Wang MJ, Ni YC (2004a) Antimalarial effect and high-performance liquid chromatography analysis of daphnetin. *Chin Remed Clin* 4:20–24
- Wang QM, Ni YC, Guo J, Wu JT, Qian YJ (2004b) Comparative study on schizontocidal activity of recrystallized or crude daphnetin against malaria parasites. *Biomed Environ Sci* 17:397–401
- Wang QM, Ni YC, Xu YQ, Ha SH, Cai Y (2000) The schizontocidal activity of daphnetin against malaria parasites *in vitro* and *in vivo*. *Chin J Parasitol Parasit Dis* 18:204–206
- Wang W, Liang YS (2016) Artemisinin: a wonder drug from Chinese natural medicines. *Chin J Nat Med* 14:5–6

- WHO (2021a) World malaria report 2021. The World Health Organization, Geneva
- WHO (2021b) Global technical strategy for malaria 2016–2030, 2021 update. The World Health Organization, Geneva
- Wu Y, Ruan HQ, Zhao CX (1995) Effect of the ethyl acetate extract from *Chrysanthemum morifolium* on *Plasmodium falciparum*. Hainan Med J 6:216
- Yang F, Dong X, Yin X, Wang W, You L, Ni J (2017) *Radix bupleuri*: a review of traditional uses, botany, phytochemistry, pharmacology, and toxicology. Biomed Res Int 2017:7597596
- Yang YZ, Ranz A, Pan HZ, Zhang ZN, Lin XB, Meshnick SR (1992) Daphnetin: a novel antimalarial agent with *in vitro* and *in vivo* activity. Am J Trop Med Hyg 46:15–20
- Yong HS (1994) Cure of malaria with Xiaochaihu Decoction during the pregnancy second trimester. J Tradit Chin Med 13:30–31
- Yuan B, Yang R, Ma Y, Zhou S, Zhang X, Liu Y (2017) A systematic review of the active saikosaponins and extracts isolated from *Radix bupleuri* and their applications. Pharm Biol 55: 620–635
- Zhao C, Ruan H, Lei Y, Wu Y, Voelter W, Jung A, Schick M (1996c) Inhibition of the development of *Plasmodium yoelii* in exoerythrocytic stage in rodents (rats) with *Chrysanthemum morifolium*. J Tongji Med Univ 16:200–202
- Zhao CX (1986) Effect of *Dichroa febrifuga* L. on chloroquinsensible and chloroquinresistant malaria parasites. J Tongji Med Univ 6:112–115
- Zhao CX, Lei Y, Ruan HQ, Wu Y (1996b) The activity of the chloroform extract of *Chrysanthemum morifolium* against the gametocyte of *Plasmodium berghei*. Hainan Med J 7:143–144
- Zhao CX, Lei Y, Wu Y, Ruan HQ (1997a) Experimental study on antimalarial action of alcohol extract from *Chrysanthemum* (1): effect on *P. yoelii* in erythrocytic stage. Central Chin Med J 21:26–27
- Zhao CX, Ruan HQ, Lei Y, Wu Y (1996d) Effect of chloroform extract of *Chrysanthemum morifolium* on *Plasmodium berghei* in exoerythrocyte. Hainan Med J 7(220–221):276
- Zhao CX, Ruan HQ, Wu Y, Lei Y (1997b) Experimental study on antimalarial action of alcohol extract from *Chrysanthemum* (2): effect on *P. yoelii* in primary exoerythrocytic stage. Central Chin Med J 21:77–78
- Zhao CX, Wu Y, Lei Y, Ruan HQ (1996a) The activity of the ethanol and chloroform extracts of *Chrysanthemum morifolium* against the erythrocytic stage of *Plasmodium berghei*. Hainan Med J 7:2–3

Index

A

Antibody, 200–206, 212–216, 264
Antigen, 72–75, 200–206, 213–216
Antimalarial activity, 282–285
Antimalarial drug, 3, 13, 24, 39, 41, 78, 81, 82, 91, 93, 98, 156–158, 166, 212, 219, 253–255, 262, 263, 268, 273, 274, 280
Artemisinin, 2, 3, 14, 41, 116, 157, 158, 160, 253, 255, 262, 268, 269, 271–274, 281, 282, 286
Artemisinin-based combination therapies (ACTs), 253–256, 258–262, 268, 281
Artemisinin resistance, 44, 267–274, 281
Artificial intelligence, 225–250
Asteraceae, 283–284, 286

B

Biological characteristics, 13, 54, 55
Bupleuri radix, 285–286

C

Challenge, 11, 14, 33, 35, 42–44, 206–207, 229, 253, 262, 274
China, 2–15, 33–44, 49, 51, 147, 206, 207, 269, 285
Clinical manifestations, 72, 75–78, 81
Control, 2, 11–13, 34, 37–44, 81, 200, 201, 203, 205, 235, 253, 263, 268, 270, 274, 281, 282, 284, 285
Control measurements, 40

D

Daphne, 284–286
Deep learning, 225–250

Drug-resistant, 78, 262–263, 273, 274
Drugs, 2, 20, 39, 78, 91, 212, 253, 268, 280

E

Elimination, 2, 11–15, 34–44, 73, 157, 200, 203, 206, 263, 280, 281, 286
Endangered regions, 20
Epidemiology, 1–15, 118
Erythrocyte invasion, 212–214

F

Feature extraction, 227, 237

G

Garlic, 282–283, 286
Ginger, 281–282, 286

H

Historical records, 3, 10
Human *Plasmodium*, 50, 51, 54–68, 72, 163

I

Immune escape, 212, 216
Immunodiagnosis, 199–207

K

kelch13 mutations, 272

L

Life cycle, 20–23, 49–68, 141, 145

M

Malaria, 1–15, 19–29, 33–44, 49–62, 71–82, 87–197, 199–207, 211–219, 225–250, 253–264, 267–274, 279–286
Malaria diagnosis, 13, 38, 40, 41, 43, 163, 200–202, 206, 225–250
Microscopic diagnosis, 13, 38, 40, 41, 43, 163, 200–202, 206, 225–250
Microscopic examination, 38, 40, 49, 87–97, 112, 118, 143–145, 156, 157, 163, 165, 226, 227
Morphology, 49–62, 87–197
Mosquitoes, 2, 14, 15, 20, 21, 39, 41–43, 49–55, 212, 216, 263, 268, 274, 280

P

Pathogenesis, 71–82, 211–219
Plasmodium, 2, 21, 49, 72, 87, 200, 211, 226, 256, 271, 280
Plasmodium falciparum, 3, 20, 43, 50, 72, 90, 201, 213, 228, 254, 268, 280

R

Re-establishment, 15, 37, 206, 207

S

Sexual differentiation, 216–219

T

Traditional Chinese medicine, 14, 279–286
Traditional methods, 226–228, 250
Transcriptional regulatory, 217, 219
Treatment, 2, 24, 38, 53, 76, 91, 201, 218, 227, 253, 268, 281

V

Vectors, 12–15, 20, 35, 41, 42, 49, 50, 109, 212, 233, 234, 241, 242, 263, 269, 274